A Nitrogen and Carbon Stable Isotope Study of some Western Australian Diamonds

Thesis

UNRESTRICTE

A nitrogen and carbon stable isotope study of some Western Australian diamonds.

A thesis submitted for the degree of Doctor of Philosophy

by

Leon Andrê van Heerden

B.Sc (Hons.), M.Sc (Cape Town)

Date of submission: 31 August 1993
Date of award: 15 November 1994

Department of Earth Science
The Open University

October, 1993

ProQuest LLC.
789 East Eisenhower Parkway
P.O. Box 1346
Ann Arbor, MI 48106 – 1346

Abstract

The carbon and nitrogen stable isotope ratios, nitrogen content and aggregation state have been measured in diamonds from Australian magmatic and alluvial sources and from a Chinese placer deposit. There are no consistent relationships between any of these properties, and there are no consistent relationships with diamond shape or colour. Both individual diamonds and diamond sources are shown to be heterogeneous and have a range of $\delta^{13}C$ and $\delta^{15}N$ values. The widest range in Western Australian magmatic diamonds occurs in Ellendale 9 samples which have $-22.1‰ \leq \delta^{13}C \leq 0.0‰$ and $-9.3‰ \leq \delta^{15}N \leq -9.9‰$. Diamonds from placer deposits have a wider range of $\delta^{15}N$ and $\delta^{13}C$ values however ($-14.8‰ \leq \delta^{13}C \leq +1.9‰$ & $-28.4‰ \leq \delta^{15}N \leq +9.7‰$ in Northern Queensland samples). This may be due to placers representing multiple primary sources.

A relationship between diamond paragenesis and $\delta^{13}C$ value is shown. Eclogitic diamonds worldwide have a mean $\delta^{13}C$ value of $-8.6 \pm 5.8‰$ and range from $\delta^{13}C = -34.5‰$ to $+1.5‰$. In contrast, peridotitic paragenesis diamonds have a mean $\delta^{13}C$ value of $-5.4 \pm 2.6‰$, and their range in $\delta^{13}C$ values is from $-23.5‰$ to $+0.1‰$. $\delta^{15}N$ data from diamonds of known provenance are scarce, but there are no significant differences between eclogitic and lherzolitic diamonds from Western Australia. Eclogitic diamonds have a mean $\delta^{15}N$ value of $4.9‰ \pm 4.6‰$ whereas lherzolitic diamonds have a mean $\delta^{15}N$ value of $4.1‰ \pm 4.9‰$. These parageneses have different mean $\delta^{15}N$ values when compared to the mean $\delta^{15}N$ value of samples thought to be of the harzburgitic paragenesis. It is provisionally suggested that carbon and nitrogen stable isotope ratios may discriminate eclogitic, lherzolitic and harzburgitic paragenesis samples.

Three Argyle diamonds and a single Ellendale diamond are zoned in $\delta^{13}C$ and $\delta^{15}N$ values, nitrogen content and aggregation state. Models for these zonation profiles are consistent with diamond formation by fractional crystallization, and fractionation factors of $\alpha \leq 1.001$ for carbon and $\alpha = 1.004$ for nitrogen during diamond growth are suggested. These samples are also zoned in age and in the most extreme case a difference of 1.2 Ga between the core and rim of a diamond 5 mm in diameter is found.

All available diamond $\delta^{15}N$ data are combined and it is concluded that $\delta^{15}N = 0‰ \pm 6‰$ is a characteristic of the sub-continental lithospheric upper mantle. Heterogeneities within this are however evident when $\delta^{13}C$ and $\delta^{15}N$ covariations are considered. It is suggested that the subduction of oceanic sediment, carbonates and peridotite into the mantle, combined with isotope fractionation processes are responsible for the stable isotope characteristics of the diamond source region. A possible trend of increasing $\delta^{15}N$ value in diamonds as their age decreases is noted, and it is speculated that this may be a result of a kinetic fractionation during mantle degassing and atmosphere formation.

For my parents

Andrê and Lenchen

whose support has made it all possible

Acknowledgements

A great number of people have been involved in this thesis and I would like acknowledge

- My supervisors, Colin Pillinger for initiating the project and Stuart Boyd for maintaining the momentum in Milton Keynes.
- Dearn Lee of Ashton Mining, Chris Smith of CRAE and Phil Plaisted of Argyle Diamond Mines for providing the samples used in this study, and Dearn Lee is thanked for clearing up some of the problems as to the origin of these diamonds.
- Judith Milledge and Monica Mendelssohn at University College, London for FTIR spectra, C.L. photographs and discussion.
- Mike Seal of Drukker & Zn. for laser sectioning the diamond plates,
- and The Open University for the three year studentship that made it all possible.

In addition, a number of people have read this thesis and I am indebted to Jeff Harris and Nick Rogers, Melissa Kirkley, Chris Harris and Stewie Smith for the comments that have significantly improved the earlier drafts. Chris and Stewie are particularly thanked for acting as unofficial supervisors while I was in Cape Town. Dave Mattey, Richard Ash, John Gurney, Steves Haggerty and Richardson, Mal McCallum, Dave Bell and Galena Bulanova have also contributed to the thesis through their discussion. I am also grateful to John Gurney and Andy Duncan for making it possible for me to complete this thesis during a very pleasant stay at the University of Cape Town.

The friends who made Milton Keynes a tolerable place to live have a lot to answer for - David Peate, Graham Hill, Lisa Robson, Arlëne Hunter, and all the members of the P.S.U., especially the lunatics of T.24 - Sara Russell, Richard Ash and Paul Yates; you lot, along with Emma Creighton and Jo Howard kept me in England for a lot longer than expected! Also much appreciated are the comments, friendship and entertainments of the "Kimberlite Kids" - Ingrid Chinn, Gail Kiewits and Steve Horwood at the University of Cape Town as well as Protea Hirschel, for the time that they all spent with me.

Special thanks go to Jacqui and Tony Lyne for sun-drenched days and rum-soaked nights in the Caribbean, just when M.K had become too much. Similar thanks are also extended to Janet Fell, for the fine food, wonderful wine and unrivalled hospitality that have made staying in Cape Town such a joy. Mark Kirby is thanked for the loan of the "red beast" without which I would have been locked immobile in Cape Town, and without Marianne Tredoux's printer, none of this would have materialised.

And finally, to all of you that I havn't named individually - the fellow students, the folks from Hoechst and Ye Olde Swan, the Skiers and the Staff of the O.U.; you know who you are... **Thank you, all of you**

Table of Contents

List of Tables

List of Figures

1 Introduction

1.1 PRELUDE

Diamond - the high pressure polymorph of carbon has several unique properties that make it valuable (Table 1.1), both intrinsically and as a tool for the earth scientist concerned with understanding the origin and the evolution of the Earth. The fact that diamonds are derived from the Earth's mantle (Kennedy and Nordlie, 1968) and may be of great age† means that they carry a record of conditions in the early Earth, possibly from depths as great as 450 km (Moore and Gurney, 1985). This record is preserved within the diamond due to its mechanical durability and resistance to most forms of chemical attack‡.

Composition	100% carbon	Purest type IIa diamond
Bonding	Covalent	hybridisation of sp3 orbitals
Crystal system	cubic	A hexagonal form known as Lonsdaleite also exists
Space group	$Fd\bar{3}m$	Holosymetric,
Point group	$\frac{4}{m}\bar{3}\frac{2}{m}$	Yacoot and Moore (1993)
Unit cell	a = 154.5pm	
Lattice dilation around N impurity	10%	Kaiser and Bond (1959)
	5 - 10%	Mainwood (1979)
	36%	Amerlaan (1981)
Hardness	10 on the Mohs scale	Hardest known
Compressibility	$\approx 1.9 \times 10^{-12}$ Nm^{-2}	Smallest known
Thermal conductivity	9.94 $W.cm^{-1}.K^{-1}$	Type I diamond
	26.2 $W.cm^{-1}.K^{-1}$	Type II diamond (Highest known)
Thermal expansion (linear)	0.8×10^{-6} at 293 K	Lowest known
Electrical resistivity	10^{13} $\Omega.cm^{-1}$	Very high
Density	3.51 $g.cm^{-3}$	
Refractive index	2.4173	
Vibrational frequency	0 to 40 x 10^{12} Hz	Widest known range

Table 1.1: Some physical and chemical properties of diamond. Thermal conductivity values are at 273 K and are very dependent on nitrogen content. See Davies (1984) for a full discussion.

† From the radiogenic dating of mineral inclusions (Richardson *et al.*, 1984). See below for further discussion.

‡ Except under conditions of high oxygen fugacity.

1.2 DIAMOND OCCURRENCE

Natural diamonds occur in two major and a number of minor environments. The major occurrences are of magmatic origin, comprising diamondiferous kimberlites and lamproites, however diamonds are often found in sedimentary (placer) deposits having been eroded out of a magmatic source. More than 3000 kimberlite and lamproite pipes are known worldwide (Lubala, 1991), although only a very small proportion of these contain diamonds, and an even smaller proportion contain sufficient diamonds to be economically viable. More than 115 lamproites, kimberlites and lamproitic or kimberlitic dykes have been identified in Western Australia alone (Jaques *et al.*, 1986b), but only the Argyle lamproite is being mined at present. Minor sources of diamonds include those in meteorites (*e.g.* Ash, 1990), those in picrites and other ultramafic rocks (Kaminsky *et al.*, 1986; Kaminsky, 1980) and those in metamorphic rocks (Sobolev and Shatsky, 1990; Shutong *et al.*, 1992). Diamonds are also known to occur in eclogite and peridotite xenoliths from kimberlite and lamproite, often at high concentrations (Gurney, 1989), and it has also been suggested that diamonds may occur in ophiolites (Pearson *et al.*, 1989). Recently, impact related diamonds have been reported from the Cretaceous/Tertiary boundary clay from Alberta, Canada (Carlisle and Bramen, 1991).

It is evident that diamonds have been intermittently carried to the earth's surface over long periods of Earth history and the oldest well documented diamond occurrences are those in the 2.6 Ga Witwatersrand Conglomerates, South Africa (Gurney, 1989). The oldest dated diamondiferous diatreme is the Premier kimberlite, South Africa (≈1250 Ma; Kramers, 1979) whilst the Noonkanbah lamproites of the west Kimberley region, Australia are amongst the youngest known primary diamond source (≈20 Ma; Jaques *et al.*, 1984b). Kimberlite (and lamproite) emplacement has been episodic and Hargraves and Onstott (1980) report some evidence for a relationship between plate tectonic motions and kimberlitic volcanism in southern Africa. A similar suggestion is made by Smith (1984) who ascribes the trend of decreasing age away from the Kimberley craton (Western Australia) shown by the west Kimberley lamproites to be a hot spot trace indicating movement of the Kimberley craton and associated rocks in a north easterly direction at about 3.7 $cm.yr^{-1}$.

1.2.1 Kimberlites and lamproites

Kimberlites and lamproites are the only commercially important primary sources of diamonds and have been thoroughly reviewed by Dawson (1980), Scott-Smith and Skinner (1984) and Mitchell (1986). Both kimberlites and lamproites are volatile-rich, ultrapotassic, ultrabasic igneous rocks intruding ancient crust as pipe like diatremes and

are similar to each other in many respects, but have several important morphological and chemical differences (Figure 1.1 and Table 1.2). Their main physical features are summarised below.

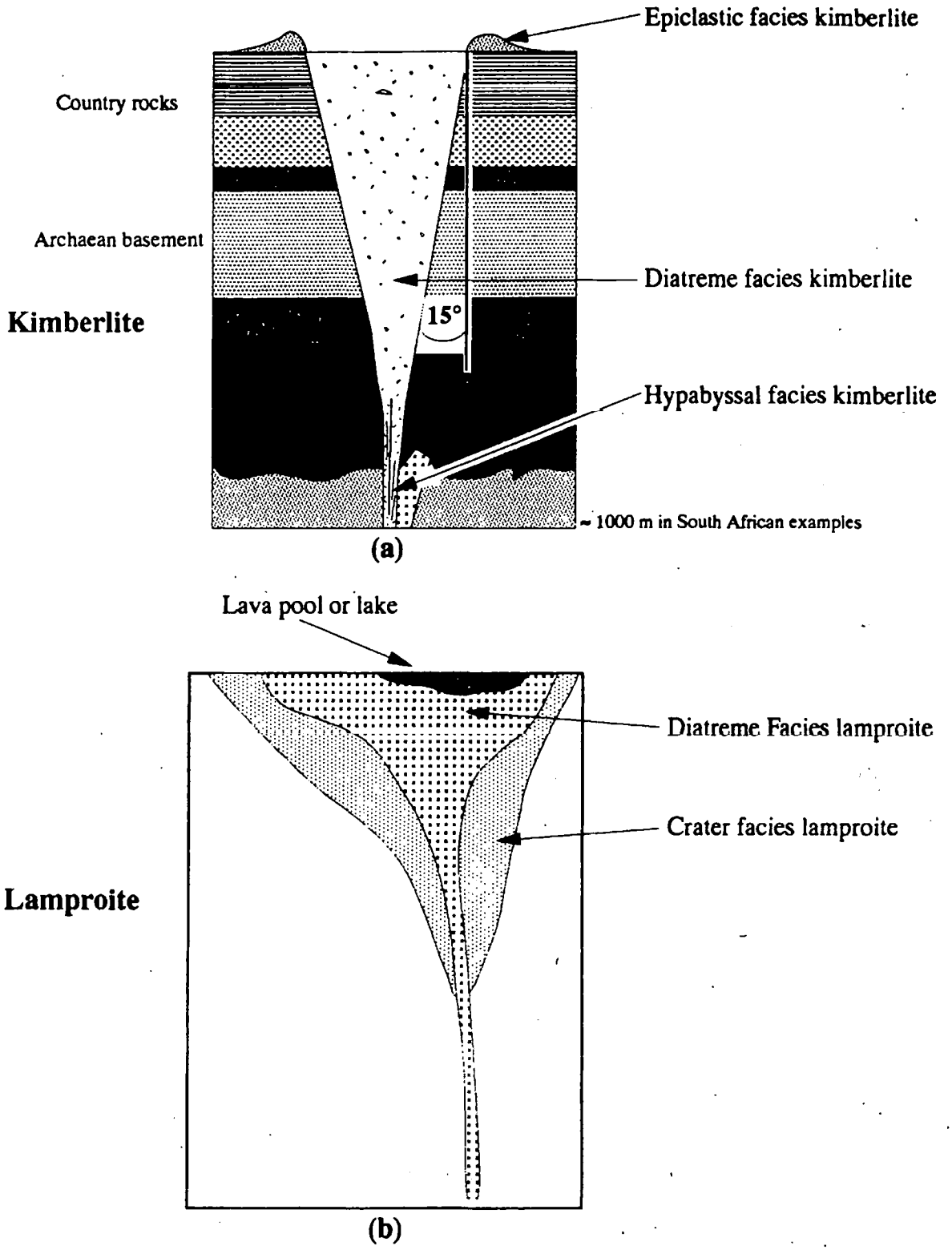

Figure 1.1: Kimberlite (a) and lamproite (b) pipes in cross section. From Hawthorne (1975) and Scott-Smith and Skinner (1984). Neither cross section is to scale.

The idealised kimberlite has been described by Hawthorne (1975) and as can be seen from Figure 1.1 tends to form a steeply dipping cone containing three distinct kimberlite facies. The uppermost epiclastic facies is produced by fluvial reworking and redeposition in crater lakes formed at the mouths of diatremes, and often contains diamond grades higher than the remainder of the pipe due to surface reworking. Craters can be from 50 to 1500m across and are preserved only in pipes that have undergone little erosion (*e.g.* Orapa, Botswana) but epiclastic facies kimberlite may be found as down-faulted blocks in the underlying diatreme facies. The diatreme facies kimberlite comprises fragments of kimberlite itself, country rock and mantle xenoliths, phenocrysts and megacrysts set in a fine-grained brecciated matrix of olivine and/or phlogopite together with perovskite, spinel, diopside, apatite, monticellite, calcite and primary serpentine.

Feeding this cone shaped diatreme facies is a series of feeder dykes or sills comprising the hypabyssal kimberlite and these are the result of in-situ solidification of kimberlitic magma that was intruded less violently than the overlying diatreme facies material. Mantle xenoliths and xenocrysts, including diamond, occur in the hypabyssal facies kimberlite but country rock xenoliths are scarcer than in the diatreme zone. Diamond grades appear to be similar in both hypabyssal and diatreme facies kimberlite (Gurney, 1986; 1989), although the diatreme facies rocks are noted for homogeneous grades whereas diamond grades in hypabyssal facies kimberlite can be very variable (Kirkley, Pers. Comm.).

In contrast to kimberlites, lamproite diatremes are commonly bowl-shaped (Figure 1.1) and often show evidence of an irregular crater filled predominantly with pyroclastic material and later intruded by magmatic lamproite forming ponded lava lakes (Scott-Smith and Skinner, 1984). The presence of the lava pools is indicative of a less violent emplacement than kimberlites and this is confirmed by lower volatile contents and particularly a lower CO_2/H_2O ratio in lamproites than in kimberlites. Further differences between lamproites and kimberlites are summarised in Table 1.2.

Both kimberlites and lamproites tend to occur in clusters or fields and it has been noted for kimberlites that if any one in a field is diamondiferous, then all kimberlites in that field are diamondiferous, although diamond grades may differ considerably (Gurney, 1989). In addition, diamonds from the same cluster of kimberlites tend to have very similar size and shape characteristics but the proportions of diamonds of different paragenesis (see section 1.3.3.1) may not always be the same (Gurney, 1989). The scarcity of data from lamproite derived diamonds prevents an evaluation of whether the above observations are valid for lamproites in general. Ellendale 4, Ellendale 9, Argyle and Prairie Creek (Arkansas, U.S.A) are the only lamproites for which diamond data are currently

available. Hall and Smith (1984) have however shown that kimberlitic and lamproitic diamonds are, in general, very similar although lamproitic diamonds do contain a higher proportion of frosted and etched diamonds, and this may indicate increased late stage corrosion.

Kimberlite	Lamproite
Cone shaped	Bowl shaped
Higher Al_2O_3 FeO, MgO & volatiles than lamproites	Higher SiO_2, TiO_2, P_2O_5, BaO, K_2O
	Lower CO_2/H_2O than kimberlites
Light REE depleted and enriched examples exist	Light REE enriched or very enriched
Very rapid or explosive emplacement	Slower emplacement
Mantle xenoliths common	Mantle xenoliths less common
No evidence for extrusive kimberlite	Lava pools & lakes common
Euhedral olivine in the groundmass	Olivine in complex crystal aggregates
Primary serpentine	No primary serpentine
Primary carbonate	No primary carbonate
Glass absent	Glass present

Table 1.2: Some differences between lamproites and kimberlites.

Diamondiferous kimberlites are thought to occur only within craton boundaries (although the Venetia kimberlite, South Africa may be an exception to this) whereas diamondiferous lamproites occur very close to craton boundaries. The currently accepted theory is that only in thick, stable lithosphere are the pressures necessary for diamond stability found within the kimberlite or lamproite source regions. Barren kimberlites, in contrast, originate off-craton, where higher heat flow (*e.g.* Haggerty, 1986) results in their roots occurring within the graphite stability field (Figure 1.2).

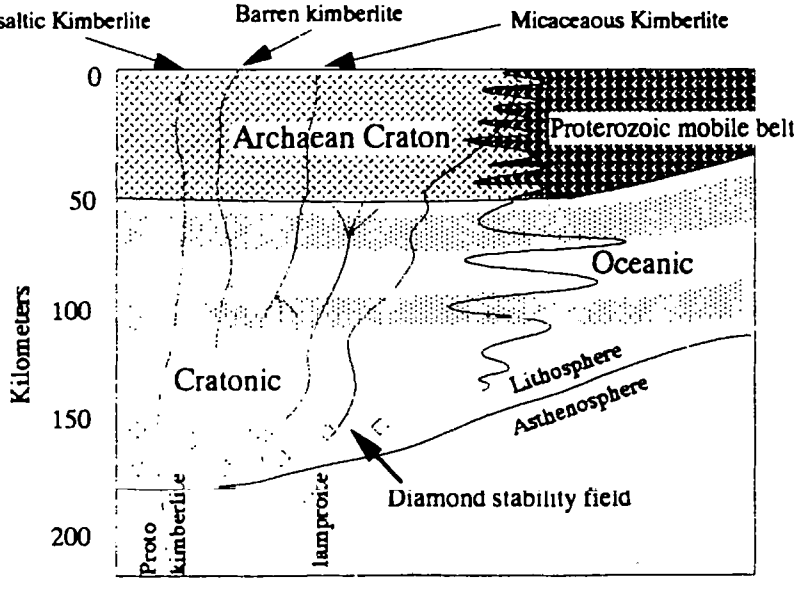

Figure 1.2: Cartoon cross section of a craton and the surrounding area showing diamond source regions. After Menzies (1988).

1.2.2 Placer deposits

Placer deposits have a similar, though more dispersed, distribution than kimberlites and lamproites and they are clearly associated with regions of ancient crust. This is a result of placer diamonds being originally derived from magmatic sources (Gurney, 1989). The outstanding feature of alluvial diamond deposits is the improvement in the average quality of diamonds with increasing distance from the primary source and this has been ascribed by Gurney (1989) to the preferential breakage of inferior crystals.

Crystals may be sorted by size and shape by hydrodynamic processes and often concentrate as a lag-gravel on a bedrock surface. When favourable conditions for trapping diamonds exist, very high grades may be attained (>250 ct.m^{-3} gravel in some marine environments†; Gurney, 1986). Most lithified gravels are however uneconomic due to low average grades and the high cost of diamond extraction.

1.2.3 Synthetic diamonds

A comprehensive review of diamond synthesis under laboratory experimental conditions is provided by Davies (1984). Most modern high pressure synthesis methods utilize a solvent-catalyst approach in which carbon, usually in the form of graphite, is dissolved in a metal heated to sufficient temperatures and pressures for the graphite to be reprecipitated as diamond, the reaction being catalysed by the solvent metal. Commonly used solvent – catalysts are Ni or Co although Fe, Pt, Pd, Mn, Cr and Ta are also suitable as they dissolve carbon. Extremely careful manipulation of the pressure and temperature conditions is necessary to ensure controlled diamond growth and pressures of ≈100kbar and temperatures of up to 1700K must be maintained despite the changing conditions in the reaction vessel. Diamond, being ≈50% more dense than graphite, occupies a correspondingly smaller volume after the transformation of the source graphite which results in a pressure decrease during reprecipitation.

By varying synthesis parameters, various morphologies and sizes of diamonds, either as single crystals or as polycrystalline aggregates, may be produced, and these are usually used as industrial abrasives for cutting and polishing. The largest synthetic diamond yet grown is a 14.2ct sample of good industrial quality (De Beers Annual Report, 1990). There is purportedly no synthetic gemstone production, although large high quality diamonds may be produced by reconstitution (Wedlake, 1979), in a manner analogous to natural diamond growth. Here the graphite source is replaced with diamond grit to avoid

---

† 1 carat = 200 mg

the problems associated with volume change, and a seed diamond is used as a nucleus to initiate growth. Gem quality synthesis is however very slow with about 5 days being necessary to produce a 1ct diamond free from metal inclusions (Davies, 1984), and as such is considered to be an uneconomic method of producing gem diamonds by the industry.

Another form of synthetic diamond of increasing importance in the diamond industry is produced by various derivatives of chemical vapour deposition (CVD). CVD diamond is grown as a thin film (from a monolayer up to several hundreds of μm thick) on virtually any substrate. Although originally patented in 1962 (Eversole, 1962), diamond growth from a gas phase was first investigated in detail by Derjaguin and Fedoseev (1977), and only recently have growth rates of CVD been sufficiently high to promote industry interest. A review of CVD diamond is provided by Angus and Hayman (1988). CVD as a mechanism for diamond growth may be analogous to shock or explosive diamond synthesis, and recently Lewis *et al.*, (1989) suggested that a growth mechanism analogous to CVD was responsible for the origin of meteoritic diamond.

1.3 THE MANTLE RECORD IN DIAMOND

The conditions in the mantle during diamond growth may be recorded in a number of ways:

- In diamond composition, both by the isotopic composition of the major constituent carbon and by the presence of trace elements within the diamond like nitrogen and the noble gases.
- In minerals and fluids occluded by the diamond during growth. Their effective isolation from their source region by diamond growth prevents re-equilibration in response to changing conditions, and makes such inclusions particularly valuable probes of the mantle and recorders of diamond growth conditions.
- In the form of structural features of the diamond crystal. Diamond growth morphology is dependent on *inter alia* the supply of volatiles (Sunagawa, 1990) while evidence of resorption may indicate periods of increased oxygen fugacity (fO_2). Lattice defects within the crystal will also provide a record of the deformation history of the diamond.

1.3.1 Carbon isotope ratios in the mantle

Carbon, electronic configuration [He] $2s^2,2p^2$, has two stable isotopes; ^{12}C and ^{13}C and the ratio in which these two occur holds important information as to the nature of the diamond source region. Throughout this thesis, this ratio is expressed in conventional

delta (δ) notation in which sample carbon isotope ratios are expressed relative to a standard which in this case is the Pee Dee belemnite (PDB), Belemnitella Americana, which occurs in the Pee Dee formation, South Carolina, U.S.A. Units are per mille (‰).

$$\delta^{13}C\ (‰) = \left(\frac{R_{sample}}{R_{reference}} - 1\right) \times 1000$$

$$\text{and } R = \frac{^{13}C}{^{12}C}$$

The first measurement of the carbon isotope ratio in diamonds was made by Nier and Gulbransen (1939) and yielded a $\delta^{13}C$ value of +0.15‰. This was followed by Craig (1953; $\delta^{13}C$ = -2.4‰ to -7.4‰, n = 6) and by Wickman (1956; $\delta^{13}C$ = -3.2‰ to -9.6‰, n = 37, mean $\delta^{13}C$ = -6.1‰) who rejected a single sample with $\delta^{13}C$ = -13.9‰ as being contaminated with organic matter. These results were similar to the range from carbonatites (*e.g.* Eckermann *et al.*, 1952; Craig, 1953) and thus lead to the conclusion that diamonds and carbonatites sampled the same mantle carbon reservoir; a hypothesis that remained unchallenged until Vinadograv *et al.*, (1966) analysed 4 samples of Brazilian carbonado and found strong ^{13}C depletion with $\delta^{13}C$ value falling between -27.8‰ and -28.4‰. Later, Kovalsky *et al.*, (1972) reported similar very light carbon isotopic composition ($\delta^{13}C$ = -32.3‰) diamonds from the Mir pipe, Siberia and the Ebelyach placer ($\delta^{13}C$ = -21.4 to -22.2‰) and the realisation that some diamonds were not simply equilibrium mantle precipitates but have a more complex origin re-ignited interest in their carbon isotopic composition. A considerable number of diamonds have since been analysed, and a compilation of the most recently available data (Table 1.3) is shown in Figure 1.3. This shows a 37‰ range in $\delta^{13}C$ ($-34.5 \leq \delta^{13}C \leq +2.8$‰), a pronounced negative skewness and a clearly defined mode at $\delta^{13}C$ = -5‰. In addition, a second, smaller but still significant mode occurs near $\delta^{13}C$ = -21‰.

The pronounced mode at $\delta^{13}C$ = -5‰ to -7‰ is close to the $\delta^{13}C$ values measured for many other mantle samples illustrated in Figure 1.4, including Mid Ocean Ridge Basalts (MORB) and Ocean Island Basalts (OIB) (Des Marais and Moore, 1984; Exley *et al.*, 1986b, 1987; Mattey *et al.*, 1989), CO_2 in MORB (Pineau *et al.*, 1976; Pineau and Javoy, 1983), carbonatites (Deines,1970; Deines and Gold, 1973) and kimberlite carbonates (Kirkley *et al.*, 1986). It is also similar to the $\delta^{13}C$ values measured from carbonaceous C1 and enstatite chondrite meteorites (Kerridge, 1985; Grady *et al.*, 1986) and this concentration of the $\delta^{13}C$ values between -5‰ and -7‰ has lead to an acceptance that this is the likely range of primordial mantle carbon isotopic compositions.

Locality	Mean	Median	Max.	Min.	Range	n	References
Angola	-8.1	-6.6	-6.1	-17.9	11.8	15	6
Argyle	-9.8	-10.4	-3.2	-16.0	12.8	190	10
eclogitic	-10.6	-10.9	-5.3	-16.0	10.7	137	10
peridotitic	-6.4	-6.9	-3.2	-9.3	6.1	17	10
Arkansas	-9.0	-5.7	-5.5	-17.0	11.5	5	6
Bultfontein	-6.2	-5.8	-2.5	-9.6	7.1	45	15
Dokolwayo	-5.7	-4.7	-1.6	-22.3	20.7	102	12
eclogitic	-5.9	-4.7	-1.6	-22.3	20.7	74	12
peridotitic	-5.5	-5.2	-3.4	-7.7	4.3	7	12
Ellendale 4	-4.9	-4.9	-3.4	-6.4	3.0	22	10
eclogitic	-4.9	-5.0	-3.8	-6.3	2.5	10	10
peridotitic	-4.8	-4.6	-3.9	-6.4	2.5	8	10
Ellendale 9	-7.1	-6.3	-4.0	-14.4	10.4	21	10
eclogitic	-10.3	-11.1	-7.2	-14.4	7.2	5	10
peridotitic	-5.6	-6.1	-4.0	-6.3	2.3	9	10
Finsch	-5.6	-5.7	-2.6	-8.6	6.0	134	6, 8
eclogitic	-5.1	-4.8	-3.1	-7.9	4.8	11	8
peridotitic	-6.0	-6.2	-2.6	-8.6	6.0	70	8
Jagersfontein	-14.0	-17.0	-3.5	-24.4	19.9	77	6, 13
eclogitic	-17.4	-18.8	-4.5	-24.4	19.9	26	13
peridotitic	-8.1	-6.1	-3.5	-19.1	15.6	14	13
Jwaneng	-9.0	-5.9	-5.0	-21.1	16.1	13	6
Koffiefontein	-5.4	-5.0	-1.8	-12.7	10.9	62	13
eclogitic	-5.5	-5.0	-1.8	-11.8	10.0	20	13
peridotitic	-5.1	-4.8	-2.7	-12.7	9.7	35	13
Lesotho	-15.3	-15.1	-4.6	-20.5	15.9	9	2
Mbuji Mayi	-7.0	-6.9	-3.4	-10.5	7.1	195	6, 3
Orapa aggregates	-12.8	-12.7	-3.8	-23.5	19.7	17	11
eclogitic	-14.0	-14.5	-4.6	-22.6	18.0	10	11
peridotitic	-9.4	-5.8	-3.8	-23.5	19.7	6	11
eclogitic nodule	-7.1	-6.1	-4.0	-22.3	18.3	45	14
Premier	-4.7	-4.7	-0.1	-12.3	12.2	124	6, 4
eclogitic	-4.7	-4.8	-2.5	-12.3	9.8	74	4
peridotitic	-4.7	-4.2	-0.1	-12.2	12.1	35	4
Roberts Victor	-6.28	-5.4	-0.2	-16.3	16.1	99	5
eclogitic	-12.69	-15.5	-4.8	-16.3	11.5	14	5
peridotitic	-5.3	-5.3	-0.2	-7.6	7.5	65	5
sulphide-bearing	-4.9	-5.1	-3.1	-6.2	3.1	20	5
Siberia	-6.58	-6.6	-5.6	-7.4	1.8	4	1
Sierra Leone	-4.3	-4.9	-1.9	-7.4	5.5	29	6
Sloan	-15.6	-17.4	-3.6	-31.4	27.8	167	7
eclogitic	-17.5	-18.4	-8.5	-31.4	22.9	119	7
peridotitic	-6.5	-5.2	-3.6	-20.7	17.1	28	7
Star	-4.3	-4.3	-2.3	-7.2	4.9	57	9
eclogitic	-2.9	-2.9	-2.3	-3.6	1.3	8	9
peridotitic	-4.67	-4.5	-3.4	-7.2	3.8	32	9
harzburgitic	-4.4	-4.3	-4.1	-4.8	0.7	3	9
lherzolitic	-4.7	-4.5	-3.4	-7.2	3.8	29	9
Udachnaya	-6.6	-6.6	-5.9	-7.1	1.2	17	6
Williamson	-4.2	-4.5	-3.3	-4.7	1.4	6	6

Table 1.3: $\delta^{13}C$ values (‰) from a variety of sources. Bultfontein data are all from the same crystal (ion probe analyses). References are: 1 = Kratsov *et al.*, (1977), 2 = Smirnov *et al.*, (1979), 3 = Javoy *et al.*, (1984), 4 = Deines *et al.*, (1984), 5 = Deines *et al.*, (1987), 6 = Boyd, (1988), 7 = Otter, (1989), 8 = Deines *et al.*, (1989), 9 = Hill, (1989), 10 = Jaques *et al.*, (1989), 11 = McCandless *et al.*, (1989), 12 = Daniels (1991), 13 = Deines *et al.*, (1991a), 14 = Deines *et al.*, (1991b) and 15 = Harte and Otter, (1992). Data from this study are not included.

On comparison of Figure 1.3 and 1.4 it is evident that diamonds show a broader spread in $\delta^{13}C$ values than most other mantle-derived samples. Of the over 2000 published diamond analyses, nearly one third fall outside the range $-9‰ < \delta^{13}C \leq -3‰$. However the carbon in some mantle diopsides is ^{13}C depleted, and $\delta^{13}C$ values from back arc basin basalts and many xenoliths recovered from alkali basalts from Hawaii (Pineau and Mathez 1990) also fall outside the -5‰ to -7‰ range expected for samples derived from "normal mantle".

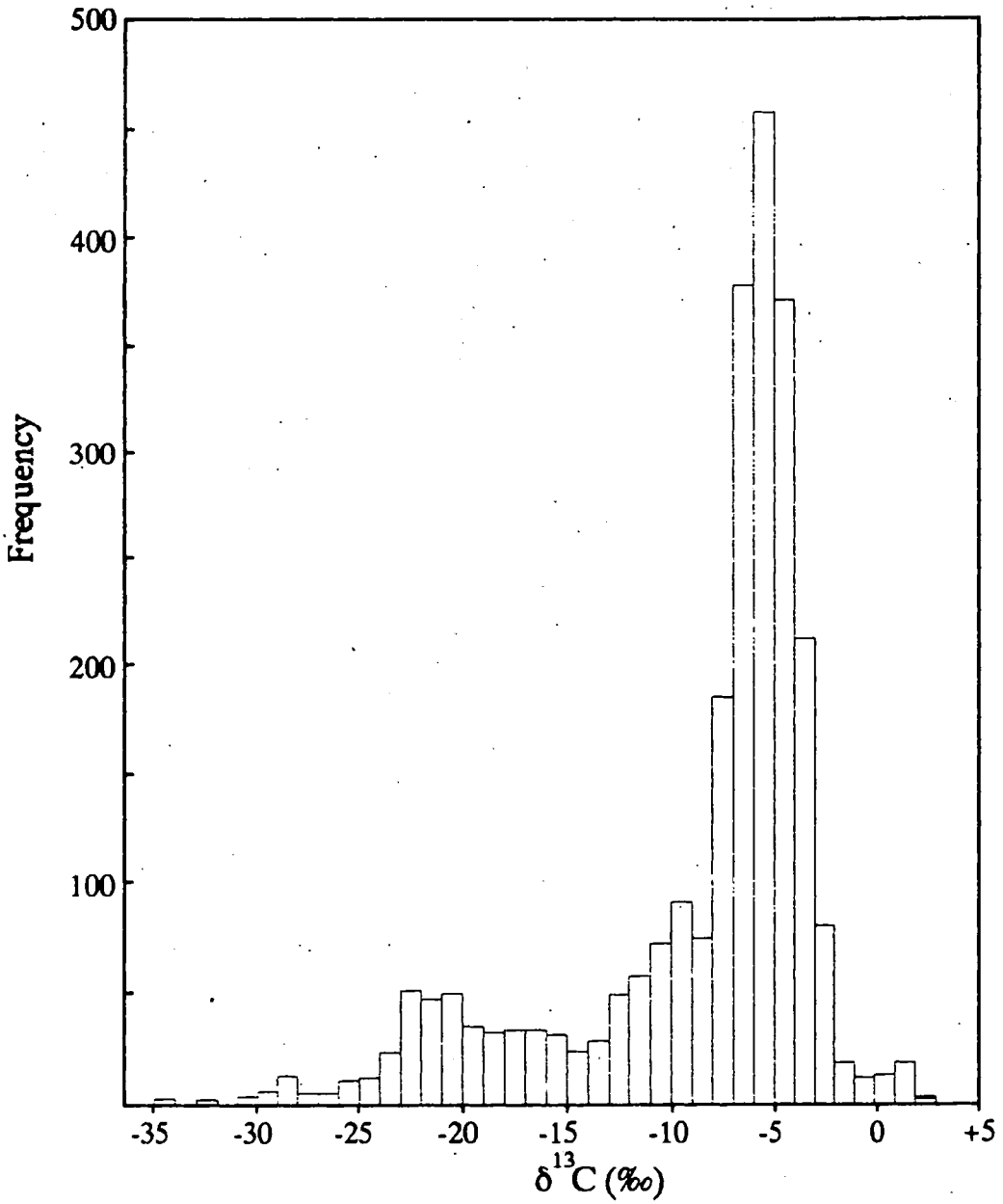

Figure 1.3: Summary histogram of diamond $\delta^{13}C$. Data from Table 1.3 and from Galimov, (1991).

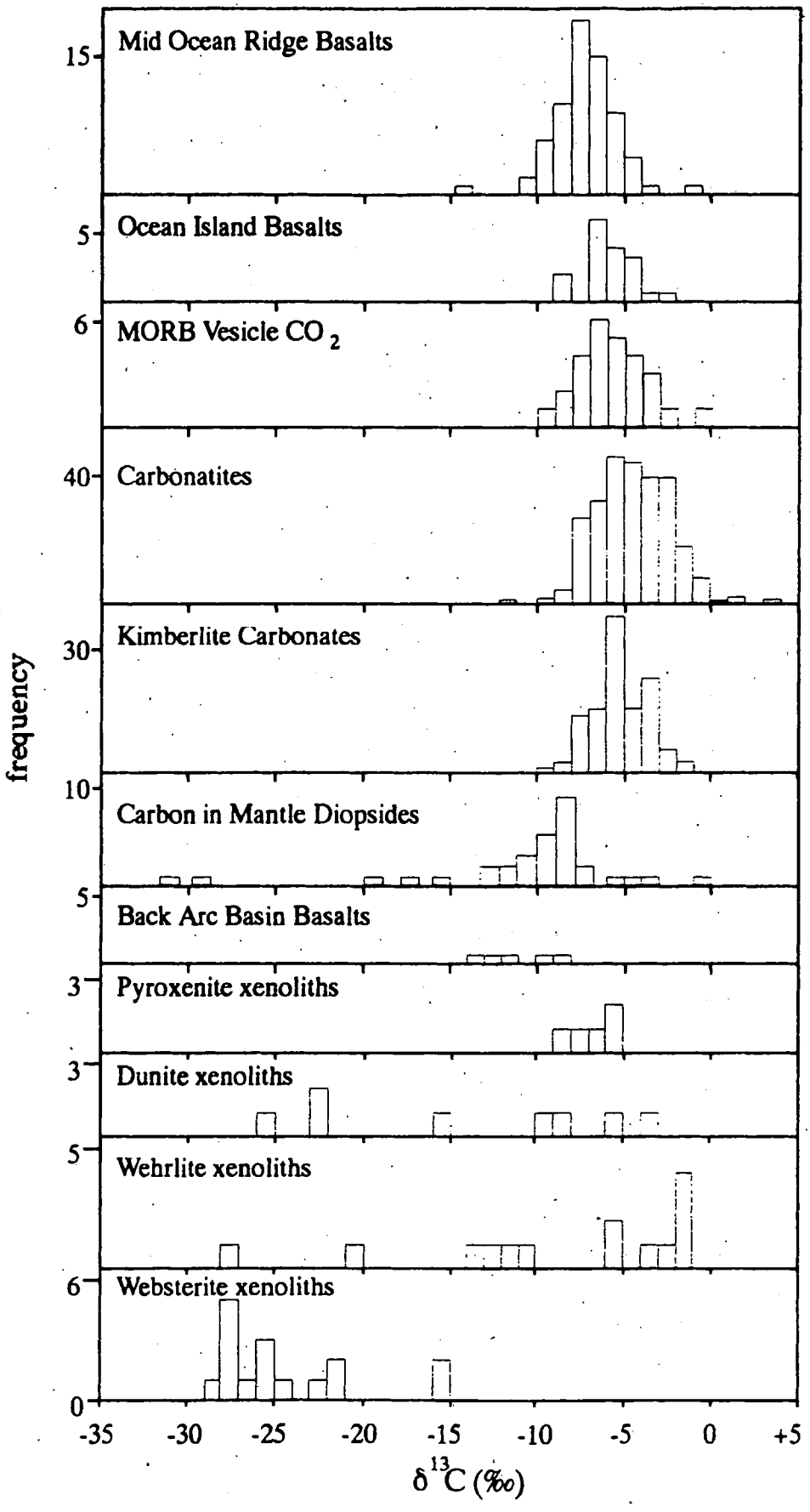

Figure 1.4: Summary histogram of the carbon isotopic composition of mantle derived material. Data from Des Marais and Moore (1984), Exley *et al.*, (1986b), Matley *et al.*, (1989), Pineau *et al.*, (1976), Pineau and Javoy (1983), Deines (1970), Deines and Gold (1973), Pineau and Mathez (1990) and Kirkley *et al.*, (1986).

The cause of this wide range in $\delta^{13}C$ values for diamonds, some mantle-derived xenoliths, diopsides and back-arc basin basalts and particularly the cause of the negative skewness shown by these samples is problematic.

- **Either** the $-7‰ \leq \delta^{13}C \leq -5‰$ range accepted as being characteristic of the normal mantle is too narrow, and this may be resolved by increasing the size of the $\delta^{13}C$ "window", or by interpreting the low temperature, low $\delta^{13}C$ so-called "reduced carbon"† in oceanic rocks as indigenous carbon (*e.g.* Tingle, 1989) rather than organic contamination introduced during sample handling (*e.g.* Mattey *et al.*, 1989)
- **or** primordial mantle with a homogeneous $\delta^{13}C$ value of -7‰ to -5‰ can produce material with more negative $\delta^{13}C$ values. This may be by means of an isotope fractionation process (equilibrium or kinetic) invoving CO_2 and CH_4 or by admixing a very ^{13}C depleted component. Subduction is considered a process that is capable of introducing ^{13}C depleted organic carbon ($\delta^{13}C \leq -25‰$) into the mantle and this possibility is compared with isotopic fractionation processes in Chapter 5.

Oxygen fugacity (fO_2) during diamond growth may significantly control diamond $\delta^{13}C$ values and mantle fO_2 is summarised in section 1.4. A comparison of carbon and nitrogen geochemistry is presented in section 1.4.2.

1.3.2 Trace constituents in diamond

A great number of impurities occur at trace level in diamonds including N, O, H, Sr, B, Mg, Ca, Si, Fe, Al and the noble gases (Raal, 1957; Kaiser and Bond, 1959; Bibby 1982; Hart *et al.*, 1991) and some of these like B and N can significantly affect the physical properties of diamond. Nitrogen is the most abundant impurity in natural diamonds and is discussed in detail in section 1.3.2.2. The presence of B in diamond makes it semiconducting, forming the rare type IIb diamond which has many potential uses in the semiconductor industry. For example, a diamond light-emitting diode

---

† Reduced carbon is carbon with a very negative $\delta^{13}C$ value (usually ≈ -25‰) that is released at temperatures below 600°C during the step heating of basaltic rocks. As it can be minimised by careful sample handling, it has been interpreted as an organic contamination (Des Marais and Moore, 1984; Exley *et al.*, 1986b,1987; Mattey *et al.*, 1989). It has also been interpreted as indigenous carbon fractionated from $\delta^{13}C \approx -7‰$ to $\delta^{13}C \approx -28‰$ by magma degassing (Javoy *et al.*, 1978, 1986). It may also be related to possibly organic, carbonaceous films, condensed on cracks and grain boundaries (Mathez, 1987).

emitting blue light has been produced in prototype (Prins Pers. Comm., 1991) and diamond is the only semiconductor to emit in the blue region of the visible spectrum.

Of all the trace constituents in diamond, nitrogen and the noble gases are at present of the greatest value for the geochemist attempting to understand the evolution of the mantle because they are (relatively) easy to analyse and are thought to have concentrated in the atmosphere by simple degassing of the mantle (See Ozima, 1989 for a review). Oxygen in diamond is also of potential use in that the mantle geochemistry of oxygen is currently under investigation (Kyser 1986, 1990; Deines *et al.*, 1991b), and bound oxygen exists in silicate and carbonate material inclusions in diamond. Trace oxygen in diamonds has also been detected by in-situ nuclear techniques (Blacic *et al.*, 1991), but it is not clear whether this is associated with micro-inclusions or is substituting for carbon in the diamond lattice.

1.3.2.1 Noble gases in diamond

The noble gases, particularly He and Ar are the most investigated trace constituents of diamond and they are useful to this study because they may place constraints on the behaviour of nitrogen. The mantle geochemistry of nitrogen is still poorly understood, however if it exists as N_2, its behaviour may be very similar to the very unreactive noble gases (Ozima, 1989).

Geochemical studies of noble gases from diamond have undergone a dual approach:

- One concerned with the dating of diamond. K-Ar, as measured by the isotopes ^{40}Ar - ^{39}Ar are most important here and
- One concerned with the identification of the primordial sources of of the various components of the Earth. These "whole-earth" geochemical approaches utilise the distinctive isotope ratios of solar, atmospheric and planetary components of many of the noble gases.

The potential for noble gas dating of diamonds was noted by Ozima *et al.*, (1983) who examined the $^3He/^4He$ ratios in diamond and found these to be anomalously high. It was suggested that the lack of U or Th in the diamond was responsible for the lack of fractionation of the primordial $^3He/^4He$ ratio and as this was very similar to the solar $^3He/^4He$ ratio it indicated an age for the diamonds close to the age of the Earth. A less contentious radiometric dating technique was applied by Zashu *et al.*, (1986) who generated a K - Ar isochron for Zaire cubic diamond, however these indicated a diamond age of 6.0 ± 0.3 Ga; an age apparently confirmed by Ozima *et al.*, (1989) using ^{40}Ar - ^{39}Ar data. This age, greater than that of the Earth, has been shown (Masuda and Akagi, 1988; Podosek *et al.*, 1988) to result from an excess of ^{40}Ar in the diamond, which effectively precludes diamond dating by noble gas methods. Podosek *et al.*,

(1988) showed that spallation was not likely to be the cause of this excess Ar and instead they speculated on the presence of a ^{40}Ar and K enriched fluid phase, while Masuda and Akagi (1988) preferred a model in which ^{40}Ar was preferentially fixed into the diamond during growth. The excess ^{40}Ar also correlates with Cl (Ozima, 1989) and Turner *et al.*, (1990) have proved the existence of a widespread Cl-rich component trapped in diamond coat, in which both ^{40}Ar and Cl are enriched by almost 4 orders of magnitude relative to the bulk upper mantle. Highly volatile enriched, potassic and chlorine rich fluids have been reported in fluid micro-inclusions in the coat of coated diamonds (Navon *et al.*, 1988; see section 1.3.3.2) and it is likely that the excess ^{40}Ar also occurs in such an environment (Ozima *et al.*, 1989) which supports the Podosek *et al.*, (1988) hypothesis.

In addition to the anomalously high $^{3}He/^{4}He$ ratios reported by Ozima *et al.*, (1983), anomalous $^{20}Ne/^{22}Ne$ and $^{129}Xe/^{130}Xe$ ratios have been reported in diamond (Honda *et al.*, 1987) and in both cases, the measured ratio in diamonds is greater than the atmospheric or planetary ratio. Unlike ^{4}He, neither ^{129}Xe nor ^{20}Ne or ^{22}Ne can be produced by terrestrial nuclear reactions and these ratios in diamonds are therefore most likely to be primordial (Ozima, 1989).

Comparison of the isotopic balance between the early Earth (from diamond samples), the modern mantle as sampled by MORB or similar rocks and the atmosphere may place constraints on planetary degassing and atmosphere evolution. Helium isotope systematics may also be useful in this respect although cognizance must be taken of the fractionation of $^{3}He/^{4}He$ by the implantation of radiogenic α particles derived from the decay of U series elements (Lal, 1989).

Additional useful constraints on nitrogen behaviour may be placed by noble gas diffusivity data (See Ozima, 1989 for a review), as nitrogen in diamonds may behave in a similar manner to the lighter noble gases (Ozima, 1989). Data for He and Ar are presented by Ozima (1989) who suggests that at mantle temperatures an approximately 0.3 mm diamond would require about 10^{9} and 10^{13} years to degas He and Ar respectively. This very slow rate of diffusion would seem to imply at least equally slow diffusion of nitrogen and this is discussed further in section 1.3.2.2.

1.3.2.2 Nitrogen in diamond

Nitrogen has been shown to be the major substitutional impurity in diamond (Kaiser and Bond, 1959) where it occurs at concentrations of up to 5000 atomic ppm (Bibby, 1982). It is analysed either spectroscopically where infrared absorption is a function of total nitrogen content, or by mass spectrometry, and there have been several geologically oriented studies using either method. These are reviewed later in this section. The highest nitrogen abundance yet directly measured by mass spectrometry is 4438 ppm (by

weight), reported in this study, but concentrations of nitrogen in diamond of less than 1000 wt. ppm are more common (Harris and Spear, 1986).

The presence of a nitrogen impurity controls several important physical characteristics of the diamond. For example
- infrared (I.R.) absorption characteristics
- colour in certain circumstances†
- thermal conductivity‡

Of these, infrared absorption characteristics are perhaps the most diagnostic. All diamonds absorb strongly in the infrared between 3μm and 6μm, and Robertson *et al.*, (1934) reported that some diamonds had additional absorption bands between 6μm and 13μm, whereas other diamonds are characterised by an ultraviolet absorption edge below 0.225μm. The former are termed type I and and the latter type II diamonds respectively (Robertson *et al.*, 1934). Kaiser and Bond (1959) later went on to show that type I diamonds were characterised by the presence of a nitrogen impurity, while type II diamonds are essentially nitrogen free. Kaiser and Bond (1959) also showed that the nitrogen occupied a substitutional site in the lattice although they were unable to deduce the structure of the defect. In addition, they showed that the the I.R. absorptions between 3μm and 6μm were the diamond lattice bands.

As well as determining diamond type, N is one of the Earth's major volatile components (*e.g.* Becker, 1982; Ozima, 1989) and the high concentration of nitrogen in diamond is valuable for constraining mantle nitrogen. This is of vital importance if the Earth's evolution, and particularly the degassing of the early Earth and formation of the atmosphere are to be properly understood.

Since nitrogen has such a significant affect on the properties of diamond, considerable attention has been paid to understanding the structure of the nitrogen-bearing defects. In particular the infrared absorption spectra in the 6μm to 13μm region have been examined in detail. This spectral region shows several different absorption bands for different nitrogen defect structures (Figure 1.5) and in future these will be referred to by wavenumber (reciprocal wavelength in cm), in line with common practise in infrared spectrometry. Two major types of N defect structure are recognised in diamond. One is paramagnetic, indicating the presence of an unpaired electron in the crystal lattice and

---

† Diamonds with an odd number of nitrogen atoms in the defect (type Ib diamond and diamond with N3 centres) are characterised by a canary yellow colour.

‡ As nitrogen content decreases, thermal conductivity increases. The material with the highest known thermal conductivity is pure type IIa (nitrogen free, boron free) diamond.

implying an odd number of nitrogen atoms in the defect and the most common of this type is the Ib defect (infrared absorption spectrum shown in Figure 1.5). The other major defect type is not paramagnetic and these are referred to as type Ia. Type Ia defects can be further subdivided into type IaA and type IaB (Sutherland *et al.*, 1954) on the basis of differences in the infrared absorption spectra (*e.g.* Woods, 1985; Woods *et al.*, 1990) and these are illustrated in Figure 1.5.

The simplest type of nitrogen defect - type Ib is very common in synthetically produced diamonds, but is rare in nature and comprises a single substitutional nitrogen atom replacing a carbon atom in the diamond lattice (Smith *et al.*, 1959). Type Ia defects in contrast comprise more complex nitrogen structures. The type IaA defect was shown by Davies (1976) to consist of two mutually bonded nitrogen atoms on adjacent lattice sites while the currently accepted structure of the IaB defect is a cluster of 4 nitrogen atoms plus a vacancy (van Tendeloo *et al.*, 1990). Diamonds are usually classified by the type of nitrogen defect which they contain and type IaA diamonds are the most commonly occurring natural samples. Only amongst diamonds from the Argyle lamproite do type IaB samples outnumber type IaA diamonds (Harris and Collins, 1985). Diamonds containing both IaA and IaB nitrogen defects do occur and these are termed type IaAB and an example of the type IaAB FTIR absorption spectra is shown in Figure 1.5. The major absorbance bands of diamond are listed in Table 1.4.

Type IaA	Type IaB
1282	1426
1203	1332
1093	1171
480	1003
	780
	328

Table 1.4: Characteristic absorbance bands of type IaA and type IaB diamonds expressed as wavenumbers (cm^{-1}). From Sutherland *et al.*, (1954) and Clackson *et al.*, (1990).

In addition to the major nitrogen defects that type diamond, nitrogen can occur in N3 centres which are believed to consist of 3 nitrogen atoms in the {111} plane (Loubser and Wright, 1973; Davies *et al.*, 1978) plus a vacancy (van Wyk, 1982). N3 centres do not give an infrared absorption but do absorb in the ultraviolet at wavenumber 24000 cm^{-1} and are often associated with diamonds of a pronounced yellow colour (Harris, 1987).

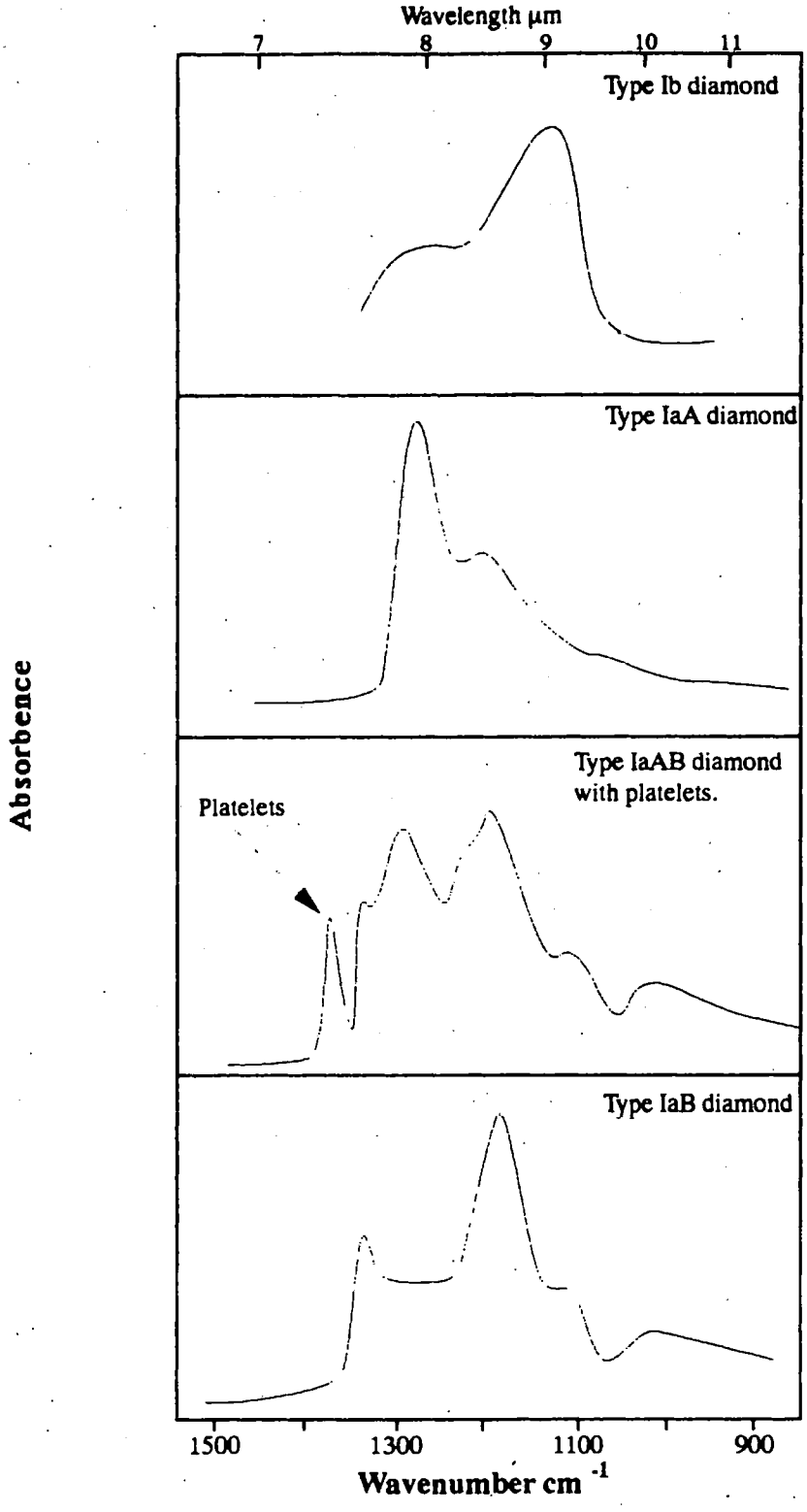

Figure 1.5: Fourier transform infrared spectra (FTIR) for type I diamond. Wavenumber = 1/wavelength in cm. After Davies (1984).

Nitrogen has also been implicated in platelets. These are planar structures lying in the {100} lattice planes of diamond and vary in diameter from 50 to 1000 atoms but are always close to 1 atom thick. These features, first identified by Evans and Phaal (1962) are believed to give rise to a characteristic absorption in the infrared at ≈1372 cm^{-1} (Clackson *et al.*, 1990), but there is still considerable controversy over their precise

structure and chemistry and particularly whether they are intimately associated with aggregated nitrogen (Lang, 1964; Allan and Evans, 1981; Berger and Pennycook, 1982). Platelets never occur in type Ib or type II diamond, but for samples termed "regular" there is a direct correlation between platelets and the B-aggregate (Woods, 1985). However, samples termed "irregular", with B-feature nitrogen but no platelet development, also exist (Woods, 1985). For the purpose of this thesis, platelets are assumed to contain negligible amounts of nitrogen.

"Voidites" may also contain nitrogen. These are linear agglomerates of low density octahedral structures lying in {100} planes (Hirsch *et al.*, 1986a). They may be a transformation feature of platelets (Hirsch *et al.*, 1986b), but like platelets, they are still poorly understood and may form from a process independent of platelet degradation (van Tendeloo *et al.*, 1990). Nitrogen has been implicated in voidites, possibly occurring as a metallic ammonia phase (Hirsch *et al.*, 1986a). As with platelets, they are assumed to contain negligible amounts of nitrogen for the purpose of this study.

The various nitrogen defects are related to one another by diffusion (Chrenko *et al.*, 1977; Evans and Qi, 1982) and Chrenko *et al.*, (1977) experimentally showed that type Ib diamond could be transformed into type IaA diamonds by a coalescing of the singly substitutional nitrogen atoms. Where sufficient transformation occurred, N3 centres were produced and the aggregation reaction was shown to follow second order kinetics:

$$\frac{1}{C} - \frac{1}{C_0} = k.t \qquad (1.1)$$

where C = concentration of Ib nitrogen at time t
C_0 = initial concentration of Ib nitrogen
t = time (seconds)
k = rate constant, units of $time^{-1}.concentration^{-1}$

The rate constant (k) is related to the activation energy by the Arrhenius equation:

$$k = A \exp^{(-E/RT)} \qquad (1.2)$$

where A = a constant pre-exponential, units of concentration per unit time
E = activation energy (J)
R = gas constant (8.31441 $J.K^{-1}.mol^{-1}$)
T = temperature (K)

Later experimental work (Allan and Evans, 1981) showed that IaB defects (also known as B-centres) could be produced by the aggregation of IaA defects (A-centres) and the kinetics of nitrogen aggregation were experimentally investigated by Evans *et al.*, (1981) and Evans and Qi (1982). A compilation of their, and other experimentally determined, activation energies for nitrogen aggregation are presented in Table 1.5. The activation energy of He and Ar diffusion are shown for comparison.

Transformation	Author	Activation energy	Note
Ib to IaA	Chrenko *et al.*, (1977)	251 kJ.mol^{-1}	
	Collins (1978, 1980)	Not given	Enhanced by ≈ 50 x
	Evans and Qi (1982)	482 kJ.mol^{-1}	
IaA to IaB	Evans and Qi (1982)	627 to 733 kJ.mol^{-1}	
	Evans and Harris (1989)	659 kJ.mol^{-1}	
	Cooper *et al.*, (1989)	800 kJ.mol^{-1}	
	Taylor *et al.*, (1990)	679 kJ.mol^{-1}	Australian samples
He and Ar diffusion	Ozima (1989)	1000 to 2000 kJ.mol^{-1}	

Table 1.5: Experimentally determined activation energies for nitrogen aggregation. Results marked "enhanced" are from diamonds that have been subjected to irradiation by high energy electrons. This creates vacancies in the lattice, facilitating the migration of nitrogen atoms (Collins, 1980) effectively decreasing the activation energy.

The low activation energy of the Ib to IaA transformation is probably responsible for the scarcity of natural type Ib diamonds. It can be calculated that even in a relatively cool mantle, N in Ib defects will aggregate to form type IaA diamonds in times that are short on a geological time scale (410 years for 500 ppm N to aggregate from type Ib to 99.9% type IaA defects at 1000°C). Activation energies for the formation of the larger nitrogen defects are however higher (Table 1.5) which accounts for the relative scarcity of type IaB diamonds.

The difference between N aggregation activation energy and those experimentally determined for noble gas diffusion may be a result of the bond extension associated with the substitution of a N atom into the carbon lattice (see Table 1.1). This bond extension will raise the overall energy of the system and its reduction may be a driving force for nitrogen diffusion and thus nitrogen aggregation.

From a knowledge of activation energy, temperature and time it should be possible to investigate diamond growth histories. There are however large uncertainties associated with this type of study. Data are at present scarce and the precision required for quantitative results is lacking (Evans and Harris, 1989). For example, calculated aggregation times are very dependent on temperature, yet seldom are geothermometric results quoted to better than 50°C. The effect of a 50°C uncertainty in temperature is illustrated in Table 1.6.

In addition, some diamonds are thought to have had an aggregation history different from the relatively simple, experimentally determined sequence of Ib → IaA → IaAB → IaB. These are termed irregular diamonds,and they are characterised by the catastrophic degradation of platelets (Woods, 1985). Here the assumption of second order kinetics

may not be valid. Furthermore, aggregation rates of N in diamonds have been experimentally enhanced by irradiation with high energy electrons which damages the diamond lattice (Collins, 1978, 1980) and it is likely that deformation in the diamond source region has a similar effect, with an associated enhancement of aggregation rate (Harris, Pers. Comm.). These problems are addressed with reference to diamonds from Argyle and Ellendale in Chapter 2, but preliminary indications are that growth times calculated on the basis of nitrogen aggregation state are likely to be of limited quantitative value. In single zoned diamonds however, ages calculated from the nitrogen aggregation state may provide a qualitative indication of the diamond's growth history and examples from Argyle and Ellendale are also presented in Chapter 2.

Temperature °C	Rate constant k	Aggregation time in Ma
1150	5.57518×10^{-14}	97
1160	8.31778×10^{-14}	65
1170	1.23409×10^{-13}	44
1180	1.82108×10^{-13}	30
1190	2.67302×10^{-13}	20
1200	3.90311×10^{-13}	14

Table 1.6: The effect of temperature on aggregation time. Calculations are for 1000 ppm N, initially in the IaA form aggregating to 25% IaB aggregates. An activation energy of 679 $kJ.mol^{-1}$ (7.03 eV) and a pre-exponential of 4.41×10^{11} $at.\%.min^{-1}$ have been assumed (Taylor *et al.*, 1990). It is evident that a 50°C rise in temperature can result in almost an order of magnitude decrease an aggregation time.

This thesis is particularly concerned with nitrogen content and nitrogen isotope ratios in diamond, and previously published work will be discussed in more detail in later chapters, however a brief summary of recent work is presented here.

1.3.2.2.1 Geological studies of the nitrogen content of natural diamond

Although the presence of nitrogen in diamonds has been known since the work of Kaiser and Bond (1959) and it was suggested as early as 1962 that nitrogen was incorporated in diamond during, rather than subsequent to, growth (Milledge and Meyer, 1962), it is only recently that systematic geochemical studies of the nitrogen content of natural diamonds have been undertaken. The first of these studies was that of Becker (1982), who reported nitrogen concentrations of 500 to 2000 ppm, and similar nitrogen concentrations were determined by Javoy *et al.*, (1984) for a suite of diamonds from Mbuji Mayi, Zaire. Javoy *et al.*, (1984) also reported an association between nitrogen content and nitrogen aggregation state, with type IaA diamonds usually having a higher nitrogen content than coexisting type IaB diamonds. This has subsequently been reported for Roberts Victor, Jagersfontein and Koffiefontein diamonds (Deines *et al.*, 1987, 1991a) and may be appropriate for Argyle diamonds which are characterised by

low nitrogen content and by high degrees of nitrogen aggregation (Harris and Collins, 1985).

Harris and Spear (1986) examined the relationship between nitrogen content and diamond paragenesis and showed that eclogitic diamonds were usually type I diamonds whereas type II diamonds were usually of peridotitic paragenesis, but they also pointed out that this was not a general rule as diamonds from both the Roberts Victor and Jagersfontein kimberlites did not adhere to it. They also showed that the histogram of diamond nitrogen content was positively skewed and that, once again, there were exceptions to this observation. Harris and Spear (1986) did not confirm any general relationship between nitrogen content and aggregation state, and nor did they find any difference between the ranges of nitrogen content for diamonds of eclogitic or peridotitic paragenesis. Similar results were obtained by Deines *et al.*, (1987) for Roberts Victor diamonds, although in this case they found that in peridotitic paragenesis diamonds only, did type IaB diamonds have lower nitrogen contents than type IaA diamonds. Deines *et al.*, (1987) also suggest that different regions of the mantle are characterised by different nitrogen contents.

The first significant differences in the nitrogen contents of eclogitic and peridotitic diamonds were reported by Deines *et al.*, (1989) for FTIR analysis of the nitrogen contents of diamonds from the Finsch and Premier mines. They, like Harris and Spear (1986) noted that eclogitic paragenesis diamonds were usually type I diamonds, and they reported a significantly higher mean nitrogen content for eclogitic paragenesis diamonds than for peridotitic paragenesis diamonds. A possible relationship between nitrogen content and $\delta^{13}C$ value is shown for certain samples characterised by variable $\delta^{13}C$ and by elevated nitrogen contents, and Deines *et al.*, (1989) interpret the different $\delta^{13}C$ and nitrogen contents of different groups of diamonds as resulting from different formation environments for each group.

Unlike Deines *et al.*, (1989), Taylor *et al.*, (1990) did not find nitrogen content to be a reliable discriminant of eclogitic and peridotitic paragenesis in a study of diamonds from Western Australia and elsewhere. They did, however, ascribe different nitrogen contents in different groups of diamonds to a heterogeneous source region, and suggested that, in certain cases, eclogitic diamonds with high nitrogen content may record the incorporation of sediment-derived nitrogen into the diamond source region. Deines *et al.*, (1991b), in an examination of diamonds from Orapa, however concluded that high nitrogen contents in eclogitic diamonds were not consistent with the expected loss of nitrogen during subduction-related metamorphism. The fate of nitrogen during subduction is still a contentious issue and is discussed in Chapter 6.

Deines *et al.*, (1991a) examined diamonds that are thought to have a deep origin, from the Jagersfontein and Koffiefontein mines. They report higher nitrogen contents in eclogitic paragenesis diamonds than in peridotite paragenesis diamonds from these localities and show that, as at Finsch, Orapa and Premier, type II diamonds from Koffiefontein are more commonly of peridotitic than of eclogitic paragenesis. The opposite however holds for Jagersfontein diamonds where type II diamonds are more commonly eclogitic. Deines *et al.*, (1991a) do not find a general relationship between nitrogen aggregation state and nitrogen content, but they do report that aggregated diamonds tend to low nitrogen contents and and are often associated with a ^{13}C depletion, and they suggest that low nitrogen contents may be a characteristic of diamonds with larger than usual depths of origin (*i.e.* asthenospheric diamonds).

From the above summary, it is evident that caution must be exercised when drawing general conclusions as to the relationships between nitrogen content, aggregation state and diamond paragenesis, that are independent of diamond provenance. The likelihood of multiple diamond sources existing, each having their own characteristic nitrogen content, thermal history (and hence proportion of nitrogen in B-aggregates) and carbon isotopic composition is high indeed! To quote Deines *et al.*, (1987): "Only through very detailed sample characterization will one be able to ascertain which minerals may have had a common origin and may be considered jointly".

1.3.2.2.2 Previous studies of nitrogen stable isotope ratios in natural diamonds

The first analysis of the isotopic composition of nitrogen in diamond were published by Wand *et al.*, (1980) in an attempt to constrain the origin and evolution of the Earth and particularly the role of mantle volatiles, in the formation of the Earth's atmosphere. These results indicated that diamonds were enriched in ^{15}N relative to the atmosphere by $\approx$1.5‰ *i.e.* they had a mean nitrogen isotopic composition of $\delta^{15}N = +1.5‰$. Similar results were obtained by Becker (1982) who also suggested that the mantle contained enough nitrogen to make its isotopic composition relevant to that of the bulk earth. The $\delta^{15}N$ values measured on 5 diamonds by Becker (1982) ranged from $0.0‰ \leq \delta^{15}N \leq +5‰$ and there was some variability, but in general, diamonds appeared to be less enriched in ^{15}N than igneous rocks of mantle affinity (*e.g.*, Becker and Clayton, 1977).

The results published by Wand *et al.*, (1980) and by Becker (1982) were both limited by the large amount of sample required, and by a lack of constraint as to diamond source. Diamonds are now known to be heterogeneous on a very fine scale (*e.g.* Boyd *et al.*, 1987) and much of the variation can be missed if too large a piece of diamond is analysed. These problems were surmounted to some extent, by Javoy *et al.*, (1984) who examined a suite of diamonds from a restricted area - Mbuji Mayi, Zaire, and included several analyses from each diamond. They could not however assign

individual samples to particular dykes or kimberlites, or individual fragments to a specific region of each sample diamond. Javoy *et al.*, (1984) showed that the mantle was probably ^{15}N depleted, with $\delta^{15}N \leq -11‰$ and that diamonds preserved evidence for isotopic mixing or fractionation processes, resulting in most having $\delta^{15}N$ values of up to 0‰. They did however report a single diamond with a positive $\delta^{15}N$ (+5.5‰) value. From these results, Javoy *et al.*, (1984) concluded that enstatite chondrites with their negative $\delta^{15}N$ values were a more likely mantle analogue than the ordinary chondrites; a suggestion incidentally supported by enstatite chondrites having oxygen isotope ratios that fall on the terrestrial fractionation line on a plot of $\delta^{17}O$ *vs.* $\delta^{18}O$ (*e.g.* Wasson, 1985).

Boyd *et al.*, (1987, 1992) and Boyd (1988) examined nitrogen isotopic composition (along with $\delta^{13}C$, nitrogen concentration and nitrogen aggregation state) on small portions of diamonds (micrograms rather than milligrams) from a wide variety of sources, and found a wide range in $\delta^{15}N$ values (-12.8‰ to +12.1‰). However in the case of "coat" on coated stones, regardless of the source of the samples, the $\delta^{15}N$ range was more restricted, falling between -8.7‰ and -1.7‰. As $\delta^{13}C$ values measured on coat ($\delta^{13}C$ = -7.2‰ to -4.1‰) fall within, or close to, the range accepted for normal mantle, Boyd *et al.*, (1987, 1992) interpreted these coats as having grown around pre-existing diamond cores from volatile rich fluids that were originally of asthenospheric origin. They also speculate that these fluids may have been related to kimberlite emplacement and that coat therefore represents a phenocrystal overgrowth around a xenocrystal core. If the isotopic characteristics of coat are indeed characteristic of normal (pristine, well mixed and primordial) mantle then these results are indicative of a mantle depleted in ^{15}N relative to the atmosphere (*i.e.* negative $\delta^{15}N$). This is in accord with the results of Javoy *et al.*, (1984, 1986) and Javoy and Pineau (1986) but apparently contradictory to the very limited results of Wand *et al.*, (1980) and Becker (1982), both of whom report a ^{15}N enrichment in the mantle relative to the atmosphere.

Comparative $\delta^{15}N$ data from other mantle sources is scarce, but available data is summarised in Figure 1.6. From this it is evident that if a ^{15}N depleted (negative $\delta^{15}N$) early mantle is assumed (*e.g.* Javoy *et al.*, 1986; Boyd *et al.*, 1987, 1992) then simple nitrogen degassing cannot have produced the atmosphere ($\delta^{15}N$ = 0‰) leaving a MORB residue with positive $\delta^{15}N$. This isotopic imbalance was noted by Javoy *et al.*, (1984) and discussed by Javoy *et al.*, (1986) who proposed a heterogeneous model for the accretion of the Earth in which an enstatite chondrite mantle overlain by a veneer of ^{15}N enriched carbonaceous chondrite material, but other models, for example the loss of atmospheric nitrogen by "evaporation" may also explain this isotopic imbalance. These are discussed in detail in Chapter 6.

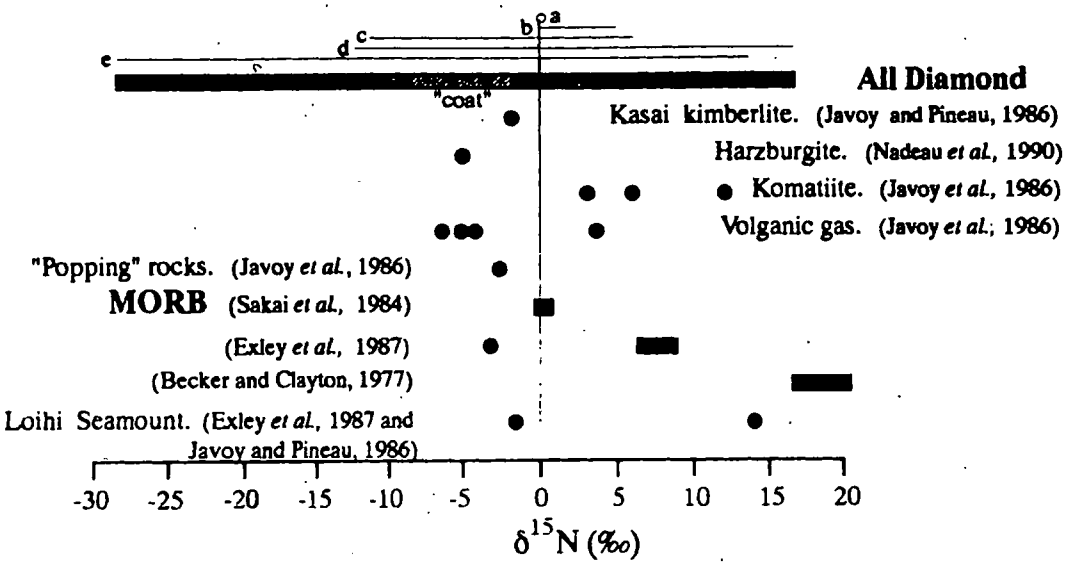

Figure 1.6: Available $\delta^{15}N$ data for mantle derived material. Air is defined as having $\delta^{15}N$ of 0‰ and is shown by the vertical bar. Dots represent individual measurements and ranges are shown by boxes. Diamond data from (a) Wand *et al.*, (1980), (b) Becker (1982), (c) Javoy *et al.*, (1984), (d) Boyd *et al.*, (1987, 1992), (d) Boyd (1988) and (e) this study. Diamond coat is shown by the hashured area.

Excluding this study, there are $\delta^{15}N$ data available for 109 diamonds (Table 1.7), and it is clear that for a systematic study of mantle-derived nitrogen more data are required. This is particularly necessary if the origin and evolution of the Earth's atmosphere is to be understood. Deines and co-workers (Deines *et al.*, 1987, 1989, 1991a, 1991b) are undertaking systematic investigations on diamonds, including nitrogen analysis, from a variety of southern African kimberlites (Orapa, Finsch, Premier, Jagersfontein, Koffiefontein) and Boyd *et al.*, (1987, 1992) examined African and Australian diamonds. This study concentrates on diamonds from Western Australia, and particularly from the Argyle and Ellendale lamproite pipes. Slowly the data necessary for understanding mantle nitrogen are accumulating.

Author		No. of diamonds studied	No. of analyses
Becker (1982)		5	5
Javoy *et al.*, (1984)		9	44
Boyd (1988)	Ladder sections	17	143
	Single diamonds	78	123
		109	315
This study	Ladder sections	10	90
	Single stones	161	169
		171	259
Totals, including this study		280	574

Table 1.7: Number of diamonds for which $\delta^{15}N$ data are available, by author. The Boyd (1988) data is also partially presented in Boyd *et al.*, (1987, 1992). As no data are available for the individual diamonds analysed by Wand *et al.*, (1980), they are not included in this compilation.

1.3.3 Inclusions in diamond

As well as incorporating trace elements, diamonds may occlude larger impurities in the form of mineral or fluid inclusions. These inclusions have usually been effectively isolated from the growth environment by being trapped within the solid diamond; the strength and chemical inertness of which ensures that they do not re-equilibrate in response to changing pressure or temperature conditions or to metasomatic events. This in effect, ensures that such inclusions provide a pristine record of mantle chemistry which makes them invaluable for earth scientists attempting to understand the mantle.

1.3.3.1 Mineral inclusions in diamond

Silicates, sulphides, oxides, metallic Fe and diamond have all been identified as mineral inclusions in diamond (Meyer, 1987). Silicate inclusions are associated with two main parageneses, eclogitic and peridotitic (sometimes referred to as basic and ultrabasic) and these have distinctive chemistry (Meyer, 1987; Gurney, 1989; McCandless and Gurney, 1989) and mineralogy (see Table 1.8). The peridotitic parageneses may be sub-divided and inclusions may have compositions characteristic of either harzburgite or lherzolite (Richardson *et al.*, 1993). A websteritic paragenesis, with compositions that are transitional between eclogitic and peridotitic parageneses inclusions has also been reported to occur at Orapa, Botswana (Gurney *et al.*, 1984; Deines *et al.*, 1993).

Peridotitic	Eclogitic	Uncertain	Epigenetic
Forsterite	**Omphacite**	Phlogopite	Serpentine
Enstatite	**Pyrope - Almandine**	Biotite	Calcite
Diopside	Kyanite	Muscovite	Graphite
Cr-pyrope	Sanadine	Amphibole	Haematite
Cr-Spinel	Coesite	Magnetite	Acmite
Mg-ilmenite	Rutile	Apatite	Richterite
Mg-wustite	Ruby	Ferro-periclase	Perovskite
Sulphides	Ilmenite	Moissanite	Mn-ilmenite
Zircon	Chromite		Spinel
Native Fe	Diamond		Sellaite
Diamond	**Sulphides**		Xenotine
	Corundum		Goetite
	Zircon		Kaolinite
	Mica		

Table 1.8: Mineral species found as inclusions within diamond. The most abundant are printed in bold type.

Sulphide inclusions occur in association with both eclogite and peridotite paragenesis inclusions and may be the most common syngenetic mineral inclusion in diamond (Gurney, Pers. Comm.). In Siberian diamonds, sulphide Ni content can be used to differentiate between eclogitic and peridotitic parageneses (Sobolev 1984), however their association is not usually defined in many diamonds in which they form the sole

inclusion type (Gurney, 1989). Meyer (1987) has suggested that sulphides may form a third paragenesis on their own, although this is not widely accepted.

The chemical differences between eclogitic and peridotitic paragenesis diamonds extend to their carbon isotopic composition (Sobolev *et al.*, 1979) *viz.* diamonds with peridotite paragenesis inclusions tend to have carbon isotopic composition similar to that reported for "normal mantle" *i.e.* $\delta^{13}C$ values clustering around -5‰. Eclogitic paragenesis diamonds in contrast, show a wider range in $\delta^{13}C$ values (-35‰ to +2‰), although they still have a (smaller) mode at $\delta^{13}C$ = -5‰. Differences in the nitrogen isotopic ratios of eclogitic and peridotitic paragenesis diamonds have not been reported previously. The relationships between diamond paragenesis and carbon and nitrogen stable isotope ratios are discussed in more detail in later chapters, with reference to Australian diamonds.

Both peridotite and eclogite paragenesis inclusions occur in all kimberlites (Gurney 1989) but the eclogite:peridotite ratio is highly variable. At Argyle more than 75% of inclusions are eclogitic (Harris and Collins, 1985) while in the Ellendale lamproites, eclogitic and peridotitic paragenesis inclusions occur in approximately equal proportions (Jaques *et al.*, 1986b). There is also no correlation between the dominant inclusion paragenesis and the most abundant xenolith type. Indeed, at some mines (*e.g.* Roberts Victor) peridotite inclusion bearing diamonds predominate, although eclogitic xenoliths are more common (Harris, Pers. Comm. and Gurney, 1989).

In general, discrete mineral grains trapped within diamonds are in chemical equilibrium with each other (Gurney, 1989) but this is not always the case, particularly when central inclusions in larger diamonds are compared with inclusions towards the margins of the host crystals, and the most dramatic examples of disequilibrium are eclogitic (Gurney, 1989). Examples of diamonds containing both peridotitic and eclogitic inclusions are very rare but do occur (Hall and Smith, 1984; Gurney, 1989) and along with disequilibrium inclusion assemblages, indicate slow or multi-stage diamond growth in a changing growth environment.

Equilibrium pairs of mineral inclusions are particularly useful in estimating diamond equilibration conditions. Most peridotitic inclusions formed in the diamond stability field close to the ambient geotherm and peridotite solidus (Figure 1.7) at pressures corresponding approximately to the highest pressures calculated for coarse grained garnet peridotite xenoliths from kimberlite (Gurney, 1989). Eclogite inclusions however formed at temperatures that may have been up to 200°C hotter (Gurney, 1989), and this may have resulted in an increase in the proportion of aggregated nitrogen in eclogitic diamonds.

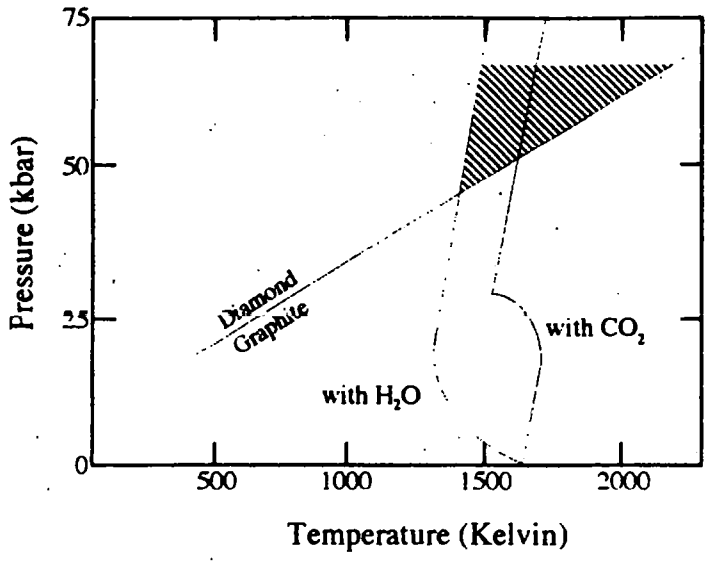

Figure 1.7: Pressure and temperature diagram showing the region of diamond formation. H_2O and CO_2 dominant peridotite solidi are shown and the diamond - graphite equilibrium is that of Berman and Simon (1985). The shaded area is the region of partially molten peridotite in which diamond is stable. From Davies (1984).

As well as having formed at temperatures greater than those of peridotitic inclusions, some eclogite paragenesis inclusions preserve evidence for very high pressure. Moore and Gurney (1985, 1989) report pressures of up to 145 kb for some eclogite paragenesis pyroxene inclusions containing a garnet component (majorite) in solid solution, in diamonds from the Monastery Mine, South Africa and suggest that these diamonds may be of asthenospheric origin. They also report temperatures of up to 1400° for polyphase websterite inclusions; a paragenesis that may be transitional between eclogite and peridotite (Moore and Gurney, 1989).

Examination of the radiogenic isotope composition of diamond inclusions (*e.g.* Burgess *et al.*, 1989) supports the suggestion that inclusions within diamonds essentially form a closed system. More useful however are the radiogenic isotope ages determined from syngenetic inclusions as these are the same as the age of formation of the host diamond. Richardson *et al.*, (1984) measured Sm - Nd ages on composite peridotitic inclusions from diamonds from the Cretaceous Kimberley and Finsch kimberlite pipes and these were clearly Archaean (≈3300 Ma) whereas eclogitic diamonds from Premier, Argyle, Orapa and Finsch are all of Proterozoic age, regardless of the age of the host diatreme (Richardson, 1986a, Richardson *et al.*, 1990). This difference between diamond age and host diatreme age is probably the best evidence for diamonds being xenocrysts rather than phenocrysts in kimberlite or lamproite.

Argon - argon dating techniques have also been applied to inclusions from Premier and other diamonds (Burgess *et al.*, 1989; Phillips *et al.*, 1989) but a general problem with argon dating is that Ar tends to diffuse out of the inclusion and remain at the inclusion -

diamond interface until it is lost when the diamonds are cleaved (Burgess *et al.*, 1992). This often results in apparent Ar ages that are younger than Sm - Nd ages obtained from the same or similar inclusions from the same diamond source. These argon ages tend to correspond to the date of kimberlite or lamproite emplacement. When the kimberlite cooled, Ar diffusion in the diamond inclusion was halted, effectively closing the Ar system.

Thus, mineral inclusions in diamond may provide information on the geothermometry and geobarometry and the age of the diamond source region and in addition may also constrain mantle fO_2; an application of inclusion chemistry that is discussed in detail in section 1.4.

1.3.3.2 Fluid inclusions in diamond

The suggestion that fluid inclusions may exist in diamond was originally made by Bibby (1982) on the basis of instrumental neutron activation analysis of diamond coat; a fibrous, rapidly precipitated overgrowth around crystalline diamond cores (Kamiya and Lang, 1965). Navon *et al.*, (1988) examined the chemistry of such fluid micro-inclusions and found them to be highly enriched in H_2O, CO_3^{2-}, SiO_2, K_2O, CaO and FeO and to have a bulk composition similar to highly potassic magmas like lamproites and kimberlites, but with some significant differences. For example, the fluid micro-inclusions have lower MgO contents, marked K_2O (and other incompatible elements) enrichment and very high K_2O/Al_2O_3 ratios. Molecular CO_2 is also occasionally present. These fluid micro-inclusions are not compositionally similar to any of the common larger inclusions of either eclogitic or peridotitic paragenesis but are associated with apatite (Lang and Walmsley, 1983; Guthrie *et al.*, 1991), biotite (Walmsley and Lang, 1992b; Guthrie *et al.*, 1991) carbonates (ankerite; Walmsley and Lang, 1992a) and quartz (Guthrie *et al.*, 1991). Navon *et al.*, (1988) interpreted these fluid micro-inclusions to be representative of mantle-derived, volatile rich fluids that had been trapped by the precipitation of the diamond coat and investigations of the internal pressure of these inclusions (Navon, 1991) supports this. Extrapolation of the room-temperature pressure determinations from these inclusions to mantle temperatures (1000°C to 1300°C) by Navon (1991) indicated that these fluid micro-inclusions were trapped at pressures of 55kb to 67kb, in general agreement with geothermobarometric determinations from peridotitic paragenesis inclusions (*e.g.* Meyer, 1987).

The composition and pressure determinations from fluid micro-inclusions in diamond coat have important implications for diamond genesis. At present, no mineralogical geobarometer exists for eclogitic paragenesis inclusions (Meyer, 1987) however Navon (1991) associates such fluid micro-inclusions with the eclogite paragenesis on the presence of sanadine, and these micro-inclusions may therefore constrain the pressure

limits of eclogitic paragenesis diamonds. Furthermore, some authors (*e.g.* Boyd, 1988) interpret diamond coat as having grown from the host kimberlite during emplacement, however the pressure determinations of Navon (1991) do not support this. Instead Navon (1991) suggests that diamond coat may be related to the megacryst suite and probably represents the residual fluids of a highly alkaline magma that suffered "heat death" (McKenzie 1989) which aborted its emplacement. In addition, Navon (1991) suggests that H_2O occurs in these inclusions as a supercooled liquid, implying the presence of (super-critical) liquids in the diamond source region and this is particularly important for isotopic fractionation processes, which can be extreme in the presence of fluids (*e.g.* Hoefs, 1987). There is evidence for isotopic fractionation processes operating during diamond growth (See Chapter 2), in which these highly fractionated fluids may be implicated.

1.3.4 Diamond morphology and structure

Diamond morphology preserves significant information on the diamond growth environment. Experimentally grown diamonds occur in two primary growth forms, octahedra and cubes (Figure 1.8) and although some natural occurring tetrahexahedral diamonds may also be primary growth forms, most natural diamonds grow in the cubic or octahedral form (Sunagawa *et al.*, 1984; Gurney, 1989; Sunagawa, 1990). These forms are then subsequently altered by resorption.

Sunagawa *et al.*, (1984) experimentally investigated the relationship between diamond growth form and carbon supply and showed that diamonds with an octahedral primary form grew by a spiral growth mechanism, probably from a solution phase in open space (melt?) and that this occurred during periods of low supersaturation of carbon. In contrast, crystals with the cubic growth form required considerably higher degrees of carbon supersaturation, and their growth rate is higher than that of octahedral forms (Moore and Lang, 1972; Sunagawa *et al.*, 1984; Sunagawa, 1990). Two types of internal structure have been reported from natural cubes (Moore, 1985, 1988). Coloured cubic diamonds have a fibrous internal structure with fibres starting at the centre of each stone and radiating out in a <111> direction to the cube corners. The second mode of cubic growth, producing colourless cubic diamond, is associated with stones termed truncated cuboids and these are stones with "central cross" growth zonation produced by periods of mixed habit growth in which normal growth on flat octahedral facets is accompanied by non-faceted growth on hummocky surfaces with a mean orientation of {100} (Lang, 1979). Both types of natural cube result from non-faceted growth which differs from synthetically produced cubic diamonds (usually smooth faced cubes) and octahedral growth forms. Orlov (1977) was the first to show that the two types of natural cubes differed (fibrous growth = variety II, associated with placers; colourless

cubes = variety III, associated with pipes) and Boyd (1988) went on to show isotopic and nitrogen aggregation state and concentration differences between the different cube types which implies different formation mechanisms for each type.

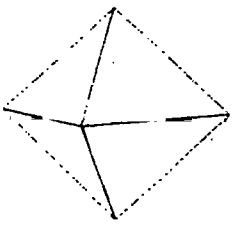

Planar octahedron

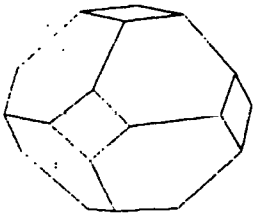

Truncated octahedron

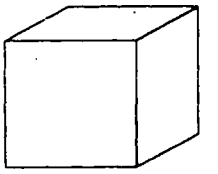

Cube

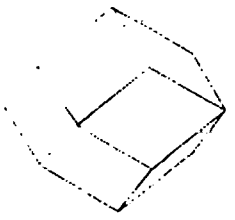

Resorbed rhombic dodecahedron

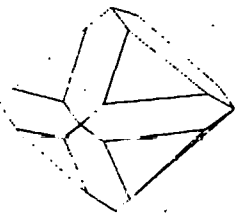

Resorbed octahedron/dodecahedron

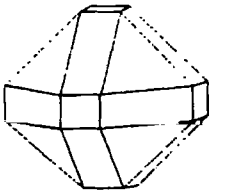

Cubo - octahedral coated stone

Figure 1.8: Some of the more common crystal forms of diamond.

In addition to octahedral and cubic forms, diamonds can occur as "lumps" (Moore, 1985) (*e.g.* the Cullinan) which are highly complex arrangements with the same number of "faces" or system of "edges" as crystals of regular rounded habits. They may also occur as the poly-crystalline aggregates carbonado, framesite, bort, stewartite, yakutite, short and hailstone bort and ballas diamond (Gurney, 1989). The origin of some of the polycrystalline forms is uncertain (Meyer, 1985) but probably involves rapid growth under supersaturation conditions (Sunagawa, 1990). Smith and Dawson (1985) have suggested that carbonado may have been formed by meteorite impacts into carbonaceous rocks early in the Earth's history, while Ozima *et al.*, (1991) present noble gas data suggesting that carbonado originates in a uranium rich, crustal environment, possibly from carbon of initially biological origin.

Crystals with both cubic and octahedral growth forms do occur, and the most common of these are coated diamonds, in which a (usually) octahedral core is surrounded by a cubic overgrowth. Investigation of the internal structure of the coat of coated stones (Kamiya and Lang, 1965) showed the coat to consist of numerous fibres growing out of the octahedral faces, maintaining the octahedral morphology. Space filling at the vertices of the octahedron and where octahedral faces intersect, leads to the development of (100) and (110) faces. The development of coat in coated stones may be associated with kimberlite emplacement (Boyd *et al.*, 1987) although this is not supported by pressure

estimates from fluid micro-inclusions (Navon, 1991; see section 1.3.3.2), and occurs during periods of supersaturation of carbon in the diamond growth region (Moore and Lang, 1972). Considerable amounts of impurities (*e.g.* fluid micro-inclusions & noble gases) are trapped between the fibres of the coat portions of coated stones.

The resorption of diamond is also an important indicator of its growth history. The end-product of diamond resorption is a rounded dodecahedral morphology and Robinson (1979) showed that to produce such crystals from initially octahedral forms requires a mass loss of at least 45%. Processes responsible for resorption are however not well constrained. The stability of diamond implies that a high fO_2 is necessary for resorption (see following section) and gaseous CO_2 may be involved as Boyd (S.R. Boyd, Pers. Comm., 1990) showed that diamonds could be efficiently resorbed by hot CO_2 in vacuo. The low CO_2/H_2O ratio in lamproites relative to kimberlites (see Table 1.2) may be a product of extensive diamond resorption, "consuming" CO_2 *via* an unknown reaction. This hypothesis would appear to be supported by the abundant resorbed diamonds in the Argyle lamproite (Harris and Collins, 1985). This does imply resorption during emplacement of the host magma, however it would be simplistic to consider all diamond resorption as occurring during emplacement, as there is considerable evidence for long mantle residence times for many diamonds (*e.g.* Richardson *et al.*, 1984 and the existence of diamonds with highly aggregated nitrogen).

Stress may also alter diamond morphology, and it has also been implicated in diamond colouration (Harris, Pers. Comm.; Gurney, 1989). It is evident in the form of lamination lines on the surfaces of resorbed diamond crystals, caused by plastic deformation and is often accompanied by a colour change to brown or pink. It is well preserved amongst diamonds from the Argyle lamproite (Hall and Smith, 1984). Such plastic deformation predates the high temperature resorption of diamonds (Robinson, 1979) and is probably restricted to occurring in the mantle (Evans, 1976) where it occurs in a stress field with grain boundary contact between deforming crystals (Gurney, 1989). Damaging the diamond lattice by this sort of deformation is likely to produce vacancies, and this should result in a decrease in the activation energy of nitrogen aggregation (*c.f.* Collins, 1980). This is a possible explanation for the large number of type IaB diamonds from the Argyle lamproite.

1.4 MANTLE OXYGEN FUGACITY, DIAMOND FORMATION AND C AND N GEOCHEMISTRY

1.4.1 Mantle fO_2 and diamond formation

The oxygen fugacity of the mantle is important in the study of diamond as it controls the speciation of mantle carbon and is thus directly related to diamond genesis (Figure 1.9). For example, in a reduced environment, CH_4, or perhaps elemental carbon, will be the dominant species, while in an oxidised environment CO_2 or carbonate (CO_3^{2-}) dissolved in a melt is expected. Mantle carbon species also have important implications for isotopic fractionation processes. Firstly, the results of fractionation processes involving gaseous phases are more extreme than those in which solid - solid or solid - fluid reactions are involved (Hoefs, 1987) and secondly, fractionation factors for CH_4 are lower than those of CO_2 for many isotope exchange processes (Richet *et al.*, 1977). In fact, Wilding and Harte (1991) have suggested that fO_2 is the most important variable in controlling the $\delta^{13}C$ value of a diamond.

Only recently has some degree of consensus been reached as to the oxidation state of the mantle and that is that it is variable. However, older, deeper, more fertile (in that significant quantities of basaltic melt have not been extracted), possibly asthenospheric mantle seems to be more reducing than younger, shallower and depleted (lithospheric?) mantle (Mattioli *et al.*, 1989; Balhaus *et al.*, 1990; Blundy *et al.*, 1991; Daniels and Gurney, 1991; Balhaus, 1993). This is broadly in line with the suggestions of Foley (1988), but not in agreement with the contention of Haggerty (1986) that the lower mantle is more oxidised than the upper mantle. There also appears to be some tectonic control, with the mantle above subduction zones being more oxidising than that in rift environments (Ionov and Wood, 1992). There is however some variation. Daniels and Gurney (1991) report that the mantle in southern Africa is laterally homogeneous yet locally diverse and that the lower mantle in this region may be sufficiently reducing for CH_4 to be the dominant volatile species, yet the coat of coated diamonds from central Africa and Siberia contains micro-inclusions associated with carbonate, indicative of oxidisation (Guthrie *et al.*, 1991; Navon, 1991; Boyd *et al.*, 1992; Walmsley and Lang, 1992a) in the source region of these coats.

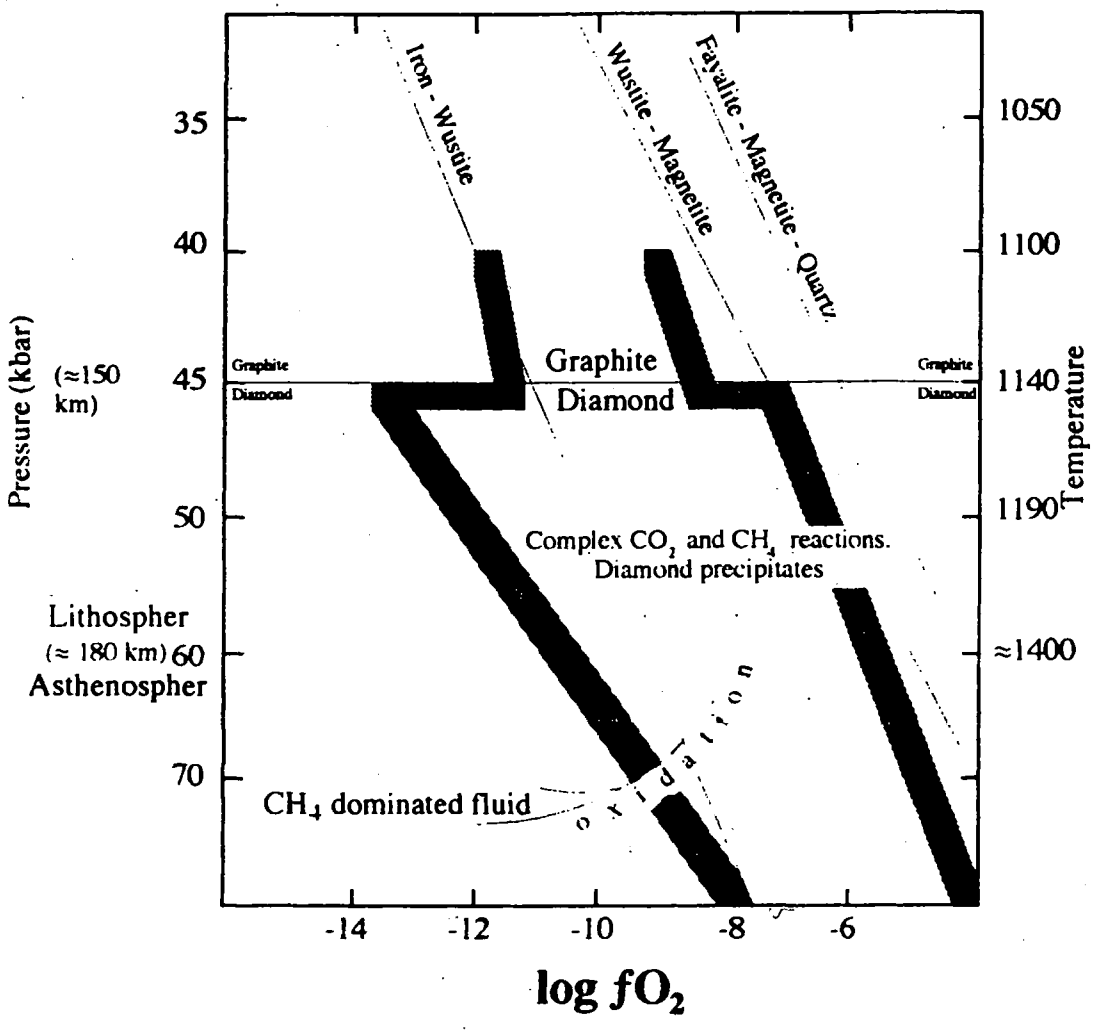

Figure 1.9: Oxygen fugacity and diamond stability within the lithosphere, modified after Haggerty (1986), to incorporate a reduced asthenosphere and more oxidising lithosphere. Diamond is stable between the heavy shaded lines.

Many processes may alter or affect mantle fO_2. For example; metasomatism (Mattioli *et al.*, 1989) particularly if the metasomatic agent is a CO_2 - H_2O rich fluid; melting and melt extraction (Amundsen and Neumann, 1992; Balhaus, 1993); possibly melt degassing (Balhaus, 1993); diamond or graphite precipitation exhausting elemental carbon (Blundy *et al.*, 1991) and geochemical enrichment and subduction (Balhaus *et al.*, 1990) may all increase mantle fO_2. Thus a range of oxygen fugacities is possible in the diamond source region, and whatever the fO_2 is depends on the history of any particular region. Some authors have however reported that partial melting, depletion or metasomatism are unlikely to alter fO_2 (*e.g.* Bryndzia *et al.*, 1989; Wood and Virgo, 1989; Chen *et al.*, 1991; Ionov and Wood, 1992), necessitating an alternative explanation for the variation in mantle fO_2.

It is accepted that diamonds formed in a variety of processes associated with two rock types - eclogite and peridotite (Gurney, 1989), but mechanisms for diamond precipitation are still contentious. Haggerty (1986) suggested precipitation from CH_4 or CO_2

dominant fluids, depending on where in the lithosphere or asthenosphere these fluids originated, while Galimov (1991) was more specific. His model is based on the interaction of reduced (*i.e.* CH_4 dominated) sub-asthenospheric fluid with more oxidised lithosphere. Peridotitic diamonds precipitate when this reduced carbon is converted partially to CO_2, and isotope exchange in the CO_2 - CH_4 system produces fractionated carbon which is then used as the source material for the formation of eclogitic diamonds. Kesson and Ringwood (1989) have a different model which intimately involves the subduction of a, presumably oxidised, slab. In their model, diamond precipitation is not from a fluid but from a melt that is produced by de-watering of bodies of former serpentenite in the slab. Eclogitic diamonds are derived from this material, while peridotitic diamonds result when these melts migrate into, and hybridise with refractory peridotite overlying the slab. The Kesson and Ringwood (1989) model is illustrated schematically in Figure 1.10.

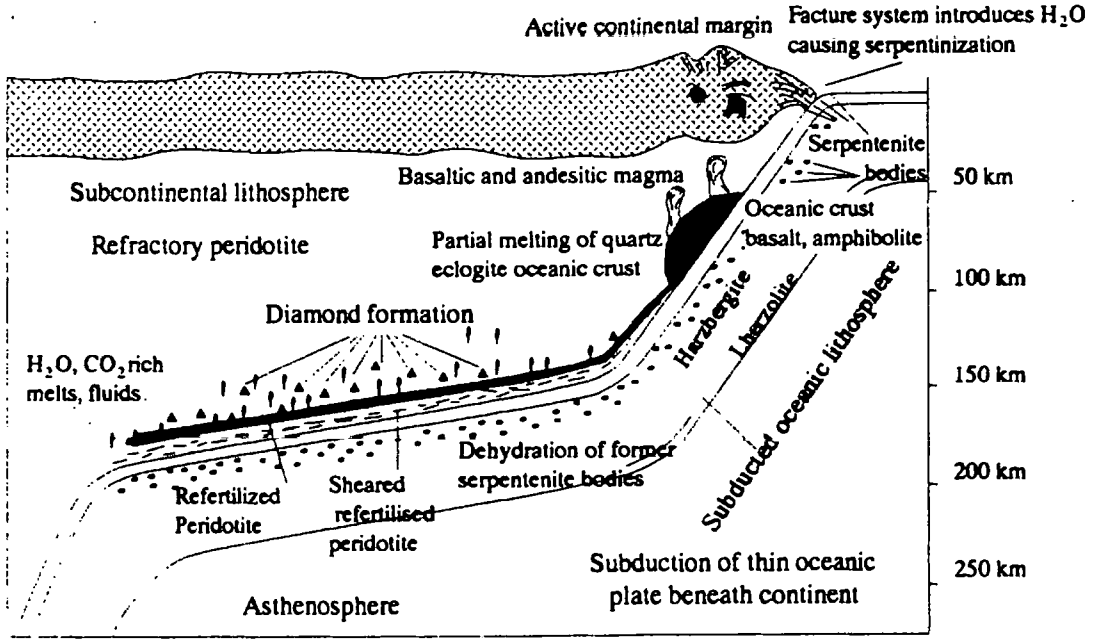

Figure 1.10: The Kesson and Ringwood (1989) model of diamond formation. See text for discussion.

Deines (1980a) examined diamond $\delta^{13}C$ and the role in determining this played by, amongst other factors, vapour composition which is determined by fO_2. He examined a variety of carbon precipitation reactions including:

$$CO_2 \rightleftarrows C + O_2 \quad (1.3)$$

$$2CO \rightleftarrows 2C + O_2 \quad (1.4)$$

$$CH_4 \rightleftarrows C + 2H_2 \quad (1.5)$$

$$CO_2 + 2H_2 \rightleftarrows C + 2H_2O \quad (1.6)$$

$$CO + H_2 \rightleftarrows C + H_2O \quad (1.7)$$

$$CO_2 + CH_4 \rightleftarrows 2C + 2H_2O \quad (1.8)$$

$$2CO + CH_4 \rightleftarrows 3C + 2H_2O \quad (1.9)$$

and showed that reactions 1.3, 1.5 and 1.8 only, were feasible for diamond precipitation from a vapour, under mantle conditions. Of these, he suggested that CH_4 dissociation under conditions of increasing fO_2 was the only mechanism that could partially reproduce the observed distribution of diamond $\delta^{13}C$ values (Figure 1.3) and the gases liberated from diamonds. Deines (1980a) however also pointed out that (1) the range of isotope effects expected to accompany precipitation from a vapour was probably very small and (2) the likelihood of a vapour phase existing in the mantle is low. From this, Deines (1980a) concluded that it was more likely that the range of $\delta^{13}C$ values recorded in diamonds were either primordial or derived from the Earth's crust, although it was not possible to be unambiguous as to whether or not a gas phase had participated in diamond formation.

1.4.2 Comparison of C and N geochemistry

A number of aspects of the geochemistry of carbon and nitrogen have been discussed earlier in this introduction, and will be further discussed again in later parts of this thesis. However, a brief resumé of the behaviour of these two elements is presented here.

Carbon in the mantle is fairly well constrained. It is thought to occur at concentrations of between 200 ppm (Gregor *et al.*, 1988), through 680 ppm (Blundy *et al.*, 1991) to up to 1000 ppm (Marty and Jambon, 1987) and the form in which it exists is controlled by mantle fO_2. In a reduced environment CH_4 is the dominant volatile species and "organic" carbon may exist, while in more oxidised regions, CO_3^{2-} will readily dissolve in a magma and CO_2 is present in many vesicles from basaltic rocks (*e.g.* Javoy *et al.*, 1982). The ranges in $\delta^{13}C$ values obtained from some mantle derived materials are summarised in Figures 1.3 and 1.4 and it is now commonly accepted that unfractionated mantle carbon has a $\delta^{13}C$ value near -5‰ to -7‰.

In contrast carbon in sedimentary rocks occurs at higher concentrations (mean [C] $\approx$ 3%; Gregor *et al.*, 1988). This carbon was originally derived from the primordial earth by CO_2 rather than CH_4 degassing, and has subsequently been recycled by biological processes (Gregor *et al.*, 1988). The degassing of CO_2 is consistent with the suggestion that younger, shallower depleted mantle is more oxidising than older, fertile and deeper mantle (see previous section) if the degassed CO_2 is derived from the upper mantle alone. If sub-asthenospheric reduced (CH_4 dominated) volatiles have been degassed, they must have oxidised prior to, or during degassing. This may occur during partial melting and melt migration (Balhaus, 1993), and may be accompanied by an increase in fO_2 (Balhaus, 1993).

The $\delta^{13}C$ range measured in sedimentary rocks is wider than that seen in the mantle as a result of the large fractionations in carbon stable isotope ratio that can occur at low temperatures. For example, during photosynthesis in plants where the intermediate stage is the production of the three carbon molecule, phosphoglyceric acid (so called C_3 plants), ^{12}C is preferentially utilised and the remaining CO_2 is correspondingly ^{12}C depleted by between 14‰ and 40‰ (Hoefs, 1987). In C_4 plants where the reaction path is *via* dicarboxylic acid, the ^{12}C enrichment of the organic material is only 2‰ to 3‰ (Hoefs, 1987) relative to the initial CO_2. Incorporation of C_3 organic material in a sedimentary rock, can thus lower the $\delta^{13}C$ value of that rock considerably. There are also stable isotope fractionations associated with chemically precipitated sedimentary rocks. When carbonates precipitate from bicarbonate dissolved in water, the reaction followed is:

$$Ca^{+} + 2HCO_3^{-} \rightarrow CaCO_3 + CO_2 + H_2O \qquad (1.10)$$

(Hoefs, 1987) and the product CO_2 is depleted in ^{13}C relative to the precipitated carbonate by up to 8‰ (Friedman and O'Neil, 1977). The net result of these fractionations of carbon stable isotope ratios in the low temperature environment, is that organic carbon (C_{org}) in sedimentary rocks is characterised by $\delta^{13}C$ values between about -19‰ and -40‰, with a mean $\delta^{13}C$ value of the order of -27‰ (Schidlowski *et al.*, 1983). In contrast, marine carbonates have a mean $\delta^{13}C$ value of about 0‰, and this has varied little since the Proterozoic (Schidlowski *et al.*, 1983).

Relative to carbon, nitrogen is still poorly understood. In an oxidised environment N_2 will be the dominant volatile form and Gregor *et al.*, (1988) suggest that in order to be consistent with CO_2 degassing, N_2 must be more important than NH_3. However, the form in which nitrogen occurs in the deeper mantle is unknown. If it does occur as N_2, then nitrogen may behave in a manner similar to the noble gases (Ozima, 1989), but if NH_3 (or the amino radical NH_2) exists, then the geochemistry is more difficult to characterise. Stevenson (1959) and Honma and Ithara (1981) have however reported fixed ammonium in igneous and metamorphic rocks and suggest that it may substitute for potassium, and Boyd and Pillinger, (1991) have produced a rubidium sulphate – ammonium sulphate solid solution for use as an experimental standard, which indicates that substitution of NH_4 for Rb is possible. Indeed, Gregor *et al.*, (1988) report that ammonium ions readily bond to clay exchange sites but the effectiveness of such a "fixing" process for nitrogen at mantle temperatures is not known. Considerably more data are required on mantle nitrogen sources and sinks.

Although the $\delta^{15}N$ value characteristic of the mantle is not known, and suggestions have ranged from as low as -40‰ (Javoy *et al.*, 1986) to positive $\delta^{15}N$ (Wand *et al.*, 1980; Becker, 1982), the opposite is the case for nitrogen in the exogeneous reservoir. The

atmosphere is defined as having $\delta^{15}N = 0‰$, and most sedimentary rocks, biological organisms and compounds dissolved in the oceans concentrate ^{15}N relative to the atmosphere. Some examples of $\delta^{15}N$ in the external reservoirs of the Earth are listed in Table 1.9.

		Range in $\delta^{15}N$ (‰)	Reference
Marine	organisms	+4 to +21	1
	particulate organic matter	+3 to +10	2
	marl oozes	+4 to +9	3
	sapropels (organic rich sediments)	+0.3 to +6	3
Seaweed		+8.1	4
Oil		+3 to +11	1
Organic matter in soils		+2 to +20	5
Catalina schist metasedimentary rocks		+1.9 to +4.3	6
Mean coastal sediments		+7	9
Air	N_2	0	by definition
	NH_4	-3 to +10	5
	NO_3	-6 to +3	5
	N_2O (marine)	+6.9 to +7.1	7
Seawater	N_2O	+6.4 to +9.4	7
	NO_3	+4.8 to +6.8	8
Rain water	NO_3	-7.2 to -3.4	4
	NH_4	-0.1 to -9.0	4

Table 1.9: The $\delta^{15}N$ values of some components of the exogenic reservoir. References are: 1 = Hoefs (1987), 2 = Saino and Hatori (1980), 3 = Calvert *et al.*, (1992), 4 = Hoering (1956), 5 = Letolle (1980), 6 = Bebout and Fogel (1992), 7 = Kim and Craig (1990), 8 = Cline and Kaplan (1975) and 9 = Lerman *et al.*, (1993).

From Table 1.9, it is evident that most nitrogen components added into the mantle by subduction are likely to be ^{15}N enriched relative to the atmosphere. Although much nitrogen is expected to be lost during metamorphism, the associated kinetic fractionation is towards ^{15}N enrichment of the rock (Bebout and Fogel, 1992) and this means that components finally added into the mantle will have even more positive $\delta^{15}N$ values, and this may cause recognisable perturbations in the $\delta^{15}N$ value of the mantle.

Estimates of the nitrogen content of the mantle are low and range from about 1 ppm to a maximum of about 20 ppm (Ganpathy and Anders, 1974; Norris and Shaeffer, 1982; Gregor *et al.*, 1988) and many mantle-derived igneous rocks have similarly low N contents (Becker and Clayton, 1977; Sakai *et al.*, 1984; Exley *et al.*, 1987; Gregor *et al.*, 1988). Nitrogen concentrations in sedimentary rocks however are higher; typically 200 to 4000 ppm (Wedepohl, 1969). Although nitrogen content decreases rapidly on diagenesis (Waples and Sloan, 1980; Bebout and Fogel, 1992) any sedimentary nitrogen that survives subduction may significantly disturb local mantle nitrogen contents.

1.5 AIMS OF THIS THESIS

Stable isotope studies of diamond and other mantle-derived material (*e.g.* Javoy *et al.*, 1986; Kyser, 1990; Kirkley *et al.*, 1991) suggest a heterogeneous mantle with respect to the light elements. Carbon and nitrogen coexist in diamonds and nitrogen abundance (*e.g.* Harris and Spear, 1986;) and a limited number of $\delta^{15}N$ data (109 stones in total) show that diamonds are also variable with respect to nitrogen. In this thesis, the database of diamonds for which C and N have been simultaneously collected has been extended from the 95 stones of Boyd (1988) to 266, with the aims of using diamond $\delta^{13}C$, $\delta^{15}N$ and nitrogen content data to address specific problems. These are:

- An analysis of the degree of variability of carbon and nitrogen isotopic composition within restricted environments, and within individual diamonds (for comparison with Boyd *et al.*, 1987 and Boyd, 1988).
- Investigation of the origin of stable isotope heterogeneities within the mantle, and an assessment of whether these are the result of fractionation (*e.g.* fractional crystallization) or mixing (*e.g.* with subducted sedimentary volatiles) processes,
- and an attempt is made to determine whether there is a restricted range of $\delta^{15}N$ values that is characteristic of the mantle, in the same way that $\delta^{13}C$ = -5‰ to -7‰is taken as characteristic of primary mantle.

In this study, efforts have been concentrated on the study of diamonds from some Western Australian sources. Some $\delta^{13}C$ data are already available for diamonds from Argyle and Ellendale (Hall and Smith, 1984; Boyd, 1988; Jaques *et al.*, 1989), and Harris and Colins (1985) and Taylor *et al.*, (1990) have described the nitrogen abundance and aggregation state characteristics of Argyle and Ellendale diamonds. In addition, Boyd (1988) present $\delta^{15}N$ data for 16 diamonds from Western Australia. Systematic carbon isotope and nitrogen abundance data are also available for comparison from a restricted number of Southern African localities (Deines *et al.*, 1984, 1987, 1989, 1991a, 1991b).

The Argyle lamproite is the richest known primary source of diamonds and diamond grades of 680 ct.100t^{-1} have been reported (Argyle project briefing, 1984). This pipe has been comprehensively investigated in terms of mineral chemistry, geology and diamond characteristics as have the Ellendale 4 and Ellendale 9 lamproites (Hall and Smith, 1984; Jaques *et al.*, 1986a,1986b). All three of these lamproites occur in regions that are tectonically similar (Hancock and Rutland, 1984), penetrating mobile belts adjacent to the Kimberley craton, Western Australia, and this provides geological control

on the diamonds used in this study. Whereas Argyle is ≈400 km from Ellendale, the Ellendale 4 and Ellendale 9 pipes are separated at the surface by less than 15 km. Any differences or similarities between these three closely proximate diamond sources could help to quantify the scale of heterogeneity in the mantle source regions.

The study presented in Chapter Two comprises an investigation of fragments broken from whole diamonds, undertaken to characterise the variability of each diamond source. This is complimented by an study of within-sample variability of nitrogen and carbon isotopic composition, nitrogen content and aggregation state in which data were obtained as a series of traverses across plates cut perpendicular to {001} for 1 carat Argyle and Ellendale 9 diamonds, and these data are discussed in Chapter 3. The data for Argyle, Ellendale 4 and Ellendale 9 diamonds are compared to other Australian and Chinese diamonds in Chapter 4, and in Chapter 5 the Western Australian macro diamonds (as described in Chapters 2 and 4) are compared to the Western Australia micro-diamond population. There have been suggestions that micro-diamonds are related to kimberlite emplacement (*e.g.* Boyd *et al.*, 1992) and this likelihood is examined.

All the data presented are used in Chapter 6 to generate a summary model of diamond genesis and to evaluate the likely role of subduction in the growth of diamond. Isotopic fractionation processes are examined as a possible alternative, and an attempt is made to constrain the $\delta^{15}N$ value of the mantle. The implications for this $\delta^{15}N$ value are discussed.

---

2 Carbon and Nitrogen characteristics of diamonds from Argyle and Ellendale

2.1 PREVIEW

In this chapter, nitrogen isotope, concentration, and aggregation state data, and carbon isotope ratios are presented for Argyle and Ellendale diamonds. Nitrogen concentration (Figure 2.1) and aggregation state (Table 2.1) data have been reported previously for Argyle diamonds (Harris and Collins, 1985; Taylor *et al.*, 1990) and the nitrogen and carbon isotopic compositions of 13 Western Australian diamonds from a commercial source (Argyle; Seal, Pers. Comm.) have been analysed by Boyd (1988). Hall and Smith (1984) examined diamonds from Argyle and Ellendale, and reported carbon isotope measurements on three diamonds from each of Argyle and Ellendale 9 (Figure 2.2), as well as describing the morphological characteristics and inclusion parageneses of diamonds from these lamproites. Jaques *et al.*, (1989) described the relationships between inclusion paragenesis and carbon isotopic composition for many more Argyle and Ellendale diamonds (Figure 2.2), and diamondiferous xenoliths from Argyle have also been examined by Jaques *et al.*, (1990). Additional analyses of the $\delta^{13}C$ values of Argyle diamonds are presented by Sobolev *et al.*, (1989).

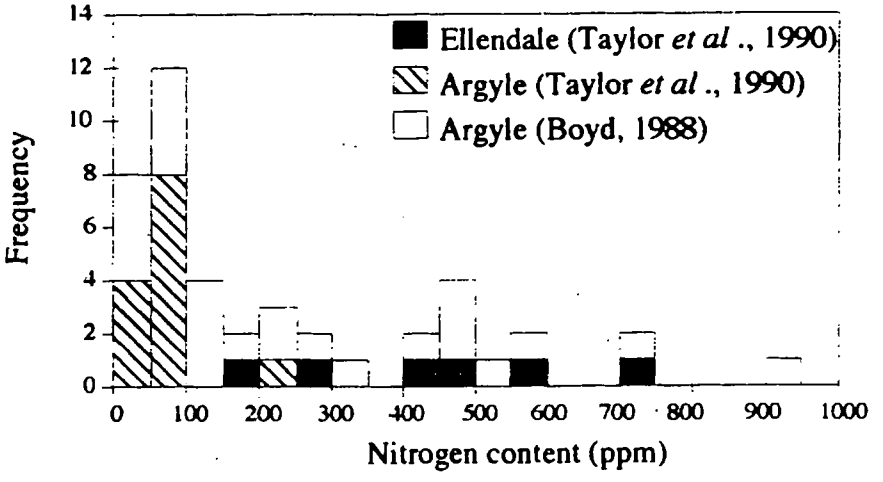

Figure 2.1: Nitrogen content histogram for Western Australian diamonds. The Boyd (1988) data represents 26 analyses from 13 diamonds. A single analysis of 1980 ppm nitrogen from Western Australian diamond (Boyd, 1988) is not shown.

The results obtained by these authors have indicated that there is a considerable variation in the morphology and carbon isotope ratios of Argyle and Ellendale diamonds. The current study extends the database by 110 diamonds with $\delta^{13}C$, $\delta^{15}N$, nitrogen abundance and nitrogen aggregation state data recorded simultaneously for all samples.

Partial data are also presented for an additional 18 stones, and all data are listed in Appendix 1.

	Argyle	Ellendale
Mean	75	25
Minimum	58	4
Maximum	95	98
Range	37	94
no of samples	13	6

Table 2.1: Percentage of nitrogen occurring in B aggregates. Data from Taylor *et al.*, (1990). In addition, Harris and Collins (1985) report that more than 75% of Argyle diamonds have greater B-feature absorption (μ_B) than A feature (μ_A) absorption.

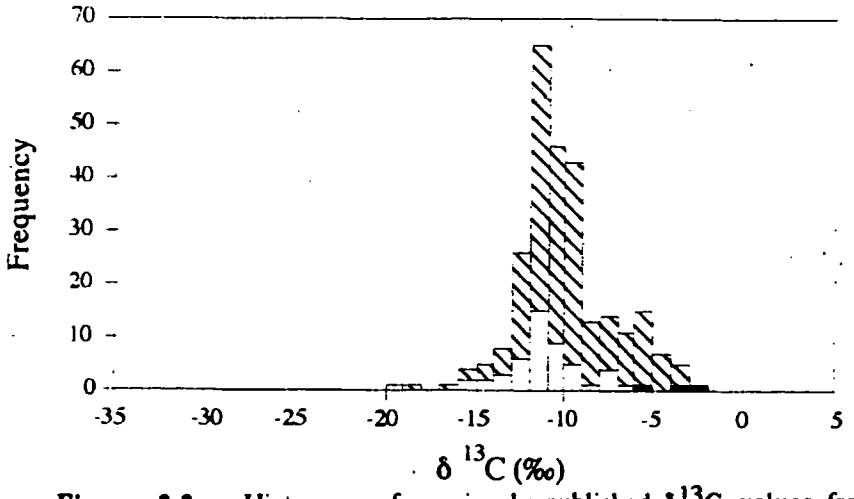

Figure 2.2: Histogram of previously published $\delta^{13}C$ values from Argyle (diagonal stripes) and Ellendale (black shading) diamonds. Data from Hall and Smith (1984), Jaques *et al.*, (1989) and Sobolev *et al.*, (1989). The $\delta^{13}C$ values from Western Australian diamonds from Boyd (1988) are shown in white.

2.1.1 General geology of Argyle and Ellendale lamproites

The geology and tectonic evolution of Western Australia has been described in detail (Gee, 1979; Hancock and Rutland, 1984; Plumb and Gemuts, 1976; Plumb, 1979; Plumb *et al.*, 1981). The Argyle and Ellendale lamproites are particularly well characterised, both chemically and geologically (Jaques *et al.*, 1986b). The diamonds used in this study are thus better constrained than is usual, in terms of source region characteristics by the following tectonic, petrological and geochemical information.

The Argyle and the Ellendale ultrapotassic alkaline intrusives are a collection of diamondiferous dykes and pipes located on the margin of the Kimberley Craton in north Western Australia (Figure 2.3) and although separated by more than 400 km and 1000 million years they occur in similar tectonic environments, all penetrating the mobile belts

bounding the craton. The presence of these diamond-bearing "kimberlites" adjacent to the Kimberley Craton was first reported in 1982 and their leucite lamproite affinities noted (Atkinson *et al.*, 1982; Jaques *et al.*, 1982). It was suggested (Scott-Smith & Skinner, 1984) that they, like the diamondiferous Prairie Creek intrusion in Arkansas, U.S.A. should be classified as lamproites and this terminology is now in general use. The Argyle intrusion is classified as an olivine-bearing phlogopite lamproite and Ellendale 4 and Ellendale 9 are olivine or phlogopite - olivine lamproites (Jaques *et al.*, 1986b).

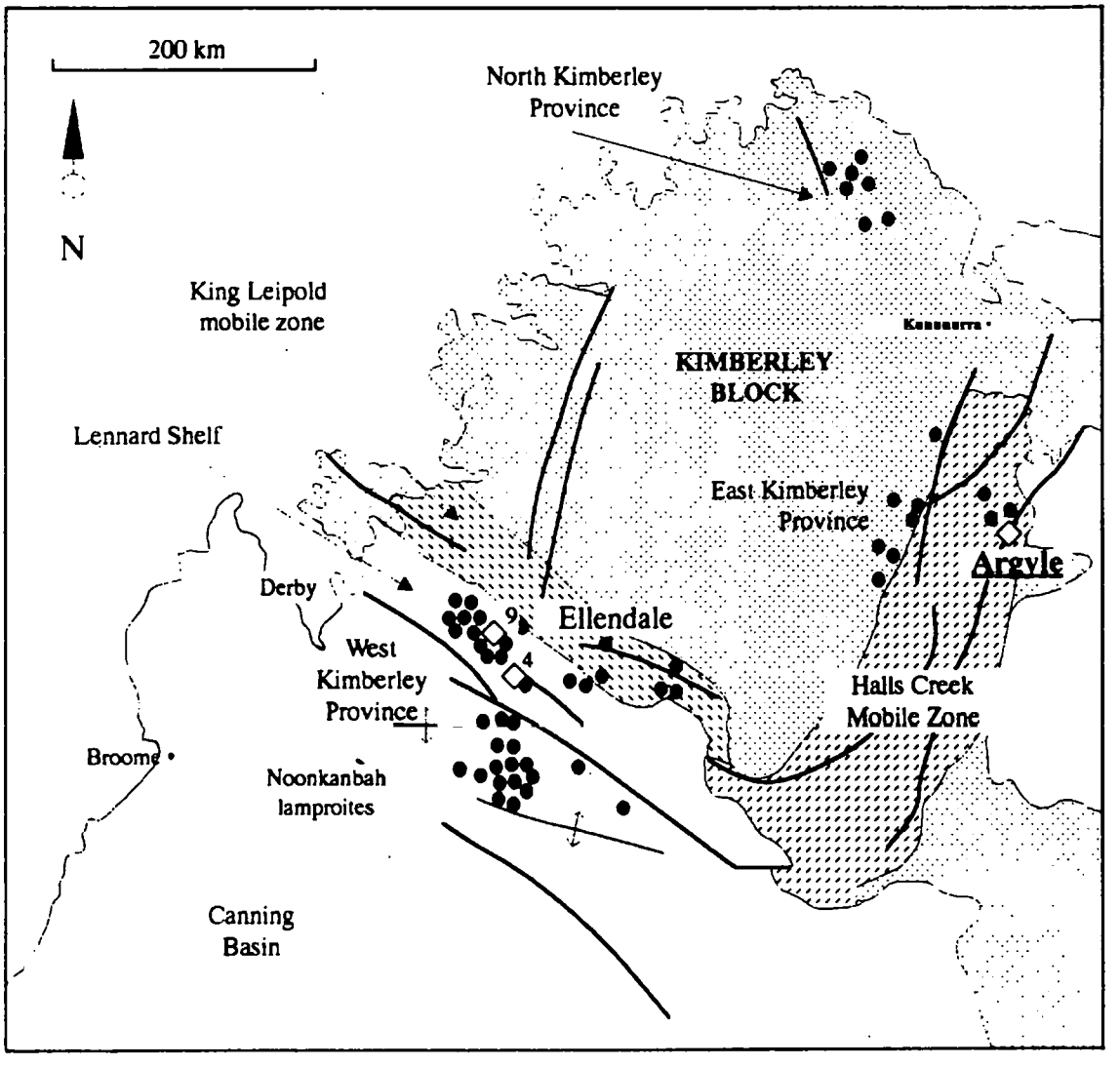

Figure 2.3: Map of north Western Australia showing major tectonic units and lamproite occurrences. Diamond occurrences shown by the diamond symbol. Ellendale 4 indicated by "4" and Ellendale 9 by "9". Modified from Jaques *et al.*, (1986b).

The Argyle lamproite pipe occurs in the East Kimberley province of Western Australia, about 200 km north east of the town of Halls Creek and it is unusual in a number of respects. Unlike other West Australian lamproites, it is isolated, not occurring in a known lamproite field, although kimberlites do occur nearby (*e.g.* the Bow Hill, Maude Creek and Lissadell Road kimberlites; Atkinson *et al.*, 1984). The Proterozoic age of the the pipe (1178 ± 47 Ma; Pidgeon *et al.*, 1989) makes it the oldest dated West Australian

alkaline intrusion, and along with the Premier kimberlite, South Africa, one of the few Proterozoic sources of diamonds. In contrast, the Ellendale lamproites; a dense cluster of 45 intrusions in the West Kimberley province occurring about 150 km east of the town of Derby (See Figure 2.3) are of early Miocene age (Jaques *et al.*, 1984b) and are thus amongst the youngest known sources of diamonds.

The tectonic evolution of this region of Western Australia has been interpreted as a sequence of cratonization around the ancient nucleus of the Kimberley block (Gee, 1979). The adjacent mobile zones are thought to represent the products of convergence of this continental block and an "oceanic" area underlain by thin crust (Hancock and Rutland, 1984). In this model, an early (≈2150 Ma) extensional phase was followed by compression and uplift (1920 Ma to 1830 Ma), accompanied by limited lithospheric subduction, crustal thickening and shortening and this is summarised in Figure 2.4.

As with all lamproites, Argyle and Ellendale 4 and Ellendale 9 are highly potassic, although unlike other leucite lamproites from the same region they are not per-potassic. They are also characterised by low Ca, Al, Fe and Na contents which are characteristic of a mildly depleted source (Jaques *et al.*, 1986b). Superimposed on this is evidence of a mantle enrichment event which elevated Rb, Sr, the light rare earth elements (LREE) and Rb/Sr ratio relative to the petrologically similar (Smith, 1984) Group 2 kimberlites (Jaques *et al.*, 1984a, 1986b). The REE patterns are also fractionated, with La/Yb ≈ 100 (Jaques *et al.*, 1986b). Further evidence of geochemical enrichment of the source material is provided by radiogenic isotopes. Epsilon (ε) Sr ranges from 118 to 282 for the West Kimberley lamproites including Ellendale 4 and 9 (Fraser *et al.*, 1985) and εSr = 22.9 for Argyle (Skinner *et al.*, 1985). Corresponding εNd values are -7.4 to -13.8 for the West Kimberley lamproites and -4.6 to -5.3 for Argyle (McCulloch *et al.*, 1983).

There is a consensus that kimberlites and lamproites are extreme products of mantle enrichment processes (*e.g.* Kramers *et al.*, 1981; Jaques *et al.*, 1984a, 1986b; Hawkesworth *et al.*, 1985; Fraser *et al.*, 1985). In an examination of Western Australian lamproites, Fraser (1987) concluded that they were derived by very small (<1%) degrees of partial melting, from a source region with a complicated evolutionary history. At least 1 Ga were necessary between enrichment and emplacement in order to explain the observed Sr and Nd isotopic characteristics. This was further constrained by Pb isotopes indicating a three stage mantle evolution, with two distinct events altering U and Pb in the mantle source. These events were modelled as occurring at ≈3.5 Ga (the age of the Archaean basement) and ≈1.8 Ga (the approximate age of the mobile belt; see Figure 2.3) by Fraser (1987), and this geochemical enrichment was superimposed on an older, formerly depleted refractory peridotite residue (Jaques *et al.*, 1986b), similar to the peridotite xenoliths found at Argyle (O'Neill *et al.*, 1986; Jaques *et al.*, 1990).

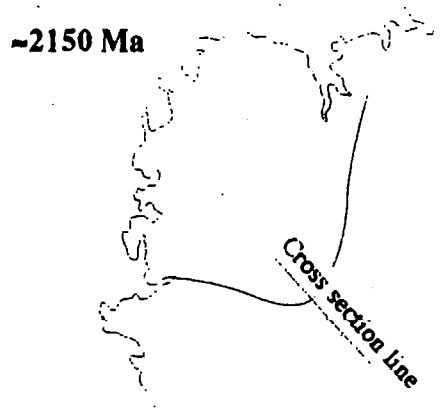

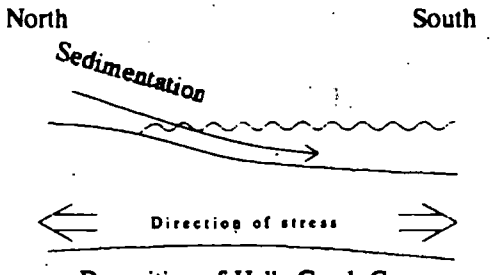

Deposition of Halls Creek Group on Archaean crust thinned during extention

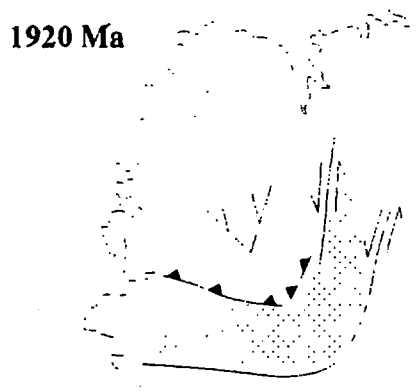

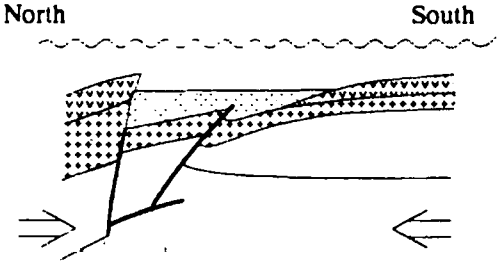

Compressional phase - Island continent converges on the Halls Creek Mobile Zone

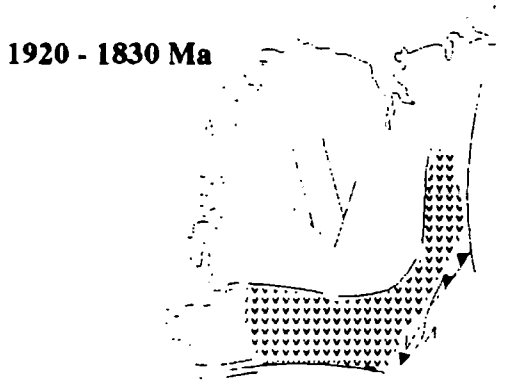

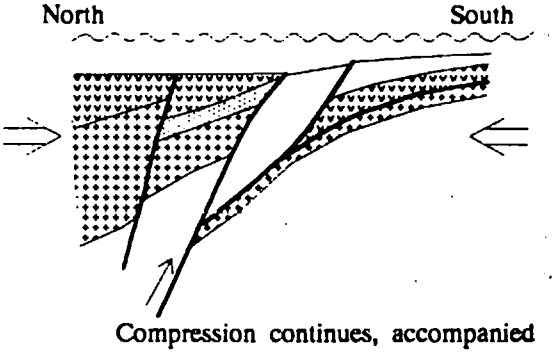

Compression continues, accompanied by "subduction" of continental material beneath the Kimberley Block. Granite emplacement terminates this phase

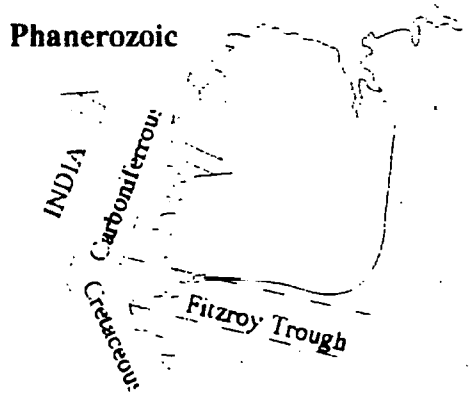

Carboniferous rifting seperates N.W. Australia and Greater India. Cretaceous extention of rift completes seperation

Fitzroy Trough represents a failed rift, filled with sediments from the Kimberley Block

Continuous movement on faults results in repeated cycles of marine transgression and regression

Figure 2.4: The structural evolution of the West Australian shield, from the model of Hancock and Rutland (1984).

Geochemical enrichment has also been reported for syngenetic inclusions in Argyle diamonds. Eclogite paragenesis diamond inclusions have been dated at 1580 ± 60 Ma by Richardson (1986b) who suggested that their origin may have been related to metasomatic events, possibly related to the formation of the Halls Creek mobile zone. The 1580 Ma age of these inclusions is some 400 Ma older than the emplacement date of the host lamproite (Pidgeon *et al.*, 1989), implying a xenocrystal relationship between diamonds and lamproite.

2.1.2 Sampling

The physical characteristics of Argyle, Ellendale 4 and Ellendale 9 diamonds and their inclusions have been described (*e.g.* Hall and Smith, 1984; Jaques *et al.*, 1984a, 1989; Harris and Collins, 1985; Griffin *et al.*, 1988, 1992). A selection was made from a single days run-of-mine production at Argyle by Chris Smith of ConZinc Rio Australia Exploration (CRAE), and a similar selection made from Ellendale 4 and 9 exploration pits, also by Chris Smith and these are the samples described in this Chapter. Samples in two size fractions were supplied. Two millimeter stones (See Table 2.2) for examining the total variability of diamonds from geographically restricted regions and larger, 1 carat stones, about 5 mm across, as plates so that internal isotopic variations could be investigated in a similar fashion to Boyd *et al.*, (1988a). A subset was chosen from the large number of two mm diameter diamonds supplied, that could be analysed in the time available, and the number of stones chosen and the number of analyses are listed in Table 2.2. The majority of these are samples of known paragenesis from CRAE or Argyle Diamond Mines (ADM) inclusion studies, or samples from which inclusions have been extracted for examination by CRAE and ADM. Additional analyses have been made of samples that are free of visible inclusions, in order to increase the amount of available data. In some cases, nitrogen concentration and isotope data are not available and this is due to either insufficient amounts of gas being available for mass spectrometric analysis, or by contamination of released nitrogen with CO_2. In these cases, $\delta^{13}C$ data were however, usually obtained.

Five one carat stones, already sawn into plates were supplied from each locality. Selected specimens were subsequently laser dissected for examination of the internal isotope variability of carbon and nitrogen in diamonds. Since early results for Argyle 2 mm diamonds indicated that there was considerable variation in $\delta^{15}N$, all Argyle plates were investigated in detail. As similar results indicated that diamonds from Ellendale 9 were more variable than those from Ellendale 4, all four Ellendale 9 diamond plates were analysed. The left hand edge of this plate E9037, (blocks 1 to 3) was lost in transit

between Drukker & Zn. and the Open University after laser-sectioning and thus could not be analysed. No plates from Ellendale 4 were examined.

		No. of diamonds analysed	Number of analyses $\delta^{13}C$	$\delta^{15}N$	[N]	FTIR*
ARGYLE						
Broken stones with eclogitic inclusions (mostly white and brown)		23	23	20	21	23
Probably peridotitic diamonds (all white)		4	4	4	4	4
Possibly peridotitic diamonds (all white)		4	4	4	4	4
Inclusion-free	Pink	2	2	2	2	2
	Grey	1	1	1	1	0
	Yellow	3	3	2	3	3
	Yellow/white macles	1	1	1	1	1
	White	10	10	9	9	10
	Brown	13	13	13	13	13
		61	61	56	58	60
ELLENDALE 4						
Inclusion-bearing		10	10	10	10	10
Inclusion-free		9	11	10	10	12
		19	21	20	21	22
ELLENDALE 9						
Inclusion-bearing		13	15	14	15	13
Inclusion-free		14	14	13	13	14
		27	29	27	28	27
TOTALS		107	111	103	104	109

Table 2.2: Two mm diamond samples analysed. Most samples of known paragenesis supplied from Argyle were analysed, as were all Ellendale diamonds from which inclusions had been extracted. Additional samples were chosen at random from inclusion-free diamonds in order to increase the pool of available data. In the case of Argyle, these additional samples were of various colours, which were analysed in approximately the same proportions as their occurrence in the lamproite. *FTIR = Fourier transform infrared analysis.

2.1.3 Analytical

As described above, initial sample selection, chosen to provide a suite of diamonds representative of the host lamproites, was undertaken by Chris Smith of CRAE and a selection of inclusion-bearing and inclusion-free diamonds of various colours, morphologies and inclusion paragenesis was supplied. A subset of these was prepared for analysis in the following manner. Whole stones (2mm size fraction) from Argyle were ultrasonically cleaned in acetone, broken in a stainless steel mortar and a fragment with mass between 100μg and 500μg, weighed to a precision of 0.1μg, selected. These chips, together with weighed chips supplied already broken as a result of the extraction of inclusions for analysis by CRAE/ADM were spectroscopically examined and several

Fourier Transform Infrared (FTIR) spectra collected for each specimen, as detailed in Appendix 2.

Samples were placed in a baked platinum bucket and held in air at a temperature of 500°C for a minimum of thirty minutes to remove surficial contamination. They were then loaded into the extraction system described by Boyd *et al.*, (1988b) and summarised in Appendix 2. After combustion in this system, liberated nitrogen was cryogenically separated from CO_2, cleaned and converted to molecular nitrogen by passing over platinum foil at 1100°C. This nitrogen was analysed in the mass spectrometer described by Wright *et al.*, (1988) where nitrogen abundance and isotopic composition were determined. The cryogenically retained CO_2 was then collected, its pressure measured on the glass line using an oil manometer and carbon isotopic composition determined on a V.G. SIRA 24 dynamic mass spectrometer. If the carbon yield did not match the mass of the sample chip to within 10%, this is indicative of either incomplete combustion or contamination, and data from that sample was discarded.

The sample preparation technique for Ellendale samples differed slightly in that FTIR spectra are collected on unbroken diamonds. Using this method provides FTIR spectra from a larger volume of diamond, improving the quality of the infrared data with the additional advantage of a much increased sample throughput. Once weighed, sample preparation was the same as for the Argyle fragments. Larger (5mm, approximately 1 carat mass) samples from Argyle and Ellendale were provided, already sawn into plates cut perpendicular to the *c* - axis, and these were photographed under plain light and in cathodo-luminescence conditions, before being laser-cut into "ladder sections" as described by Boyd (1988). Subsequent sample preparation and infrared and isotope analysis of these plates was as for the broken samples.

Boyd (1988) undertook a very thorough evaluation of the mass spectrometer used for nitrogen analysis and quotes an internal (machine) precision of 0.2‰ - 0.5‰ for the $\delta^{15}N$ measurement of 23 ng of nitrogen (Appendix 2). This precision varies with the amount of nitrogen analysed, from ± 3‰ on a 0.6ng aliquot to ≤0.6‰ for aliquots of nitrogen larger than 2ng. All nitrogen analyses in this study are of more than 2ng of gas. Nitrogen mass spectrometer performance is monitored by multiple analyses of a reference gas between every sample analysis for nitrogen. The internal precision of the SIRA 24 mass spectrometer used for determination of carbon isotopic composition is regularly checked as part of a technical support program using a variety of NBS standards and is known to be better than 0.05‰. Results here are given against regularly calibrated working standards supplied to users of the instrument and users have only to check the balance of the instrument by performing a zero enrichment test.

Nitrogen analyses from a working reference gas bulb were regularly plotted against a calibration graph and periodically the accuracy of the mass spectrometer was tested by the analysis of a rubidium sulphate – ammonium sulphate standard. This technique (Boyd and Pillinger, 1991) was developed after the bulk of the analytical work done in this thesis, however the results obtained subsequently suggested that the previous procedure using ammonium sulphate, local air and standard steel (NBS-133a) for accuracy calibrations was acceptable. Accuracy determinations using ammonium sulfate standards N-1 and N-2 give $\delta^{15}N$ values always within 1‰ (and usually within 0.5‰) of the expected value (Boyd, Pers. Comm), and nitrogen abundance is quoted to ±5% (Boyd and Pillinger, 1991).

Diamond type (IaA, IaAB or IaB, See section 1.3.2.2) is determined by inspection of the infra-red absorption spectrum, and nitrogen aggregation state is estimated using the spectral deconvolution method of Davies (1981) from the relative size of the A and B feature nitrogen absorption peaks (See Appendix 2). There are large uncertainties associated with these aggregation state estimates (≈40%; See Appendix 2), as absolute absorption coefficients were not obtained due to samples being fragments of diamond with irregular morphology, rather than polished specimens. For the same reason, no attempt has been made to determine nitrogen content spectroscopically. Indeed, the calibration factors for the spectral determination of nitrogen abundance in diamonds are of considerable dispute and they are the subject of continuing study (Pillinger, Pers. Comm., 1992 Diamond Conference). The presence of platelets and the hydrogen absorption peak at wavenumber 3107cm^{-1} is noted for each spectrum and all data are listed in Appendix 1.

2.2 RESULTS

In this section, the results for each size fraction from each diamond source studied will be presented individually. Implications of the results are discussed in Chapter 3. Descriptions of samples and Tables of data are presented in Appendix 1.

2.2.1 Argyle 2 mm diamonds

2.2.1.1 Carbon isotope variations

The carbon isotope composition of 59 Argyle 2 mm diamonds measured in this study fall within the range -13.0‰ ≤ $\delta^{13}C$ ≤ -4.5‰ (Figure 2.5). The mean $\delta^{13}C$ value is -9.9‰, the standard deviation = 1.6‰, and there are 2 analysis of each of eclogitic-diamond A5 and brown-octahedra A1. The median $\delta^{13}C$ value is -10.2‰. There are groups in this data, and eclogitic diamonds and diamonds identified as being of peridotitic

paragenesis on the basis of sharp edged octahedral morphology (90% certainty; Chris Smith, Pers. Comm. 1988) have different $\delta^{13}C$ values. Eclogitic diamonds have a wider overall range in $\delta^{13}C$ values than peridotitic diamonds, and have a mode at a more negative $\delta^{13}C$ value than peridotitic diamonds. The $\delta^{13}C$ range for eclogitic diamonds also encloses that of samples of unknown paragenesis. Ranges, means and median $\delta^{13}C$ values for Argyle diamonds are presented in Table 2.3.

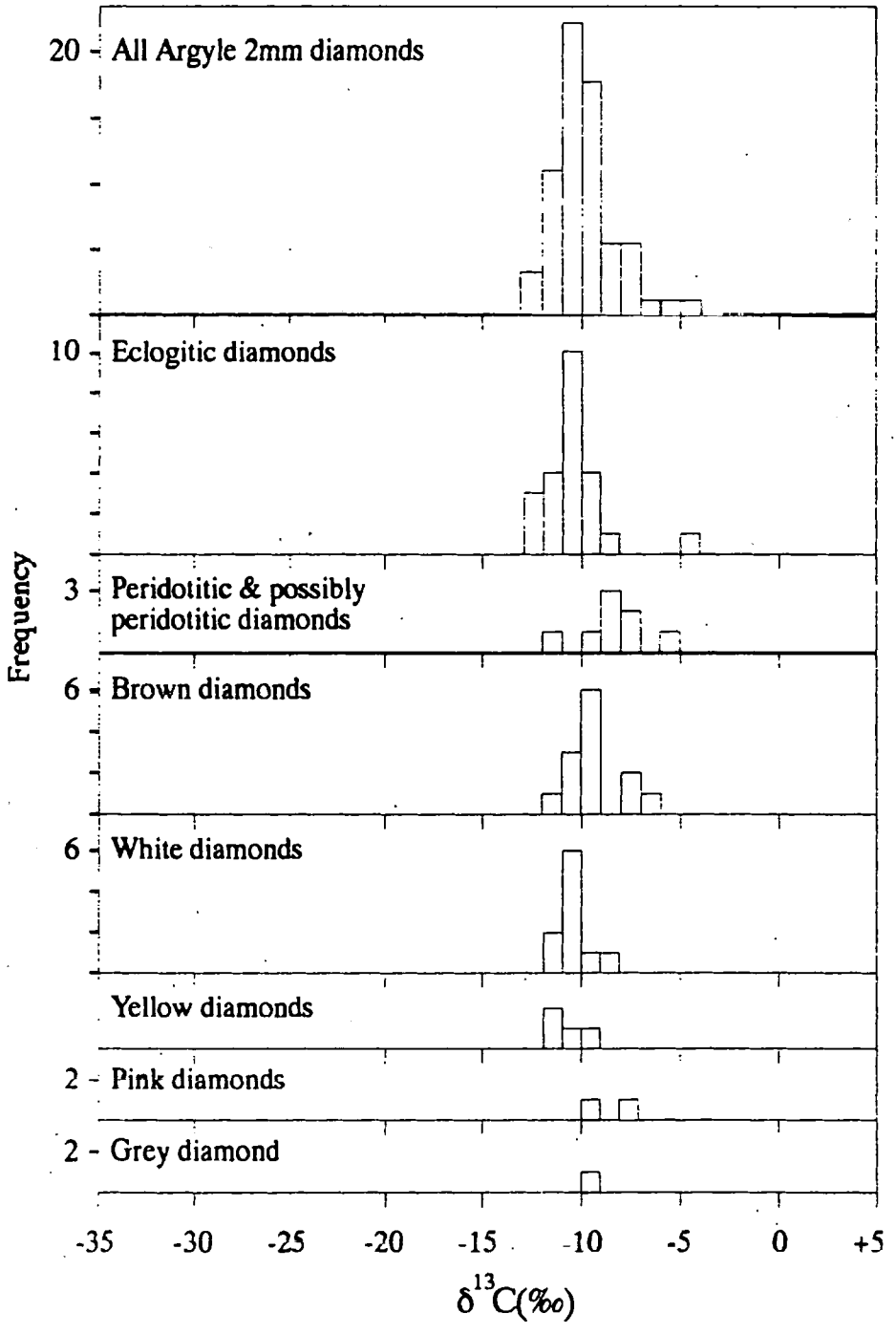

Figure 2.5: Histogram showing $\delta^{13}C$ distribution of Argyle 2 mm diamonds. Eclogitic and peridotitic paragenesis diamonds are shown. Coloured samples are of unknown paragenesis as they do not contain inclusions.

Sample	Range (‰)	Mean and std. error on mean (‰)		Median (‰), population std deviation (‰) and n		
Eclogitic diamonds	-13.0 to -4.5	-10.4	0.3	-10.8	1.6	23
Peridotitic & possibly peridotitic diamonds	-12.0 to -5.8	-8.5	0.6	-8.2	1.8	8
Unknown paragenesis	-11.6 to -6.2	-9.8	0.2	-9.8	1.3	30
Brown diamonds	-11.4 to -6.2	-9.4	0.4	-9.8	1.5	13
White diamonds	-11.6 to -8.19	-10.3	0.3	-10.6	1.0	10
Yellow diamonds	-11.4 to -9.7	-10.6	0.4	-10.6	0.8	4

Table 2.3: Descriptive statistics for $\delta^{13}C$ values from Argyle 2mm diamonds. "n" = number of analyses.

There are no relationships between $\delta^{13}C$ value and diamond morphology or diamond type evident in these Argyle samples. Amongst inclusion-free samples of unknown paragenesis however, there is a relationship between colour and $\delta^{13}C$. Brown diamonds have a $\delta^{13}C$ peak at marginally less negative values than white diamonds (Table 2.3 and Figure 2.5). Yellow and white diamonds have similar median and mean $\delta^{13}C$ values, and may thus be grouped whereas the mean $\delta^{13}C$ value of brown diamonds of unknown paragenesis is -9.4‰. There are insufficient data to comment on the two pink diamonds and the grey diamond, other than to say that they do not differ from the general distribution.

2.2.1.2 Nitrogen

2.2.1.2.1 Nitrogen content; The nitrogen content of 55 Argyle diamonds ranges from 0 ppm (Type II diamond) to a maximum of 2198 ppm in a bright yellow type IaAB diamond, and the mean nitrogen concentration is 313 ppm. The standard deviation is 475 ppm and there are 2 analyses of each of eclogitic diamond A5 and brown octahedra A1. The distribution is skewed towards low nitrogen abundances and has a median value of 98 ppm (Figure 2.6). Of the samples with detectable nitrogen, yellow diamonds contain the greatest amounts (625 ppm and 2200 ppm) while pink and brown diamonds have lower mean nitrogen contents of 63 ppm and 99 ppm respectively. White diamonds have an intermediate mean nitrogen content of 220 ppm.

Peridotitic paragenesis diamonds contain more nitrogen than those of eclogitic paragenesis and have a maximum nitrogen content of 1317 ppm. The maximum for eclogitic paragenesis diamonds is 571 ppm. Type II spectra occur in diamonds from both parageneses, but the lowest measured nitrogen concentration in peridotitic diamonds is 79 ppm For eclogitic diamonds, the minimum measured N concentration is 14 ppm.

The mean nitrogen content of peridotitic paragenesis diamonds is 620 ppm (σ = 174 ppm) and the mean nitrogen content of eclogitic diamonds is 161 ppm (σ = 38 ppm).

Unusually, 13 diamonds that were initially identified as type II from their FTIR spectra contain nitrogen. This ranges from 10 ppm for white dodecahedron-A4 and reaches a maximum of 555 ppm for the octahedral diamond, probably-peridotitic-A4. It is likely that these diamonds are type IaAB or type IaB diamonds, however the poor quality of the FTIR spectra, as a result of their irregular surfaces, prevents their classification. Alternative explanations are that these samples are either very heterogeneous, and that recorded FTIR spectra sampled only low-nitrogen parts of the diamond chip, or that the nitrogen is present in a non-infrared active form (*e.g.* N3 centres or molecular nitrogen). Nitrogen content by spectral type is tabulated in Table 2.4.

Spectral type	Range	Mean	No. of samples
II	10 to 555	164	13
IaA	14 to 1317	802	3
IaAB	0 to 2198	330	25
IaB	26 to 973	216	14

Table 2.4: Analysed nitrogen content listed by spectral type. The type II samples are only those 13 that yielded nitrogen on combustion. Range and nitrogen content in parts per million.

Three "genuine" type II diamonds were also analysed. FTIR spectra of eclogitic diamond A15, Yellow diamond A3 and Brown macle A2 indicated no nitrogen and in all three cases, none was detected by mass spectrometric analysis. In addition, white octahedron A1, spectrally a type IaAB diamond, bearing platelets had a nitrogen concentration below mass-spectrometric detection limits.

There is no relationship between nitrogen content and carbon isotope ratios, and furthermore, there is no evidence for groups with high and low nitrogen contents occurring within any of the groups defined on the basis of colour. There is also no evidence for any relationship between nitrogen content and diamond shape for samples of unknown paragenesis. Amongst peridotitic diamonds (sharp edged octahedra) however, 3 of the possibly peridotitic samples (A2, A3 and A4) have significantly higher nitrogen content than the remaining 5 diamonds. Nitrogen contents are 1317, 973 and 1181 ppm respectively (see Figure 2.6).

The range, mean and median values of the nitrogen contents of the different groups of Argyle 2 mm diamonds are presented in Table 2.5.

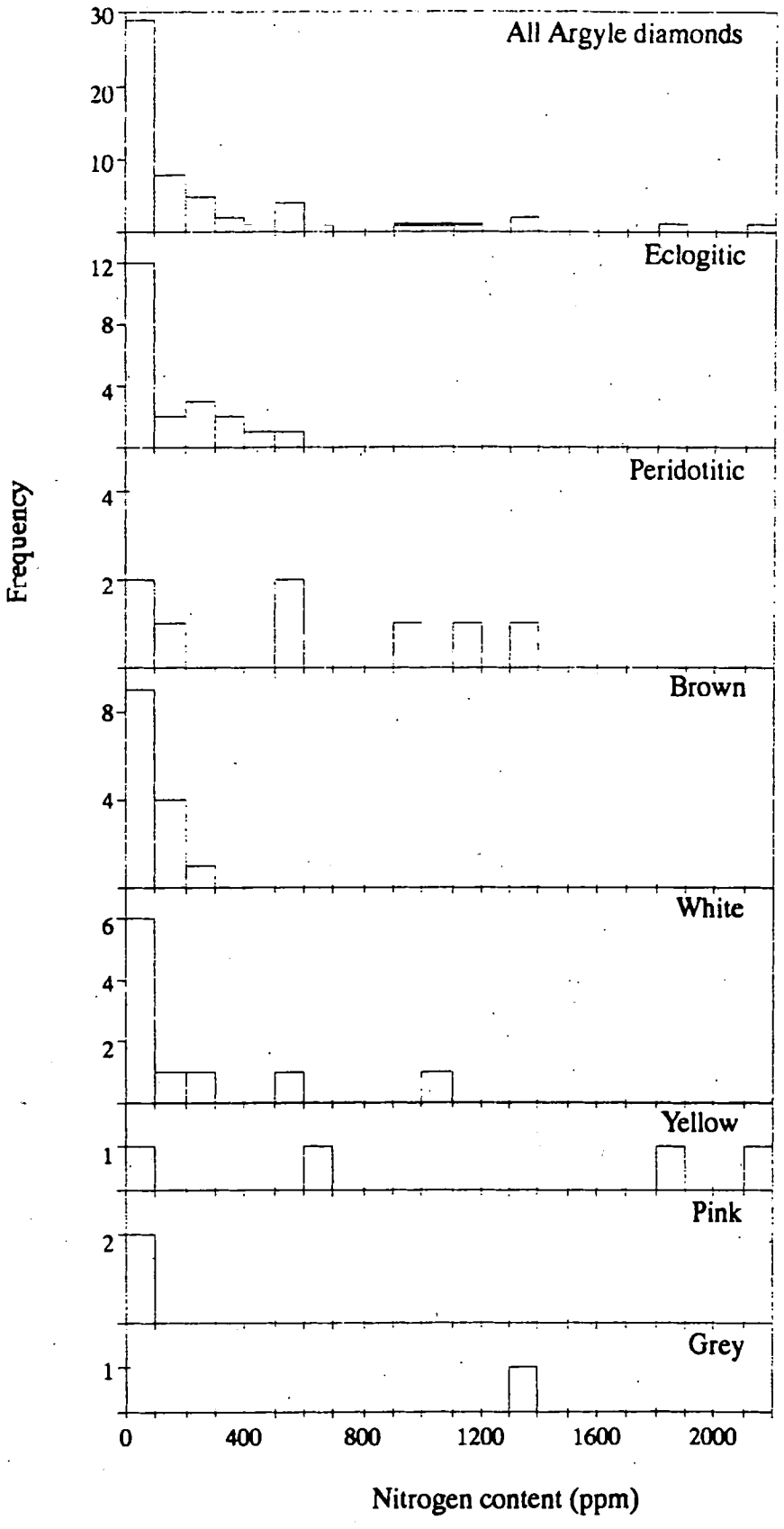

Figure 2.6: Nitrogen content histogram for Argyle 2mm diamonds. All analysed data, including measured N concentrations in diamonds that are spectral type II are displayed.

Sample	Range (ppm)	Mean and std. error on mean (ppm)		Median (ppm), population std deviation (ppm) and n.		
Eclogitic diamonds	0 to 571	153	37	55	171	21
Peridotitic diamonds	79 to 1317	620	174	568	492	8
Yellow diamonds	0 to 2198	1176	518	Not applicable		4
White diamonds	0 to 1074	220	108	92	343	10
Brown diamonds	0 to 291	92	22	62	83	14
Pink diamonds	33 and 93	63	30	Not applicable		2
Grey diamond	1364	Not applicable		Not applicable		1

Table 2.5: Descriptive statistics for nitrogen contents of Argyle 2mm diamonds.

2.2.1.2.2 Nitrogen aggregation state: Type I diamonds ranging from pure type IaA to nearly pure type IaB occur in the Argyle 2 mm diamond population, and nitrogen aggregation state seems to be related to diamond paragenesis. Samples of peridotitic paragenesis are less aggregated than samples of eclogitic paragenesis and this is illustrated in Figure 2.7.

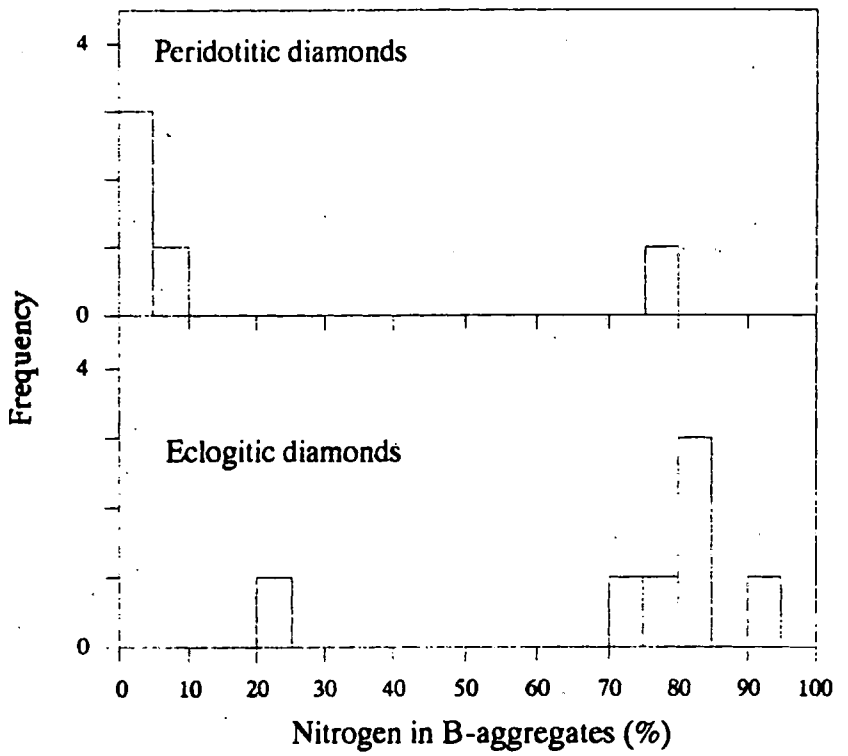

Figure 2.7: Aggregation states of eclogitic (7) and peridotitic (5) paragenesis 2mm diamonds from Argyle. Data are listed in Appendix 1.

Estimates of the proportions of nitrogen occurring in B aggregates have mean values of 18% and 73% for peridotitic and eclogitic diamonds respectively. Estimates of aggregation state for samples of unknown paragenesis are less certain, however only in yellow diamonds is any distinct correlation with colour noted. Both yellow diamonds

that contain nitrogen contain mostly A-centres. These contain 12% and 22% B-aggregates respectively. White and brown diamonds span the entire range of aggregation states from 0% to 100% B-aggregates with mean values of 50% and 51% B-aggregates. These semi-quantitative (uncertainty ≈ 40%) estimates of the proportion of nitrogen in B-aggregates were possible for 6 white and 9 brown diamonds. There is no relationship between aggregation state and diamond shape for these Argyle 2mm diamonds.

2.2.1.2.3 Nitrogen isotope variation; All 55 analysed Argyle 2 mm diamonds have nitrogen isotopic composition falling within the range -2.5‰ ≤ $\delta^{15}N$ ≤ 13.4‰ and the mean $\delta^{15}N$ value is 6.3‰. The median $\delta^{15}N$ value is 5.7‰ and the standard deviation is 3.6‰. There are 2 analyses of each of eclogitic-diamond A5, brown-octahedra A1 and grey-diamond A1. The $\delta^{15}N$ characteristics of the different groups of Argyle diamonds are presented in Table 2.6. There is no obvious relationship between diamond paragenesis and $\delta^{15}N$ value and peridotitic diamonds have $\delta^{15}N$ values within the range of eclogitic diamonds (Figure 2.8).

Sample	Range (‰)	Mean and std. error on mean (‰)		Median (‰), population std deviation (‰) and n.		
Eclogitic diamonds	-2.5 to 11.8	5.5	0.9	4.8	4.0	20
Peridotitic diamonds	0.1 to 8.5	4.9	1.0	4.6	2.9	8
Yellow diamonds	2.3 to 4.0	3.1	0.5	Not applicable		3
White diamonds	1.2 to 13.4	8.2	1.1	8.6	3.7	9
Brown diamonds	5.7 to 12.1	8.4	0.6	8.5	2.1	13
Pink diamonds	1.7 and 13.5	7.6	5.9	Not applicable		2
Grey diamond	4.5 and 4.7	4.6	0.1	Not applicable		2

Table 2.6: The $\delta^{15}N$ values of Argyle 2mm diamonds.

Amongst samples of unknown paragenesis, only yellow diamonds have distinct nitrogen isotopic composition with all three $\delta^{15}N$ values clustering in a narrow range. Pink and white diamonds have a similar range of $\delta^{15}N$ values and this encompasses the $\delta^{15}N$ values measured for brown diamonds.

There is no relationship between $\delta^{15}N$ and diamond morphology for white diamonds. For brown diamonds, octahedra and dodecahedra have similar $\delta^{15}N$ (between 6.4‰ and 12.1‰) whereas the brown macles A1, A3 and A4, have $\delta^{15}N$ values at the lower end of this range ($\delta^{15}N$ = 6.7‰, 5.7‰ and 5.7‰ respectively).

When the relationships between nitrogen isotopic composition and nitrogen content, and between $\delta^{13}C$ and $\delta^{15}N$ are considered, a number of trends are apparent (Figure 2.9 and 2.10).

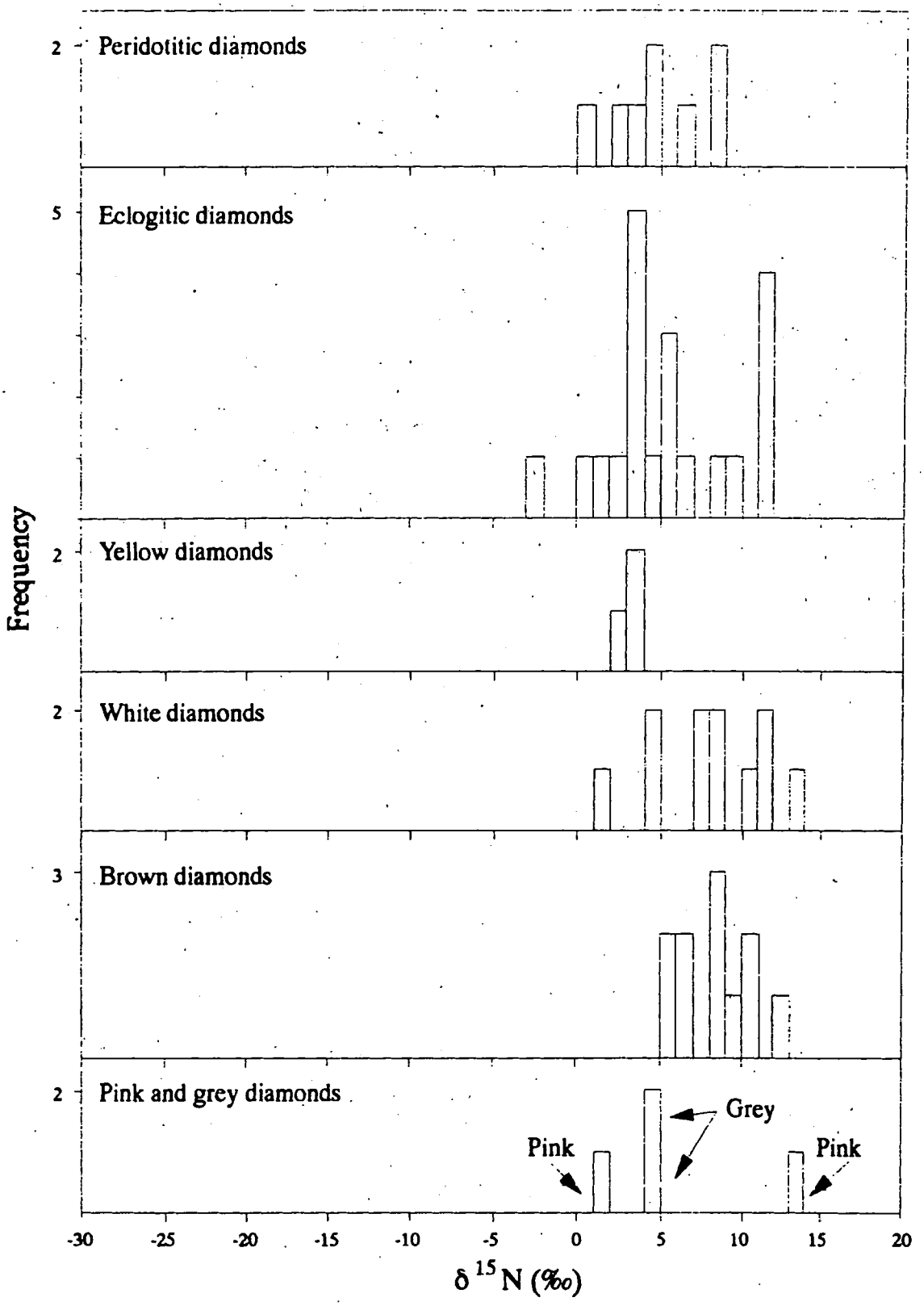

Figure 2.8: $\delta^{15}N$ histogram showing the different groups of Argyle 2 mm diamonds.

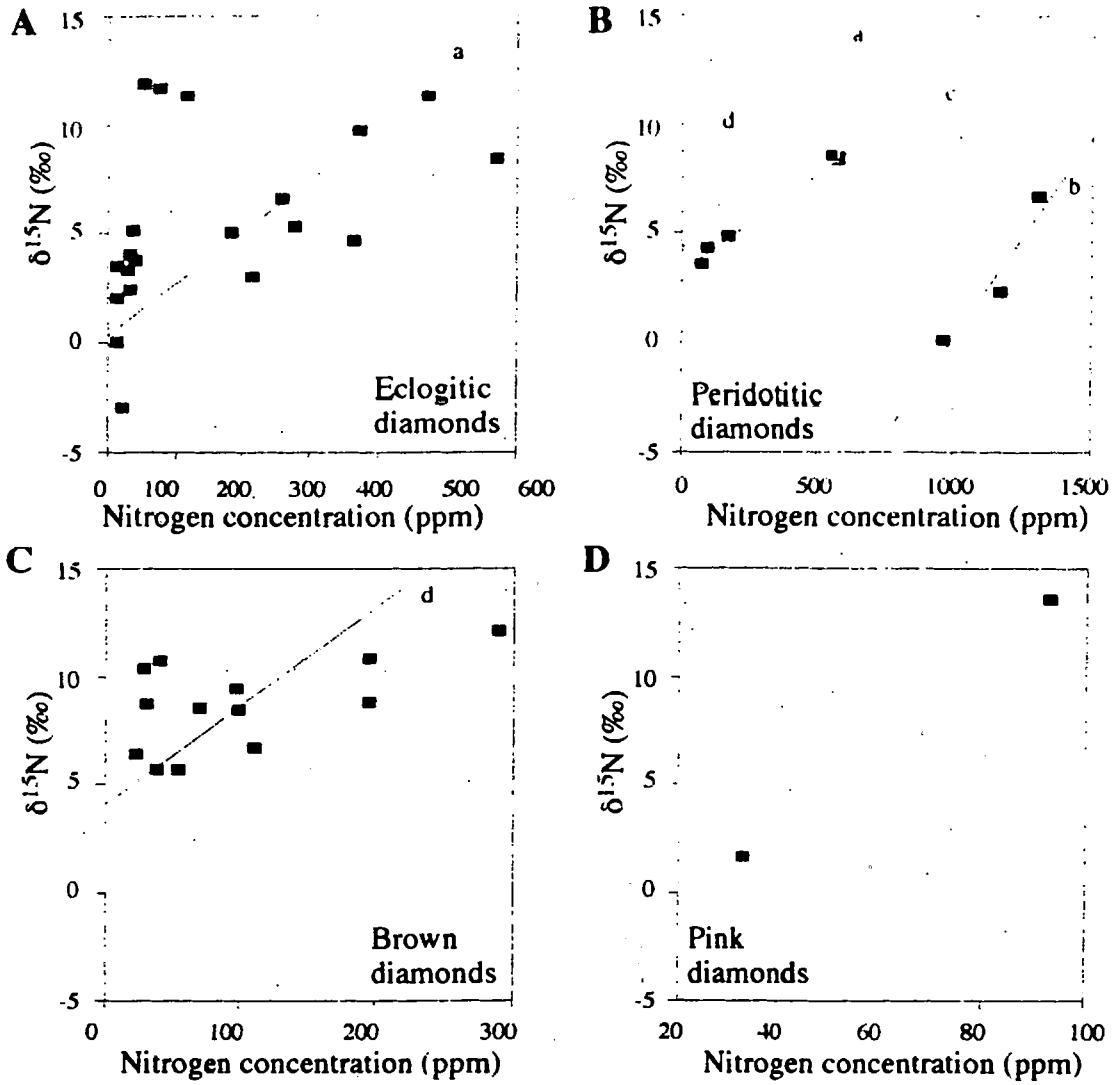

Figure 2.9: Relationship between $\delta^{15}N$ and nitrogen content for some Argyle 2 mm diamonds. Regression lines have slopes (a) = 43, (b) = 49, (c) = 106, and (d) = 22 (ppm.‰$^{-1}$) respectively. Eclogitic diamonds A22, A23 and A25 not included in fitted line. When they are included, slope drops to 19 ‰.ppm^{-1}. Correlation coefficients are 0.62, 0.91, 0.99, and 0.30 for (a), (b), (c) and (d), but the correlations are only significant at 99% confidence levels for lines (a) and (c). Lines (b) and (d) are only significant at a confidence level of 85%. The slope of a line joining the two pink diamonds has slope = 5 ppm.‰$^{-1}$.

Amongst eclogitic diamonds, there is a general trend of increasing nitrogen content with increasing $\delta^{15}N$ (Figure 2.9a), although there are three exceptions to this (A22, A23 and A25). There is no such trend when all peridotitic diamonds are considered together (Figure 2.9b). However, if peridotitic diamonds with high nitrogen content (> 950 ppm) and low nitrogen content are considered individually, then a positive correlation between $\delta^{15}N$ and nitrogen content is evident for each group (lines b & c). The brown diamonds define a broad group, and this group too, has an overall positive slope (Figure 2.9c). The two pink diamonds show the same relationship, with the sample with the lower nitrogen content having the lower $\delta^{15}N$ value (Figure 2.9d). There is no such relationship evident in either yellow diamonds or white diamonds and when all 2 mm diamonds from Argyle are considered together, the relationship is obscured.

When the covariation of carbon and nitrogen isotopic composition is considered, eclogitic and peridotitic paragenesis diamonds form overlapping clusters (Figure 2.10). There is no grouping on the basis of colour.

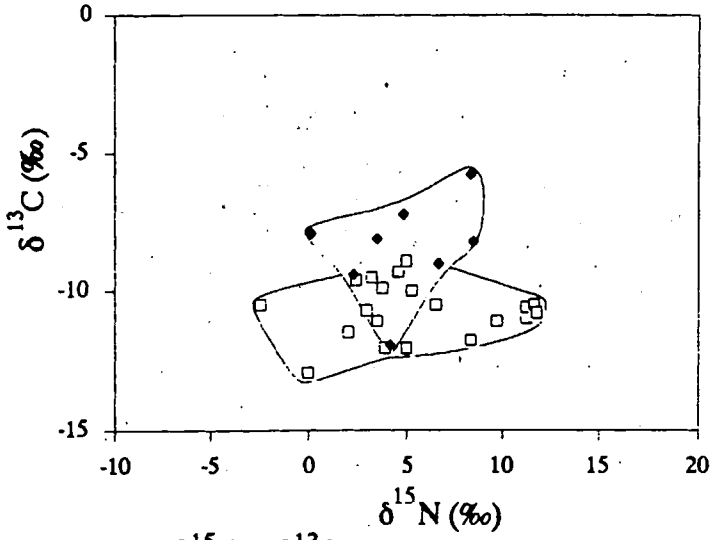

Figure 2.10: $\delta^{15}N$ - $\delta^{13}C$ plot showing eclogitic and peridotitic paragenesis diamonds. Eclogitic samples are shown by open squares and peridotitic samples by filled diamonds.

There are no correlations between the nitrogen isotopic compositions and the nitrogen aggregation state for eclogitic or peridotitic paragenesis 2 mm Argyle diamonds (Figure 2.11), despite eclogitic paragenesis diamonds persistently containing more aggregated nitrogen than peridotitic paragenesis samples. Nor is there any relationship between $\delta^{15}N$ value and the proportion of B-aggregates in brown or white coloured diamonds. In the two yellow samples for which both $\delta^{15}N$ and the proportion of B-aggregates are available, the lower $\delta^{15}N$ sample shows the least amount of nitrogen aggregation, but given that only 2 samples comprise this group, this is likely to be coincidental.

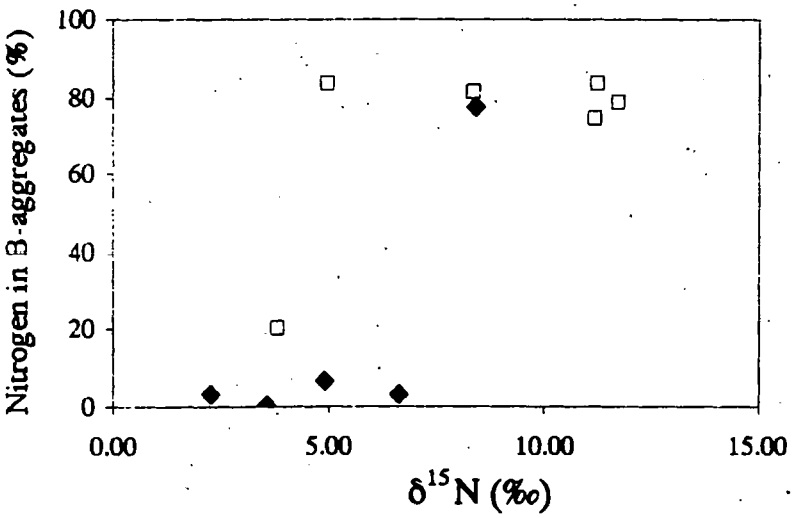

Figure 2.11: Plot of $\delta^{15}N$ *vs.* % B-aggregates for eclogitic (open squares) and peridotitic (filled squares) paragenesis diamonds.

2.2.2 Argyle diamond plates

Five diamond plates from Argyle were were supplied for this study and they had octahedral (150701 #8, #12-8, #12-1 & #12-4) or dodecahedral (150701 #1) morphology prior to cutting (C.B. Smith, Pers. Comm.). Inclusions from three of these plates were identified by laser Raman microprobe by CRAE Exploration staff and plates 150701 #1 and 150701 #8 both contain eclogitic garnet. Plate 150701 #12-8 contains an orthopyroxene of peridotitic paragenesis. The paragenesis of the remaining two (inclusion free) plates cannot be ascertained.

2.2.2.1 Cathodoluminescence

Cathodoluminescence is a technique useful for the location of low concentrations of impurities within diamonds, and is also particularly effective at revealing the internal structure of diamonds. An electron beam is directed at an earthed sample, and the excitation of electrons from the valance band to the conduction band and their subsequent return to the ground state produces a characteristic luminescence. Several optical centres of characteristic energies have been described in the recent literature (*e.g.* de Sa and Davies, 1977; Yamamoto *et al.*, 1984; Collins and Woods, 1987; Collins, 1989) and most appear to be associated with the presence of impurities in diamonds, for example nitrogen, boron, the H3 or H4 centres (Davies, 1979), or the presence of donor-acceptor pairs arranged along dislocations (Yamamoto *et al.*, 1984).

In this study, cathodoluminescence has been used qualitatively, to reveal the internal structure of diamond plates, and Argyle plates under cathodoluminescence conditions are illustrated in Figures 2.12 to 2.16. These all show various shades of the yellow-blue luminescence characteristic of nitrogen-bearing diamonds (Milledge, Pers. Comm), and all show a bright yellow rim. Streaks the same colour as the rim, run diagonally across all five diamond plates. This yellow rim is similar to that seen on many radiation damaged diamonds (Milledge, Pers. Comm.) however the scarcity of clear diamonds with the thin green coat associated with radiation damage at Argyle (Hall and Smith, 1984) suggest instead that this bright rim is not a function of radiation damage, but rather represents cathodoluminescence reflections (Harris, Pers. Comm.). The diagonal streaks may thus be reflections on the striations left by the sawing process.

The central regions of these diamond plates are characterised by a bright blue luminescence that is associated with abundant nitrogen, and this is particularly well illustrated in diamond 150701 #8. There is no evidence for a relationship between this blue luminescence and nitrogen in A-aggregates as has been reported for some diamonds (*e.g* Boyd, 1988). Surrounding this central region, is a "dead" zone with reduced, mostly yellow, luminescence in which octahedral growth zonation is evident.

2.2.2.2 Carbon isotope variation

All data for these Argyle plates are given in Figure 2.12 to 2.16, which shows the variation of carbon and nitrogen as traverses across the diamonds. The sample numbers or letters along the bottom axis represent the position in the traverse and each traverse is from one rim to the opposite rim. The centre of each diamond plate corresponds to the middle position on the bottom axis. Missing data, due to mass spectrometer malfunction, insufficient gas to analyse or the FTIR spectra indicating that the block is a piece of type II diamond and therefore nitrogen free are shown by a gap left in the traverse. Error bars are shown by vertical lines passing through data points. The traverse across diamond 150701 #8 was hampered by the large size of each of the laser-cut blocks and these were fractured prior to analysis. These analyses were then combined (weighted by the mass of the analysed fragment) to give the mean values plotted on Figure 2.13. This has a smoothing effect on the data presented in Figure 2.13.

When all the Argyle plates are considered simultaneously, these have a range in $\delta^{13}C$ values from -14.1‰ to -4.5‰ which is larger than the overall $\delta^{13}C$ variation shown by the 2 mm diamonds (Section 2.2.1.1). For the most part however, these diamond plates show only small intra-sample variations in $\delta^{13}C$ values. The Argyle plate with the greatest variation in carbon isotopic composition is 150701 #12-8 (Figure 2.12). This sample has $\delta^{13}C$ = -9.3‰ at the left hand edge of the plate, decreasing to $\delta^{13}C$ = -14.1‰ for a single block towards the centre of the diamond and then starting to rise towards the right hand edge. As only a single $\delta^{13}C$ value of -14.1‰ is available it will have to be accepted as a possible outlier, and if this is the case the rest of the diamond has a $\delta^{13}C$ value of -10.2 ± 1.5‰. A portion of the ladder section near the right hand edge (piece "H") was regrettably lost during analysis due to a mass spectrometer fault, and it is therefore impossible to comment on whether the traverse is symmetrical with respect to carbon isotopic composition.

Samples 150701 #8 (Figure 2.13) and 150701 #12-1 (Figure 2.14) show a $\delta^{13}C$ increase towards the centre of the plate. This shift towards less negative $\delta^{13}C$ values is less marked than the decrease in sample 15070 #12-8 (Figure 2.12) and the edge to centre variation of $\delta^{13}C$ is 1.3‰ for 150701 #8 and 1.3‰ for 150701 #12-1. Pieces 1 and 1A for plate 150701 #8 are relatively homogeneous for carbon, $\delta^{13}C$ varying by less than 0.3‰ in each fragment, however $\delta^{13}C$ analyses of broken fragments of piece 2 vary from -4.5‰ to -6.0‰: a range of 1.5‰. The least negative $\delta^{13}C$ value for this piece occurs in the middle of the diamond.

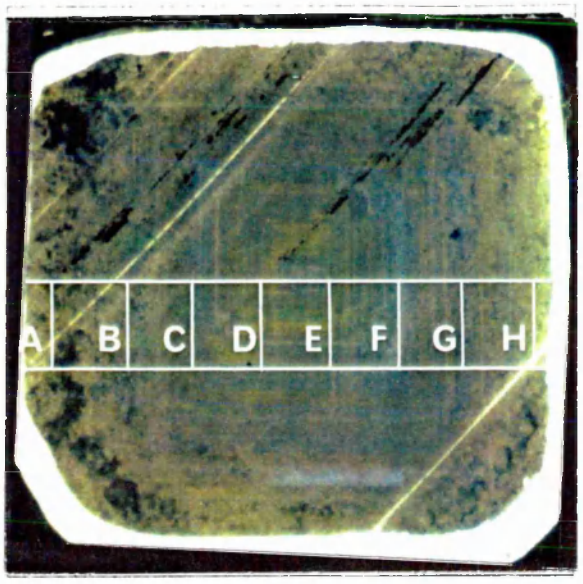

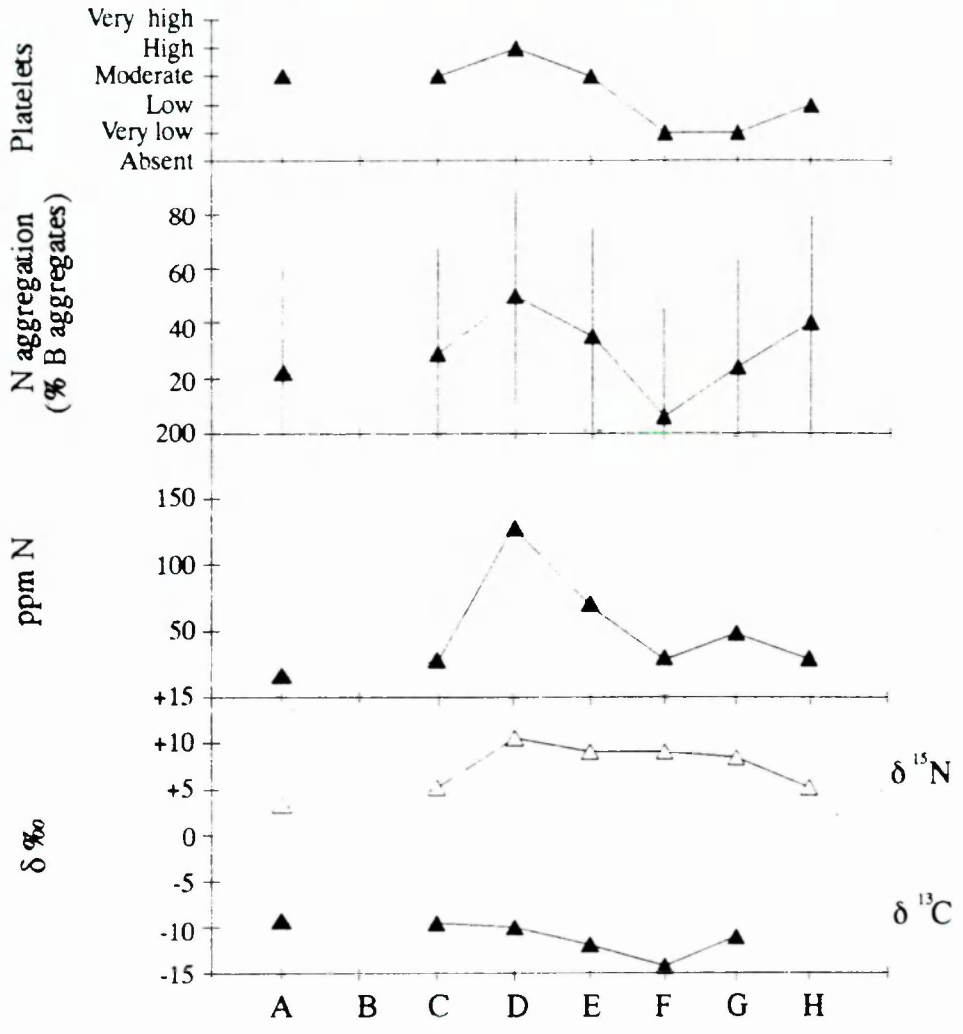

	A	B	C	D	E	F	G	H
$\delta^{13}C$ (‰)	-9.3	-	-9.3	-9.8	-11.7	-14.1	-10.8	-
$\delta^{15}N$ (‰)	3.3	-	5.4	10.6	9.1	9.1	8.6	5.5
[N] (ppm)	17	-	29	135	73	29	55	34
%B	22	-	29	50	35	6	24	40
Type	IaAB+p	-	IaAB+p	IaAB+p	IaAB+p	IaAB+p	IaAB+p	IaAB+p

Figure 2.12: Plot for 150701 #12-8. The diamond is 5mm across.

Ladder sections 150701 #1 (Figure 2.15) and 150701 #12-4 (Figure 2.16) show no clear variation of $\delta^{13}C$ with position in the across-sample traverse. There is some fluctuation in $\delta^{13}C$ values near the left hand edge of 150701 #1 (-10.1‰ to -8.7‰) but the remaining blocks all have $\delta^{13}C$ within one standard deviation (0.5‰) of the mean $\delta^{13}C$ for the complete traverse (-9.8‰). Ladder section 150701 #12-4 is the most uniform Argyle diamond plate in terms of $\delta^{13}C$ variation across the sample. The $\delta^{13}C$ values all fall within the range $-12.9‰ \leq \delta^{13}C \leq -12.3‰$ and the mean $\delta^{13}C$ value of this ladder section is -12.6‰ (σ = 0.1‰).

There is a relationship between $\delta^{13}C$ value and diamond paragenesis in that the peridotitic diamond plate 150701 #12-8 has a wider range in $\delta^{13}C$ values (4.8‰) than either of the two eclogitic plates 150701 #8 or 150701 #12-1. A comparison of the $\delta^{13}C$ values of individual plates with the 2 mm Argyle diamonds is given in Table 2.7.

	Range	Mean	Standard deviation
150701 #12-8	-14.1 to -9.3	-10.8	1.8
150701 #8	-6.6 to -4.5	-5.7	0.6
150701 #12-1	-9.1 to -7.2	-8.3	0.7
150701 #1	-10.2 to -8.7	-9.8	0.5
150701 #12-4	-12.9 to -12.3	-12.6	0.1
All 2 mm diamonds	-13.0 to -4.5	-9.9	1.6

Table 2.7: A comparison of the $\delta^{13}C$ values of individual diamond plates and the Argyle 2 mm diamonds.

2.2.2.3 Nitrogen

2.2.2.3.1 Nitrogen content: The nitrogen content of these Argyle plates is variable between 0 ppm and 1435 ppm, and the greatest fluctuations are shown in the brown diamond 150701 #8. Mean nitrogen contents in this ladder section range from 0 ppm for type II fragment 4 at the extreme edge, up to a maximum of 840 ppm for piece 1A. There is however, considerable variation within each analysed block. Block 1 was broken into two fragments which contained 402 and 145 ppm N respectively (weighted mean = 227 ppm) while the three fragments of block 1A contained 588 ppm, 1267 ppm and 1056 ppm (weighted mean = 840 ppm). The greatest within-block concentration range occurs in block 2, where fragments containing 447 ppm, 284 ppm and 1435 ppm were analysed (weighted mean = 551 ppm), and the highest concentration fragment has an edge that abuts block 1A. Block 3 was also broken into three fragments which contained 53 ppm, 124 ppm and 232 ppm respectively (weighted mean = 120 ppm).

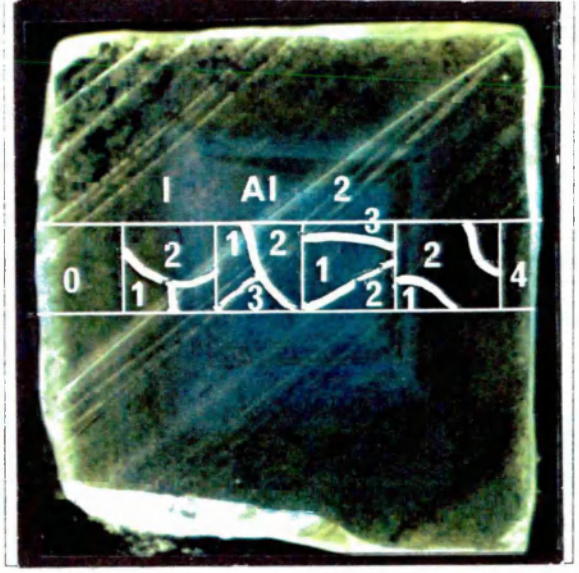

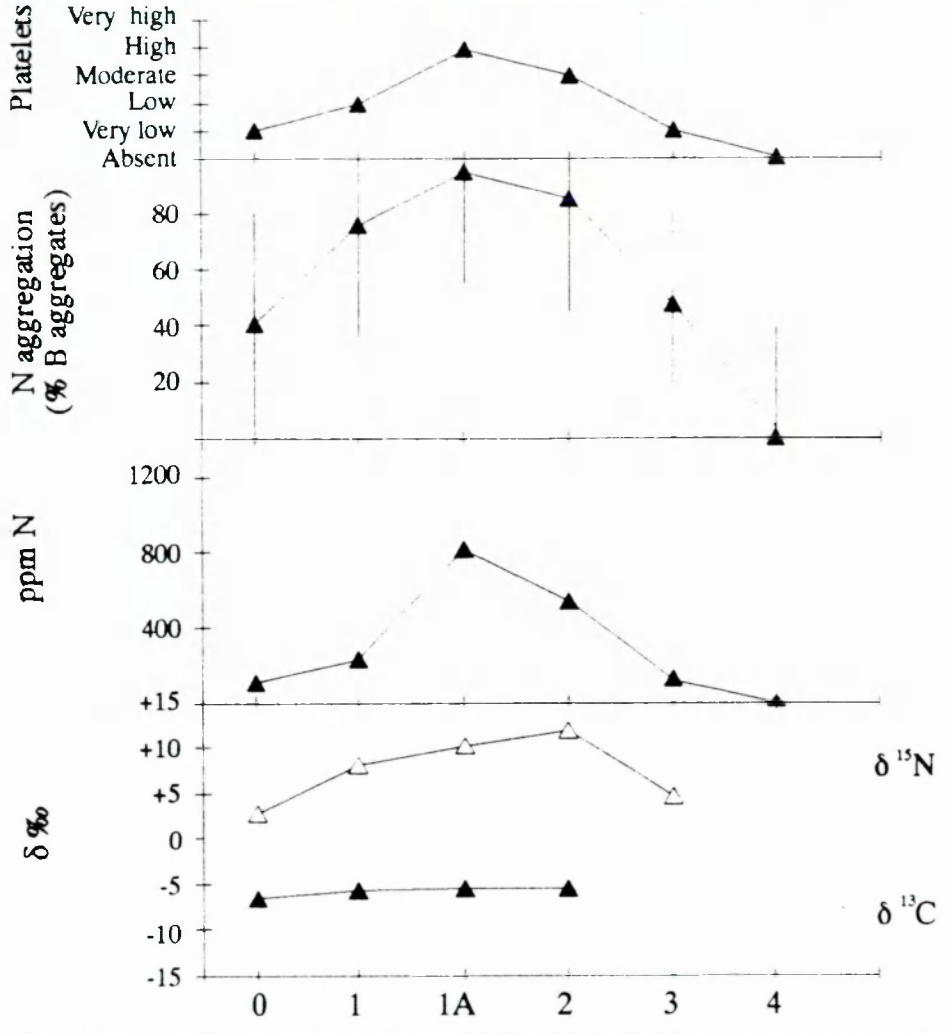

	0	1	1 A	2	3	4
$\delta^{13}C$ (‰)	-6.6	-5.8, -5.9	-5.7, -5.6, -5.5	-6.0, -4.5, -5.4	lost	lost
weighted mean		-5.8	-5.7	-5.3		
$\delta^{15}N$ (‰)	2.7	9.8, 7.1	10.5, 7.9, 13.6	12.2, 10.3, 11.1	2.5, 4.3, 8.3	-
weighted mean		8.0	10.1	11.6	4.5	
[N] (ppm)	105	402, 145	588, 1267, 1056	447, 284, 1435	53, 124, 232	-
weighted mean		227	840	551	120	
%B	38	74	94	84	45	0
Type	IaAB+p	IaAB+p	IaB+p	IaAB+p	IaAB+p	II

Figure 2.13: Plot for 150701 #8. The diamond is 5mm across.

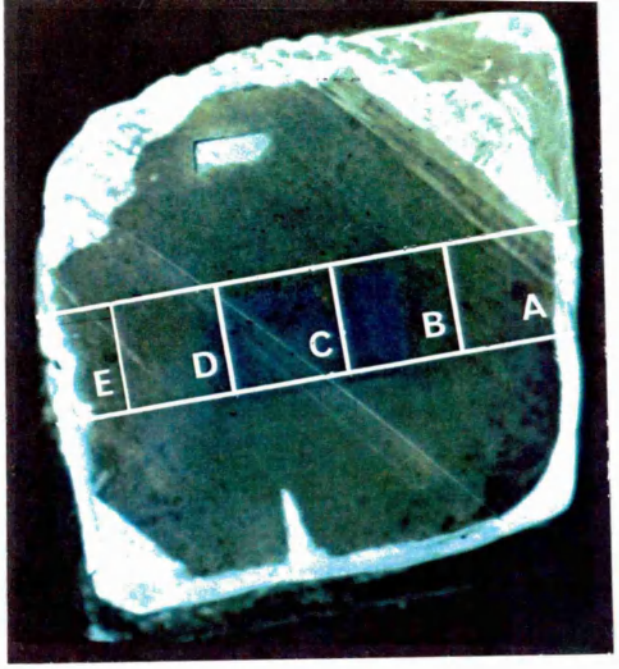

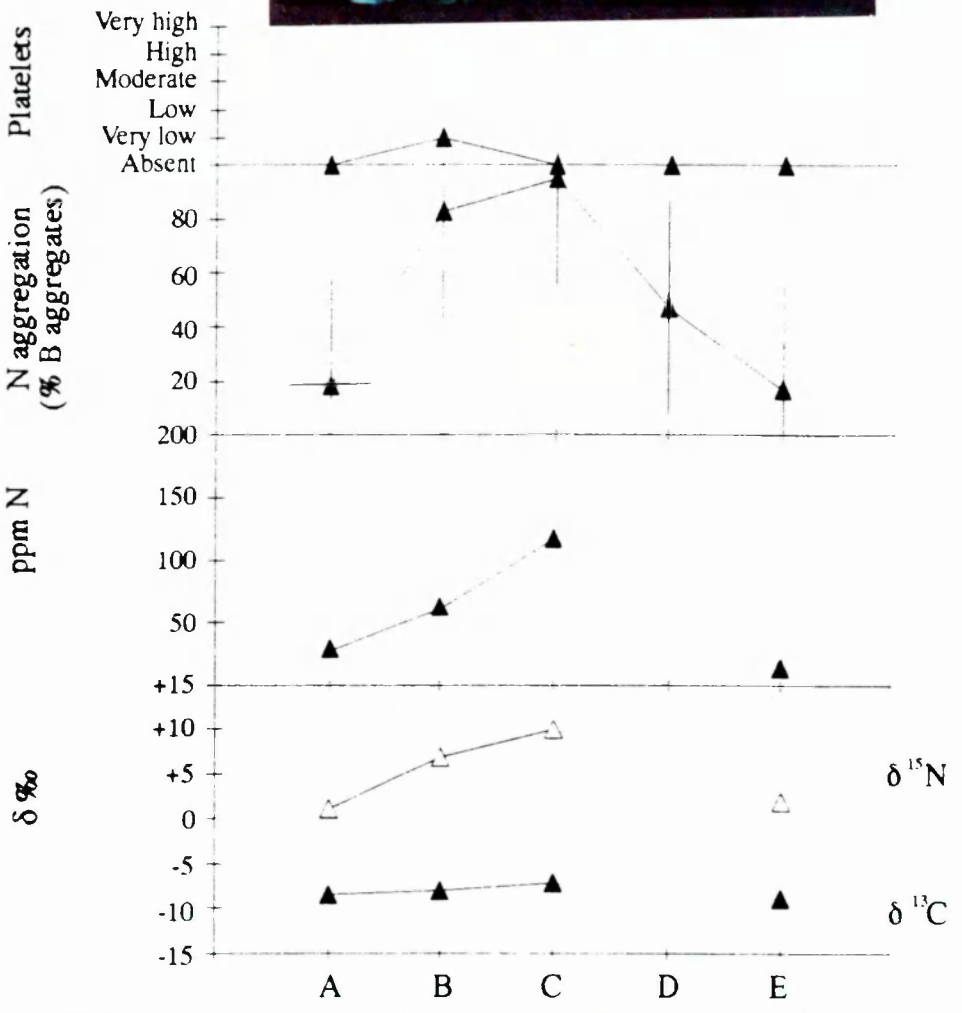

	A	B	C	D	E
$\delta^{13}C$ (‰)	-8.5	-8.0	-7.5	-	-8.9, -9.1
weighted mean					-9.0
$\delta^{15}N$ (‰)	1.1	6.9	10.0	-	0.9, 3.0
weighted mean					2.0
[N] (ppm)	41	74	123	19	23
weighted mean					21
%B	18	83	95	47	17
Type	II	IaAB+p	IaB	IaAB	IaAB

Figure 2.14: Plot for 150701 #12-1. The diamond is 5mm across.

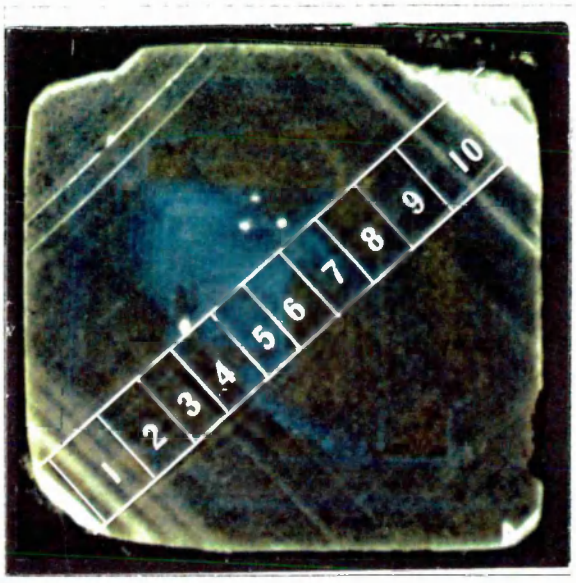

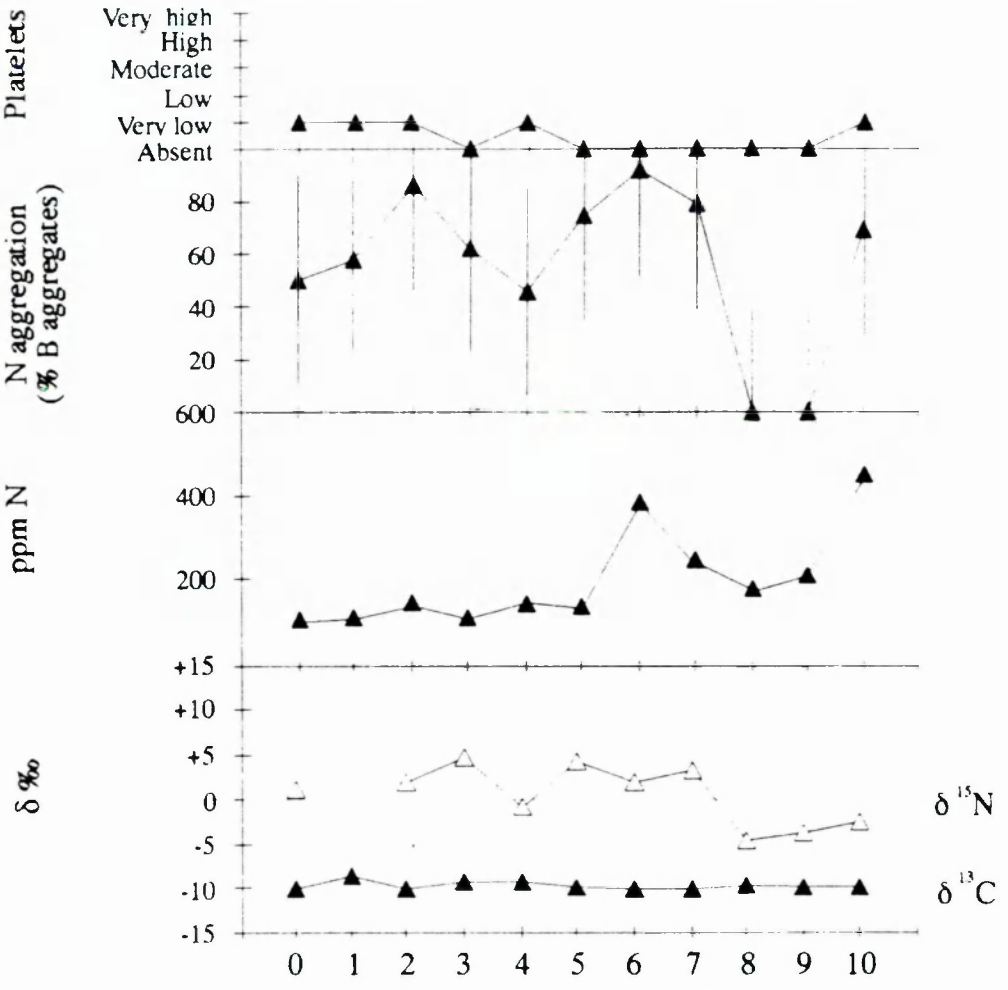

	0	1	2	3	4	5	6	7	8	9	10
$\delta^{13}C$ (‰)	-10.1	-8.7	-10.2	-9.3	-9.4	-9.9	-10.1	-10.2	-9.8	-9.9	-9.9
$\delta^{15}N$ (‰)	1.2	-	1.9	4.7	-0.7	4.2	2.0	3.3	-4.6	-3.7	-2.5
[N] (ppm)	107	107	148	110	147	140	380	247	181	203	456
%B	50	58	86	62	46	75	92	79	0	0	69
Type	IaAB+p	IaAB+p	IaAB+p	II	IaAB+p	IaB	IaB	IaAB	II	II	IaB+p

Figure 2.15: Plot for 150701 #1. The diamond is 5mm across.

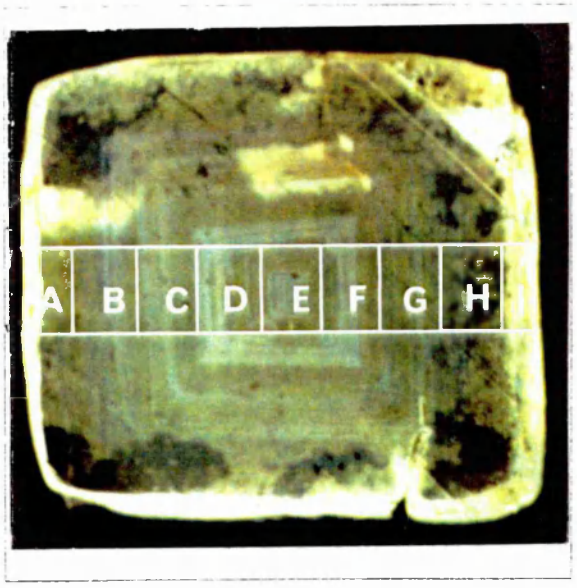

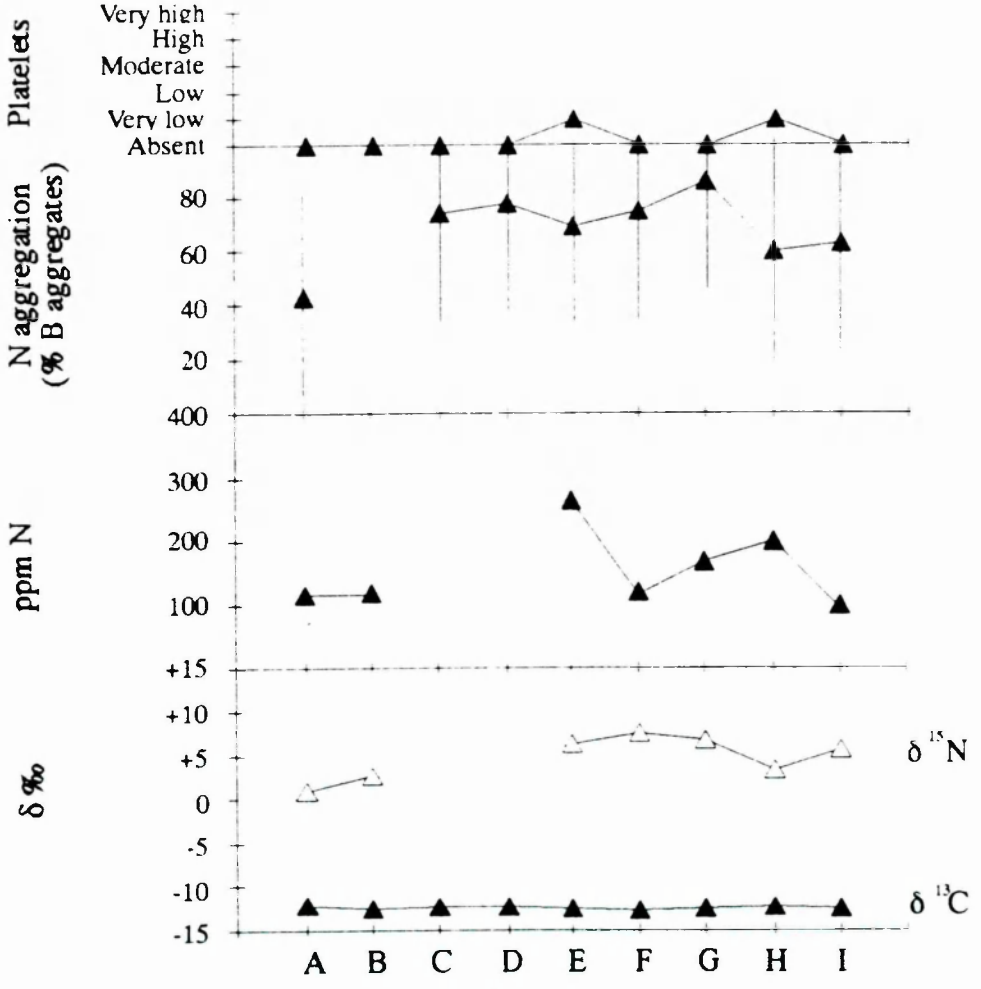

	A	B	C	D	E	F	G	H	I
$\delta^{13}C$ (‰)	-12.3	-12.6	-12.6	-12.6	-12.6	-12.9	-12.7	-12.5	-12.6
$\delta^{15}N$ (‰)	0.9	2.6	-	-	6.1	7.4	6.6	3.3	5.7
[N] (ppm)	114	106	-	-	253	108	157	192	89
%B	43	-	74	78	69	75	86	60	63
Type	IaAB+p	IaAB+p	IaB	IaB	IaB	IaB	IaAB	IaAB	IaAB

Figure 2.16: Plot for 150701 #12-4. The diamond is 5mm across.

When the mean nitrogen content of each block from 150701 #8 is considered, it is evident that nitrogen content rises from the edge of the diamond towards the centre (Figure 2.13). This same trend is evident in sample 150701 #12-1 (Figure 2.14), but here nitrogen contents of 41 ppm (left hand edge) and 21 ppm (right hand edge) bracket the highest nitrogen content of 123 ppm in the centre of the traverse (position C).

Complex nitrogen zonation patterns occur in samples 150701 #12-8 (Figure 2.12) and 150701 #12-4 (Figure 2.16). In 150701 #12-8 the highest nitrogen concentrations occur towards the central regions of the diamond and lower concentrations are found at the edges. The edge to centre variation is less regular than 150701 #8. Sample 150701 #12-4 is another diamond plate in which the highest nitrogen content occurs towards the central region (Figure 2.10) with lower nitrogen contents at the edges, but the transition between centre and edge is more complex. Zones of low and high nitrogen content alternate and this is evident in the right hand side of the traverse (positions 6 to 9) as illustrated in Figure 2.16.

The most complex pattern of nitrogen concentration zonation occurs in sample 150701 #1 (Figure 2.15). The left hand side of this ladder section is characterised by nitrogen contents lower than 150 ppm. A local maximum then occurs at position 6 (380 ppm) from which nitrogen concentration decreases to 181 ppm (position 8) before increasing again to a maximum of 456 ppm on the right edge of the ladder section. Unlike the other diamond plates, this sample was laser-sectioned on the diagonal rather than perpendicular to the growth zones which may be an explanation for the marked asymmetry of this traverse.

It must also be borne in mind that as there is nitrogen content variability on a very small scale (for example in the individual analyses of fragments of the blocks in 150701 #8), and some of the structure seen in these plates may be the result of inhomogeneity in sampling.

2.2.2.3.2 Nitrogen aggregation state; Notwithstanding the large errors associated with estimates of the proportion of nitrogen in B-aggregates, there are still three styles of aggregation state zonation evident in these Argyle plates. The first of these, shown by samples 150701 #8 and 150701 #12-1 is characterised by an increase in the proportion of B-aggregates towards the centre of the diamond plate. In the central regions of both of these samples B-aggregates are estimated to contain more than 94% of the nitrogen present.. The rims, in contrast, are characterised by 17% and 18% B-aggregates (150701 #12-1) and 38% B-aggregates (150701 #8) respectively. The right hand edge of sample 150701 #8 is made of type II diamond, which cannot, by definition contain any B-aggregates. In both of these samples, there is a relationship between nitrogen

aggregation state and nitrogen content (Figure 2.17). As nitrogen content increases, so does the proportion of B-aggregates.

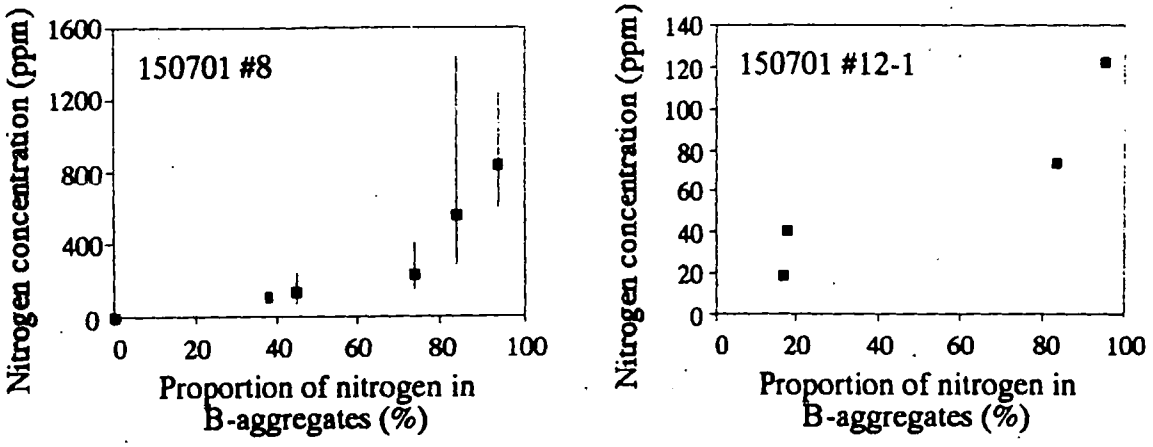

Figure 2.17: The relationship between estimates of the proportion of nitrogen in B-aggregates and nitrogen concentration for samples 150701 #8 and 150701 #12-1. These two samples show an increase of aggregated nitrogen and higher nitrogen contents in their central regions. Vertical bars show the range in nitrogen content within individual blocks.

The second aggregation state pattern is flat. Within the associated uncertainties, nitrogen aggregation state across samples 150701 #12-8 and 150701 #12-4 does not vary significantly with position in the traverse (Figure 2.13 and 2.16). It is however likely that in 150701 #12-8 the greatest amount of aggregation has occurred in the region of highest nitrogen concentration (Figure 2.12). The mean proportion of B-aggregates in 150701 #8 and 150701 #12-4 are 29% and 69% respectively.

The left hand side of diamond plate 150701 #1 also has a flat aggregation state pattern when uncertainties in the aggregation state estimates are considered (Figure 2.15). The right hand side however has a complex aggregation state pattern that, given the uncertainties involved, may be following the nitrogen abundance profile. The right hand side is marked by two blocks being spectral type II, both of which contain nitrogen (181 ppm for block 8 and 203 ppm for block 9). The U-shaped profile on the right hand side of this diamond may be an artifact, arising either as a result of the poor quality of the FTIR spectra. Alternatively, the low nitrogen contents of these two blocks may reflect the incorporation of small regions of type II diamond in the analysed fragment, implying a markedly heterogeneous diamond.

2.2.2.3.3 Nitrogen isotope variation; The $\delta^{15}N$ zonation evident in these Argyle plates is, for the most part, relatively simple. The diamond plate with the greatest variation in measured $\delta^{15}N$ is, as for nitrogen abundance, plate 150701 #8 which has a minimum $\delta^{15}N$ value of 2.5‰ (fragment 2, block 3) and a maximum $\delta^{15}N$ = 13.6‰ (fragment 3, block 1A) giving a range of 11.1‰. When the mean $\delta^{15}N$ value of each block is considered however, their nitrogen isotopic compositions fall within the range

2.7‰ ≤ $\delta^{15}N$ ≤ 11.7‰. This sample also shows the most simple zonation pattern, with the highest $\delta^{15}N$ values occurring in the centre of the plate (positions 1A and 2) and the lowest $\delta^{15}N$ values occurring at or towards the the edges (Figure 2.13).

Two other samples have $\delta^{15}N$ values increasing regularly towards the centre. In sample 150701 #12-1, edge $\delta^{15}N$ values are low, 1.1‰ and 1.9‰ respectively, and the maximum measured $\delta^{15}N$ value of 10.0‰ is for a block in the middle of the plate (Figure 2.14). Lower $\delta^{15}N$ values also occur at the edges of 150701 #12-8 ($\delta^{15}N$ = 3.3‰ and 5.5‰) when compared to blocks from the middle of this ladder section ($\delta^{15}N$ = 9.1‰ to 10.6‰), but the transition from centre to edge not perfectly symmetrical (Figure 2.12).

The highest $\delta^{15}N$ measurement from ladder section 150701 #12-4 occurs in block E ($\delta^{15}N$ = 7.4‰), just off centre, while the lowest measured $\delta^{15}N$ value of 0.9‰ is for the block on the leftmost edge. The right-hand side of this sample is characterised by a kick towards a higher $\delta^{15}N$ value of 5.7‰ (see Figure 2.16), and thus the concave-down $\delta^{15}N$ zonation evident in diamond plates 150701 #12-8, 150701 #8 and 150701 #12-1 is not apparent here.

The most complex $\delta^{15}N$ profile is that found in ladder section 150701 #1. The right hand side where type II diamond occurred is characterised by negative $\delta^{15}N$, and this is the only Argyle plate with $\delta^{15}N$ < 0‰. For blocks 10 to 8, $\delta^{15}N$ values decrease from -2.5‰ at the edge of the diamond to -4.6‰ moving inwards. The next block in, has a positive $\delta^{15}N$ (3.3‰), and nitrogen isotopic variations across the central region of this diamond fluctuates in the range -0.7‰ ≤ $\delta^{15}N$ ≤ +4.7‰. The left hand edge is characterised by low, but positive $\delta^{15}N$ (1.2‰ to 1.9‰). This profile is illustrated on Figure 2.15.

When nitrogen content is plotted against the $\delta^{15}N$ value (Figure 2.18), a broad group for plate 150701 #8 is defined and this is characterised by a positive slope. Diamonds 150701 #12-1 and 150701 #12-8 form nearly linear trends, also with positive slope, while no trends are apparent for samples 150701 #1 and 150701 #12-4.

The variable nitrogen concentration range in these Argyle plates (up to to 1435 ppm) prevents direct comparison of these trends, and in Figure 2.19, nitrogen isotopic composition is plotted against nitrogen content expressed as a percentage of the maximum measured nitrogen content within each individual plate. From Figure 2.19 it is evident that in the three Argyle diamonds in which nitrogen content and aggregation state are related, *vis.* 150701 #12-8, 150701 #8 and 150701 #12-1, the covariation of nitrogen content and $\delta^{15}N$ defines regular trends. These have important implications for the fractionation of nitrogen isotopes and the possibility that they may represent mixing or Rayleigh distillation curves will be discussed in detail in a later section. It is also worth

noting that samples 150701 #8 and 150701 #12-1 which show the best nitrogen trends (Figures 2.13 and 2.14) are also the two samples in which there is a slight increase in the $\delta^{13}C$ values towards the centre of the plate.

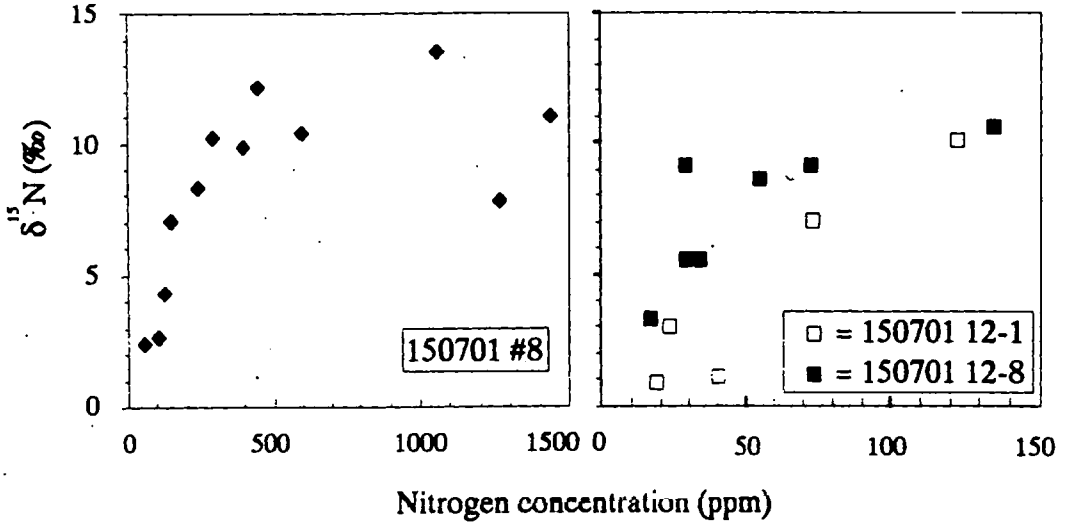

Figure 2.18: Nitrogen isotopic composition plotted against nitrogen content for Argyle plates 150701 #12-8 (Filled squares), 150701 #8 (Filled diamonds) and 150701 #12-1(Open squares). No groupings are apparent for the remaining Argyle plates.

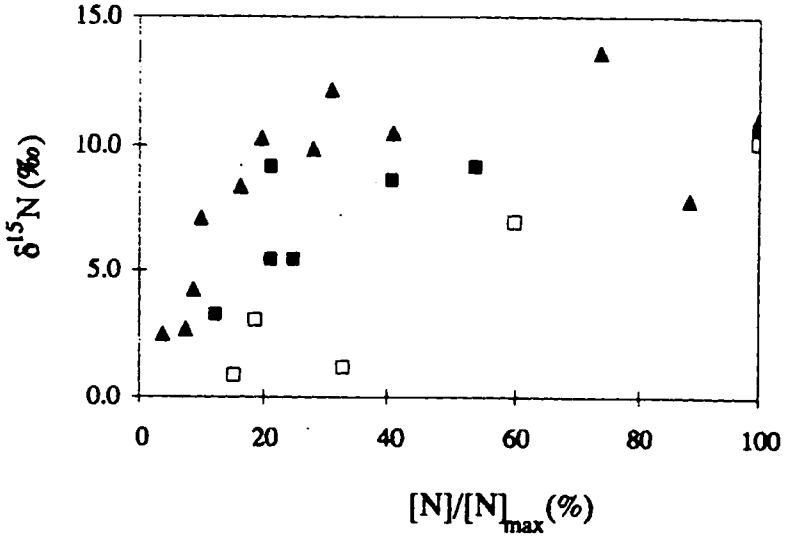

Figure 2.19: $\delta^{15}N$ plotted against normalised nitrogen concentration for Argyle plates 150701 #12-8 (Filled squares), 150701 #8 (Filled triangles) and 150701 #12-1 (Open squares). Normalising values are 135 ppm, 1435 ppm and 123 ppm respectively.

Nitrogen and carbon isotope covariation for Argyle plates is plotted in Figure 2.20, and from this, it is apparent that, with the exception of 150701 #12-8, plates show little variation in $\delta^{13}C$ value over a wide range of $\delta^{15}N$ values. In samples 150701 #1 and 150701 #12-8 there is no apparent relationship between $\delta^{15}N$ and $\delta^{13}C$. There is a slight positive slope to the $\delta^{15}N$ - $\delta^{13}C$ group for diamonds 150701 #8 and 150701 #12-1 and a negative slope in the case of 150701 #12-4. Such relationships are unusual and may be related to isotopic fractionation processes differentially affecting carbon and nitrogen isotopes. This possibility is discussed in Chapter 3.

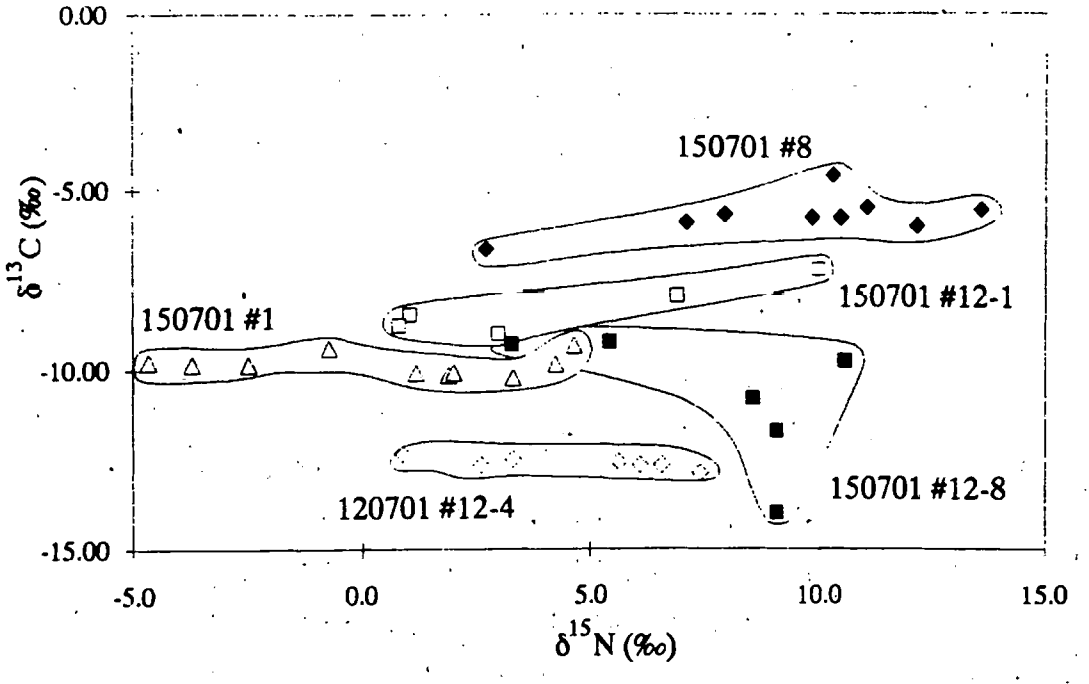

Figure 2.20: $\delta^{15}N$ - $\delta^{13}C$ plot for Argyle diamond plates, 150701 #12-8 (filled squares), 150701 #8 (filled diamonds), 150701 #12-1 (open squares), 150701 #1 (open triangles) and 150701 #12-4 (open diamonds).

Estimates of the proportion of nitrogen in B-aggregates for all Argyle plates is plotted against $\delta^{15}N$ in Figure 2.21.

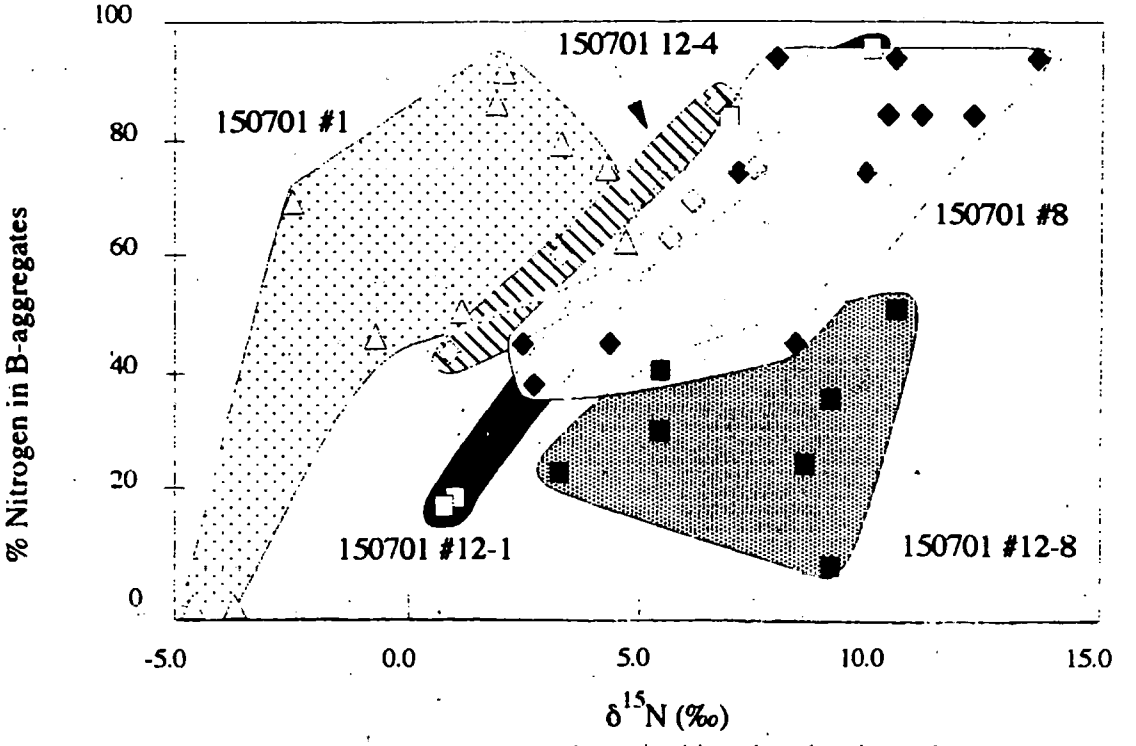

Figure 2.21: Nitrogen isotopic composition plotted against estimates of nitrogen in B-aggregates.

Although there is considerable scatter in the data, a crude positive correlation is visible for plates 150701 #8, 150701 #12-1 and 150701 #12-4. Diamond 150701 #12-8 defines a broad group, with no apparent relationship between $\delta^{15}N$ and the proportion of nitrogen

in B-aggregates. Sample 150701 #1 also defines a broad group, distorted by the presence of two blocks that are spectral type II, yet contain sufficient nitrogen for isotopic analysis. If the uncertainty in these data are considered, there is no apparent relationship between B-aggregates and $\delta^{15}N$ for this sample.

2.2.3 Comparison of plates and 2 mm diamonds from Argyle

The 5 diamond plates resemble 2 mm diamonds in all respects. Measured nitrogen content and nitrogen aggregation states from diamond plates fall within the ranges defined by 2 mm diamonds and mean nitrogen content and aggregation state values are between the mean values for Argyle eclogitic and peridotitic diamonds. The isotopic compositions of these plates, also have mean δ values ($\delta^{13}C$ = -9.5‰, $\delta^{15}N$ = +5.1‰) between the eclogitic and peridotitic diamond mean values (See Table 2.3). In addition to similar mean $\delta^{13}C$ and $\delta^{15}N$ values, there are only slight differences in the isotopic composition ranges of diamond plates and the 2 mm diamonds. For 2 mm diamonds, $\delta^{13}C$ ranges from -13.0‰ to -4.5‰ and the corresponding range for diamond plates is from $\delta^{13}C$ = -14.1‰ to -4.5‰. For nitrogen, 2 mm diamonds have $\delta^{15}N$ ranging from -2.5‰ to +13.5‰ and the range in diamond plates is from $\delta^{15}N$ = -4.6‰ to +13.6‰. This is illustrated in Figure 2.22.

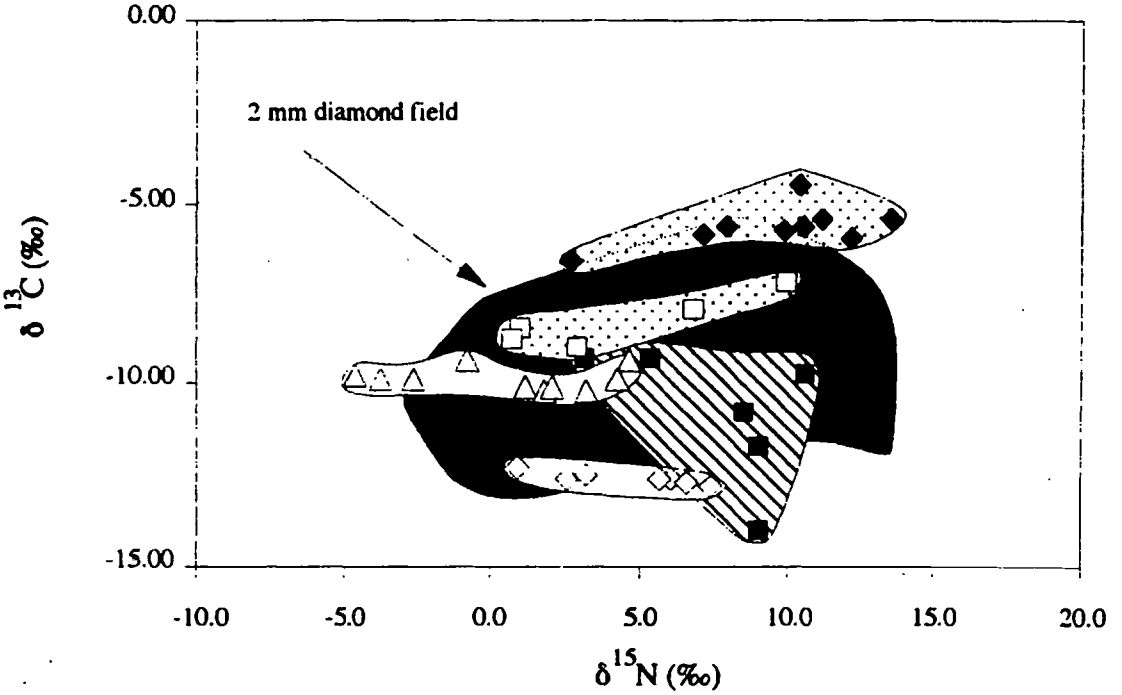

Figure 2.22: $\delta^{15}N$ - $\delta^{13}C$ plot showing individual diamond plates superimposed on a field for all Argyle diamonds. Plot symbols as for Figure 2.20 and 2.21.

Amongst individual plates however, the variation of both $\delta^{15}N$ and $\delta^{13}C$ values is less than the overall variation seen in all 2 mm diamonds. The maximum intra-sample variation of $\delta^{13}C$ is 4.8‰, in sample 150701 #12-8, and the maximum variation of $\delta^{15}N$

is 11.1‰ which occurs in sample 150701 #8. Corresponding maximum variations for 2 mm diamonds are 8.4‰ in $\delta^{13}C$ values, and 16‰ in $\delta^{15}N$ values, but the maximum isotopic difference between nearest-neighbours is only $\delta^{13}C$ = 1.3‰ and $\delta^{15}N$ = 2.5‰. Nearest-neighbour isotopic differences are thus less than the intra-sample $\delta^{13}C$ and $\delta^{15}N$ variation. This is significant in that it indicates that the variability observed in the 2 mm diamond population may be accounted for by the heterogeneity inherent within Argyle diamonds.

2.2.4 Ellendale 2 mm diamonds

Nineteen 2 mm diamonds from Ellendale 4 and 27 from Ellendale 9 are described in this section. Samples are separated on whether they are inclusion-bearing or inclusion-free, and 8 of the inclusion-bearing Ellendale 9 diamonds have had their inclusion mineral paragenesis investigated by CRA/ADM mineralogists, using Raman spectroscopy. Three of these are of peridotitic paragenesis (E9006, E9008 and E9013) and contain colourless to pale green inclusions, while the remaining 5 (E9001, E9002, E9004, E9007 and E9012) contain eclogitic paragenesis, orange garnet inclusions. There are replicate analyses for one eclogitic (E9012) and one peridotitic (E9013) diamond. The parageneses of Ellendale 4 inclusions are not known.

2.2.4.1 Carbon isotopic composition

Ellendale 4 two mm diamonds have the narrowest range of $\delta^{13}C$ values seen in this study, with a maximum $\delta^{13}C$ of -2.0‰ and a minimum of -6.2‰. When inclusion-bearing and inclusion-free samples are considered individually, these ranges are slightly narrowed (Table 2.8). Mean and median $\delta^{13}C$ values for all samples (-4.6‰ and -4.7‰ respectively) are very similar, although inclusion-bearing samples are marginally ^{13}C depleted (*i.e.* have more negative $\delta^{13}C$) relative to inclusion-free samples. This is reflected in the mean $\delta^{13}C$ values of inclusion-bearing and inclusion-free diamonds differing by 0.6‰ (See Table 2.8). The corresponding difference in median $\delta^{13}C$ values is 1.1‰. A $\delta^{13}C$ histogram for all 2mm diamonds from Ellendale 4 is shown in Figure 2.23.

In contrast to Ellendale 4 samples, 2 mm diamonds from Ellendale 9 have a far wider range in $\delta^{13}C$ values (Table 2.8), and both inclusion-free and inclusion-bearing diamonds have similar $\delta^{13}C$ ranges. Inclusion-free samples are however, marked by a single outlier with a very negative $\delta^{13}C$ (E9015: $\delta^{13}C$ = -22.1‰). The remaining inclusion-free samples fall within the range $-7.7‰ \leq \delta^{13}C \leq -4.3‰$. Descriptive statistics for both inclusion-bearing and inclusion-free samples are presented in Table 2.8, and sample E9015 is included in the calculated mean and median values for

inclusion-free samples. When this sample is omitted, the median $\delta^{13}C$ value shifts to -5.5‰ and the mean $\delta^{13}C$ value becomes -4.9‰.

Sample	$\delta^{13}C$ Range (‰)	Mean and std. error on mean (‰)		Median (‰), population std deviation (‰) and n		
All Ellendale 4	-6.2 to -2.0	-4.6	0.3	-4.7	1.2	21
E4 Inclusion-bearing	-6.2 to -3.1	-4.9	0.4	-5.0	1.1	10
E4 Inclusion free	-5.8 to -2.0	-4.3	0.3	-3.8	1.2	11
All Ellendale 9	-22.1 to -0.0	-7.8	1.0	-5.8	5.4	29
E9 Inclusion free	-22.1 to -4.3	-7.1	1.2	-6.0	4.4	14
E9 Inclusion-bearing	-21.7 to -0.0	-8.6	1.6	-5.8	6.2	15
E9 Eclogitic	-21.7 to -8.5	-14.1	2.1	-13.4	5.0	6
E9 Peridotitic	-5.8 to -3.0	-4.9	0.7	Not applicable		4

Table 2.8: Descriptive statistics for $\delta^{13}C$ values from Ellendale 2 mm diamonds.

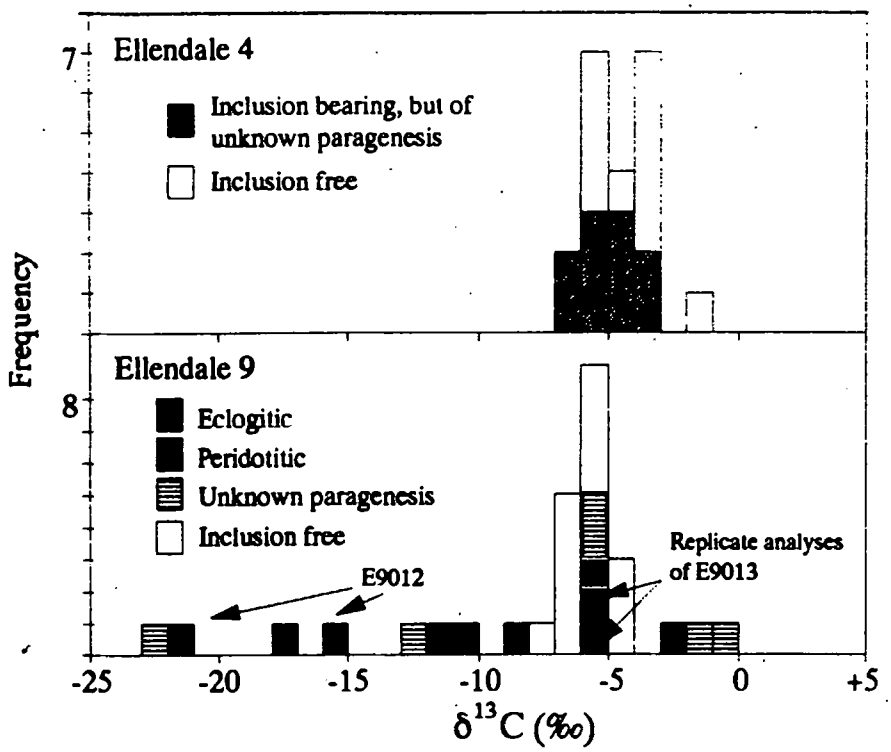

Figure 2.23: $\delta^{13}C$ histogram for Ellendale 4 and Ellendale 9 two millimeter diamonds. Ellendale 9 samples of known paragenesis are identified. Replicate analyses (E9012 and E9013) are shown.

Ellendale 9 diamonds of known paragenesis have distinct $\delta^{13}C$ distributions. Eclogitic samples E9001, E9002, E9004, E9007 and E9012 (two analyses) have more negative $\delta^{13}C$ than peridotitic samples E9006, E9008 and E9013 (two analyses) and this is illustrated in Figure 2.23. There is no overlap between the two parageneses in the analysed 2mm diamonds from Ellendale 9.

2.2.4.2 Nitrogen

2.2.4.2.1 Nitrogen content; The maximum nitrogen contents of the Ellendale 2 mm diamonds are high; up to 4125 ppm for Ellendale 4 and 4438 ppm for Ellendale 9, and there is considerable variation amongst diamonds from each lamproite. Nitrogen free diamonds occur at both Ellendale 4 and Ellendale 9. A single type II specimen from Ellendale 9 was identified, and sample E4014 from Ellendale 4 did not contain sufficient nitrogen for analysis, despite having a type IaAB FTIR spectrum. Despite having similar ranges in nitrogen content (Table 2.9), the distributions from Ellendale 4 and Ellendale 9 are distinct (Figure 2.24). Ellendale 4 samples are characterised by higher mean and median nitrogen contents (1240 ppm and 1205 ppm) than Ellendale 9 diamonds (717 ppm mean nitrogen content, median = 283 ppm), and this is indicative of Ellendale 4 having a larger proportion of nitrogen-rich diamonds than Ellendale 9. At Ellendale 9, 13 out of 28 analyses are of less than 100 ppm nitrogen (46%) while at Ellendale 4, only 2 out of 21 analyses are of this low a nitrogen content (9.5%). Less than half the Ellendale 9 samples (42%) contain more than 500 ppm nitrogen, yet more than 70% (15 out of 21) of the Ellendale 4 diamonds have nitrogen contents of more than 500 ppm.

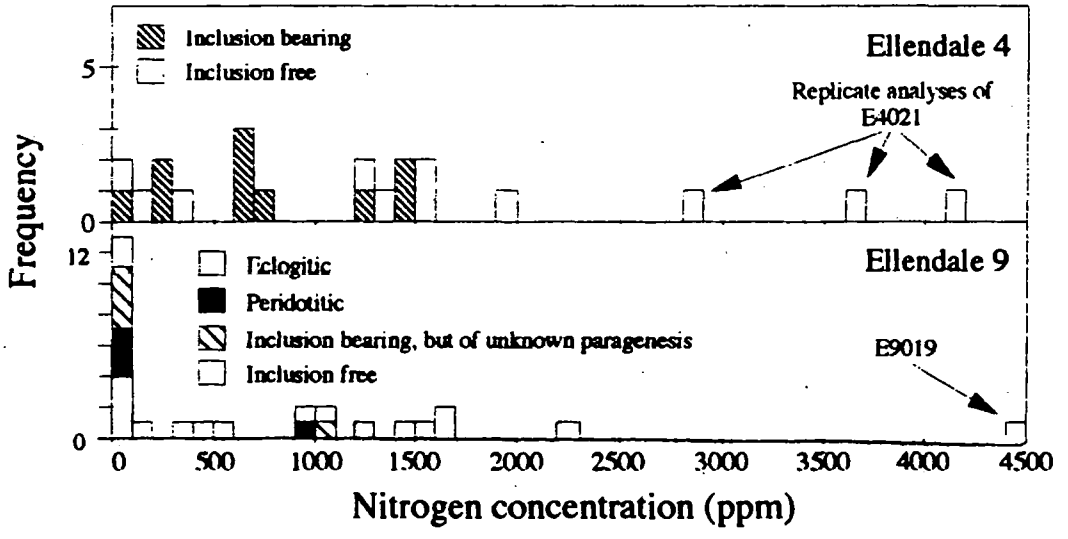

Figure 2.24: Nitrogen content of Ellendale 4 and Ellendale 9 two millimeter diamonds. Replicate analyses of E9012 and E9013 all fall within the first class for Ellendale 9.

At both Ellendale 4 and Ellendale 9, inclusion-bearing samples have a smaller range of nitrogen contents (up to 1425 ppm for Ellendale 4; up to 1413 ppm for Ellendale 9) than their inclusion-free counterparts and in each case, mean (and median) nitrogen contents are lower for inclusion-bearing than for inclusion free samples (See Table 2.9).

Of the Ellendale 9 samples of identified paragenesis, eclogitic diamonds have a wider range in nitrogen content than peridotitic diamonds, and they have a higher mean nitrogen content. Two of the five eclogitic diamonds contain more than 1000 ppm nitrogen (E9001, 1294 ppm and E9004, 1413 ppm), while the remainder contain less than 63 ppm

(63 ppm, 0 ppm and 17 to 27 ppm for E9002, E9007 and E9012). Peridotitic diamonds include only a single sample with high nitrogen content (E9006, with 904 ppm). E9008 and E9013 contain 27 ppm and 45 to 48 ppm respectively.

Sample	Range (ppm)	Mean and std. error on mean (ppm)		Median (ppm), population std deviation (ppm) and n		
All Ellendale 4	0 to 4125	1240	248	1205	1136	21
E4 Inclusion-bearing	60 to 1425	730	155	674	489	10
E4 Inclusion free	0 to 4125	1703	412	1502	1366	11
All Ellendale 9	0 to 4438	717	186	283	985	28
E9 Inclusion free	9 to 4438	1153	336	923	1211	13
E9 Inclusion-bearing	0 to 1413	338	137	45	532	15
E9 Eclogitic	0 to 1413	468	280	45	686	6
E9 Peridotitic	27 to 904	256	216	Not applicable		4
E9 Unknown	13 to 1082	248	209	Not applicable		5

Table 2.9: Descriptive statistics for the nitrogen content of Ellendale 2 mm diamonds.

There is some within-sample heterogeneity. Analyses of three fragments of E4021 yielded 2872, 3650 and 4125 ppm nitrogen. Two fragments of the eclogitic diamond E9012 had nitrogen contents of 27 and 16 ppm respectively and two fragments of the peridotitic diamond E9013 contained 45 ppm and 48 ppm nitrogen. For both of these diamonds, each fragment had the same $\delta^{13}C$ value but different $\delta^{15}N$ values.

There is no relationship between nitrogen content and carbon isotopic composition for any of the Ellendale two millimeter diamonds.

2.2.4.2.2 Nitrogen aggregation state: Despite the large errors associated with estimates of the proportion of nitrogen occurring in B-aggregates, it is evident from Figure 2.25 that the majority of Ellendale samples contain poorly aggregated nitrogen (*i.e.* near type IaA diamonds dominate).

Diamonds from both lamproites have similar ranges in the proportion of B-aggregates; namely 5 to 80% B-aggregates at Ellendale 4 and 0 to 100% B-aggregates at Ellendale 9. However the mode for Ellendale 4 diamonds is at 10 to 20% B-aggregates, with a single outlier at 80% B-aggregates. The Ellendale 9 diamonds have an extended distribution from a peak occurring at 0 to 10% B-aggregates, to 100% B-aggregates. The effect is that a higher proportion of aggregated diamonds occur amongst the Ellendale 9 samples than amongst the Ellendale 4 samples. Only 1 (out of 26) Ellendale 4 diamonds contains more than 50% B-aggregates, while 4 (out of 25) of the Ellendale 9 diamonds contain such highly aggregated nitrogen.

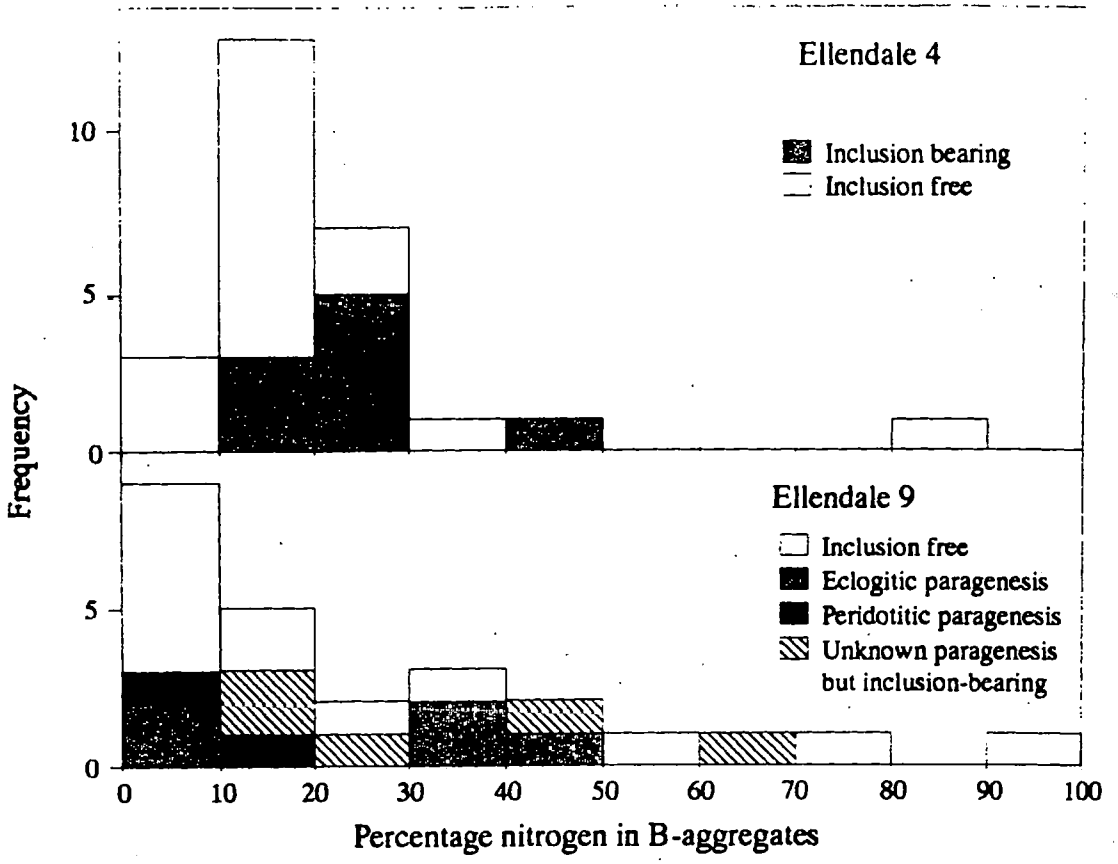

Figure 2.25: Histogram showing the distribution of nitrogen in B-aggregates for Ellendale 4 and Ellendale 9 samples. For Ellendale 4, mean = 21%, σ = 15% and n = 26. For Ellendale 9, mean = 26%, σ = 25%, median = 17% and n = 25.

There is no grouping in nitrogen aggregation state amongst Ellendale 4 diamonds on the basis of colour, morphology or carbon isotopic composition and the same holds for Ellendale 9 diamonds. Amongst Ellendale 9 diamonds of known paragenesis, eclogitic samples have a wider range in the proportion of B-aggregates (0 to 46%) than peridotitic samples (6 to 17%), and they also have higher mean (24% *cf.* 12%) and median (31% *cf.* 12%) values. The large uncertainties associated with these data, and the scarcity of samples of known paragenesis from Ellendale 9, means that, at present, the difference between eclogitic and peridotitic diamonds in terms of nitrogen aggregation state is at best equivocal, but does warrant further examination.

2.2.4.2.3 Nitrogen isotopic composition; The isotopic composition of 2 mm diamonds from Ellendale 4 falls within the range -10.4‰ $\leq \delta^{15}N \leq$ +3.7‰ and there is an even spread of values, with no significant peak, between these two extremes. Ellendale 9 diamonds of the same size have a wider range of nitrogen isotopic compositions, from $\delta^{15}N$ = -9.3‰ to $\delta^{15}N$ = +9.9‰ and also show an even spread of $\delta^{15}N$ values. The mean and median $\delta^{15}N$ values of Ellendale 4 diamonds (-2.3‰ and -1.0‰ respectively) are more negative than the corresponding values of $\delta^{15}N$ for Ellendale 9 (0.2‰ and

0.0‰), and this is a result of 6 of the 27 Ellendale 9 diamonds (22%) having $\delta^{15}N$ values greater than the maximum measured for Ellendale 4.

There are no apparent distinctions between inclusion-bearing and inclusion-free samples in terms of overall nitrogen isotopic composition (Figure 2.26) at either Ellendale 4 or Ellendale 9. Amongst Ellendale 9 diamonds of known paragenesis, eclogitic diamonds have less variable $\delta^{15}N$ values ($-3.3‰ \leq \delta^{15}N \leq 8.6‰$) than peridotitic samples ($-9.3‰ \leq \delta^{15}N \leq 3.7‰$), and the mean (1.3‰) and median (0.0‰) $\delta^{15}N$ values of eclogitic samples are greater than those of peridotitic samples (-3.3‰ and -3.8‰ for mean and median $\delta^{15}N$) indicating a concentration of ^{15}N in these eclogitic diamonds. Analyses from diamonds of known paragenesis are identified on Figure 2.26.

There are no visible relationships between measured $\delta^{15}N$ value and diamond colour or morphology. There is, however a relationship between the nitrogen content and $\delta^{15}N$ value for Ellendale 4 inclusion-bearing diamonds and this is illustrated in Figure 2.27. This relationship does not hold when all Ellendale 4 diamonds are considered together, and there is no such relationship for Ellendale 9 diamonds. Furthermore, the negative correlation evinced here differs from the positive correlation seen in Argyle diamonds (Figure 2.9). There are no relationships between nitrogen aggregation state and nitrogen isotopic composition for any of the different groups of Ellendale two millimeter diamonds considered here.

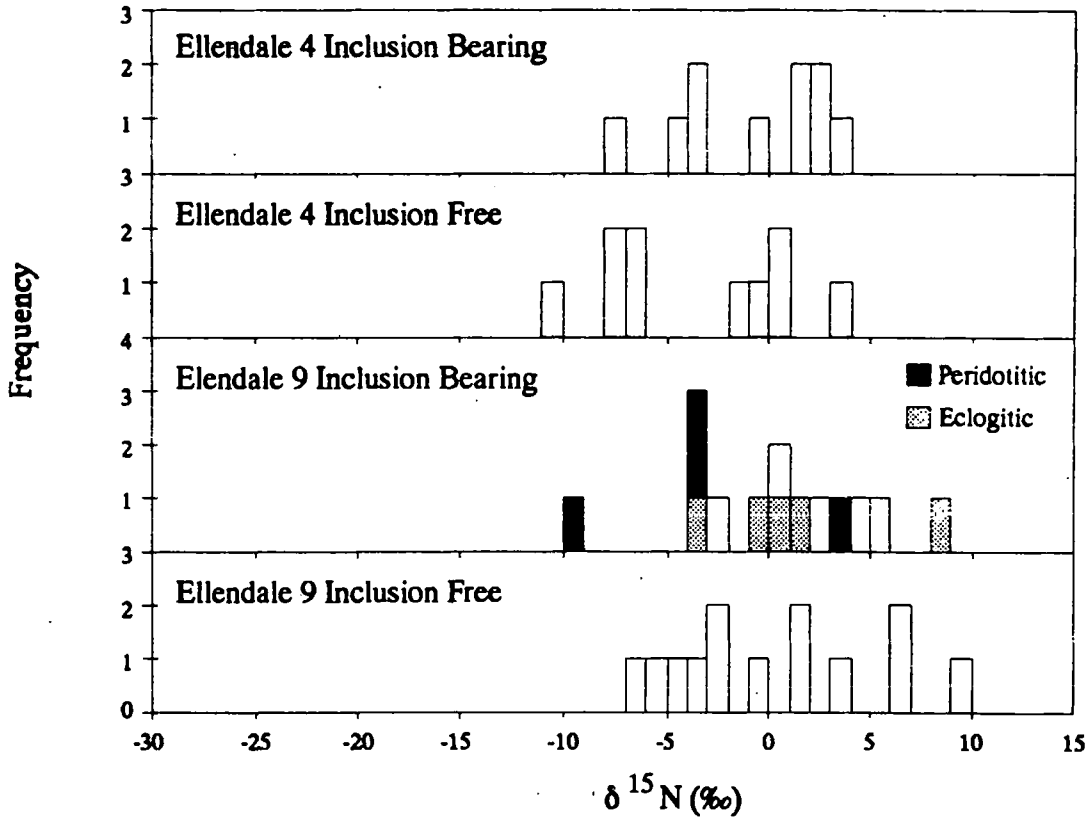

Figure 2.26: $\delta^{15}N$ histogram for 2 mm Ellendale diamonds.

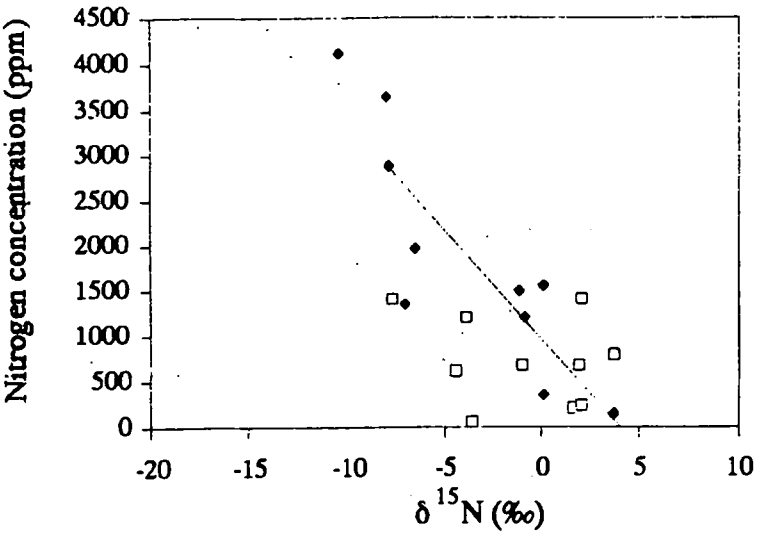

Figure 2.27: $\delta^{15}N$ plotted against nitrogen concentration for Ellendale 4 diamonds. Inclusion-bearing diamonds shown by filled diamonds. Inclusion-free diamonds shown by open squares. The line through the inclusion-bearing samples is a least squares linear regression and has the equation $[N] = -243 \cdot \delta^{15}N + 955$. The correlation coefficient $r = 0.75$, and this is significant at a 98% confidence level.

When carbon and nitrogen isotopic covariation is considered, Ellendale 4 and Ellendale 9 are distinct. Ellendale 4 defines a tight group extended along the $\delta^{15}N$ axis (Figure 2.28) and there is considerably more scatter in Ellendale 9 diamonds (Figure 2.29). In addition, Ellendale 9 diamonds of known paragenesis are distinct. The peridotitic paragenesis diamonds plot at less negative $\delta^{13}C$ values and generally lower $\delta^{15}N$ values than diamonds of eclogitic paragenesis.

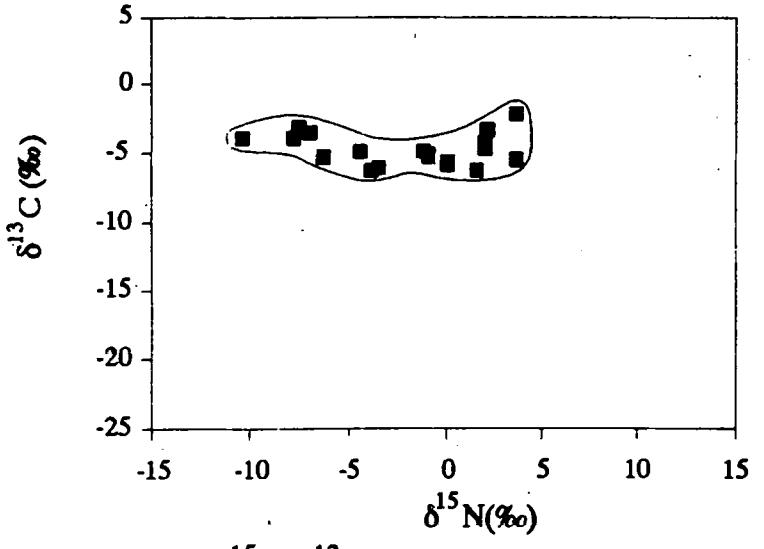

Figure 2.28: $\delta^{15}N$ - $\delta^{13}C$ plot showing all Ellendale 4 two millimeter diamonds.

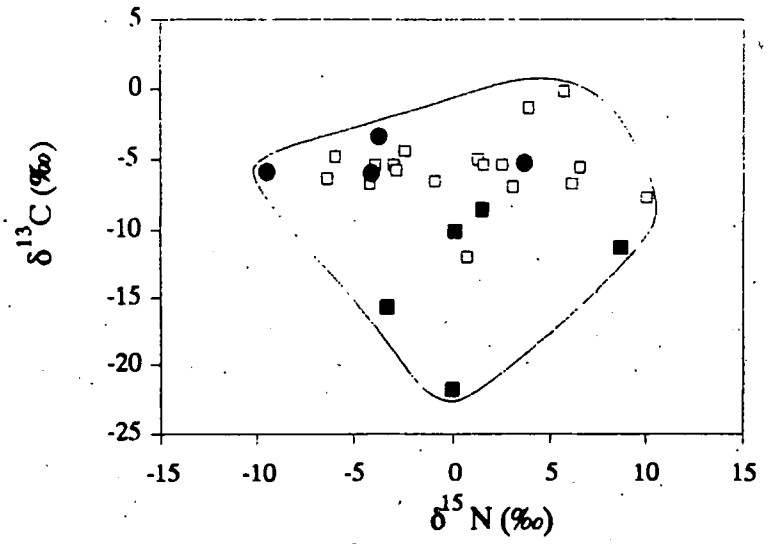

Figure 2.29: $\delta^{15}N$ - $\delta^{13}C$ plot showing Ellendale 9 two millimeter diamonds. Eclogitic paragenesis diamonds shown by filled squares and peridotitic paragenesis diamonds shown by filled grey circles. There are no $\delta^{15}N$ data available for E9037 or E9015 and they are not shown.

2.2.5 Ellendale 9 diamond plates

Five diamond plates from Ellendale 9 were supplied for this study. Of the five diamonds, sample E9039 arrived shattered and, apart from being examined under cathodoluminescing conditions, was not studied. The remaining four diamonds were reportedly inclusion-free (apart from graphite), and had dodecahedral morphology prior to sectioning (Chris Smith, Pers. Comm.).

2.2.5.1 Cathodoluminescence

Ellendale 9 diamond plates are broadly similar to the Argyle plates illustrated in Figures 2.12 to 2.16, under cathodoluminescing conditions (C.L.). All are characterised by a bright blue central region, surrounded by a zone of less intense yellow-blue and octahedral growth zonation (picture frame zonation) is visible in all zones. Bright yellow rim reflections are present on all samples, but are best developed in E9037 and E9039 (not sectioned). The brightness contrast between the different growth zones evident in C.L. amongst Ellendale 9 diamond plates is not as marked as the contrast in Argyle plates. There is no consistent relationship apparent between cathodoluminescence intensity and nitrogen content or aggregation state.

2.2.5.2 Carbon isotope variations

Two groups are evident in the $\delta^{13}C$ measurements from Ellendale 9 plates. The first of these comprises samples E9037 and E9038 and is characterised by $\delta^{13}C$ values near -11‰, while the second group, comprising samples E9040 and E9041 is characterised by $\delta^{13}C$ values near -5‰. The first group has a more variable carbon isotopic

composition, with nearly 3‰ variation in $\delta^{13}C$ across E9037, and E9038 has an overall $\delta^{13}C$ variation of 1.1‰. The maximum $\delta^{13}C$ variation in the second group is 0.8‰ (E9040). The least variation in $\delta^{13}C$ occurs in sample E9041 where the total $\delta^{13}C$ range is 0.3‰. None of the plates analysed showed the marked ^{13}C depletion evident in some of the 2mm Ellendale 9 diamonds ($\delta^{13}C$ values down to -22.1‰), and this may reflect the fact that 2 mm diamonds with extreme $\delta^{13}C$ values are all inclusion bearing, whereas all plates are inclusion free. The range in $\delta^{13}C$ values and mean and median $\delta^{13}C$ values of these Ellendale 9 diamond plates are presented in Table 2.10.

Sample	Range (‰)	Mean and std. error on mean (‰)		Median (‰), population std deviation (‰) and n		
E9037	-10.9 to -7.9	-10.0	0.4	-10.3	1.0	8
E9038	-12.1 to -10.9	-11.7	0.1	-11.7	0.3	12
E9040	-4.8 to -4.0	-4.6	0.1	-4.7	0.2	9
E9041	-5.2 to -4.9	-5.1	0.0	-5.0	0.1	10
All 2 mm stones	-22.1 to -0.0	-7.8	1.0	-5.8	5.4	29

Table 2.10: Descriptive statistics for $\delta^{13}C$ values from Ellendale 9 diamond plates. Two millimeter diamonds shown for comparison.

There are subtle variations in $\delta^{13}C$ across each diamond plate and these are illustrated in Figure 2.30 to Figure 2.33. In sample E9037, the central region of the diamond (blocks 5 to 7) has higher $\delta^{13}C$ values than those measured for blocks on either side. The least negative $\delta^{13}C$ measurement (-10.1‰) occurs in block 6, and minimum $\delta^{13}C$ values of -10.8‰ are seen in blocks 8 and 9. The right hand edge of the sample is characterised by a marked increase in $\delta^{13}C$ up to the maximum of -7.9‰ measured in block u.n. Regrettably, the symmetry of this profile could not be checked due to sample loss.

A contrasting pattern occurs in sample E9038. Here the most negative $\delta^{13}C$ measurement occurs towards the centre of the diamond (position 6; $\delta^{13}C$ = -12.0‰) and there is a smooth increase in $\delta^{13}C$ value on the right hand side to a maximum of -11.4‰. The profile on the left hand side of this diamond is also one of increasing $\delta^{13}C$ away from the central region of the diamond to a maximum of $\delta^{13}C$ = -10.9‰ in the unnumbered block, however this transition is marred by the anomalously negative $\delta^{13}C$ measurement in block 1 (-12.0‰).

Diamond plate E9040 is also characterised by a $\delta^{13}C$ profile which has the lowest values in the centre, and the highest values towards the edge. The total variation across this plate is however small (less than 1‰, see Table 2.10). The most negative $\delta^{13}C$ value (-4.8‰) occurs in the centre of the diamond (block 5) and $\delta^{13}C$ smoothly increases towards either edge. The maximum $\delta^{13}C$ measured for this plate (-4.0‰) is for the un-numbered block on the extreme right hand side.

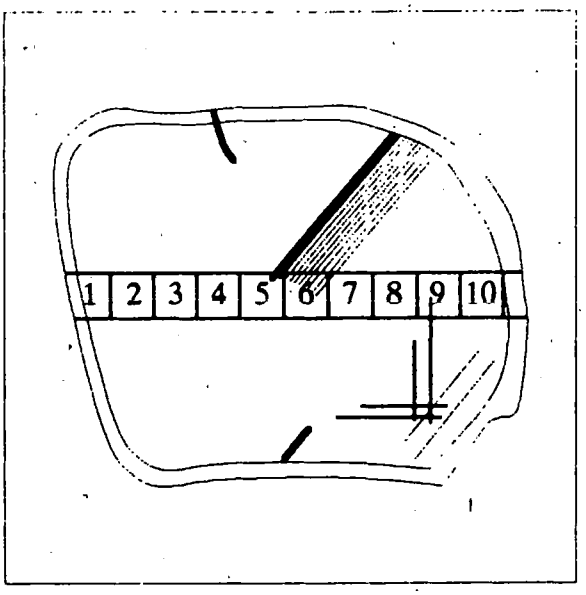

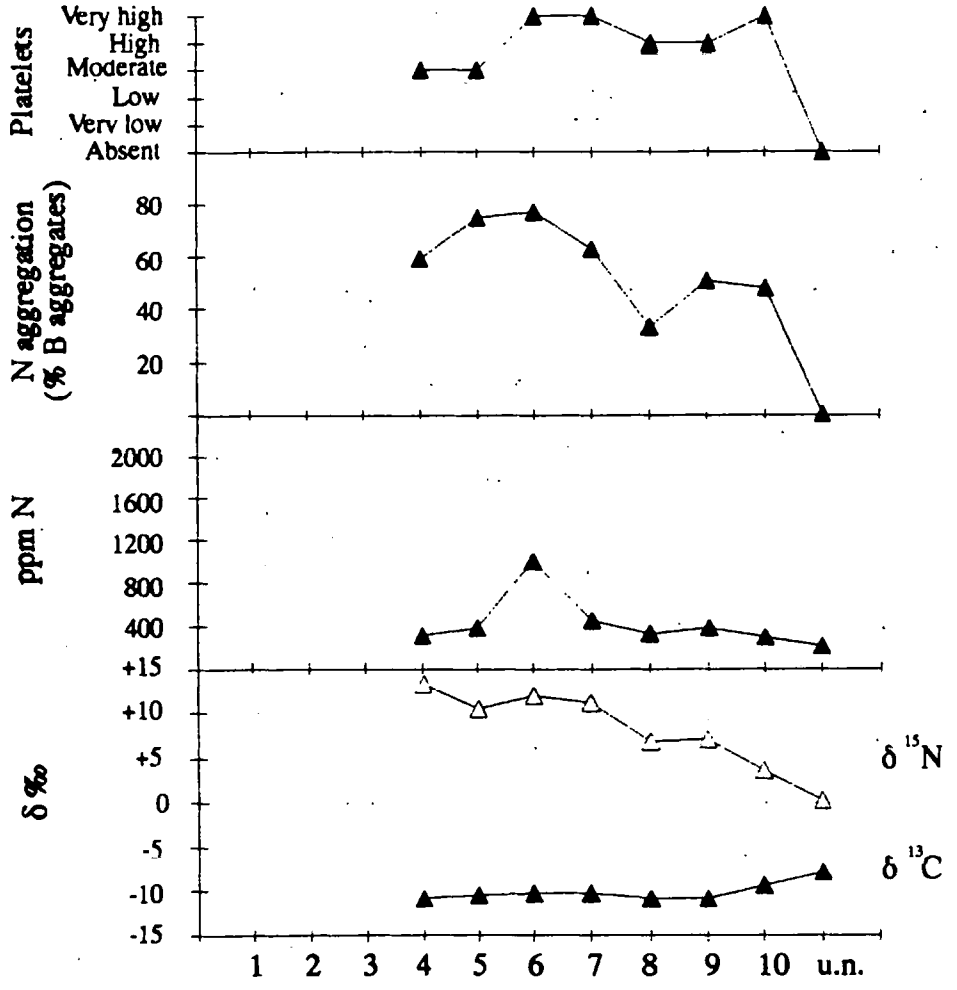

	1	2	3	4	5	6	7	8	9	10	u.n
$\delta^{13}C$ (‰)	Lost in transit			-10.7	-10.3	-10.1	-10.2	-10.8	-10.8	-9.4	-7.9
$\delta^{15}N$ (‰)	"			13.2	10.4	12.0	11.2	6.9	7.0	3.8	0.3
[N] (ppm)	"			313	387	1052	453	340	398	299	213
%B	"			59	75	77	63	33	51	48	0
type	"			IaAB+p	IaAB+p	IaAB+p	IaAB+p	IaAB+p	IaAB+p	IaAB+p	IaA

Figure 2.30: Plot across E9037. The diamond is 5mm across.

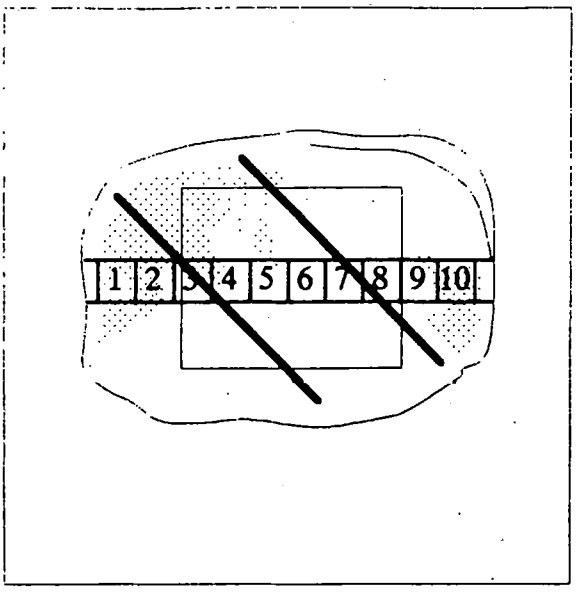

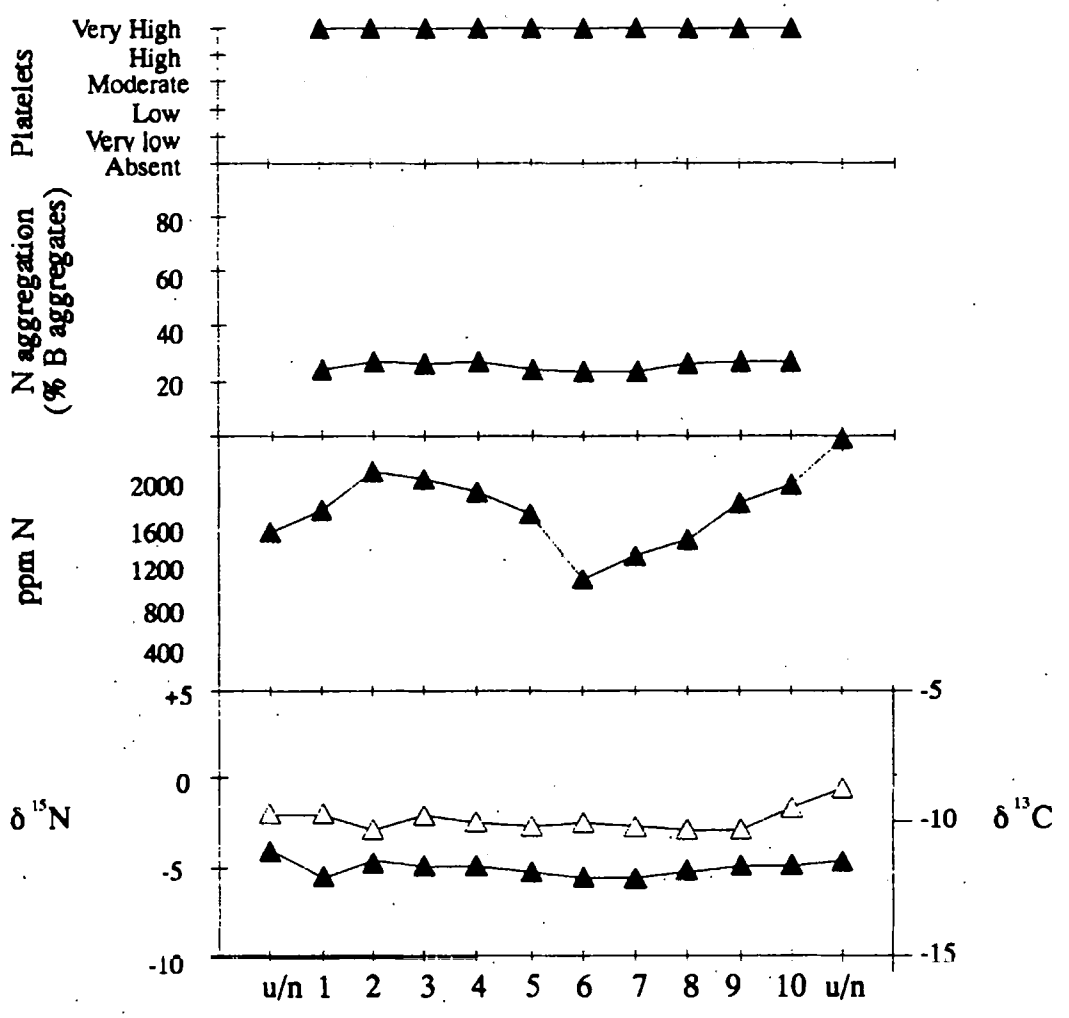

	u.n	1	2	3	4	5	6	7	8	9	10	u.n
$\delta^{13}C$ (‰)	-10.9	-12.0	-11.5	-11.6	-11.6	-11.9	-12.0	-12.0	-11.9	-11.8	-11.6	-11.4
$\delta^{15}N$ (‰)	-2.0	-2.0	-2.9	-2.1	-2.5	-2.7	-2.6	-2.8	-2.9	-2.9	-1.7	-0.7
[N] (ppm)	1486	1691	2052	1986	1858	1659	1042	1279	1418	1757	1928	2358
%B		24	27	26	27	24	23	23	26	27	27	
type	----------					All type IaAB+p						----------

Figure 2.31: Plot across E9038. Note the differing scales for the $\delta^{13}C$ and $\delta^{15}N$ axes. $\delta^{15}N$ shown by open symbols and $\delta^{13}C$ by filled symbols. The diamond is 5mm across.

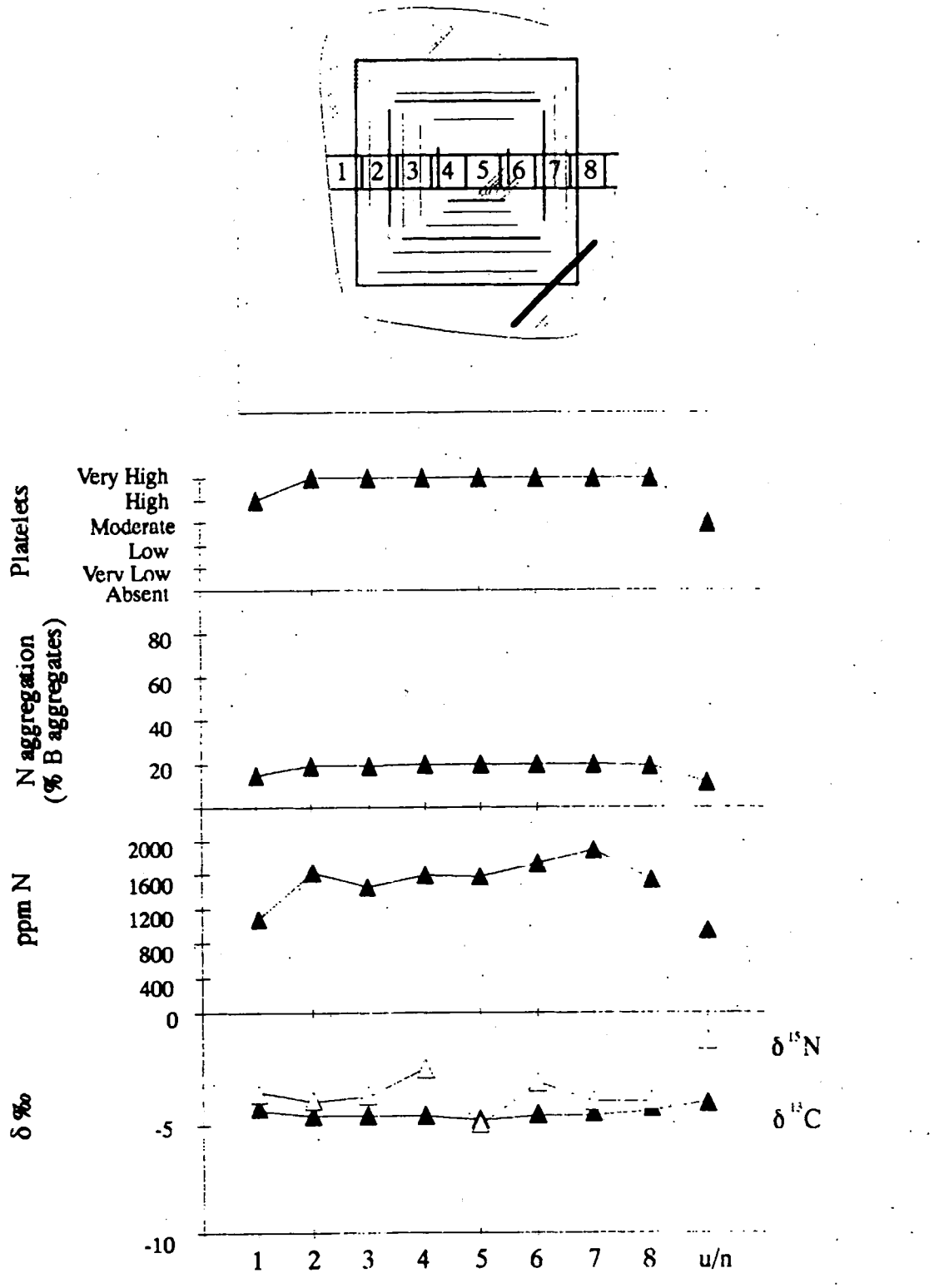

	1	2	3	4	5	6	7	8	u.n.
$\delta^{13}C$ (‰)	-4.4	-4.7	-4.7	-4.7	-4.8	-4.7	-4.6	-4.5	-4.0
$\delta^{15}N$ (‰)	-3.6	-4.0	-3.8	-2.5	-5.0	-3.2	-4.0	-4.0	-1.2
[N] (ppm)	1081	1633	1463	1588	1578	1738	1879	1537	953
%B	15	19	19	20	20	20	20	19	11
type	IaAB+p	IaAB+p	IaAB+p	IaAB+p	IaAB+p	IaAB+p	IaAB+p	IaAB+p	IaA+p

Figure 2.32: Plot across E9040. The diamond is 5mm across.

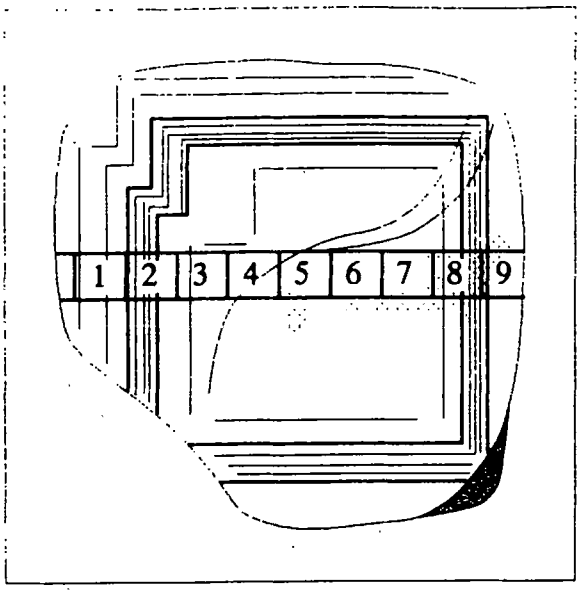

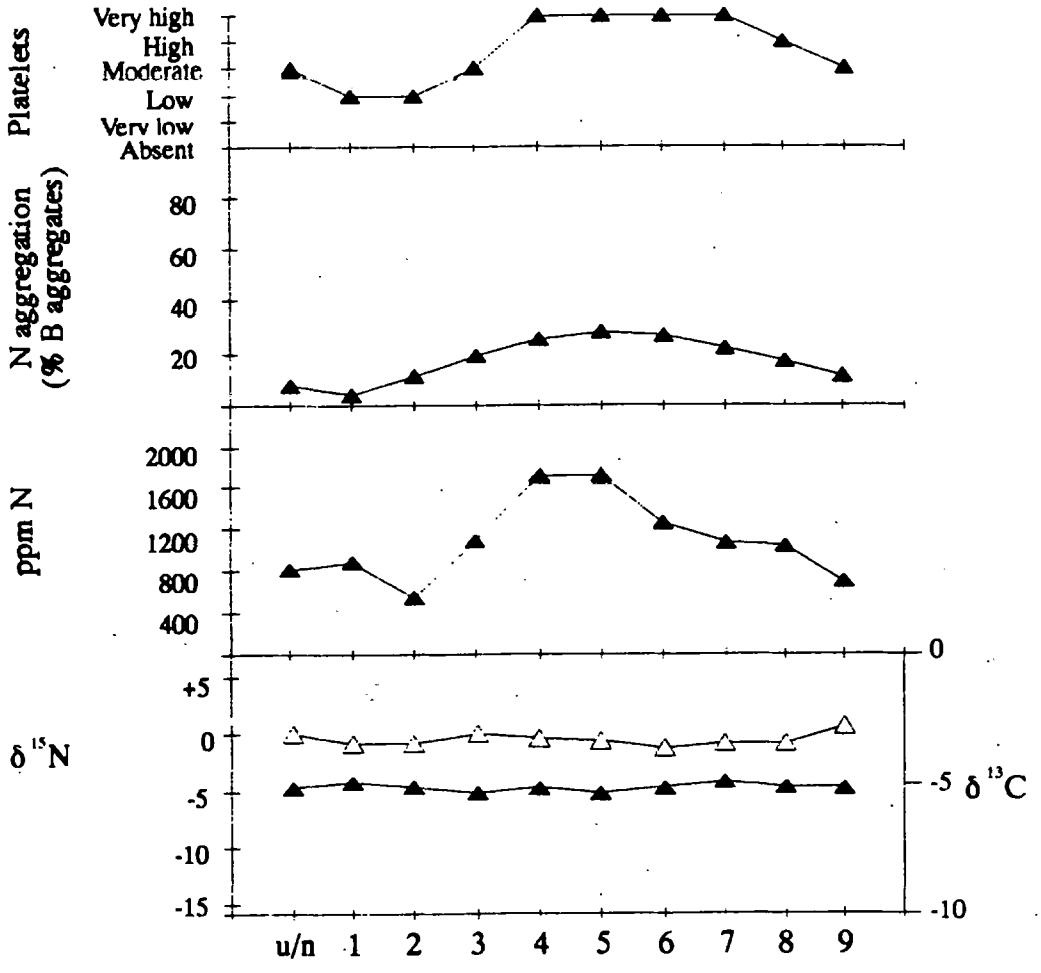

	u.n.	1	2	3	4	5	6	7	8	9
$\delta^{13}C$ (‰)	-5.1	-4.9	-5.0	-5.2	-5.1	-5.2	-5.0	-4.9	-5.0	-5.1
$\delta^{15}N$ (‰)	0.1	-0.9	-0.7	-0.1	-0.4	-0.6	-1.2	-0.7	-0.9	-0.8
[N] (ppm)	805	887	545	1084	1716	1712	1257	1072	1040	692
%B	8	4	11	19	25	28	27	22	17	11
type	IaA+p	IaA+p	IaA+p	IaAB+p	IaAB+p	IaAB+p	IaAB+p	IaAB+p	IaAB+p	IaA+p

Figure 2.33: Plot across E9041. Note the differing scales for the $\delta^{13}C$ and $\delta^{15}N$ axes. $\delta^{15}N$ shown by open symbols and $\delta^{13}C$ by filled symbols. The diamond is 5mm across.

Extremely small (less than 0.3‰) variations in $\delta^{13}C$ also characterise E9041. As with E9040 and E9038, the most negative $\delta^{13}C$ measurement is from the central region of the diamond (block 5, $\delta^{13}C$ = -5.2‰), but in this sample, there is no smooth transition to less negative $\delta^{13}C$ values towards the edges. Instead, $\delta^{13}C$ fluctuates across the sample, with the central region being flanked by a zone of increased $\delta^{13}C$ (blocks 1 and 2 and 6 and 7). The outer edges of the sample are again ^{13}C depleted (*i.e.* have a more negative $\delta^{13}C$) relative to this zone, but they are not as ^{13}C depleted as the central region of this stone.

2.2.5.3 Nitrogen

2.2.5.3.1 Nitrogen content; Ellendale 9 diamond plates have variable nitrogen contents, with a single sample, E9037 containing significantly less nitrogen than the remaining samples. E9037 has a mean nitrogen content of 432 ppm, while other Ellendale 9 plates all have mean nitrogen contents in excess of 1000 ppm (See Table 2.11). In addition, E9037 is marked by having only one block with more than 500 ppm nitrogen (Block 6, 1052 ppm) and this sample occurs in the middle of the diamond plate (Figure 2.30). The high nitrogen concentration in the centre of this diamond plate tapers off to 213 ppm nitrogen on the right hand edge, but the transition is not smooth. Block 8 contains less nitrogen than block 9, indicative of small scale fluctuations in nitrogen content within this diamond. The left hand samples also contain less nitrogen than the centre, decreasing from the high of block 6 to 387 ppm nitrogen in block 5 and 313 ppm in block 4. There are no further nitrogen concentration data available for this diamond, so it is not possible to comment on whether the concentration decrease from core to rim is either a general trend, or symmetrical about the centre of E9037. However, it is suggested that variations in nitrogen abundance occur in the same places as changes in the $\delta^{13}C$ value (Figure 2.30).

Sample	Range (ppm)	Mean and std. error on mean (ppm)		Median (ppm), population std deviation (ppm) and n		
E9037	213 to 1052	432	92	364	261	8
E9038	1042 to 2358	1710	105	1724	364	12
E9040	953 to 1879	1494	99	1578	298	9
E9041	545 to 1716	1081	124	1056	393	10

Table 2.11: Descriptive statistics for the nitrogen content of Ellendale 9 diamond plates.

In sample E9038, unlike E9037 or any of the other Ellendale plates, the lowest nitrogen content occurs towards the centre of the diamond ((Block 6, 1042 ppm nitrogen; See Figure 2.31). From this central sample, nitrogen content increases smoothly towards the

right hand edge, reaching a maximum of 2358 ppm at the extreme right (Figure 2.25). The variation from the centre towards the left hand edge is however more complex. Nitrogen content initially increases, peaking at 2052 ppm (block 2), before dropping off sharply to 1486 ppm on the left hand edge. Such a profile is in accord with the suggestion, from the $\delta^{13}C$ data, that the diamond is symmetrical about block 6 and that there has been some additional growth on the left hand edge.

The nitrogen content variation across diamond plate E9040 (Figure 2.32) is such that it appears lowest at the right hand edge where $\delta^{13}C$ values are the highest, and fairly constant but 50% higher across the interior of the diamond where it is accompanied by lower $\delta^{13}C$ values. The greatest amount of nitrogen occurs in block 7 (1879 ppm), on the right hand side on the diamond, while the lowest nitrogen content in this central region is found in block 3 (1463 ppm) on the left. With the exception of blocks 3 and 7, the nitrogen abundance measurements from the central region are within experimental error of each other. The two edge-blocks however, contain significantly less nitrogen than the central blocks. The left hand edge (block 1), containing 1081 ppm nitrogen and the right hand, un-numbered edge piece having the lowest measured nitrogen content from this sample (953 ppm).

Diamond plate E9041 is similar to E9037 in that the highest nitrogen concentrations occur in the central parts of the stone. In this case, nitrogen contents of 1716 ppm and 1712 ppm occur in blocks 4 and 5 respectively, and the nitrogen content then decreases towards the edges of the plate. One the right hand side of the central region (Blocks 6 to 9), this nitrogen concentration decrease is smooth, reaching the minimum content of 692 ppm at the extreme right hand edge. One the left hand side of the centre however, the smooth nitrogen content decrease is marred by an anomalously low nitrogen content in block 3 (545 ppm), which is not within error of the adjacent blocks. With the exception of this block, there is a regular nitrogen content profile across diamond E9041, with high nitrogen contents in the centre being surrounded by lower nitrogen contents towards the edges.

There is no relationship between nitrogen content and carbon isotopic composition for plates E9037 and E9041. Diamond E9038 shows an increase in $\delta^{13}C$ value with increasing nitrogen content (Figure 2.34), with a single outlier lying off a least squares regression line which has the equation: $[N] = 1608 \times \delta^{13}C + 20644$. The correlation coefficient $r = 0.86$, which is significant at a 99.95% confidence level. The outlier point is the un-numbered block on the extreme left hand edge of the diamond.

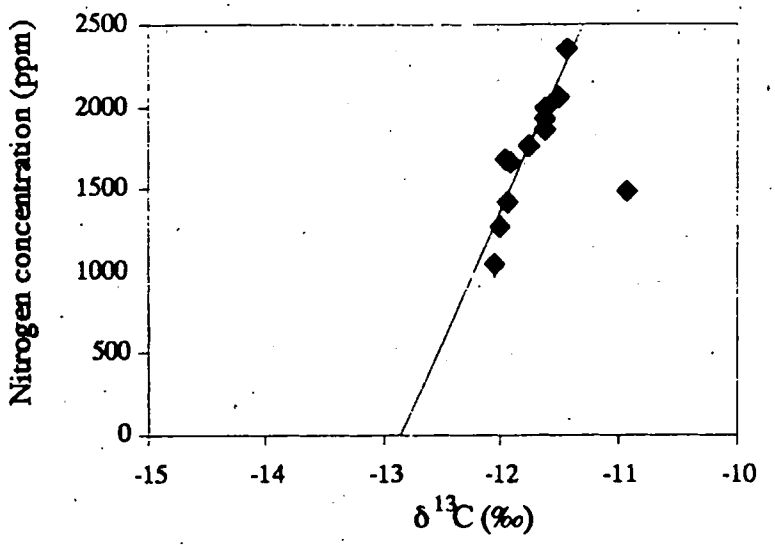

Figure 2.34: Nitrogen content plotted against $\delta^{13}C$ for E9038. The line is a least squares regression (correlation coefficient r = 0.86) omitting the outlier.

Sample E9040 also shows a relationship between nitrogen content and $\delta^{13}C$ value, but in this case, $\delta^{13}C$ values decrease with increasing nitrogen content (Figure 2.35) *i.e.* this line has the opposite slope to that found in E9038. The regression line calculated for this relationship has the equation: nitrogen content = -1027 x $\delta^{13}C$ - 3190.

The opposite sense of these two lines may be evidence for two component mixing rather than for a fractionation process. This possibility is discussed in section 2.3, where further evidence from the relationships between $\delta^{13}C$ and $\delta^{15}N$ values, nitrogen content and aggregation state are also considered.

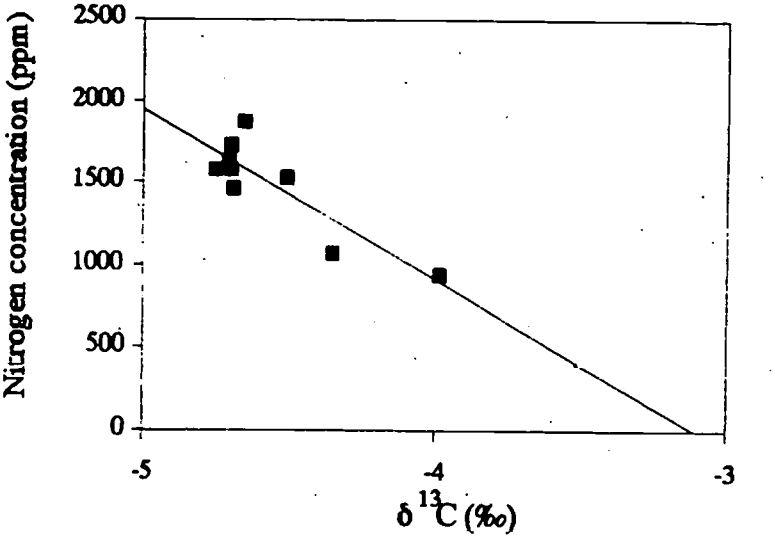

Figure 2.35: Nitrogen content plotted against $\delta^{13}C$ for diamond plate E9040. The calculated regression line has r = 0.74, which is significant at a 99% confidence level.

2.2.5.3.2 Nitrogen aggregation state; Considerable variation in the proportion of nitrogen occurring in B-aggregates is evident in sample E9037 (Figure 2.30). In this sample, the most aggregated nitrogen occurs in the centre of the sample (blocks 5, 6 and 7), than is found at the right hand edge (pure type IaA - no B-aggregates). In plates E9038 (Figure 2.31) and E9040 (Figure 2.32), nitrogen aggregation state is, within the associated uncertainties, the same across the entire diamond. There is an indication however that the edge blocks of E9040 may contain fewer B-aggregates than blocks wholly within the diamond plate. In sample E9041 (Figure 2.33), the more aggregated nitrogen occurs towards the centre of the diamond plate (blocks 1 to 6), and there is a smooth decrease in the proportion of B-aggregates towards either edge, except at the extreme left hand side (un-numbered block) where there is a small (4%) increase in the proportion of B-aggregates.

Platelets are present in varying proportions in all 4 Ellendale 9 diamond plates (Figure 2.30 to Figure 2.33). Their distribution across E9037 has no regular pattern, but they are most abundant in the centre of the sample and least abundant on the extreme right hand edge. In sample E9038, platelets show no variation across the sample: they occur in uniformly high concentrations. Sample E9040 shows an apparent relationship between platelet content and nitrogen aggregation state in that the two edge samples, characterised by reduced proportions of nitrogen in B-aggregates are also characterised by reduced platelets, and these two blocks also have the lowest nitrogen contents for this diamond. In sample E9041, platelets distribution is not symmetrical, but empirically follows the proportion of nitrogen occurring in B-aggregates, and using the terminology of Woods (1985) this is termed a regular diamond. In the central region, platelets are most abundant, and these decrease towards both the right hand and left hand edges. However, the extreme left hand edge of this sample is marked by an increase in the proportion of platelets. This is the same block that shows the increased proportion of B-aggregates.

There is no relationship between nitrogen aggregation state and $\delta^{13}C$ value for plates E9037 and E9041. Diamond plates E9038 and E9040, the plates for which a $\delta^{13}C$ – [N] relationship exists, however also show a relationship between carbon isotopic composition and nitrogen aggregation state. In E9038, as $\delta^{13}C$ becomes less negative, the proportion of B-aggregates increases, while in E9040 the opposite happens. This is illustrated in Figure 2.36.

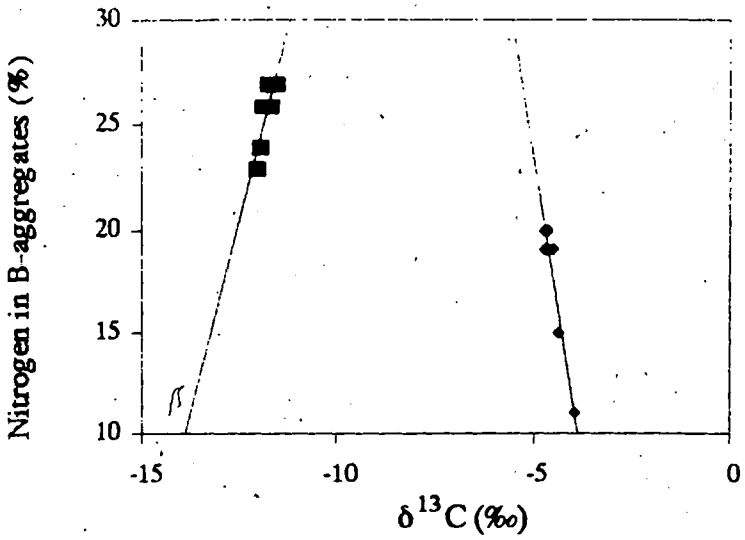

Figure 2.36: Nitrogen aggregation state plotted against carbon isotopic composition for Ellendale plates E9038 (squares) and E9040 (diamonds). Lines are least squares regressions. The equation for E9038 is $\%B = 7.5 \cdot \delta^{13}C + 114$ ($r = 0.75$) and for E9040 is $\%B = -12.1 \cdot \delta^{13}C - 37$ ($r = 0.94$). Both lines are significant at a 99% confidence level.

There is no relationship between nitrogen aggregation state and nitrogen content in diamond E9041. In samples E9038 and E9040 lines with positive slope are defined, and these may represent either mixing lines or fractionation curves. They are illustrated in Figure 2.37 where nitrogen content is normalised to the maximum nitrogen content in each ladder section. A broad group with a positive slope is defined for E9037 when normalised nitrogen content is plotted against the proportion of nitrogen in B-aggregates, and this is similar to E9038 and E9040 in that the minimum nitrogen contents are related to the least aggregated nitrogen (see Figure 2.37). Possible causes and the implications of these trends are discussed in Chapter 3.

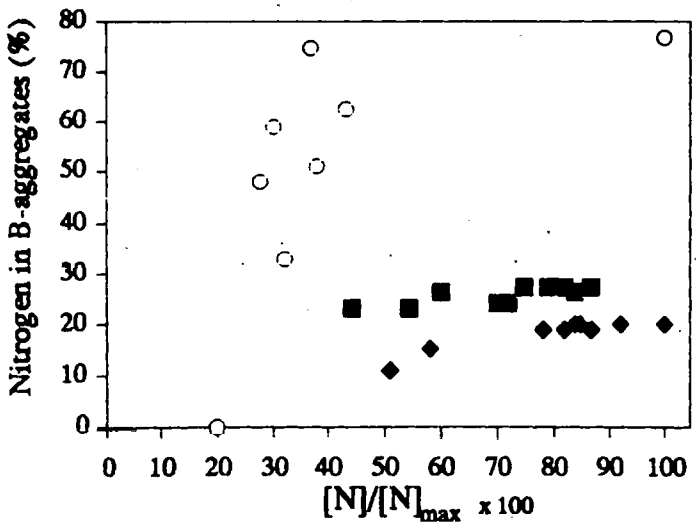

Figure 2.37: Nitrogen aggregation state plotted against normalised nitrogen content. E9037 shown by open circles, E9038 shown by filled squares and E9040 shown by filled diamonds. See also Figure 2.17.

2.2.5.3.3 Nitrogen isotope variation: Two of the Ellendale 9 diamond plates (E9037 and E9040) have variable $\delta^{15}N$ values, and of these two, E9037 shows the greatest range in nitrogen isotopic composition ($0.3‰ \leq \delta^{15}N \leq 13.2‰$; see also Table 2.12). It is also the only Ellendale 9 plate which has all $\delta^{15}N$ values greater than 0‰. The variation in $\delta^{15}N$ across this diamond plate follows a regular pattern as already seen for all 4 of the other parameters investigated. The centre of the sample is characterised by high $\delta^{15}N$ values and these decrease to the minimum at the right hand edge, but this decrease is not a smooth transition (see Figure 2.30). Left of the central region, $\delta^{15}N$ values decrease to +10.4‰ (block 5) before rising again to the possible outlier value of $\delta^{15}N$ = +13.2‰ (block 4).

Sample	Range (‰)	Mean and std. error on mean (‰)		Median (‰), population std deviation (‰) and n		
E9037	0.3 to 13.2	8.1	1.6	8.7	4.4	8
E9038	-2.9 to -0.7	-2.3	0.2	-2.6	0.7	12
E9040	-5.0 to -1.2	-3.5	0.4	-3.8	1.1	9
E9041	-1.2 to +0.8	-0.5	0.2	-0.7	0.6	10
All 2mm diamonds	-9.3 to +9.9	0.2	0.9	0.0	4.8	27

Table 2.12: Descriptive statistics for $\delta^{15}N$ values from Ellendale 9 diamond plates.

In contrast to E9037, sample E9040 has the minimum $\delta^{15}N$ value in the centre of the diamond (block 5, $\delta^{15}N$ = -5.0‰; See Figure 2.25). This is flanked on either side by a blocks with less negative $\delta^{15}N$ (block 4, $\delta^{15}N$ = -2.5‰; block 6, $\delta^{15}N$ = -3.2‰). $\delta^{15}N$ values then decrease towards either edge (down to $\delta^{15}N$ = -4.0‰) however the extreme edge pieces on either side is ^{15}N enriched relative to this trough. Edge pieces have $\delta^{15}N$ = -3.6‰ (left hand side) and $\delta^{15}N$ = -1.2‰ (right hand side).

Samples E9038 and E9041 show little variation in $\delta^{15}N$ value across the diamond plate (Figures 2.31 and 2.33) and plate E9038 is symmetrical about blocks 6 and 7 with respect to $\delta^{15}N$ values. Both plates show a kick to less negative $\delta^{15}N$ at at least one edge, and this is particularly pronounced in E9041. The first two blocks on the left hand edge ($\delta^{15}N$ = +0.1 and -0.9‰) have $\delta^{15}N$ 1‰ apart while the right hand edge is marked by a 1.7‰ $\delta^{15}N$ contrast (block 8, $\delta^{15}N$ = -0.9‰; block 9, $\delta^{15}N$ = +0.8‰). This "kick" is not present on the left hand edge of E9038 but on the right hand edge, there is a 1‰ $\delta^{15}N$ difference between block 10 ($\delta^{15}N$ = -1.7‰) and the un-numbered block ($\delta^{15}N$ = -0.7‰).

There is no general relationship between nitrogen and carbon isotope ratios and on a $\delta^{13}C$ - $\delta^{15}N$ plot (Figure 2.38), each diamond plate defines a distinct field. E9038, E9040 and E9041 form tight groups, elongated along the $\delta^{15}N$ axis while E9037 shows more

more scatter. This plate shows a crude trend of decreasing $\delta^{13}C$ with increasing $\delta^{15}N$, but the correlation coefficient of a least squares regression line through these data (0.55) is too low to be significant at more than a 90% confidence level. If the extreme edge portions of plate E9037 are omitted (the blocks with the lowest $\delta^{15}N$ values), the remaining data are positively correlated and in section 2.3 it is shown that this may arise from either an isotopic fractionation mechanism or from a mixing process.

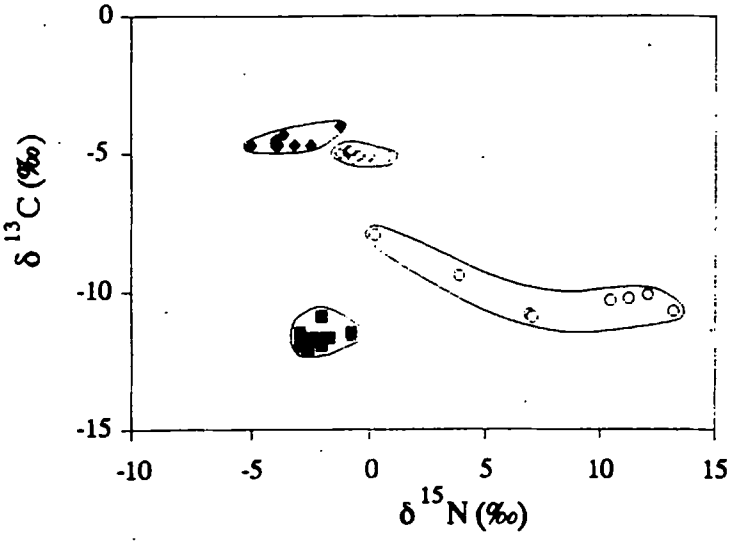

Figure 2.38: $\delta^{13}C$ - $\delta^{15}N$ plot for Ellendale 9 diamond plates. E9037 shown by open circles, E9038 shown by filled squares, E9040 shown by filled diamonds and E9041 shown by open diamonds.

There is no general relationship between nitrogen content and nitrogen isotopic composition. When $\delta^{15}N$ is plotted against normalised nitrogen content, E9038, E9040 and E9041 form linear arrays, extended along $[N]/[N]_{max}$ (Figure 2.39). Plate E9037 is an exception to this however. As normalised nitrogen content increases, $\delta^{15}N$ increases. All these lines have different slopes and this may be used to resolve the mechanisms relating nitrogen content and isotopic composition (and possibly nitrogen aggregation state) in diamonds and is discussed in section 2.3.

Only in diamond plate E9037 is there a definite relationship between nitrogen aggregation state and nitrogen isotopic composition (Figure 2.40). As the proportion of nitrogen in B-aggregates increases, the $\delta^{15}N$ value increases. No such trend is seen in any of the remaining Ellendale diamond plates. E9038 and E9040 define tight groups on Figure 2.40 due to their limited $\delta^{15}N$ variation, whereas E9041 forms a group extended along the aggregation state axis This line may show a slight decrease in $\delta^{15}N$ values with increasing proportions of nitrogen in B-aggregates.

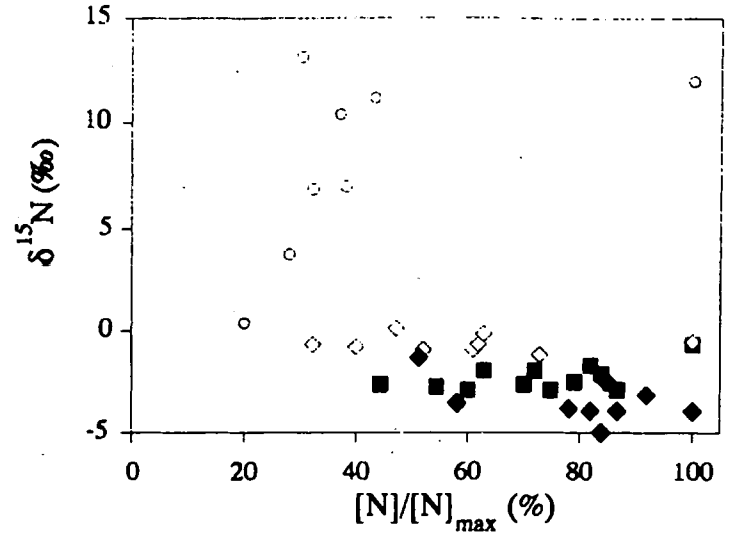

Figure 2.39: $\delta^{15}N$ plotted against normalised nitrogen content for Ellendale 9 diamond plates. E9037 shown by open circles, E9038 shown by filled squares, E9040 shown by filled diamonds and E9041 shown by open diamonds.

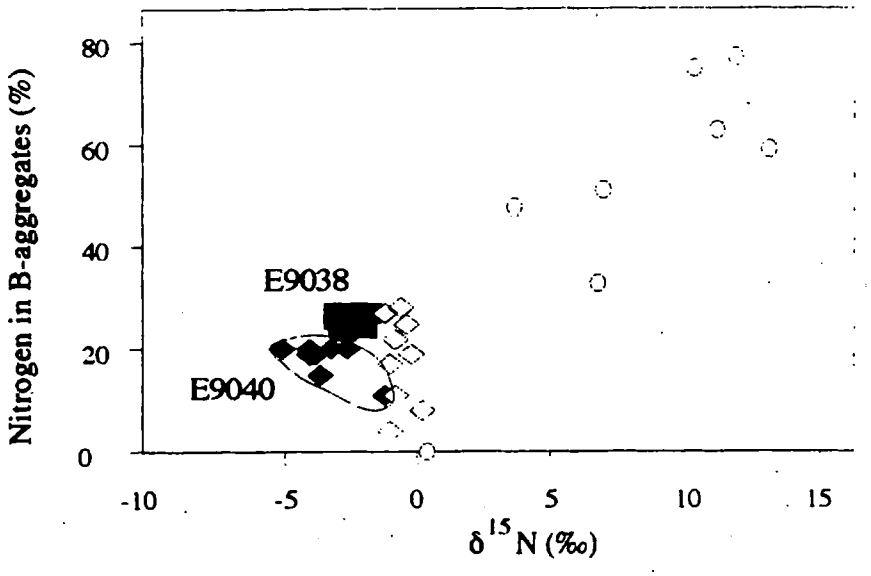

Figure 2.40: Proportion of nitrogen in B-aggregates plotted against $\delta^{15}N$ for Ellendale 9 diamond plates. Plot symbols as for Figure 2.38 and 2.39. Note the E9037 block at 0% B-aggregates and $\delta^{15}N$ = +0.3‰.

2.2.6 Comparison of 2 mm diamonds and diamond plates from Ellendale 9

Comparison of the carbon and nitrogen isotopic composition of Ellendale 9 diamond plates and the 2 mm diamonds of known paragenesis from the same locality is facilitated by means of a $\delta^{13}C$ - $\delta^{15}N$ diagram (Figure 2.41). From this, it is evident that plates

E9040 and E9041 are totally bounded within the limits placed by peridotitic paragenesis diamonds. For diamond plates E9037 and E9038, most $\delta^{13}C$ values fall within the limits imposed by eclogitic paragenesis diamonds, the single exception being the maximum $\delta^{13}C$ value from E9037 (-7.9‰, block u.n). The most positive $\delta^{13}C$ value from eclogitic paragenesis diamonds is $\delta^{13}C$ = -8.5‰. The lower limits of the $\delta^{15}N$ values for plates E9037 and E9038 are similar to the lower limits for eclogitic paragenesis diamonds, but plates show a far wider range of $\delta^{15}N$ values than eclogitic 2 mm diamonds. The maximum $\delta^{15}N$ value for 2 mm eclogitic diamonds is +8.6‰, and the maximum $\delta^{15}N$ measurement from plates E9037 and E9038 is +13.2‰. The field for 2 mm, eclogite paragenesis Ellendale 9 diamonds therefore does not enclose plates E9037 or E9038 completely, but the weighted mean $\delta^{13}C$ and $\delta^{15}N$ values from each of these plates ($\delta^{13}C$ = -10.1‰ and -11.8‰ respectively, $\delta^{15}N$ = 8.2‰ and -2.5‰) do fall just within the field defined by the eclogitic paragenesis diamonds.

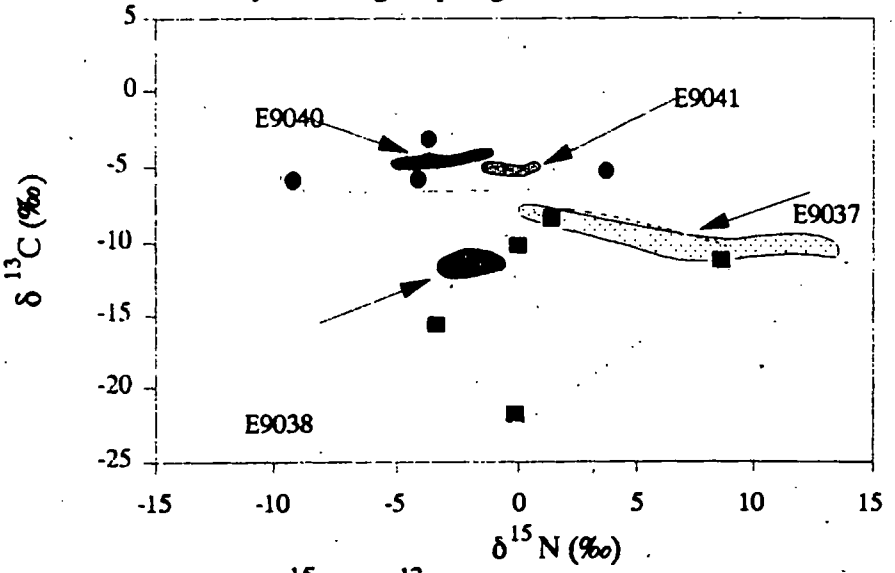

Figure 2.41: $\delta^{15}N$ - $\delta^{13}C$ plot of Ellendale 9 diamond plates. Superimposed on this are Ellendale 9 two millimeter diamonds of known paragenesis. Peridotitic diamonds are shown by filled grey circles and eclogitic paragenesis diamonds are shown by filled squares.

In terms of nitrogen content, Ellendale 9 plates fall well within the 4438 ppm range measured from all Ellendale 9 two millimeter diamonds. The mean nitrogen content of E9037 (432 ppm) is very similar to the mean nitrogen content of eclogitic paragenesis diamonds (468 ppm) but no further groupings are evident on paragenetic grounds. The remaining three Ellendale 9 plates all have mean (and median) nitrogen contents in excess of 1000 ppm and only inclusion-free Ellendale 9 two millimeter diamonds have mean nitrogen contents approaching this.

As with nitrogen content, there is a complete overlap of the aggregation state of two millimeter diamonds with the aggregation state of Ellendale 9 diamond plates. None of the groups of 2 mm diamonds however have mean nitrogen aggregation states as high as those evident in plate E9037 (mean B-aggregates = 51%). The highest mean aggregation

state for 2 mm Ellendale 9 diamonds occurs in inclusion-bearing diamonds (mean proportion of B-aggregates = 30%), but this is a specious comparison. This mean is raised by the marked skewness of the aggregation state histogram (See Figure 2.25). A more valid comparison is of the median aggregation state values. Eclogitic 2 mm diamonds have a median aggregation state of 31% B-aggregates. This is lower than the median of 55% B-aggregates in E9037; similar to the median for E9038 (26% B-aggregates) and higher than the median values for E9040 and E9041 (19% and 18% B-aggregates respectively). The median proportions of B-aggregates for the later two plates are more similar to the median aggregation state for peridotitic 2 mm diamonds from Ellendale 9 (12% B-aggregates).

2.3 SUMMARY AND DISCUSSION

In this section, the carbon and nitrogen characteristics of each diamond source are summarised, and the relationships between them are compiled in Table 2.13. Possible causes for these relationships include isotope fractionation and mixing and these are quantitatively evaluated and discussed in the following Chapter.

2.3.1 Argyle diamonds

The Argyle 2 mm diamonds have C and N stable isotope and other characteristics that are largely dependent on diamond paragenesis. Eclogitic paragenesis diamonds are characterised by more negative mean $\delta^{13}C$ values than peridotitic paragenesis diamonds (t-statistic = -2.9; D.O.F = 29, significant at better than 99%), as has been reported for diamonds of known paragenesis elsewhere (*e.g.* Kirkley *et al.*, 1991). The overall $\delta^{15}N$ range for peridotitic paragenesis diamonds is smaller than the corresponding range for eclogite paragenesis diamonds. Furthermore, eclogite paragenesis diamonds from Argyle are characterised by lower nitrogen concentrations and by higher degrees of nitrogen aggregation than the peridotitic paragenesis diamonds. In addition, peridotitic paragenesis Argyle 2 mm diamonds are morphologically distinct from the eclogitic paragenesis diamonds in that resorbed forms do not occur; all peridotitic diamonds are sharp-edged octahedra.

Diamonds of unknown paragenesis from Argyle may be classified into two groups; strongly coloured and less coloured. The strongly coloured samples are thought to have been have been affected by plastic deformation which results in graphite deposition (Harris, Pers. Comm; Gurney, Pers. Comm) and is responsible for a brown, pink or grey colouration. The less coloured (white and yellow) samples are those that show little or no evidence of plastic deformation. The plastically deformed diamonds are usually characterised by more positive mean $\delta^{13}C$ values, and by lower nitrogen contents than

samples that show little evidence for deformation. Both groups have similar ranges of $\delta^{15}N$ values and there is some evidence of a relationship between nitrogen content and nitrogen isotopic composition in samples that have been plastically deformed (See Figure 2.9), as well as in some eclogitic paragenesis diamonds. In these cases, decreasing nitrogen content correlates with decreasing $\delta^{15}N$ value in the diamonds. This may be indicative of (amongst other possibilities) an isotopic fractionation resulting from the preferential loss of the ^{15}N isotope from the diamond, or may arise from the preferential fixing of the ^{15}N isotope into a crystallizing diamond. Of these two options, the latter is preferred for, in general, chemical bonds to ions with high ionic potential and low atomic mass are associated with high vibrational frequencies and have a tendency to preferentially incorporate the heavy isotope (O'Neil, 1977). This has been shown in a variety of minerals which concentrate ^{18}O relative to ^{16}O, ^{34}S relative to ^{32}S and deuterium relative to hydrogen (See O'Neil, 1977, 1986 for reviews). By analogy, diamonds are expected to concentrate ^{15}N relative to ^{14}N on crystallization. Nitrogen loss as a fractionation mechanism, although theoretically feasible is difficult to conceive. In such a case the lighter, more mobile ^{14}N isotope would be expected to be preferentially lost, leading to an increase in $\delta^{15}N$ value with decreasing nitrogen content. This type of kinetic fractionation is, in any respect, not expected to be important at mantle temperatures (O'Neil, 1986, Hoefs, 1987). An alternative model for the differences between these diamonds is that plastically deformed diamonds record growth in a heterogeneous mantle, and that their isotopic characteristics are a function of the mixing of two or more end-member components. Isotopic fractionation mechanisms are discussed in more detail in Chapter 3.

Argyle diamond plates contain both eclogitic and peridotitic paragenesis inclusions and all show evidence of octahedral growth zonation. There are variations in $\delta^{13}C$ values across diamond plates and the peridotitic sample 150701 #12-8 shows an increase in the proportion of ^{13}C towards the sample edges. Eclogitic paragenesis diamond 150701 #8, and the unknown paragenesis sample 150701 #12-1 have the opposite $\delta^{13}C$ zoning pattern. In these samples, edge $\delta^{13}C$ values are more negative than those from the central parts of the diamond. There is no relationship between the style of carbon isotopic zoning and diamond paragenesis, and the eclogitic diamond 150701 #1 and the sample of unknown paragenesis 150701 #12-4 show no variation in $\delta^{13}C$ with position in the diamond. Where $\delta^{13}C$ value varies across diamond plates, the magnitude of the fluctuations are much larger than is expected at mantle temperatures (O'Neil, 1986; Hoefs, 1987). This, and the nitrogen evidence summarised below, reflects the complex crystallization history of the Argyle diamonds.

Measurements of nitrogen isotope ratios, content and aggregation state across the Argyle plates are variable, and there are many small scale fluctuations across these samples.

However, $\delta^{15}N$ values, nitrogen content and the proportion of nitrogen in B-aggregates appear to be related and this is particularly evident in samples 150701 #12-8, 150701 #8 and 150701 #12-1 (See Figures 2.12 to 2.14, 2.19 and 2.21). In these samples, high nitrogen concentrations, greater proportions of aggregated nitrogen and an increase in the proportion of ^{15}N occur towards the centres of the plates. The zoning profiles are however seldom smooth and this is ascribed to small scale heterogeneities within individual diamond plates, such as are evident in the fine laminations visible on cathodoluminescence images of these diamond plates. The relationships between nitrogen content, aggregation state and isotope ratio are not governed by diamond paragenesis. Increasing proportions of aggregated nitrogen towards the central regions of diamonds have been reported previously (Allen and Evans, 1981) and in coated stones, the core regions are often ^{15}N enriched relative to the coat (Boyd *et al.*, 1992). There is an exception to the general trends described above. Diamond 150701 #1 shows a pronounced break in nitrogen isotopic composition, aggregation state and concentration at the right hand edge, and this may arise from multiple growth events in an environment in which nitrogen concentration and stable isotope ratios are changing. This sample has a complex internal structure (Figure 2.15) and contains giant platelets (Milledge, Pers. Comm.) indicating a complex growth history.

As with plastically deformed and eclogitic paragenesis Argyle diamonds, the relationships between nitrogen content, aggregation state and isotopic composition of Argyle plates may arise from either multi-component mixing or from an isotopic fractionation mechanism. These possibilities are discussed in section 2.3.3.

2.3.2 Ellendale diamonds

All Ellendale 4 diamonds have $\delta^{13}C$ values close to the range for normal mantle (see Chapter 1), as do the majority of Ellendale 9 diamonds. There are however exceptions at Ellendale 9. Diamonds that are ^{13}C depleted occur and these appear to be related to an eclogitic paragenesis. Peridotite paragenesis diamonds at Ellendale 9 however have $\delta^{13}C$ values clustering around $\delta^{13}C = -5‰$. Similar differences in $\delta^{13}C$ value between eclogitic and peridotitic paragenesis diamonds have been reported previously (*e.g.* Kirkley *et al.*, 1991).

The nitrogen content of Ellendale 4 and Ellendale 9 diamonds is higher than that of Argyle, and the Ellendale 4 diamonds have a higher mean nitrogen content than the Ellendale 9 samples, which may be indicative of small scale (15 km) variability in mantle nitrogen contents. There are no apparent differences between the different paragenesis diamonds identified at Ellendale 9. Ellendale 9 diamonds contain marginally greater proportions of aggregated nitrogen than Ellendale 4 diamonds and there appears to be a

loose relationship between lower nitrogen contents and higher degrees of nitrogen aggregation for both the Argyle and Ellendale 9 diamond populations. Both of these have a higher number of more aggregated diamonds than the Ellendale 4 diamond population with higher nitrogen content. Amongst the Ellendale 9 diamonds, eclogitic paragenesis samples show slightly greater degrees of nitrogen aggregation than peridotitic paragenesis samples, however there is a considerable amount of overlap between the two parageneses. There are also (weakly defined) differences in nitrogen isotopic composition between eclogitic and peridotitic paragenesis Ellendale 9 diamonds. Eclogitic diamonds are slightly enriched in ^{15}N relative to peridotitic paragenesis samples, although there is still a considerable amount of overlap of the two groups. Unlike the plastically deformed Argyle diamonds, there is no general relationship between nitrogen content and nitrogen isotopic composition and there is no obvious evidence of nitrogen fractionation for 2 mm diamonds from Ellendale 4 or Ellendale 9.

Ellendale 9 diamond plates show only minor fluctuations in $\delta^{13}C$ value with position in the sample. The nitrogen variations across samples however are more extreme, and three of the four plates show higher nitrogen contents towards the central regions of the traverse than at the rims. Nitrogen aggregation is also usually more advanced towards the centres of these samples, although this aggregation is less advanced than it is in Argyle plates. There are also variations in nitrogen isotopic composition across the Ellendale 9 diamond plates, but only in sample E9037 do these correspond to nitrogen content and aggregation state zonation patterns. There is a higher proportion of ^{15}N in the central region of this sample than there is at the rim, and this is similar to the zonation patterns evident in Argyle diamond plates. For the remaining Ellendale 9 diamond plates, nitrogen isotopic variations occur on a small scale, and this may be obscuring subtle relationships between nitrogen isotopic composition and nitrogen aggregation state and content.

	ARGYLE	**ELLENDALE 4**	**ELLENDALE 9**
$\delta^{13}C$ *vs.* diamond paragenesis.	Peridotitic diamonds have more positive $\delta^{13}C$ values than eclogitic diamonds. The intra-diamond range of $\delta^{13}C$ values is larger for peridotitic than for eclogitic diamond plates.	•	Peridotitic diamonds have more positive $\delta^{13}C$ values than eclogitic diamonds.

Table 2.13: Relationships between the characteristics of Argyle, Ellendale 4 and Ellendale 9 diamonds. Table 2.13 is continued overleaf.

	ARGYLE	ELLENDALE 4	ELLENDALE 9
$\delta^{13}C$ *vs.* shape.	Peridotitic diamonds have sharp edged, octahedral morphology, whereas eclogitic diamonds are more commonly resorbed.	•	•
$\delta^{13}C$ *vs.* colour.	Brown (sheared) diamonds have more negative $\delta^{13}C$ values than white or yellow diamonds.	•	•
$\delta^{13}C$ value *vs.* nitrogen abundance.	There is a good positive correlation evident in diamond plate 150701 #12-1. There is also a positive trend for 150701 #8, although there are some outliers.	•	There is a positive correlation between nitrogen abundance and carbon isotopic composition in plate E9038. In plate E9040, the correlation is negative.
$\delta^{13}C$ *vs.* nitrogen aggregation state.	There is a positive correlation in plate 150701 #12-1. The trend is also positive for 150701 #8, although it is less good. The slope for plate 150701 #12-4 is negative.	•	There is a positive correlation between $\delta^{13}C$ and the proportion of nitrogen in B-aggregates in plate E9038. In plate E9040, the correlation is negative.
Nitrogen content *vs.* paragenesis.	Peridotitic diamonds contain less nitrogen than eclogitic paragenesis diamonds.	•	Eclogitic diamonds have a wider range in, and higher mean nitrogen content than peridotitic diamonds.
Nitrogen content *vs.* presence of inclusions.	•	There is a smaller range in nitrogen contents in inclusion-bearing diamonds than there is in inclusion-free diamonds.	There is a smaller range in nitrogen contents in inclusion-bearing diamonds than there is in inclusion-free diamonds.

Table 2.13 continued: Relationships between the characteristics of Argyle, Ellendale 4 and Ellendale 9 diamonds.

	ARGYLE	ELLENDALE 4	ELLENDALE 9
Nitrogen content *vs.* colour.	Brown diamonds contain less nitrogen than yellow diamonds.	•	•
Nitrogen content *vs.* nitrogen aggregation state.	There is a positive correlation between proportion of B-aggregates and nitrogen abundance in plates 150701 #8 and 150701 #12-1.	•	There is a positive correlation between nitrogen aggregation state and abundance in plate E9037, E9038 and E9040.
Nitrogen aggregation state *vs.* diamond paragenesis.	Peridotitic diamonds tend to contain nitrogen in less aggregated form than eclogitic diamonds.	•	There is a wider range in aggregation state, and a higher mean proportion of B-aggregates for eclogitic diamonds.
$\delta^{15}N$ *vs.* diamond paragenesis.	•	•	Eclogitic diamonds are less variable and have a higher mean $\delta^{15}N$ value than peridotitic diamonds.
$\delta^{15}N$ *vs.* shape.	Macles have lower $\delta^{15}N$ values than octahedra or dodecahedra.	•	•
$\delta^{15}N$ *vs.* nitrogen content.	There is a positive correlation for eclogitic diamonds and for brown diamonds. There are positive correlations between nitrogen content and isotopic composition for plates 150701 #8, 150701 #12-1 and 150701 #12-8.	There is a negative correlation between nitrogen content and isotopic composition for inclusion bearing diamonds.	There is a positive correlation between nitrogen abundance and $\delta^{15}N$ value in plate E9037.
$\delta^{15}N$ *vs.* nitrogen aggregation state.	There is a positive correlation in plates 150701 #8, 150701 #12-1 and 150701 #12-4.	•	There is a positive correlation in plate E9037.

Table 2.13 continued: Relationships between the characteristics of Argyle, Ellendale 4 and Ellendale 9 diamonds.

	ARGYLE	ELLENDALE 4	ELLENDALE 9
$\delta^{15}N$ *vs.* $\delta^{13}C$.	Eclogitic and peridotitic 2mm diamonds form two overlapping groups. There is a positive correlation between carbon and nitrogen stable isotope ratios for plates 150701 #8 and 150701 #12-4 and a negative correlation in plate 150701 #12-4.	There are no linear trends.	Elongated groups occur for three of the diamond plates. For plate E9040, there is a positive slope to the group, whereas the slope for plates E9037 and E9041 is negative. No line can be fitted confidently through plate E9038.

Table 2.13 continued: Relationships between the characteristics of Argyle, Ellendale 4 and Ellendale 9 diamonds.

3 Processes affecting stable isotope ratios

3.1 INTRODUCTION

There are large ranges in the carbon and nitrogen stable isotopic composition of both Argyle and Ellendale diamonds. This may result from either fractionation of the stable isotope ratios in the source regions of these diamonds or from multi-component mixing, where each component has a distinct stable isotope signature. Fractionation of carbon stable isotope ratios was first proposed by Deines (1980a) who examined potential diamond forming reactions (See section 1.4.1) and concluded that only in the unlikely cases in which diamond precipitated from a vapour phase were isotopic fractionations likely to be significant. The magnitude of these isotopic fractionations would, however, be limited due to the low expected equilibrium fractionation factors in the diamond – vapour system at mantle temperatures. Deines (1980a) noted that the maximum isotopic fractionation was likely to be of the order of 15‰ and that this would occur if diamonds were precipitated from a CO_2 dominated fluid. In such an environment, a distribution of $\delta^{13}C$ values skewed towards more positive values would result, as is seen, for example, in the Argyle diamonds (Figure 2.5). This contrasts with the combined $\delta^{13}C$ distribution for all diamonds (See Figure 1.3), which is skewed to more negative values. Such a distribution would result if diamonds precipitated from a CH_4 dominated vapour, but in such a case, the maximum isotopic fractionation of carbon is likely to be of the order of 5‰. In any respect, neither a 15‰ nor a 5‰ isotopic fractionation are sufficient to alone explain the full range in diamond carbon isotopic compositions, which globally fall within the range $-35‰ \leq \delta^{13}C \leq +3‰$ (See Chapter 1 and Figure 1.3).

Swart *et al.*, (1983) examined the differences in carbon isotopic composition between the cores and coats of coated diamonds and concluded that the approximately 4‰ differences in $\delta^{13}C$ value between core and coat might be consistent with a Rayleigh distillation process operating during diamond growth, although this interpretation was later discounted by Boyd *et al.*, (1987) who showed that diamond cores could be both ^{13}C enriched and ^{13}C depleted relative to diamond coat. Galimov (1984a), in contrast, suggested that theoretical fractionations in the diamond – CO_2 – CH_4 – graphite system could explain minor fractionations of the $\delta^{13}C$ value of diamonds, but that such isotopic fractionation processes could not explain ^{13}C depleted diamonds successfully.

An alternative hypothesis has been proposed by Javoy *et al.*, (1986) who suggested that a "global Rayleigh distillation" is sufficient to explain the full range of $\delta^{13}C$ values observed for diamonds and other mantle derived samples. In this open-system model, CO_2 is lost from a homogeneous source which has a $\delta^{13}C$ value within the mantle range.

An approximately 4‰ fractionation between diamond and CO_2 (or carbon trapped in a melt, as CO_3^{2-}, and CO_2) is able to fractionate the $\delta^{13}C$ values of diamond and residue significantly. This hypothesis is also supported by Bottinga and Javoy (1989, 1990) for explaining the carbon isotopic compositions of MORB, but the fractionation factor used in the model is controversial. Based on experimental studies, Mattey *et al.*, (1990), suggested that 4‰ is an overestimate and that a fractionation factor of the order of 2.0‰ to 2.6‰ is the maximum possible. An approach similar to that of Javoy *et al.*, (1986) and Bottinga and Javoy (1989, 1990) was followed by Otter (1989) who examined the possibility of carbon isotopic variations in diamonds from the Sloan diatremes, North America, being caused by isotopic fractionation during fractional crystallization. Otter (1989) concluded that while a Rayleigh process may be responsible for minor variations in $\delta^{13}C$ values within sub-groups of diamonds, it is not possible to explain the full range of carbon stable isotopic compositions evident in these samples by simple fractionation mechanisms, despite the larger fractionation factor of 4‰ being used.

More recently, Galimov (1991) presented a model for explaining the full range of carbon isotopic compositions occurring in mantle derived samples, and in kimberlites and related rocks in particular. In this model, isotopic fractionations are thought to occur as a result of a combination of Rayleigh distillation processes and isotopic exchange in the CO_2 – CH_4 – solid carbon system. Partial dissociation of CH_4-dominated fluids on entering a region with increased fO_2 is expected to produce CO_2, with an associated isotopic fractionation. Galimov (1991) suggested that diamonds of eclogitic paragenesis are related to this fractionated carbon, and that diamonds of peridotitic paragenesis are related to the "primary", unfractionated fluids.

To date, little is known about the fractionation of nitrogen isotopes within diamond. Boyd *et al.*, (1988a) examined the fractionation of nitrogen isotopes in synthetic diamonds of mixed crystal habit, and reported that regions of reduced nitrogen content have increased $\delta^{15}N$ values. This is growth sector dependent; cubic growth sectors are enriched in ^{15}N by some 4.5‰ relative to octahedral growth sectors, and contain about a factor of 2 less nitrogen. Boyd (Pers. Comm.) suggested that this may be a function of differing interfacial energies for differing growth zones.

Nitrogen isotope fractionation and multi-component mixing were both considered by Javoy *et al.*, (1984) as possible explanations for an anti-correlation noted between $\delta^{15}N$ value and nitrogen abundance in diamonds from Mbuji Mayi, Zaire. From the few data that were available, Javoy *et al.*, (1984) were not able to choose between either mechanism. They did, however point out that there were two groups on a $\delta^{13}C$ *vs.* $\delta^{15}N$ plot which may represent two distinct source regions, but that there was also an inverse correlation between $\delta^{13}C$ and $\delta^{15}N$ values for large diamonds. This, they

suggested may represent stages in a distillation (*i.e.* fractionation) process. At present, no further reports of nitrogen isotopic fractionations in diamond are known, although there are relationships, summarised in Table 2.13, between the nitrogen content, aggregation state and isotopic compositions of the Argyle and Ellendale diamonds that may represent either isotopic fractionation or mixing processes.

In the following sections, Rayleigh distillation and condensation and two-component mixing are examined as possible causes of the carbon and nitrogen stable isotope variations in the Argyle and Ellendale diamonds. Rayleigh condensation is equivalent to fractional crystallization and fractional (Rayleigh) melting is indistinguishable from Rayleigh distillation. The relevant fractionation equations are (Hoefs, 1987):

Rayleigh condensation $$\frac{R_v}{R_{v_0}} = F^{(\alpha - 1)} \qquad (3.1)$$

Rayleigh distillation $$\frac{R_v}{R_{v_0}} = \frac{1}{\alpha} F^{\left(\frac{1}{\alpha} - 1\right)} \qquad (3.2)$$

In these equations, α = the fractionation factor, F = the fraction of carbon remaining in the residue, R_{v_0} = the isotope ratio in the source material and R_v = the isotope ratio in the residue.

The general mixing equation is hyperbolic and has the form (Langmuir *et al.*, 1978):

$$Ax + Bxy + Cy + D = 0 \qquad (3.3)$$

where x and y = general variables along the abscissa and ordinate respectively. The calculation of coefficients A, B, C and D and the mathematical manipulations for using equations 3.1 and 3.2 for modelling variations in δ values are given in Appendix 3.

Also presented in Appendix 3 is a discussion of the efficacy of both open and closed system equilibrium crystallization and batch melting on the fractionation of stable isotope ratios. These three processes are all limited to small maximum fractionations; a few per mille at most and they are thus not considered here. Kinetic effects are also not considered in this Chapter, due to both the complexities of the mathematics involved and the fact that at magmatic temperatures, kinetic effects are expected to be minimal (*e.g.* Hoefs, 1987). Jambon (1980) has, however produced a kinetic model for isotopic fractionations in crystals growing from magmatic melts.

3.2 ISOTOPE RATIO MODELLING

3.2.1 Two millimeter diamonds

Although there are large ranges in $\delta^{13}C$† and $\delta^{15}N$ value for Western Australian diamonds, there are no obvious correlations between carbon and nitrogen stable isotope compositions for any of the Argyle, Ellendale 9 or Ellendale 4 data sets as a whole. Therefore no simple fractionation process can be used to explain the stable isotope characteristics of all these diamonds. Indeed the only clear relationships that do occur, are between nitrogen content and $\delta^{15}N$ value. Amongst eclogitic and brown diamonds from Argyle, there is a positive correlation between nitrogen abundance and isotopic composition, and a negative correlation occurs between these two variables for inclusion-bearing diamonds from Ellendale 4. There is no relationship evident in any of the sub-groups of Ellendale 9 diamonds. This lack of constancy in the $\delta^{15}N$ – nitrogen abundance relationship is evidence against a simple fractionation process, and it suggests that whatever the mechanism responsible for this variation in nitrogen, it is not universal, but rather represents a set of circumstances particular to each case.

As the lack of any consistent relationship between $\delta^{13}C$, $\delta^{15}N$, nitrogen abundance and nitrogen aggregation state in Argyle, Ellendale 4 and Ellendale 9 diamonds is evidence against a simple fractionation process relating these variables, a heterogeneous source region for each diamond population is suggested. Data are scattered around the average composition (Table 3.1) which is distinct for each pipe. This heterogeneity would seem to occur on the scale of a few kilometers. Ellendale 4 and Ellendale 9 are closely proximate (15 km) at the surface, and assuming similar depths of diamond entrainment, have different source region $\delta^{13}C$ and $\delta^{15}N$ characteristics (Table 3.1).

Additional evidence against equilibrium or fractional crystallization being responsible for the observed range in $\delta^{13}C$ values in the Argyle, Ellendale 4 and Ellendale 9 diamonds is that, for credible fractionation factors (≈4‰ or less), very large degrees of crystallization are necessary to generate the observed range of $\delta^{13}C$ values from a homogeneous source

---

† Argyle diamonds $\delta^{13}C$ range is 9.5‰ (Table 2.7)
Ellendale 9 diamonds $\delta^{13}C$ range is 22.1‰ (Table 2.8).
Ellendale 4 diamonds $\delta^{13}C$ range is 4.3‰ (Table 2.8).
$\delta^{15}N$ range is 22.8‰ for Argyle diamonds (Table 2.6)
Ellendale 9 $\delta^{15}N$ range is 22.5‰ (Section 2.2.4.2.3).
Ellendale 4 $\delta^{15}N$ range is 14.1‰.(Section 2.2.4.2.3).

	$\delta^{13}C$ (‰)	$\delta^{15}N$ (‰)	[N] ppm	% B-aggregates
Argyle	-9.8	+5.8	282	56
Ellendale 4	-4.7	-2.3	1122	19
Ellendale 9	-7.7	+0.1	998	28

Table 3.1: Average compositions of diamonds from the Argyle, Ellendale 4 and Ellendale 9 lamproites. Data from Hall and Smith (1984), Jaques *et al.*, (1989), Sobolev *et al.*, (1989) and Taylor *et al.*, (1990), together with data reported in this and later chapters have been included in the calculation of these averages.

that has a $\delta^{13}C$ value = -6‰. From equation 3.1, it is possible to calculate that at least 96% crystallization is required at Argyle, 65% crystallization at Ellendale 4 and 99.4% crystallization at Ellendale 9 to explain the range of $\delta^{13}C$ values in these pipes, when the fractionation factor $\alpha = 1.004$ (Table 3.2). If lower fractionation factors are used (*e.g.* Mattey *et al.*, 1990), even more crystallization is necessary. Furthermore, in order to explain the $\delta^{13}C$ shift to more negative values, a process which concentrates ^{13}C in the diamond is required (Deines 1980a). One possibility is diamond precipitating from CH_4 rather than from CO_2, however if CH_4 is involved in diamond genesis then carbon fractionation factors lower than $\alpha = 1.004$ are expected (Bottinga, 1969; Friedman and O'Neil, 1977).

Start composition: $\delta^{13}C$ = -6‰
Fractionation factor α = 1.004

Fractional crystallization $\frac{R_v}{R_{v_o}} = F^{(\alpha - 1)}$

% crystallization	F	$\delta^{13}C_{min}$ (‰)	
96.0	0.040	-14.8	$\delta^{13}C_{min}$ at Argyle is -14.1‰
99.4	0.006	-22.2	$\delta^{13}C_{min}$ at Ellendale 9 is -22.1‰
65.0	0.350	-6.21	$\delta^{13}C_{min}$ at Ellendale 4 is -6.2‰

Table 3.2: Minimum $\delta^{13}C$ values that can be attained by fractional crystallization from a starting $\delta^{13}C$ value of -6‰. The fractionation factor $\alpha = 1.004$ is extrapolated from Bottinga (1969) and Friedman and O'Neil, (1977) to mantle temperatures.

Whether very large degrees of crystallization are geologically feasible is difficult to assess. If diamond precipitates from small volume, volatile-rich fluids, crystallization may completely exhaust available carbon on a local scale of perhaps a few centimeters. Crystallization of diamond in such a single crystal–sized reservoir may be evident in the isotope zonation patterns of individual diamonds and these are described in the following section. On a larger scale however, there is no evidence either for or against a mantle-wide depletion of carbon associated with diamond genesis. Volatile-rich fluids, of asthenospheric origin have, however, been shown to be widespread in the lithospheric mantle (Boyd *et al.*, 1992), and such fluids are likely to constantly replenish the carbon available in the region of diamond formation. This may prevent high degrees of crystallization from being reached.

Thus large degrees of crystallization are not the preferred model for explaining the range in $\delta^{13}C$ values seen in these 2 mm diamond populations. Instead a heterogeneous mantle model is suggested in which each pipe samples a different source region. Possible causes of source region heterogeneity are discussed in Chapter 6, but some of the heterogeneity may be time-related, with different pulses of volatile-rich fluid, each with different stable isotope signatures occurring at different times, and each precipitating a new generation of diamond. It is possible that the peridotitic paragenesis diamonds at Argyle are the product of one such pulse and the eclogitic paragenesis diamonds the product of another.

It is possible that mixing of different source regions, with different isotopic characteristics, may be responsible for some of the variability seen within these diamond populations. However, the lack of consistent linear relationships between the $\delta^{13}C$ and $\delta^{15}N$ values of the 2 mm diamonds precludes simple two-component mixing. If mixing is implicated, either more than two end-member components are required, or each end-member must in turn have a range of $\delta^{13}C$ and $\delta^{15}N$ values. For example, mixing an Argyle type source with an Ellendale 4 type source may give rise to the range of $\delta^{13}C$ values seen in the Ellendale 9 diamond suite. Two-component mixing within individual diamond crystals is quantitatively examined in the following section.

3.2.2 Diamond plates

Examining individual diamonds may allow an assessment of the processes that have operated during their crystallization. Stable isotope variability within individual crystals is almost as great as that within the bulk population, and these variations may result from

- either multiple cycles of diamond growth, each from an isotopically distinct source material,
- or from a fractionation of the stable isotope ratios during crystallization in a closed system,
- or may result from diamond growth in an open system where fluids of different composition are mixing. These possibilities can all be investigated.

Multi-stage diamond growth has been described in the case of coated stones (*e.g.* Boyd *et al.*, 1987, 1992). In the Argyle and Ellendale diamonds, distinct growth phases may be identified by any or all of the following: (1) changes in cathodoluminescence characteristics and evidence of resorption (See for example the corners of plate 150701 #12-1, Figure 2.14); (2) abrupt changes in the isotopic characteristics, nitrogen abundance and nitrogen aggregation state of different portions of the crystal and (3) by sudden changes in mantle residence times as calculated from nitrogen aggregation state

(see section 3.3). Such changes in the isotope characteristics are evident in diamond plates 150701 #1, 150701 #12-4, and on the left hand edge (blocks A and C) of 150701 #12-8 from Argyle. The isotopic variability in plate E9038 and on the rim of E9041 may have a similar cause. Multiple phases of diamond growth have been related to injections of new volatile-bearing fluid passing through diamond source region by Boyd *et al.*, (1992), but unlike the coated stones described by Boyd *et al.*, (1987, 1992) the Argyle and Ellendale overgrowths are not characterised by a uniform "normal mantle" composition. Rather, the later generations of diamond growth are characterised by variable composition and possible causes of these variable compositions will be discussed in Chapter 6.

Both fractional crystallization and mixing will result in regular changes in the $\delta^{13}C$ and $\delta^{15}N$ values, nitrogen content and nitrogen aggregation state across the diamond crystal. Regular zonation of these variables is evident in the Argyle diamond plates 150701 #8, 150701 #12-1 and on the right hand side of 150701 #12-8 (blocks D to H), as well as being evident in E9037 (Table 3.1). An attempt is now made to model the isotopic variations in the four of these diamonds that show the widest range in isotopic composition (Table 3.3) by fractional crystallization and by mixing.

Diamond plate	$\delta^{13}C$ range (‰)	$\delta^{15}N$ range (‰)
150701 #12-8	-14.1 to -9.3	3.3 to 10.6
150701 #8	-4.5 to -6.6	-2.5 to 13.6
150701 #12-1	-7.2 to -9.1	0.9 to 10.8
E9037	-10.9 to -7.9	0.3 to 13.2

Table 3.3: Diamond plates that have regularly zoned stable isotope compositions. See also Figures 2.18, 2.19 and 2.39. Sample 150701 #8 is of peridotitic paragenesis and 150701 #12-1 is of eclogitic paragenesis. The parageneses of the other two samples is not known.

Note that the relationships between $\delta^{13}C$ and $\delta^{15}N$ value, nitrogen content and aggregation state occur in a limited number of stones, and those in which they do occur are those with the most simple internal structure as revealed by cathodoluminescence. The results of the modelling cannot provide the definitive model for diamond crystallization. They shed light on processes that may be operating only during the most simple cases of diamond genesis.

Firstly an attempt is made to model nitrogen zonation patterns in these samples as a fractional crystallization process (equation 3.1) operating during growth, and the following assumptions are made:

(1) Nitrogen behaves as a compatible element during diamond growth and partitions preferentially into the growing crystal. This is supported by the nitrogen content zonation within these four diamonds (higher nitrogen content in earlier precipitated diamond). If nitrogen behaves as an incompatible element, an

increase in diamond nitrogen content from core to rim during fractional crystallization is expected.

(2) These diamonds precipitate in a closed system. Crystal growth is accompanied by a decrease in the nitrogen content of the source material (fluid/magma) which will result in a concomitant decrease in diamond nitrogen content with continuing diamond growth, as is seen in the samples under discussion.

(3) The regions of the diamond with maximum nitrogen content represent the starting conditions. These are always found towards the central (earliest forming) regions of these diamond crystals.

(4) Assuming a linear relationship between nitrogen content and diamond growth. Normalising the nitrogen content of the blocks constituting the ladder section, to the nitrogen content of the block with the most abundant nitrogen provides an indication of the degree of crystallization. This assumption is a first-order approximation in light of the lack of published nitrogen - diamond partition coefficient data. The normalised nitrogen content ($[N]/[N]_{max}$) is equivalent to the "F" value as used in equations 3.1 and 3.2. As diamond growth proceeds, $[N]/[N]_{max}$ deceases to a minimum at the sample edges.

(5) The ^{15}N isotope preferentially partitions into diamond. This is shown by the more positive $\delta^{15}N$ values measured in the central regions of these 4 diamond plates than at the edges.

The slopes (Δ fractionation) and intercepts ($\delta^{15}N_{initial}$) of power regression curves through normalised nitrogen concentration and $\delta^{15}N$ data are presented in Table 3.4. Curves constrained by being forced through data with the minimum or maximum and both minimum and maximum values of $[N]/[N]_{max}$, as well as curves in which all data are equally weighted are reported. Theoretical fractional crystallization curves are illustrated graphically in Figure 3.1.

The curves illustrated in Figure 3.1 are fractional crystallization curves, calculated from equation 2.5, for average α values and initial $\delta^{15}N$ obtained from Table 3.4. They show a close fit to the actual $\delta^{15}N$ values measured in plates 150701 #8, 150701 #12-1 and 150701 #12-8. The $\delta^{15}N$ data from E9037 do not fit the calculated fractionation curve. The calculated "best-fit" and weighted fractionation factors range from $\alpha = 1.0027$ to $\alpha = 1.010$ with a mean value of $\alpha = 1.0044$. Rounding this to $\alpha = 1.004$ ($\Delta = 4‰$), consistent with the precision of the data, provides a fractionation factor that may explain the nitrogen stable isotope variations in diamond plates 150701 #8, 150701 #12-1 and 150701 #12-8.

Note that on the scale of Figure 3.1, the shapes of fractionation curves for $\alpha = 1.003$, $\alpha = 1.004$ and $\alpha = 1.005$ are not readily distinguished visually. The position of the curve

depends on the $\delta^{15}N_{initial}$ value and the effect of changes in this is illustrated on Figure 3.2.

Diamond plate	Initial $\delta^{15}N$	Δ fractionation	r
150701 #8			
All data with equal weight	10‰	3.5‰	0.81
Forced through minimum F	10‰	3.2‰	
Forced through maximum F	10‰	3.5‰	
Forced through both min and max F	8‰	2.7‰	
150701 #12-1			
All data with equal weight	5‰	5.1‰	0.81
Forced through minimum F	5‰	4.2‰	
Forced through maximum F	5‰	5.1‰	
Forced through both min and max F	5‰	4.8‰	
150701 #12-8			
All data with equal weight	8‰	2.9‰	0.88
Forced through minimum F	8‰	4.1‰	
Forced through maximum F	8‰	2.9‰	
Forced through both min and max F	7‰	3.5‰	
E9037			
All data with equal weight	8‰	4.2‰	0.65
Forced through minimum F	7‰	10.‰	
Forced through maximum F	6‰	4.2‰	
Forced through both min and max F	5‰	7.2‰	

Table 3.4: Modeling results for $\delta^{15}N$ variations in Argyle and Ellendale plates. The curves have been calculated by the Hewlett-Packard™ program "GRAFIT" to minimise the sum of squares of residuals, and the r value is the correlation coefficient, which is only meaningful for unforced curves.

The fit of the $\delta^{15}N$ data for Argyle plates 150701 #8, 150701 #12-1 and 150701 #12-8 to the fractionation curves may be fortuitous, but if it is indeed indicative of a stable isotope fractionation during diamond precipitation, then it also indicates that (1) the source region of these diamonds is heterogeneous with respect to initial $\delta^{15}N$ value and (2) that ^{15}N is concentrated in the crystallizing diamond by about 4‰. A heterogeneous source region has already been postulated from the $\delta^{15}N$ values of the 2 mm diamonds. Here it is suggested that, for these diamond plates the initial $\delta^{15}N$ value ranges from $\delta^{15}N \approx +5‰$ to +10‰.

The range in fractionation factors determined from the three Argyle diamonds from just under $\alpha = 1.003$ to just over $\alpha = 1.005$ is very large, given the temperatures at which diamond are expected to precipitate. Possible causes for this variation in model α include: (i) varying temperatures of diamond crystallization. An $\alpha = 1.0004$ fractionation factor at 1050°C will become $\alpha = 1.00022$ at a temperature of 1500°C using the equation linking α and temperature (Equation A3.3, Appendix 3). Temperature estimates from Argyle and Ellendale diamonds range from 1050° to 1500°C (Hall and

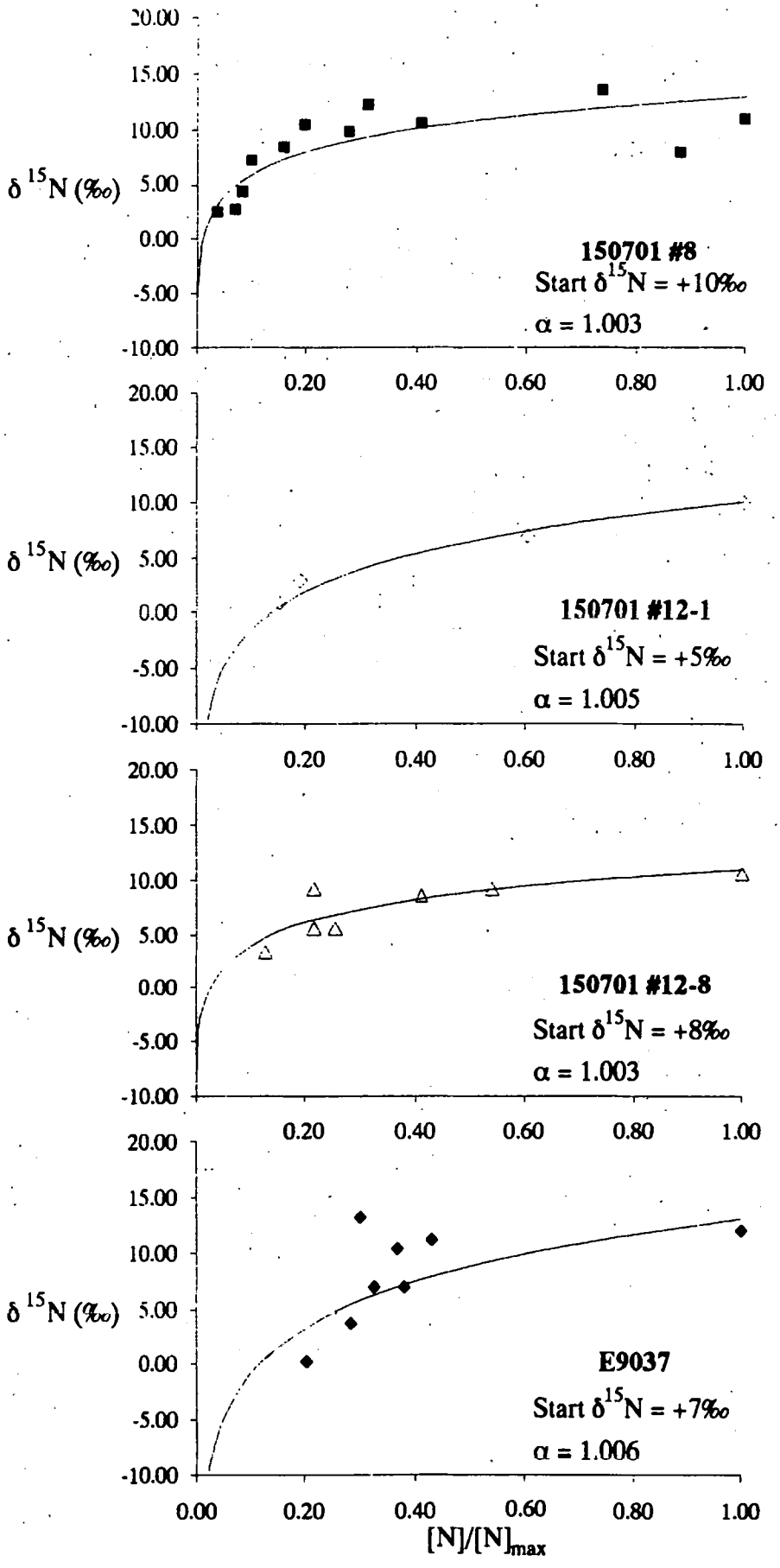

Figure 3.1: Fractionation curves passing through diamond plates that show evidence of nitrogen isotopic fractionation. Initial $\delta^{15}N$ values and fractionation factors are the means from the data in Table 3.4. Note that "Start $\delta^{15}N$" refers to the source composition.

Smith, 1984; Jaques *et al.*, 1989; Taylor *et al.*, 1990); (ii) variable fO_2 affecting nitrogen speciation with different fractionation factors being applicable, for example, for NH_4, for NH_3^+ or for N_2 and (iii) the relative proportions of volatile species (CO_2, CH_4, H_2O, F and N) affecting the nitrogen fractionation factor. These are just three speculative possibilities and it is likely there are further affects that will only become evident in a comprehensive study of nitrogen fractionation factors in the diamond – source material system.

The likelihood of carbon isotope fractionations also occurring during diamond formation can be investigated in a manner similar to that used for nitrogen. Once again, normalised nitrogen content is used as an indicator of the degree of crystallization (F), and calculated fractionation curves through the $\delta^{13}C$ values of these diamond samples are plotted in Figure 3.2. The slope and intercept values for power regression lines through the $\delta^{13}C$ data, minimising the sum of squares of residuals, are listed in Table 3.5.

Diamond plate	Initial $\delta^{13}C$	Δ fractionation	r
150701 #8	-5.6‰	0.2‰	0.74
150701 #12-1	-8.3‰	0.9‰	0.93
150701 #12-8 (All data)	-10.1‰	3.0‰	*
E9037	-10.3‰	0.5‰	*

Table 3.5: Power regression curves passing through the $\delta^{13}C$ values of diamonds that show evidence of nitrogen fractionation. Samples marked with a * have been constrained by omitting outliers.

The carbon stable isotopic compositions within diamond plates 150701 #8 and 150701 #12-1 plot close to calculated fractional crystallization curves, as do the $\delta^{13}C$ values from the right hand side (blocks D to G) of 150701 #12-8. The $\delta^{13}C$ values from E9037 however do not fit the calculated fractionation curve. This indicates that some, but not all, diamonds might precipitate under closed system conditions, and that carbon isotopes could be fractionated during this crystallization. The magnitude of the fractionation effects are however small and a fractionation of less than 3‰ is indicated ($\alpha < 1.003$) and values of $\alpha \leq 1.001$ are probable. As is the case with nitrogen fractionation factors, the model fractionation factors vary and the role of temperature and fO_2 on this variation need to be investigated.

The initial $\delta^{13}C$ values indicated by the fitted fractionation curves range from $\delta^{13}C$ = -5‰ to just less than -10‰, which encompasses the major peak in diamond $\delta^{13}C$ values near -6‰. The scatter in these initial $\delta^{13}C$ values may be a result of either isotopic fractionation effects during the formation of the diamond-precursor fluid, or more probably by diamonds crystallising within an initially heterogeneous source region.

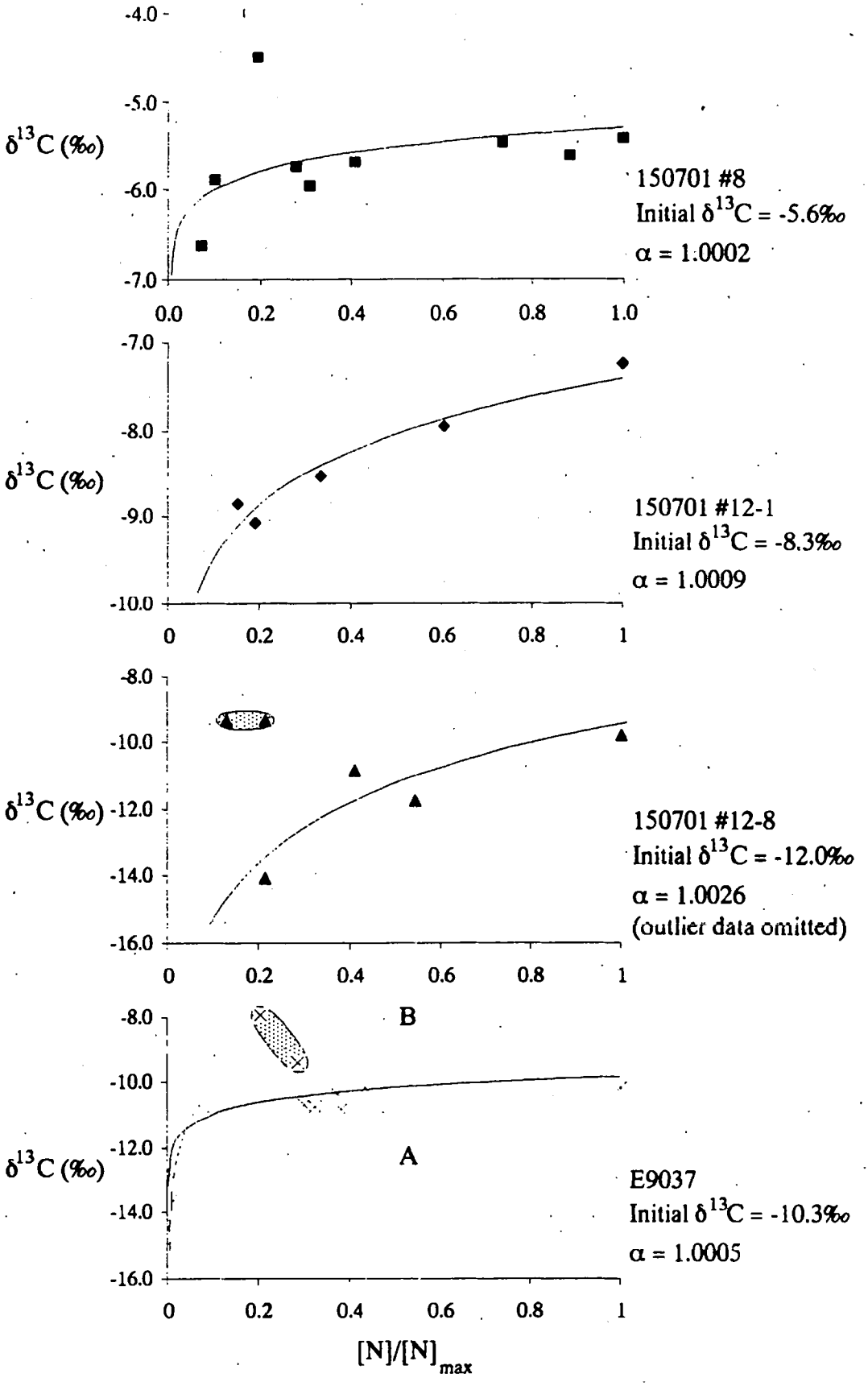

Figure 3.2 Fractional crystallization curves plotted through $\delta^{13}C$ *vs.* normalised nitrogen content. Outlier data (marked) on 150701 #12-8 and E9037 are a function of non-symmetrical diamond growth. Note that "Start $\delta^{13}C$" refers to the source composition. Superimposed on the plot for E9037 are two dotted lines that illustrate the sensitivity of fractionation curves to changes in α and $\delta^{13}C_{initial}$. Curve A has the same fractionation factor (α = 1.0005) as the model curve for E9037, but has a lower $\delta^{13}C_{initial}$ (-12‰). Curve B has the same $\delta^{13}C_{initial}$ as curve A, but the fractionation factor, α = 1.005 is 10 times larger than that of curve A.

Better estimates of possible fractionation factors and initial $\delta^{15}N$ and $\delta^{13}C$ values may be obtained by considering carbon and nitrogen stable isotope covariation (Figure 3.3). This can account for non-symmetrical diamond growth as in the case in samples 150701 #12-8, and E9037. The intersection of fractionation vectors for each side of the diamond plate may provide a possible source composition. Data for the fractionation vectors shown in Figure 3.3 are summarised in Table 3.6.

			Fractionation factor	
Plate	$\delta^{13}C_{initial}$	$\delta^{15}N_{initial}$	Carbon	Nitrogen
150701 #8 (both sides)	-5.6‰	+10‰	1.0003	1.003
150701 #12-1(both sides)	-8.3‰	+5‰	1.0009	1.005
150701 #12-8 (left had side)	-9.0‰	+10‰	1.0003	1.005
(right hand side)	"	"	1.004	1.001
E9037 (left hand side)	-9.75‰	+14‰	1.003	1.003
(right hand side)	"	"	1.0005	1.003

Table 3.6: Possible source region stable isotope characteristics and fractionation factors explaining $\delta^{13}C$ - $\delta^{15}N$ covariation in diamond plates that show evidence of fractional crystallization.

The $\delta^{13}C$ and $\delta^{15}N$ data for samples 150701 #8 and 150701 #12-1 correspond closely to the calculated fractionation vectors. There is, however a considerable scatter around the "best fit" lines for $\delta^{13}C$ and $\delta^{15}N$ data from 150701 #12-8 and E9037 and for this reason, fractional crystallization is not considered to be the most likely explanation for the stable isotope covariation in these two samples. From Table 3.6, it is evident that a mean nitrogen fractionation factor $\alpha_{diamond\text{ - }source}$ close to 1.003 is indicated for these samples whereas for the most part carbon fractionation factors are much lower with $\alpha_{diamond\text{ - }source}$ usually < 1.001. This is consistent with the large differences in the fractionation of nitrogen and carbon stable isotope ratios reported for synthetic diamond of mixed crystal habit (Boyd *et al.*, 1988a) where no significant changes in $\delta^{13}C$ value across the sample were associated with an up to 45‰ variation in $\delta^{15}N$ values in different growth sectors of the diamond. Causes of the differences between nitrogen and carbon fractionation factors are not known, but it may be related to differences in the binding energy of the carbon and nitrogen atoms in the diamond lattice. The differences in fractionation factors for different samples and for different sides of diamond plates 150701 #12-8 and E9037, may be a result of changes in temperatures during diamond growth and, in the case of carbon, changes in the source region fO_2 affecting the CO_2/CH_4 ratio.

There is no evidence of a similar closed system fractionation of either nitrogen or carbon isotopes across the core regions of any of the diamond plates examined by Boyd *et al.*, (1987, 1992). These plates have smaller ranges in nitrogen content in their core regions,

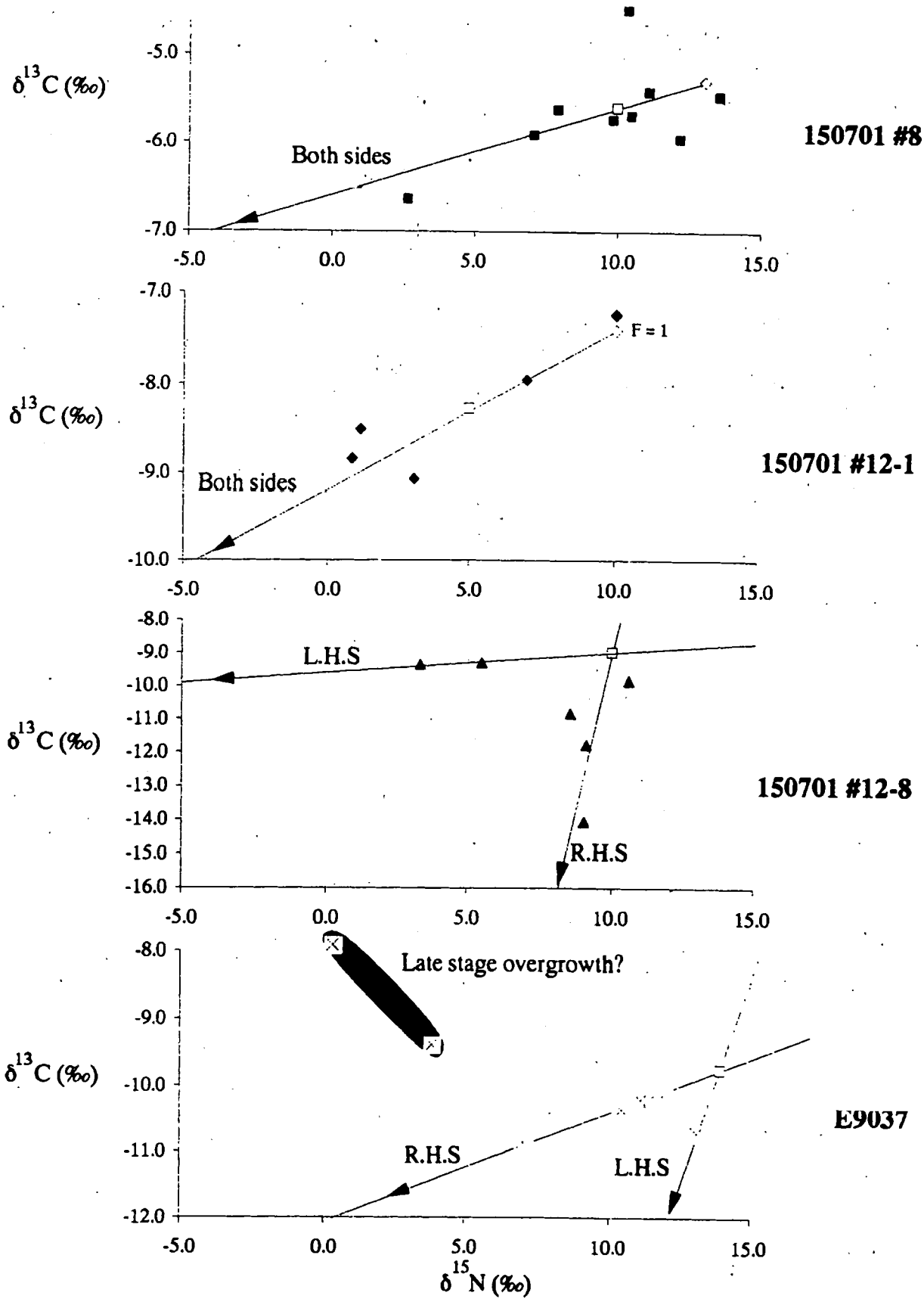

Figure 3.3: $\delta^{15}N$ - $\delta^{13}C$ plot for diamonds showing evidence of stable isotope fractionation. Fractionation vectors for fractional crystallization (equation 2.5) from an assumed starting composition (open square) and the composition of the first precipitated diamond (open diamond) at F = 1 are shown. L.H.S = left hand side and R.H.S = right hand side of the diamond plate, as plotted in Figures 2.12 to 2.14 and 2.30. Arrows on vectors show increasing crystallization.

than the three Argyle and one Ellendale plates examined. In these cases $[N]/[N]_{max}$ does not vary from 1 to 0 and hence does not provide a complete record of the different stages of crystallization. In the samples examined by Boyd *et al.*, (1987, 1992), nitrogen and carbon stable isotopic characteristics of the core and coat are distinct, but the differences between coat and core are not adequately explained by the closed system fractional crystallization model presented here for diamond plates 150701 #8, 150701 #12-1, 150701 #1 and E9037. Instead, the model of Boyd *et al.*, (1987, 1992) in which the coat forms in an event separated in time, and possibly space, from the main diamond growth event is preferred.

Thus closed system fractional crystallization is a model that may be appropriate in the most simple cases of diamond precipitation. As the model applies only to the crystallization of single diamonds from a reservoir that is restricted in size to a single crystal it cannot be applied to diamonds in general, without some modification. Furthermore, it is possible that the trends that here fit fractionation curves may also be the result of mixing between two isotopically distinct components. This possibility is now investigated.

Mixing lines on a plot of $\delta^{13}C$ *vs.* $\delta^{15}N$ are curved (Appendix 3) and consistent trends on such plots (Figures 2.20 and 3.3) indicate that mixing is an appropriate model to consider. Whether it occurs may be tested by considering the variation of $\delta^{15}N$ and $\delta^{13}C$ values with nitrogen content. Mixing trends, when δ values are plotted against reciprocal nitrogen content, define straight lines (*e.g.* Javoy *et al.*, 1984).

There are no clear correlations between reciprocal nitrogen content and both the $\delta^{15}N$ and $\delta^{13}C$ values for diamond plates 150701 #8, 150701 #12-8 or E9037 (Figures 3.4 and 3.5). For these three diamond plates, linear regression lines on $\delta^{15}N$ *vs.* 1/[N] have correlation coefficients of $r^2 = 0.71$, 0.73 and 0.54 respectively (see Figure 3.4), but the corresponding regression lines for $\delta^{13}C$ *vs.* 1/[N] have correlation coefficients of $r^2 =$ 0.28, 0.02 and 0.39 respectively (Figure 3.5). This lack of any relationship between reciprocal nitrogen content and the diamonds $\delta^{13}C$ value is taken as evidence that the isotopic relationships seen in these samples are not a result of simple two component mixing, where the two components are characterised by nitrogen contents at the highest and lowest extremes.

Only sample 150701 #12-1 shows consistent linear trends for isotopic composition *vs.* nitrogen abundance, and data always plot close to a calculated mixing line (Figures 3.4 and 3.5). For these reasons, mixing may be an appropriate model for this diamond.

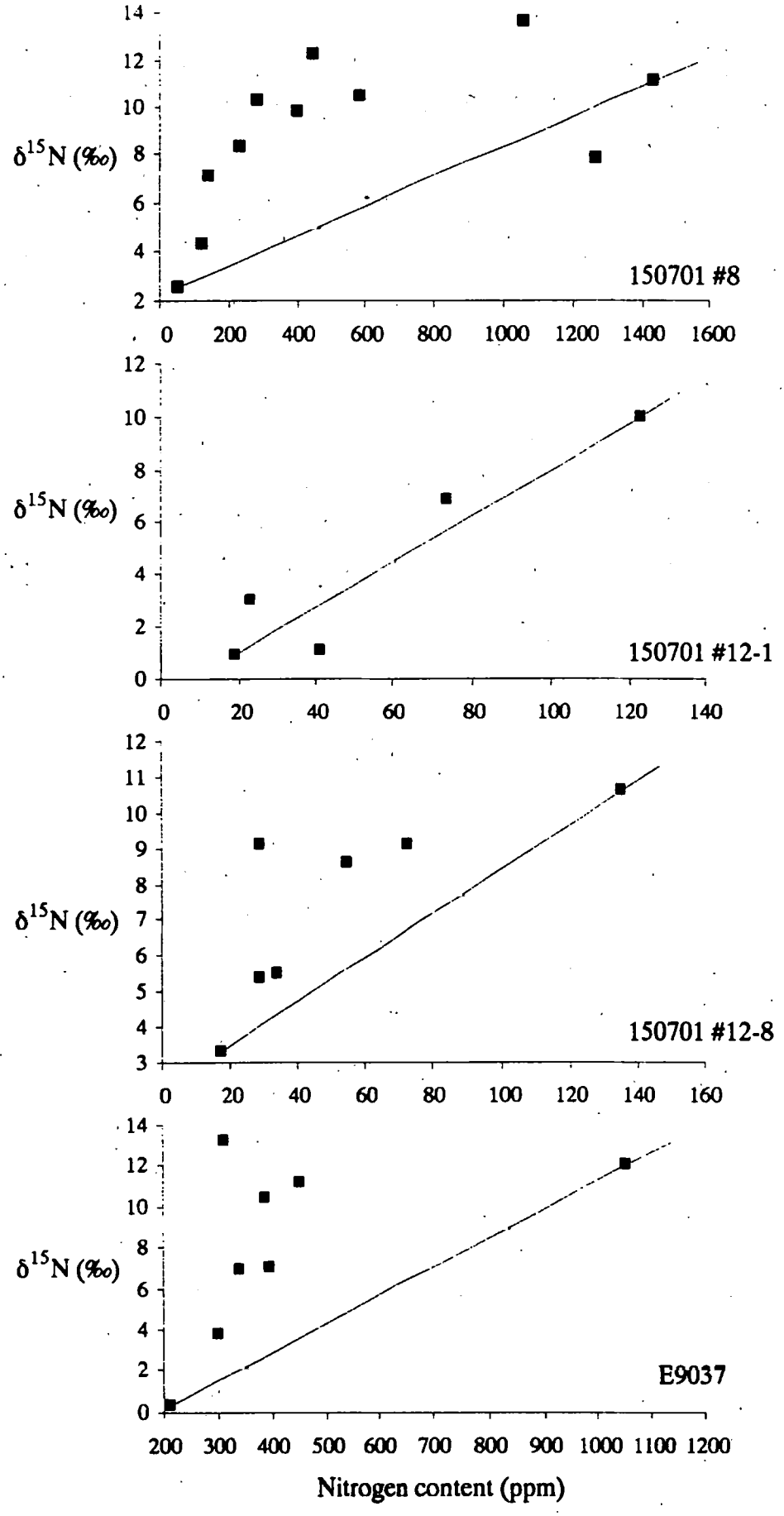

Figure 3.4: $\delta^{15}N$ plotted against nitrogen abundance.

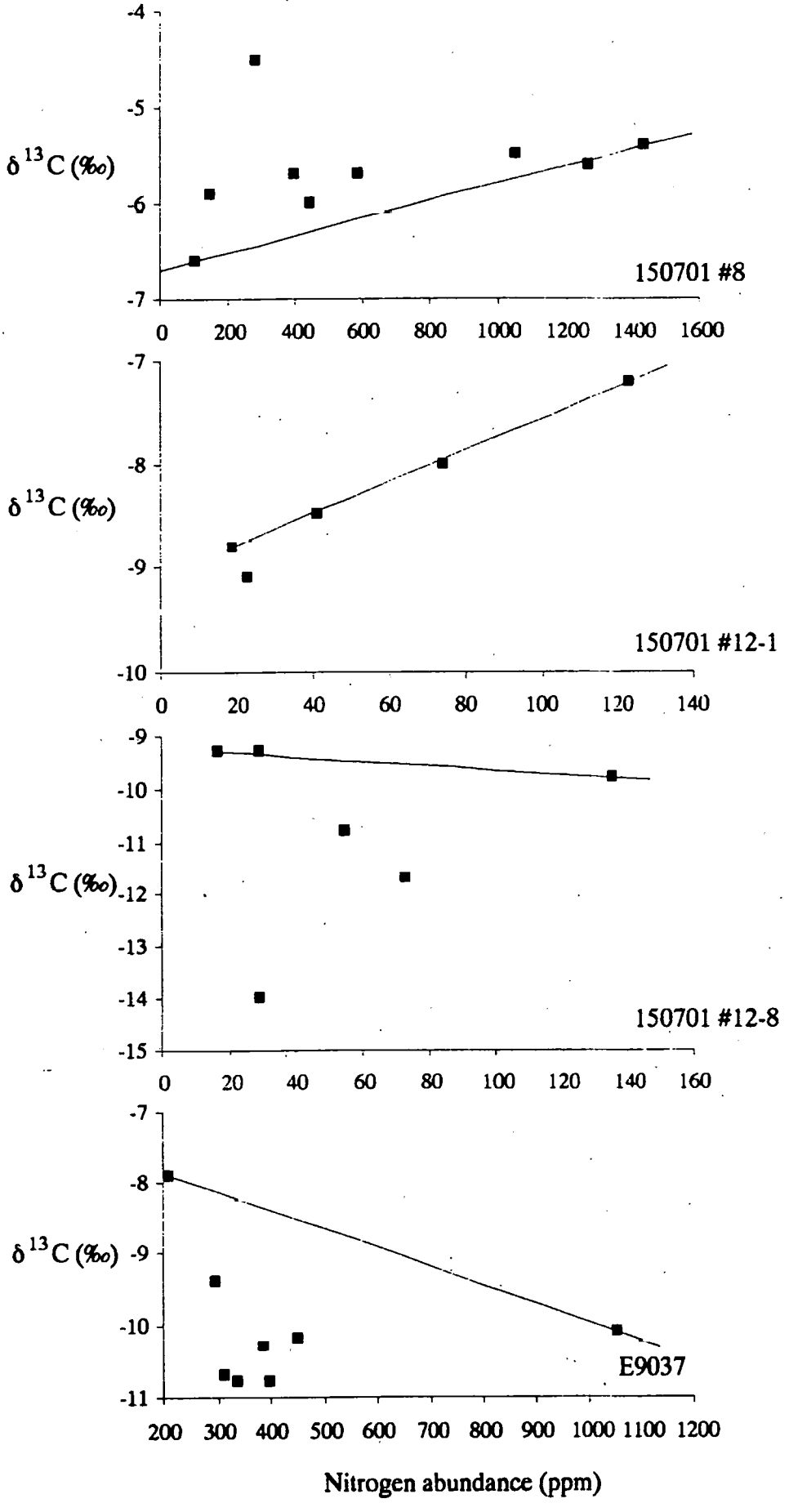

Figure 3.5: $\delta^{13}C$ plotted against nitrogen abundance.

The (largely unsuccessful) mixing models above have concentrated on two component mixes in which one component is represented by the core region of the diamond plate and the other component is represented by the rim of the plate. If more complex mixes are involved, for example three component mixing, then all the observed stable isotope variability in diamond plates and in 2 mm diamonds may be explained by a mixing model when the components have the characteristics summarised in Table 3.7.

Component 1	Positive $\delta^{15}N$	Very negative $\delta^{13}C$	*e.g.* Argyle eclogitic
Component 2	Positive $\delta^{15}N$	"Mantle" $\delta^{13}C$	*e.g.* Argyle peridotitic
Component 3	Negative $\delta^{15}N$	"Mantle" $\delta^{13}C$	*e.g.* Ellendale 4

Table 3.7: Components required in order for a three component mix to explain the observed isotopic variability in Argyle and Ellendale diamonds.

3.2.3 The role of nitrogen aggregation

It is evident from Figures 2.21 and 2.40 (see also Table 2.13) that there is a positive correlation between the $\delta^{15}N$ value and the nitrogen aggregation state for the 4 diamonds that show evidence for regular zoning patterns For this reason, the possibility that there is a cause-effect relationship with the process of nitrogen aggregation directly fractionating the nitrogen stable isotope ratios must be considered. The lack of high precision measurements of nitrogen aggregation state, for reasons discussed elsewhere, prevents quantification of any possible relationship, however presented below is a discussion of the possible role of the aggregation process.

There are two effects that are likely to be important in the fractionation of nitrogen stable isotope ratios and both of these are mass dependent. The first is the kinetic effect which states that "light isotopes" are likely to be more mobile than "heavy isotopes" and implies that A-aggregates that form when two $m/z = 14$ nitrogen atoms combine are likely to be more mobile than A-aggregates with a mass of 29 ($^{14}N + {}^{15}N$) or 30 ($^{15}N + {}^{15}N$). Low-mass A-aggregates therefore have a higher probability of meeting and forming B-centres, than do A-aggregates with higher mass. The net result of this process is a preferential fixing of low-mass aggregates into the more aggregated B form. Older, more aggregated portions of the diamond crystal could therefore be expected to relatively enriched in the lighter isotope.

The second factor to consider has the opposite effect. For crystal chemical reasons, it is thought likely that diamonds will concentrate ^{15}N relative to ^{14}N (see section 2.3.1), and the heavier isotope is thus thought to be more strongly bound into the diamond lattice. Similarly, high-mass A- and B-aggregates ($m/z = 30$ or 60) are thought to be more stable and less prone to dissociation than low-mass A- or B-centres. High mass B-centres are therefore expected to be enriched in the older and more aggregated regions of a

diamond crystal relative to low-mass B-centres and this will result in a relative increase in the $\delta^{15}N$ values of these parts of the diamond crystal.

It is probable that both of these effects are operating within a diamond crystal during nitrogen aggregation, although there is little direct evidence with which to demonstrate this. The evidence that exists is the positive correlation between the proportion of nitrogen occurring within B-aggregates and $\delta^{15}N$ value, and this is the relationship expected to arise from the second process; the preferential retention of high-mass aggregates into the diamond lattice. This process can be thought of as being akin to distillation-condensation, with the retention of high-mass aggregates and the "loss" of low-mass aggregates, and as such it should be possible to model the consequent fractionation of nitrogen stable isotope ratios. This is prevented at present however, by a lack of understanding of the relationships between the isotope fractionations that are thought to occur during diamond precipitation and the possible fractionations that may occur during the aggregation of nitrogen. It is compounded by a lack of constraint on variables like the duration, temperature and rate of diamond growth. Clearly, the effect of nitrogen aggregation on nitrogen stable isotope ratios must be experimentally investigated before the problem will be resolved. Suffice it to say that nitrogen aggregation is considered likely to play some role in fractionating nitrogen stable isotope ratios.

3.2.4 Summary and discussion

Fractional crystallization can explain the isotopic and nitrogen content variations in 150701 #8 and in 150701 #12-1. It cannot explain the variations in E9037 or 150701 #12-8. Mixing between edge and rim may be a mechanism for explaining the isotopic characteristics of 150701 #12-1, although the relationship of the $\delta^{13}C/\delta^{15}N$ ratio to nitrogen abundance does not fully confirm this possibility. Thus, it seems likely that fractional crystallization may explain some, but not all the isotopic variability of in Argyle and Ellendale diamonds. Mixing does not appear to be an important process for generating intra-sample isotopic variability, although mixing of individual diamond sources, with distinct isotopic characteristics is a possible cause of the spectrum of $\delta^{13}C$ and $\delta^{15}N$ values observed at individual localities. Nitrogen aggregation may play a role in the fractionation of nitrogen stable isotope ratios within individual diamond crystals, but this process has not been investigated.

Fractionation of the stable isotope ratios of carbon and nitrogen appears to occur during diamond growth and in very simple cases, the $\delta^{15}N$ and $\delta^{13}C$ zonation patterns across individual diamonds may be explained by closed system fractional crystallization. In these simple systems, fractionation factors for carbon are low, $\alpha_{diamond\text{ - }source} \leq 1.003$

and probably less than 1.001. Nitrogen fractionation factors are larger with $\alpha_{diamond\text{-}source} \approx 1.004$. It is probable that there is a temperature effect on both the carbon and the nitrogen fractionation factors but this cannot be quantitatively assessed due to the lack of cogenetic inclusion phases within the diamond samples used here. Oxygen fugacity may also be important in controlling fractionation factors.

The models presented also indicate that the initial stable isotope ratios in the source regions are not the same. The initial δ values in a single lamproite (Argyle) range from $\delta^{15}N = +5‰$ to +10‰ and $\delta^{13}C = -5.6‰$ to -8.3. At Ellendale 9, $\delta^{13}C_{initial} \approx -10‰$ and $\delta^{15}N_{initial}$ is between +5‰ and +14‰. This is important as it is very strong evidence for a mantle source that is heterogeneous. On the scale of diamond entrainment in a lamproite, variations in initial δ value of at least 5‰ are possible On a regional scale, the $\delta^{15}N$ variation is at least 9‰.

Within individual diamond crystals, large amounts of crystallization of the source material are indicated. In the case of 150701 #8, the minimum F - equivalent ($[N]/[N]_{max}$) is 0.03 which corresponds to 97% crystallization, and almost as much crystallization is evident in samples 150701 #12-8 and 150708 #12-1. Such complete crystallization trends will only be evident if the initial source reservoir is of a similar size to that of the product diamond, and this has important implications for diamond genesis. From temperature determinations that are hotter than the volatile-free peridotite solidus, Griffin *et al.*, (1992, 1993) concluded that African and Siberian diamonds grew in the presence of melts and perhaps volatile phases. Small-volume fluid phases that are dominated by H_2O are likely to be immobile in the mantle as experimentally determined dihedral angles between water and olivine or clinopyroxene are larger than 60° (Watson *et al.*, 1990; Watson and Lupulescu, 1993), but the same is not true for volatile-rich silicate or carbonatite melts. Volatile-rich frozen melt phases have been identified as micro-inclusions in diamond coat from Zaire (Navon *et al.*, 1988) and from microdiamonds from Coanjula, Australia (Lee *et al.*, 1991 and see Chapter 5) and it is possible that such small volume phases are the source material from which diamonds precipitate. Such phases may form as the result of localised melting events or may even represent volatile-rich (CO_2 - CH_4) "bubbles" or "melt droplets" percolating up from the asthenosphere or even deeper. Haggerty (Pers. Comm., 1993) suggests that the initial source for these volatile phases may even be as deep as the core-mantle boundary.

If small-volume volatile-rich phases are indeed the source material for diamond precipitation, variations in stable isotope ratio in different portions of individual diamonds are readily explained. Each isotopically distinct region, for example the different sides of 150701 #12-8 or E9037, could simply precipitate from a different drop of carbon-rich melt. Complicated mixtures of different precursors may be the explanation for the lack

of clear zonation patterns in the diamond plate 150701 #1 (Figure 2.15). A similar model has been proposed by Boyd *et al.*, (1992) explaining the coat on coated diamonds as the result of precipitation from a volatile-rich asthenospheric fluid around a seed crystal that formed some time before the overgrowth.

Closed system fractional crystallization in very small reservoirs may thus explain a large proportion of the carbon and nitrogen stable isotope variability within individual diamond source regions. The precursor volatile-rich phases are however heterogeneous and the presence of a number of diamonds with differing initial $\delta^{13}C$ and $\delta^{15}N$ values within the same lamproite suggests that there is a constant flux of volatiles through the diamond source region.

3.3 NITROGEN AGGREGATION STATE VARIATIONS ACROSS INDIVIDUAL DIAMOND PLATES

The aggregation state of nitrogen in diamonds is a second order kinetic function of mantle residence time and the temperature of mantle storage (See Chapter 1, equations 1.1 and 1.2). If the temperature is known, the duration of mantle storage can be calculated, and this added to the emplacement date of the diamond-bearing diatreme will give the age of the diamond.

In this section, nominal mantle residence times are calculated for each of the different portions of Argyle and Ellendale diamond plates and the zonation patterns (Figure 3.6 and 3.7) across these diamonds examined. These residence times are calculated by substituting nitrogen aggregation state measurements (from FTIR analyses - see Appendix 2) and nitrogen contents measured directly by mass spectrometry, into the second order kinetic equation; $\frac{1}{C} - \frac{1}{C_0} = k.t$ (Equation 1.1, page 18). The rate constant k is calculated from the Arrhenius equation (Equation 1.2) assuming an activation energy of 679 kJ.mol.$^{-1}$ and time averaged aggregation temperatures of 1255°C for Argyle and 1193°C for Ellendale, in line with the determinations of Taylor *et al.*, 1990.

Results presented graphically here are not quantitative for a number of reasons, including (1) the spectra are not of perfect quality; (2) no account is taken of D-defect absorbance which is critical in recognizing aggregation state in B-defect rich diamonds like Argyle (Clark and Davey, 1984); (3) only relative proportions of A and B defects have been determined and these have large associated uncertainties (See Appendix 2); (4) the rate constants of nitrogen aggregation are still poorly constrained (Evans and Harris, 1989) and (5) the likelihood of mantle temperatures remaining constant over the duration of diamond residence are slim indeed.

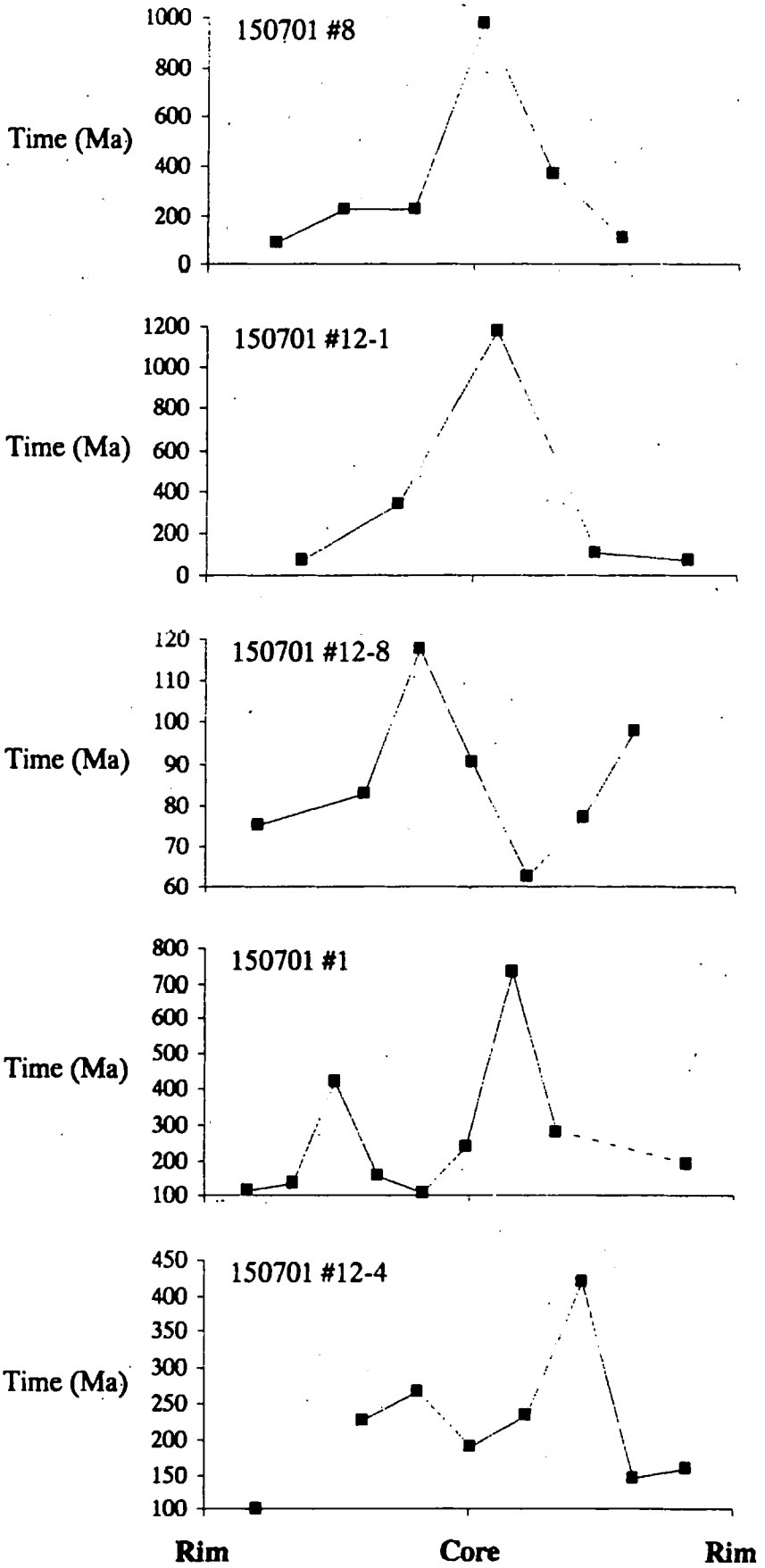

Figure 3.6: Variation in nominal mantle residence time across Argyle diamond plates. The activation energy and pre-exponential of Taylor *et al.*, (1990) have been used in conjunction with an assumed temperature of 1255°C. Each plate represents a rim to rim traverse across the diamond.

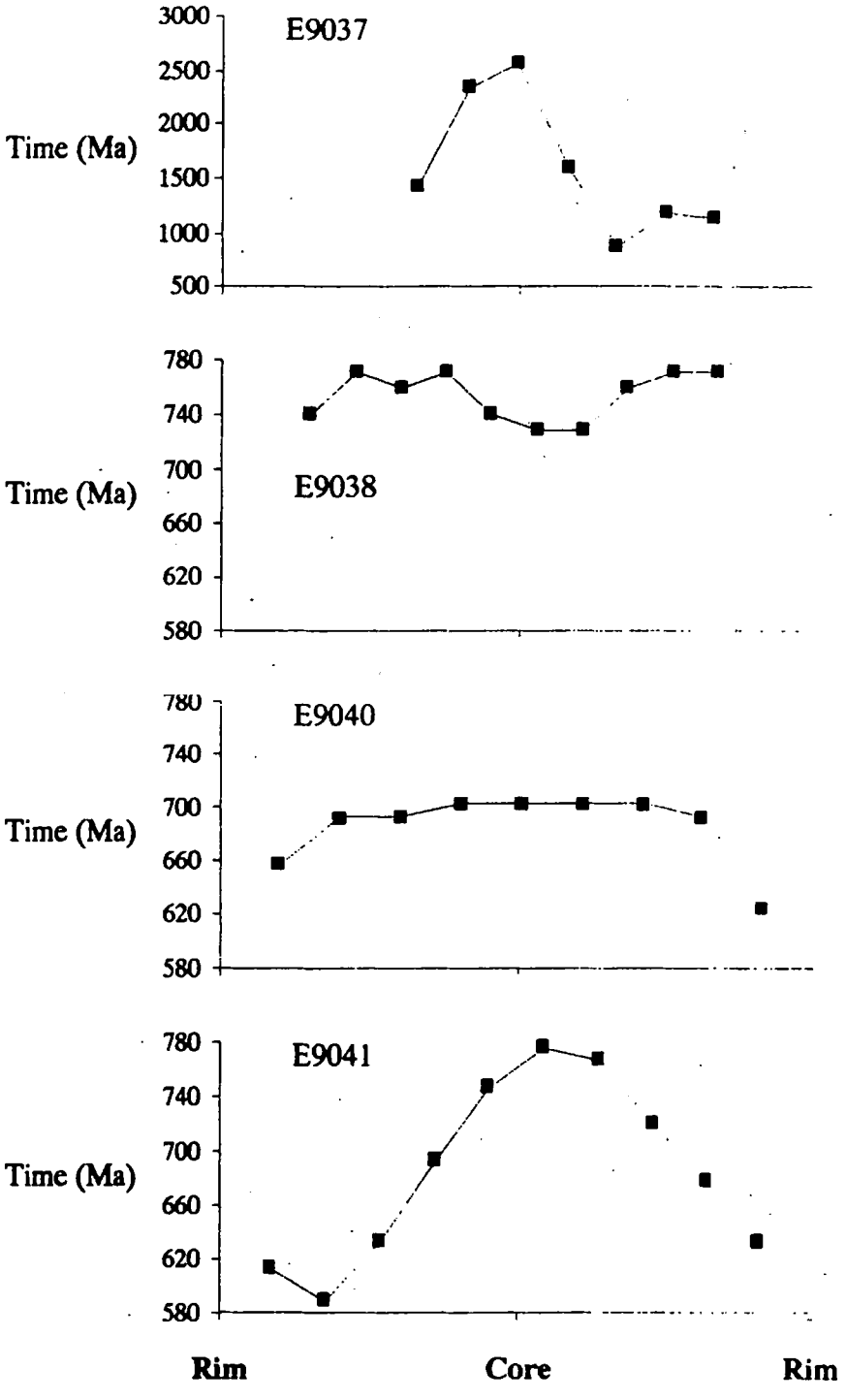

Figure 3.7: Variation in nominal mantle residence time across Ellendale 9 diamond plates. The activation energy and pre-exponential of Taylor *et al.*, (1990) have been used in conjunction with an assumed temperature of 1193°C. Each plate represents a rim to rim traverse across the diamond.

Taylor *et al.*, (1990) examined nitrogen aggregation in Australasian diamonds including Argyle and Ellendale samples and determined an activation energy for nitrogen aggregation of 679 kJ.mol.$^{-1}$ (7.03 eV) similar to results reported previously (See Table 1.5). They also found that nitrogen aggregation was sensitive to time-averaged temperatures, which in the case of Argyle was ≈1255°C, and which for two Ellendale 9

diamonds was 1193°C. These results have been used to construct the nominal mantle residence time profiles across Argyle and Ellendale diamonds, which are those presented in Figures 3.6 and 3.7.

It is evident from Figures 3.6 and 3.7 that there are large differences in the nominal duration of mantle residence between the core and the edge regions of these diamond plates. In the case of the Argyle diamonds 150701 #8 and 150701 #12-1 these differences may be nearly a thousand million years. This is not in agreement with the diamond formation ages determined by Richardson (1986a) which imply mantle storage of about 400 Ma. The data indicate that the oldest part of these Argyle diamond plates (150701 #12-1, block C) formed some 2.4 Ga ago which was followed by residence in the mantle for some 1172 Ma, followed by emplacement of the Argyle pipe at 1180 Ma (Pidgeon *et al.*, 1989). This ≈ 2.4 Ga age is, incidentally, similar to the age of the oldest portion of the Ellendale 9 diamond plates (E9037, block 6; 2442 Ma). The data are also interesting in that they imply that diamond growth is slow, taking millions of years to produce a diamond about 5 mm in diameter, the size of these samples. These qualitative results certainly indicate that a quantitative determination of nitrogen aggregation times should be undertaken.

Samples that show evidence for regular isotopic zonation, like 150701 #8, 150701 #12-1 and the central region of E9037, also have smooth "age" profiles. Samples that do not however show regular isotopic zonation have more complex "age" profiles. It is suggested that this is evidence for multiple phases of diamond growth, with each peak in the age curve corresponding to a separate seed crystal or precursor volatile phase and that these have subsequently been joined by a later overgrowth of diamond (Figure 3.8). This may be the reason for the lack of isotopic zonation patterns. On this basis, samples E9040 and E9041 which have smooth mantle residence time profiles should be good candidates for showing isotopic zonation patterns, however if such patterns exist, they are obscured by the small range in the $\delta^{15}N$ and $\delta^{13}C$ values of these diamond plates.

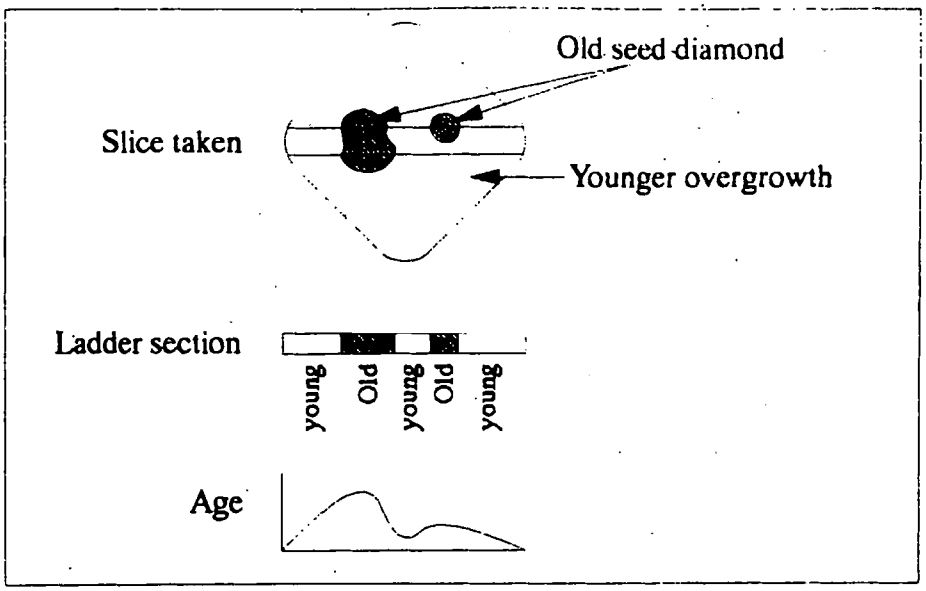

Figure 3.9: A mechanism for explaining irregular "age" profiles across diamonds.

4 The C and N characteristics of diamonds from other sources

4.1 OVERVIEW

In this chapter, the first C and N stable isotope, nitrogen content and nitrogen aggregation state data are presented for diamonds from a number of localities in Australia and an alluvial source in China. These are compared with similar data for diamonds from Argyle and Ellendale and with other published diamond analyses. An aim of the study is to increase the overall number of localities for which nitrogen isotope data from diamonds are available. To illustrate the need for this: with the exception of the results from Chinese diamonds presented here, the only other $\delta^{15}N$ analyses available for diamonds from Asia are the 17 analyses of 3 Udachnaya diamonds presented by Boyd (1988). A further aim of the study is to examine differences in the stable isotope ratios, aggregation state and concentrations of nitrogen in diamonds from alluvial deposits and those from unequivocally magmatic sources. This has a potential application in diamond prospecting in that it may be possible to identify the number of primary diamond sources contributing to a placer deposit.

The samples used in this comparison (Table 4.1) are derived from a CRA exploration prospect in north Western Australia and from Ashton diamonds prospects in China, the Northern Territories and northern Queensland, Australia. The Western Australian samples come from the Morelli's Fox alluvial site on the King George River, which is located on the Kimberley Plateau at 127°19.5'E 14°17.5'S, and the Northern Queensland diamonds are also of alluvial origin (Figure 4.1). The Chinese diamonds come from the Hunan Province alluvials in central south China (D. Lee, Pers. Comm, 1993). There have been previous reports of diamonds from China, from the Sino-Korean craton and the Yangzi craton (Dawson, 1989; Wan, 1989; Zhang *et al.*, 1989), and these two cratons are both in north eastern China.

Diamonds from the Morelli's Fox site have been investigated previously, and a comparison made of the morphology, inclusions and carbon isotopic composition of some of these diamonds with those from Argyle (Sobolev *et al.*, 1989), but no measurements of nitrogen abundance, state of aggregation or $\delta^{15}N$ were made by Sobolev *et al.*, (1989). The Morelli's Fox diamonds used in this study were classified by shape prior to arrival at the Open University, using the same criteria as Sobolev *et al.*, (1989), and these shape classifications have been used here to define separate groups of Morelli's Fox diamonds. No published data are available from the Northern Queensland diamonds or those from China.

		No. of stones	$\delta^{13}C$	$\delta^{15}N$	[N]	FTIR
Morelli's Fox	Frosted octahedra	8	8	7	8	8
	Discoid type	8	8	8	8	8
	Plateau type	2	2	2	2	10*
	Argyle type	2	2	2	2	10*
		20	20	19	20	36
Northern Queensland		34	34	22	23	29
China		19	20	19	19	18†

Table 4.1: Two mm diamond analyses reported in this Chapter. FTIR spectra have been obtained for several Morelli's Fox diamonds for which $\delta^{13}C$ or nitrogen data could not be obtained, and these are marked by an asterisk. †There are two analyses of separate fragments of diamond C.3.

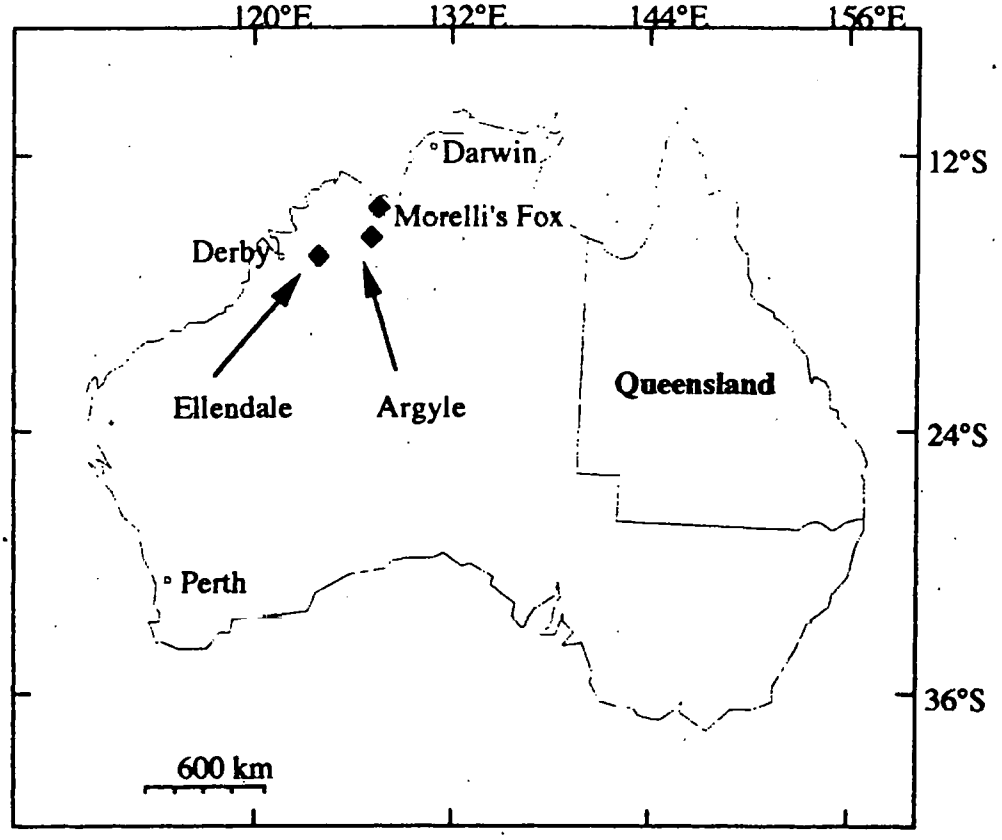

Figure 4.1: Outline map of Australia, showing sampling localities.

4.2 RESULTS

4.2.1 Diamond morphology

Morelli's Fox diamonds were sorted on a morphological basis prior to their receipt at the Open University and are divided into four groups; Frosted Octahedra, Argyle type diamonds, Plateau type diamonds and Discoids, using the classification system of Sobolev *et al.*, (1989). The morphology and other characteristics of these groups, and the Northern Queensland and Chinese diamonds are summarised in Table 4.2.

Samples	Classification	Shape	Colour	Other features	Inclusions
Morelli's Fox					
MF101 - 110	Frosted Octahedra	octahedral	Brown rare white or green	Always frosted. Occasionally step layered	Rare, Black
MF112 - 120	Discoid	Mostly dodecahedral	Green, brown or yellow	Etched and broken	Very rare, Black
MF124 & 127	Plateau	Dodecahedra or octahedra/ dodecahedra	Brown, white, green or grey	Etched and broken. Dissolution features. Green or brown spots	Very rare, Black
MF131 & 135	Argyle	Dodecahedra/ macles or dodecahedra/ aggregates	White or brown	Frosted. Hexagons and glide planes	Black
Northern Queensland					
N.Q 12 & 17	Blue	Irregular		Occasionally resorbed	
N.Q 8 & 21	Brown	Octahedral & irregular		N.Q. 8 is octahedral.	
N.Q. 10, 15, 20 30 & 38	Yellow	Irregular		Never resorbed	
N.Q. 4, 5, 11, 13 14, 26 & 36	White	Dodecahedral		Occasionally resorbed	
N.Q. 19, 23, 24, 29, 32 & 34	"	Irregular		Occasionally resorbed	
N.Q. 1, 3, 7, 16, 25, 28, 31, 33, 37 39, 39 & 40	"	Octahedral		Occasionally resorbed	
China					
C1 to C20	Alluvial	Rounded dodecahedra	White, brown and yellow	Commonly polished. Occasionally frosted.	

Table 4.2: Characteristics of Morelli's Fox, Northern Queensland and Chinese diamonds.

Northern Queensland diamonds are divided on the basis of colour and shape (Table 4.2). The Chinese diamonds all have a dodecahedral morphology (Table 4.2), and a particular characteristic of these diamonds is that they proved extremely difficult to fracture prior to analysis, leading to the inference that the crystals under examination are free from stress or damage. This is consistent with an alluvial source for these diamonds, as Gurney (1989) suggests preferential breakage of inferior crystals in the fluvial environment.

The Argyle type, the Plateau type and the Discoid type sub-populations of the Morelli's Fox diamonds are similar to the dodecahedral habit diamonds which dominate the Argyle, Ellendale 4 and Ellendale 9 (Hall and Smith, 1984) diamond populations. The Morelli's Fox frosted octahedra however are morphologically akin to the peridotite paragenesis octahedral diamonds from Argyle. In addition, the Discoid type, Plateau type and

Argyle type diamonds from Morelli's Fox all show evidence for resorption, similar to the Argyle and Ellendale diamond populations.

In contrast, diamonds from Northern Queensland are unlike the Argyle or Ellendale populations, in that dodecahedral forms are scarce and in that there is an approximately equal distribution of rounded and sharp-edged octahedral crystal forms. Sharp-edged crystal forms are scarce amongst the Argyle and Ellendale diamond populations (Hall and Smith, 1984). The Chinese diamonds are also quite unlike either the Argyle or Ellendale diamonds in terms of present morphology. They are extensively resorbed and only in very few cases is evidence of the primary, octahedral growth morphology preserved. An "orange peel" surface texture is present on some of these Chinese diamonds and this is interpreted as a result of etching of the diamond by a caustic medium, either while they were resident in the mantle, or during transport to the surface.

4.2.2 Carbon isotopic composition

A description of the $\delta^{13}C$ values of the Morelli's Fox, Northern Queensland and Chinese diamonds are presented in Tables 4.3 and 4.4. Histograms illustrating the $\delta^{13}C$ distribution for these diamonds are shown in Figures 4.2 to 4.4.

Sample	Range (‰)	Mean and std. error on mean (‰)		Median (‰), population std. deviation (‰) and n		
All Morelli's Fox	-11.8 to -3.3	-5.8	0.4	-5.4	1.9	20
Frosted octahedra	-6.0 to -4.1	-5.1	0.2	-5.1	0.6	8
Discoid type	-7.6 to -4.4	-5.8	0.4	-5.6	1.0	8
Plateau type	-5.2 & -3.3	-4.3	1.0	Not applicable		2
Argyle type	-11.8 & -9.4	-10.6	1.1	Not applicable		2

Table 4.3: Descriptive statistics for $\delta^{13}C$ values from Morelli's Fox diamonds.

From Table 4.3 and Figure 4.2, it can be seen that the two Argyle type diamonds are characterised by the most negative $\delta^{13}C$ values occurring at this locality, and one of the two Plateau type diamonds has the least negative $\delta^{13}C$ value of -3.3‰. Frosted octahedra and Discoid type diamonds both have mean and median values, and a mode between $\delta^{13}C$ = -5‰ to -6‰, but two of the Discoid type diamonds have $\delta^{13}C$ values just more negative than the frosted octahedra. Thus they also have slightly more negative mean and median $\delta^{13}C$ values.

Sample	Range (‰)	Mean and std. error on mean (‰)		Median (‰), population std. deviation (‰) and n		
All N.Q. diamonds	-14.8 to +1.9	-5.9	0.6	-5.1	3.3	34
White	-14.8 to -2.3	-5.7	0.6	-5.1	2.8	24
Brown	-10.5 and -9.1	-9.8	0.7	Not applicable		2
Blue	-3.7 and -3.4	-3.6	0.2	Not applicable		2
Yellow	-11.1 to +1.9	-7.3	2.4	-8.7	5.3	5
Octahedra	-11.7 to -2.6	-6.1	0.8	-5.3	2.7	11
Dodecahedra	-14.8 to -3.1	-7.2	1.7	-6.2	4.2	6
Irregular	-11.1 to +1.9	-5.6	0.8	-5.4	3.4	16
All Chinese diamonds	-16.2 to +2.0	-5.3	0.9	-4.6	4.1	20

Table 4.4: Descriptive statistics for $\delta^{13}C$ values from North Queensland and Chinese diamonds.

In the Northern Queensland diamonds, extreme values of $\delta^{13}C$ are not generally exhibited by white samples, but are found in both brown ($\delta^{13}C_{min}$ = -10.5‰) and yellow diamonds ($\delta^{13}C_{max}$ = +1.9‰, $\delta^{13}C_{min}$ = -11.1‰). There are, however 2 exceptions to this; N.Q. 36 ($\delta^{13}C$ = -14.8‰) and N.Q. 40 ($\delta^{13}C$ = -11.7‰) are both white stones. There is no relationship between $\delta^{13}C$ value and diamond morphology in that all three shape categories (octahedra, dodecahedra and irregular diamonds) of Northern Queensland diamonds all have similar ranges in $\delta^{13}C$ value.

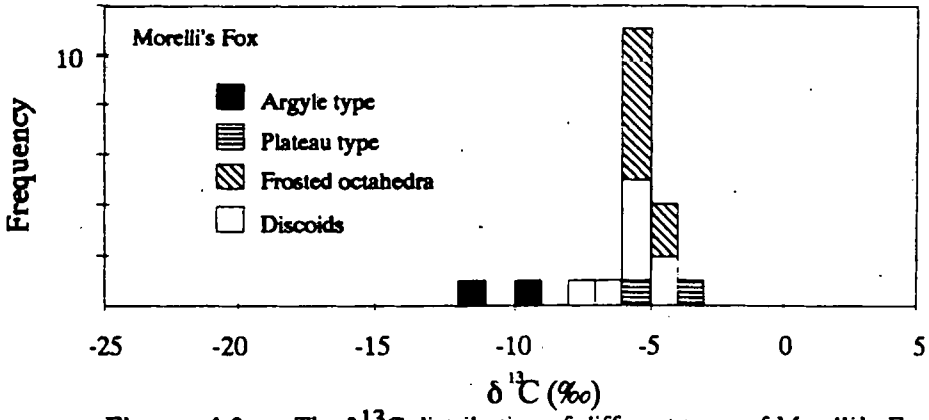

Figure 4.2: The $\delta^{13}C$ distribution of different types of Morelli's Fox diamonds.

There are also no obvious relationships between carbon isotopic composition and diamond colour, surface texture or shape for any of the Chinese diamonds. The diamonds are however heterogeneous. Analysis of separate fragments from C.3 yielded $\delta^{13}C$ values of -3.4‰ and +2.0‰ respectively; a more than 5‰ difference within a single diamond.

When compared to one another (Figure 4.5), the Morelli's Fox, Northern Queensland and Chinese diamonds all have similar median and mean $\delta^{13}C$ values, near the "normal"

mantle value of -5‰ to -6‰ (See Figures 4.2 to 4.4), with the Chinese samples being very slightly ^{13}C enriched relative to the other two groups (Median $\delta^{13}C$ = -4.6‰ *cf.* $\delta^{13}C$ = -5.4‰ (Morelli's Fox) and $\delta^{13}C$ = -5.1‰ (N.Q)). The 4 groups of Morelli's Fox diamonds however have less variable carbon isotopic composition than diamonds from Northern Queensland and China. The total variation in $\delta^{13}C$ value at Morelli's Fox is 8.5‰, but this is considerably reduced when individual sub-populations are examined. Maximum variations in the $\delta^{13}C$ value of Northern Queensland and Chinese diamonds are 16.6‰ and 18.2‰ respectively. The restricted range of $\delta^{13}C$ values for Morelli's Fox diamonds is similar to that for Argyle diamonds in general, and the Argyle type sub-group of the Morelli's Fox diamonds has $\delta^{13}C$ values that correspond to the major mode in $\delta^{13}C$ values from Argyle eclogitic paragenesis diamonds. The remaining Morelli's Fox sub-groups have $\delta^{13}C$ values that do not correspond to any of the Argyle sub-groups.

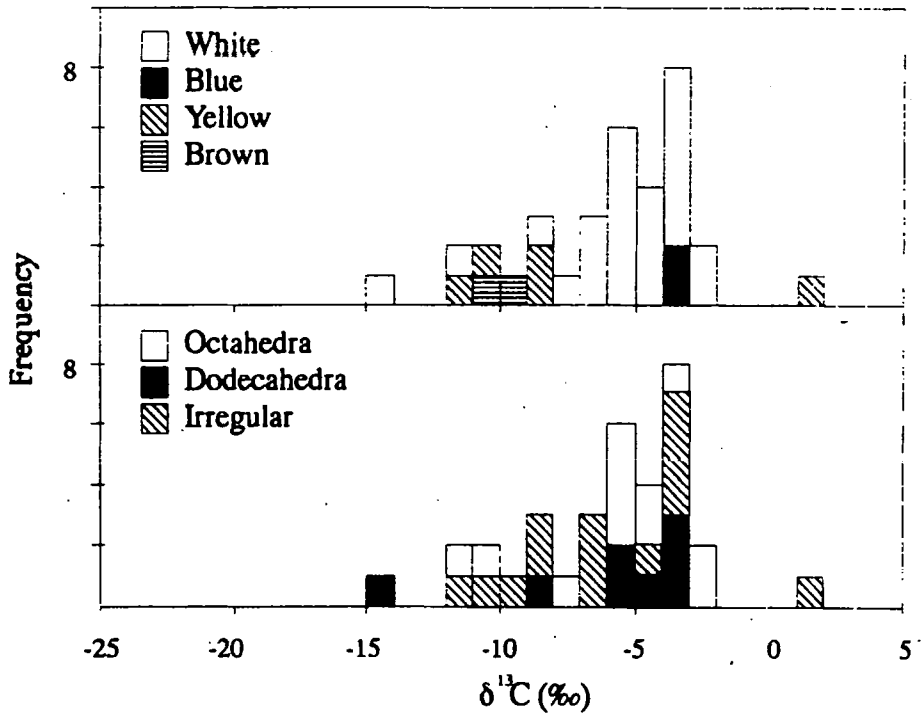

Figure 4.3: The $\delta^{13}C$ distribution of North Queensland diamonds.

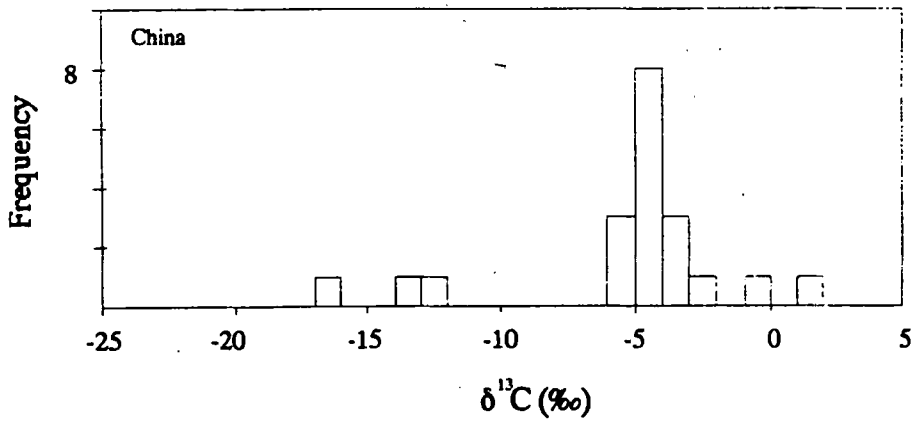

Figure 4.4: The $\delta^{13}C$ distribution of Chinese diamonds.

The wide $\delta^{13}C$ range in Northern Queensland and Chinese diamonds has a counterpart in the Ellendale 9 diamond population (Figure 4.5). Although no diamonds with positive $\delta^{13}C$ values have however been recovered from Ellendale 9, the Northern Queensland and Chinese populations each have one such sample. The mode in North Queensland and Chinese $\delta^{13}C$ values corresponds to the mode for Ellendale 4 and Ellendale 9 diamonds and also corresponds to the $\delta^{13}C$ values determined for Ellendale 9 diamonds of peridotitic paragenesis. This mode occurs within the $\delta^{13}C$ range expected from samples derived from "normal" mantle and does not overlap with any of the Argyle sub-groups.

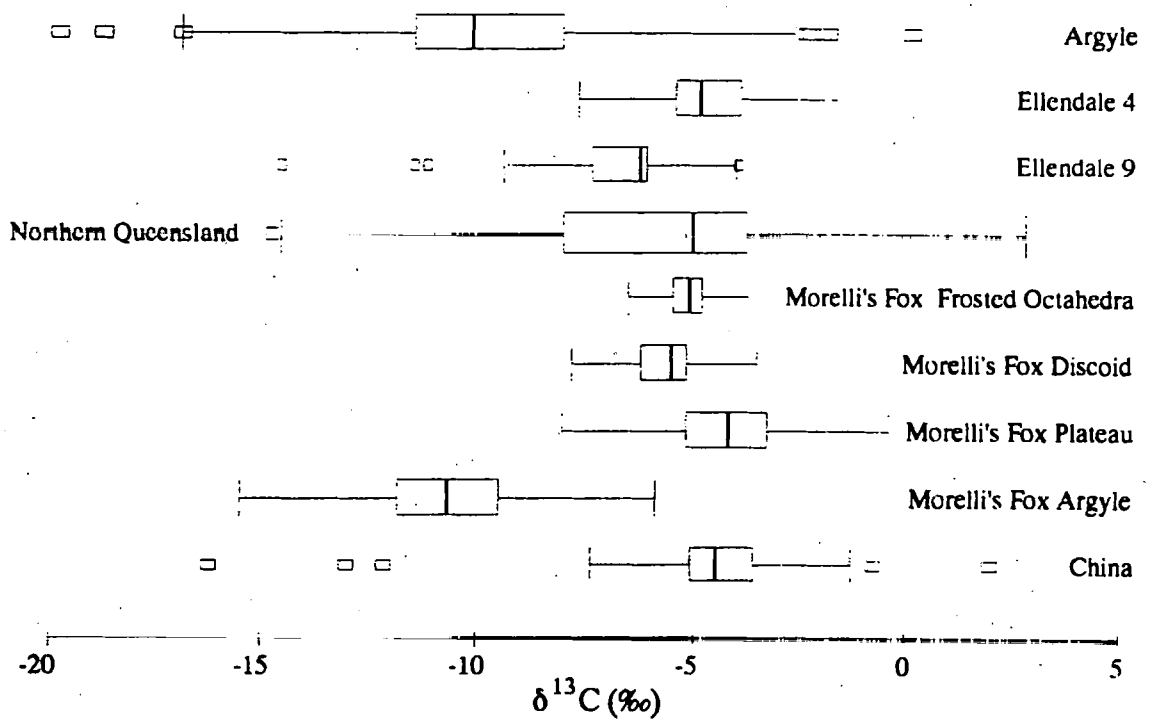

Figure 4.5: Box and whisker plots for the comparison of the $\delta^{13}C$ values of Argyle, Ellendale 4 and Ellendale 9, Morelli's Fox, Northern Queensland and Chinese diamonds. The "boxes" show the inter-quartile ranges and whiskers are at 3 standard deviations from the median, shown by the heavy vertical line. Argyle, Ellendale 4 and Ellendale 9 data includes that reported by Hall and Smith (1984), Jaques *et al.*, (1989) and Sobolev *et al.*, (1989).

4.2.3 Nitrogen

4.2.3.1 Nitrogen content

Spectral studies show that there are no type II diamonds amongst the Morelli's Fox samples, and the lowest measured nitrogen content from these samples was 18 ppm in the type IaA frosted octahedra M.F. 108. The highest measured nitrogen content occurs in the type IaAB Discoid sample M.F. 117 which contains 1587 ppm nitrogen. The groups reported from morphological studies all have different mean and median nitrogen

contents (see Table 4.5), however only Discoid type samples are readily distinguishable on the basis of nitrogen content. This group is characterised by far higher nitrogen contents than the other Morelli's Fox samples and this is illustrated on Figure 4.6.

Sample	Range (ppm)	Mean and std. error on mean (ppm)		Median, population std. deviation (ppm) and n		
All Morelli's Fox	18 to 1587	374	105	139	472	20
Frosted Octahedra	18 to 976	172	116	44	329	8
Discoid type	171 to 1587	721	181	681	512	8
Plateau type	79 and 106	93	14		Not applicable	2
Argyle type	38 and 105	72	36		Not applicable	2

Table 4.5: Descriptive statistics for the nitrogen content of Morelli's Fox diamonds.

Argyle type and Plateau type diamonds are characterised by low nitrogen contents, with Plateau diamonds having marginally higher contents than the Argyle samples. Frosted Octahedra include a single outlier with high nitrogen content (M.F. 107, [N] = 976 ppm) and if this sample is omitted from the statistical calculations, then this group compares with Plateau and Argyle type samples, with a maximum nitrogen content of 180 ppm, a mean nitrogen content of 58 ppm and a median [N] value of 39 ppm (*cf.* Table 4.5).

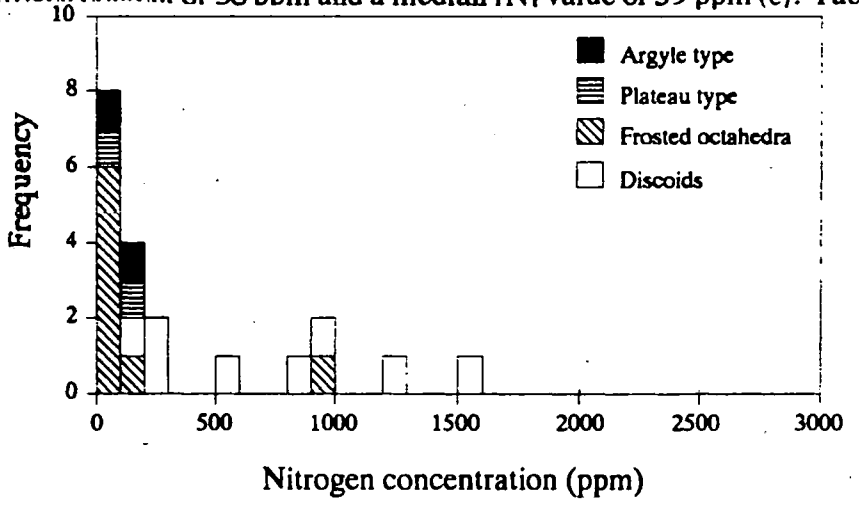

Figure 4.6: Nitrogen content histogram of the Morelli's Fox diamonds. The different shape classes are indicated.

Type II diamonds are rare amongst the North Queensland samples and only three examples were recognised from FTIR spectra. One of the spectral type II samples (the blue diamond N.Q. 17) contains 25 ppm nitrogen, and a brown nitrogen-free sample (N.Q. 21) was too opaque for a spectral identification of diamond type to be made. The 23 samples for which nitrogen abundance have been determined, have a smooth distribution (Figure 4.7) from low to high abundance and 8 of the samples (35%) contain less than 100 ppm nitrogen. The maximum nitrogen concentration in the Northern Queensland samples is 2710 ppm, and occurs in the white dodecahedron N.Q. 36. This

is more than a factor of two more nitrogen than that found in other diamonds from the same locality. Descriptive statistics of nitrogen content in the different shape and colour groups of North Queensland diamonds are listed in Table 4.6.

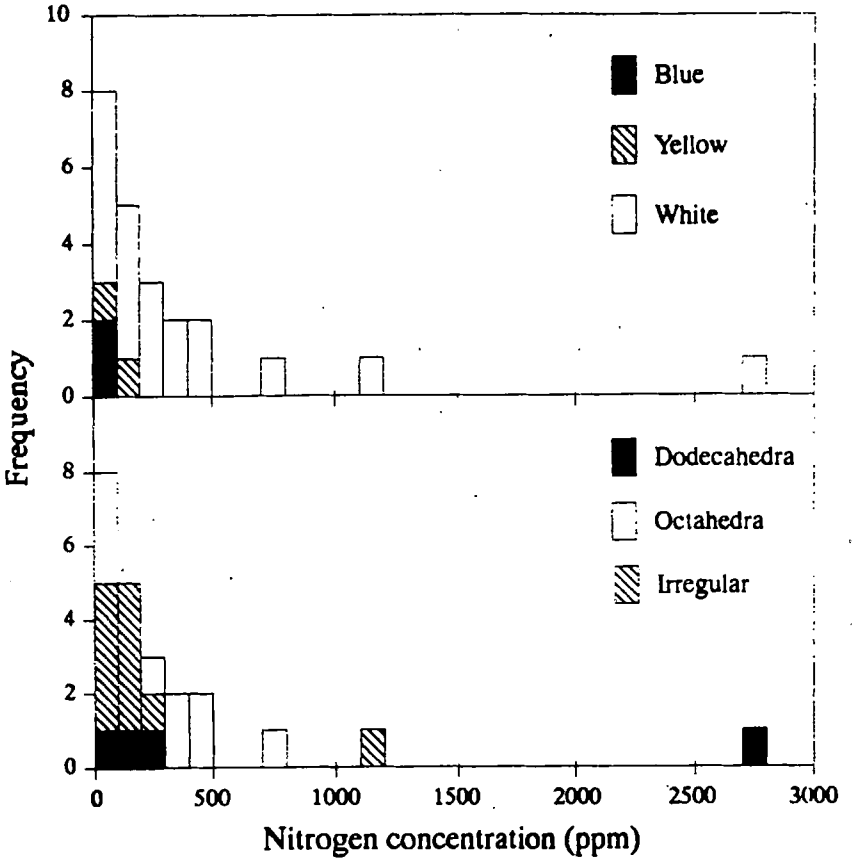

Figure 4.7: The nitrogen content histogram for North Queensland diamonds.

Sample	Range (ppm)	Mean and std. error on mean (ppm)		Median, population std. deviation (ppm) and n		
All N.Q. diamonds	20 to 2710	351	121	182	581	23
White	20 to 2710	425	143	216	622	19
Brown	Both type II					—
Blue	25 and 63	44	19		Not applicable	2
Yellow	64 and 154	109	45		Not applicable	2
Octahedra	35 to 410	218	58	296	154	7
Dodecahedra	80 to 2710	846	625		Not applicable	4
Irregular	20 to 1196	234	94	137	324	12
All Chinese diamonds	0 to 2238	463	133	193	580	20

Table 4.6: Descriptive statistics for the nitrogen content of North Queensland and Chinese diamonds.

A description of the nitrogen contents of the 19 Chinese diamonds (plus one replicate analysis) is included in Table 4.6 and a histogram of nitrogen content is shown in Figure

4.8. Four of the Chinese diamonds are identified as spectral type II, however three of these contain sufficient nitrogen for analysis (C10, 33 ppm; C17, 104 ppm and C18, 201 ppm). Of the 19 diamonds for which nitrogen abundance has been determined, 14 are characterised by nitrogen contents of less than 500 ppm and 4 samples (C2, C4, C7 and C20) have nitrogen concentrations in the range 800 ppm to 1208 ppm. A single outlier (C16) exists at the highest measured concentration (2238 ppm) and, like the Northern Queensland outlier (N.Q. 36), this sample contains a factor of two more nitrogen than other diamonds from the locality.

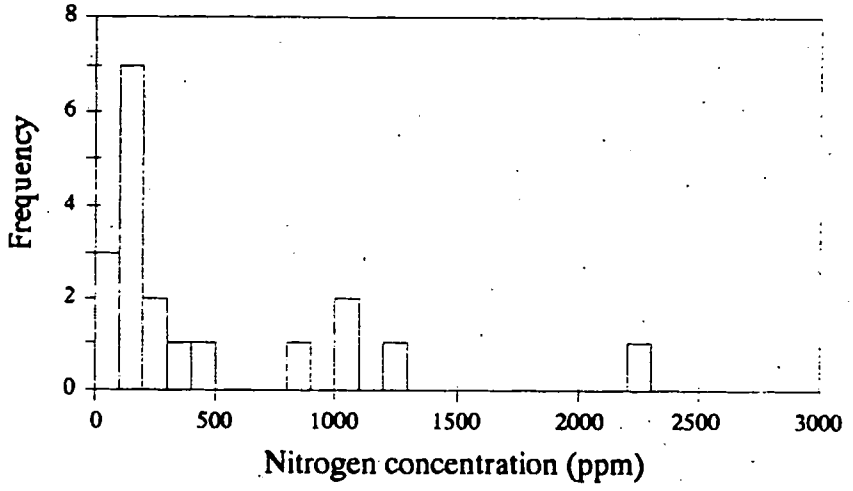

Figure 4.8: The nitrogen content of Chinese diamonds.

The Chinese diamond C3, which has highly variable carbon isotopic composition, is also heterogeneous with respect to nitrogen content. Separate fragments yielded 193 ppm and 107 ppm nitrogen respectively. There is no distinct correlation between nitrogen content and carbon isotopic composition for the Chinese diamonds, however samples with $\delta^{13}C$ values outside the "mantle range" (*i.e.* $\delta^{13}C \leq -7‰$ or $\geq -3‰$) tend to have low nitrogen contents. In all cases these are ≤ 201 ppm.

There is also no general relationship between nitrogen content and the $\delta^{13}C$ value of the Morelli's Fox diamonds or the Northern Queensland diamonds. For Morelli's Fox Argyle and Plateau type samples however, the higher nitrogen content sample is also the sample with the less negative $\delta^{13}C$ value, but further analyses are necessary in order to confirm this observation.

Morelli's Fox, Northern Queensland and Chinese diamonds are all marked by low median nitrogen contents (139 to 193 ppm), and only the Discoid sub-population of the Morelli's Fox diamonds has a high median nitrogen content (681 ppm). The maximum nitrogen concentration measured from these localities occurs in the Northern Queensland outlier N.Q. 36 (2710 ppm), although this group has the fewest samples with nitrogen contents of over 1000 ppm (2 out of 23 or 9%). Diamonds with high nitrogen content are most abundant in the Chinese sample with 4 of the 19 samples (21%) containing over

1000 ppm nitrogen. There are 2 (out of 20 or 10%) such samples amongst the Morelli's Fox diamonds and both of these belong to the Discoid type sub-population.

The low median nitrogen contents of the Morelli's Fox, Northern Queensland and Chinese diamonds are similar to the Argyle diamond population and markedly different from the Ellendale diamond suites (Figure 4.9). The median nitrogen content of the Morelli's Fox Argyle type sub-population (72 ppm) is similar to that of the Argyle eclogitic paragenesis (67 ppm) and brown diamonds (71 ppm) described in Chapter 2, and the Discoid type sub-population at Morelli's Fox has nitrogen contents (mean = 720 ppm) of the same order as the nitrogen contents of Argyle peridotite paragenesis diamonds (mean [N] = 620 ppm).

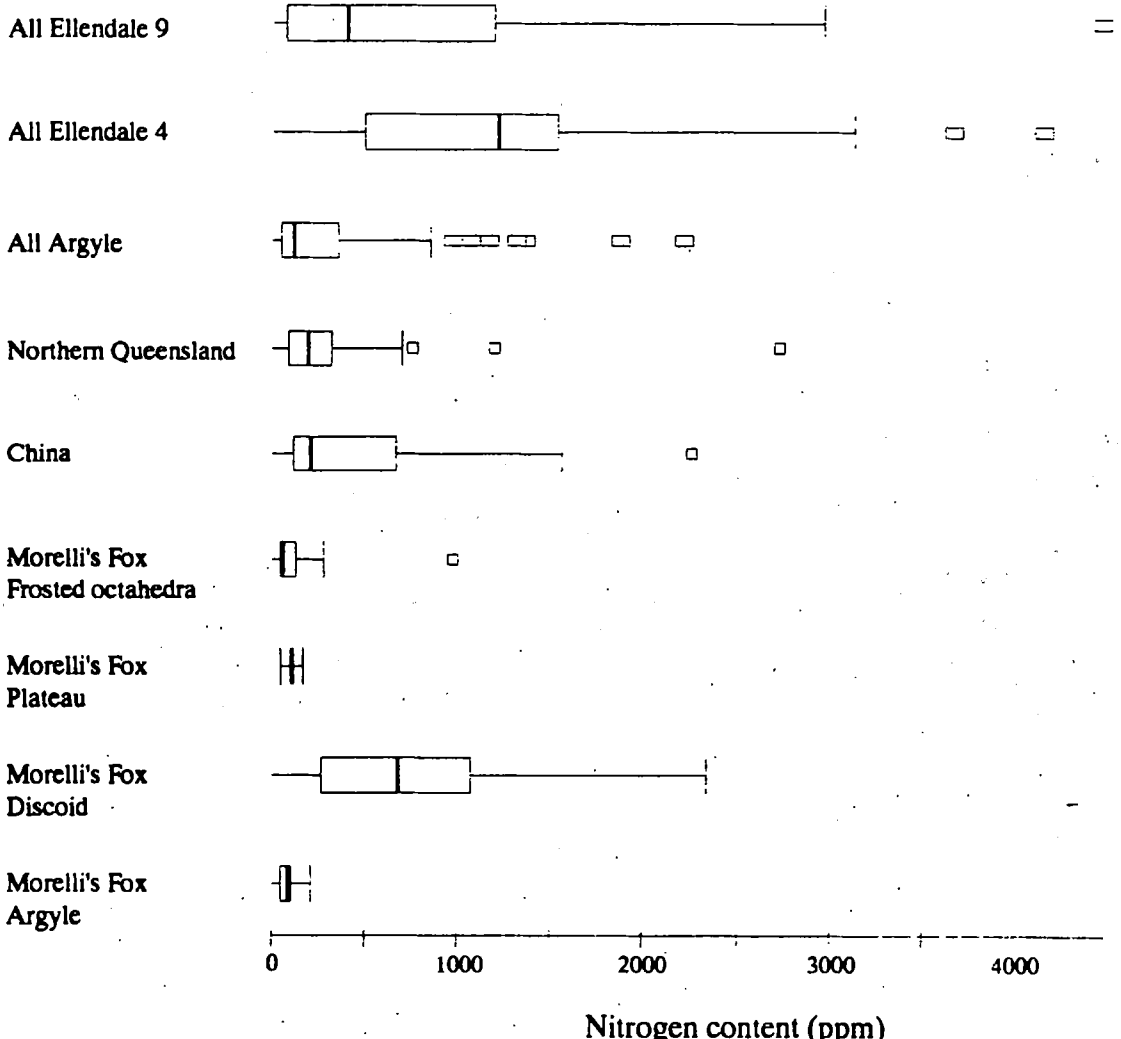

Figure 4.9: Box and whisker plots for a comparison of the nitrogen contents of Argyle,and Ellendale diamonds with the diamonds from Morelli's Fox, Northern Queensland and China.

Argyle is characterised by a low proportion of diamonds containing more than 1000 ppm nitrogen (6 out of 57 or 11% of the samples described in Chapter 2) and this is similar to the Morelli's Fox and North Queensland diamonds. Chinese diamonds with 21% of the samples having more than 1000 ppm nitrogen are similar to the Ellendale 9 diamonds

(25% of samples have > 1000 ppm nitrogen). The Ellendale 4 diamond distribution is unique amongst the samples studied with 52% of the analysed diamonds containing nitrogen in excess of 1000 ppm.

4.2.3.2 Nitrogen aggregation state

The nitrogen aggregation state of the different morphological groups of Morelli's Fox diamonds, including those for which there are no $\delta^{13}C$, $\delta^{15}N$ or nitrogen abundance data are distinct (Figure 4.10). All frosted octahedra contain less than 50% B-aggregates while Argyle type diamonds are more aggregated, always having more than 40% B-aggregates. There is a range in the aggregation state of the Discoid diamonds from 14% to 84% B-aggregates, while Plateau type diamonds have either < 25% B-aggregates (6 samples) or >85% B-aggregates (4 samples). Carbon isotopic composition and nitrogen isotopic composition and content could determined from the first of these sub-groups of Plateau type diamonds; the remaining samples had been earmarked for an alternative mineralogical examination by Dr H.J. Milledge, at University College, London.

Semi-quantitative estimates of the proportion of nitrogen in B-aggregates was possible for 27 of the North Queensland diamonds, illustrated on Figure 4.11, and these diamonds have spectral type varying from pure IaA to pure IaB. Nine samples have between 0 to 10% B-aggregates, and a further 5 contain less than 20% B-aggregates, and low degrees of aggregation are thus most common (51% of samples have ≤ 20% B-aggregates). Ten samples contain between 30% and 70% B-aggregates and only two contain more than 80% B-aggregates. The two blue samples contain nitrogen in a low state of aggregation (0% and 7% B-aggregates), whereas yellow diamonds have aggregation states ranging from 2% to 30% B-aggregates. White samples have a range of aggregation states from 0% to 100% B-aggregates, and both brown diamonds are are nitrogen free.

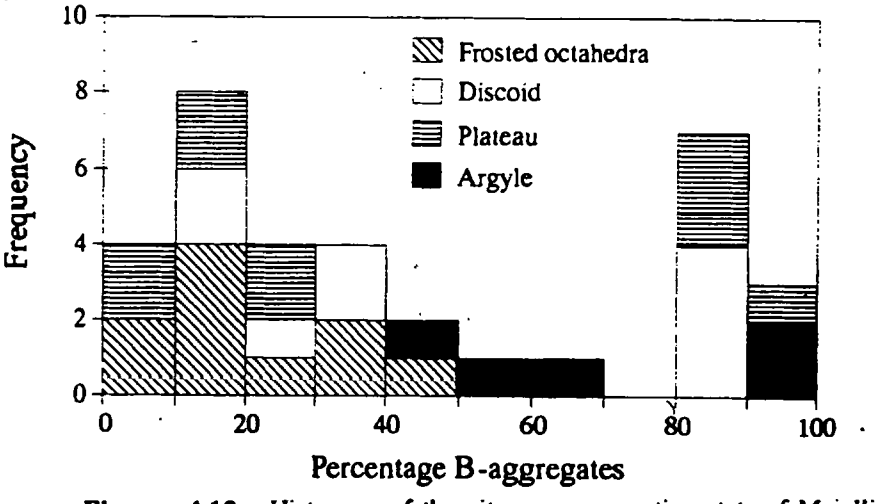

Figure 4.10: Histogram of the nitrogen aggregation state of Morelli's Fox diamonds. Different groups are shown.

There is no general grouping in nitrogen aggregation state of Northern Queensland diamonds on the basis of sample morphology. Dodecahedral samples have a slightly narrower range in the proportion of nitrogen occurring in B-aggregates than octahedral diamonds. Nearly 50% of the irregular diamonds (5/11) however are poorly aggregated and contain less than 10% B-aggregates. The most aggregated irregular diamond contains 57% B-aggregates, and the median for the proportion of nitrogen in B-aggregates for irregular samples is 12%. This is lower than the median aggregation state for octahedral diamonds (47% B-aggregates) and for dodecahedra (37% B-aggregates).

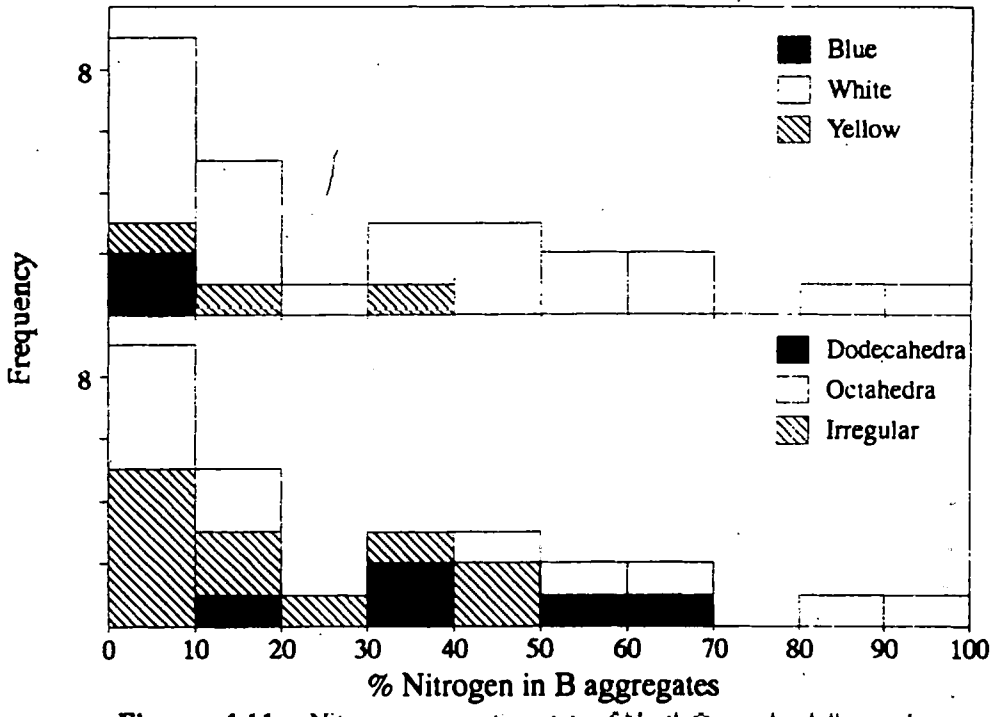

Figure 4.11: Nitrogen aggregation state of North Queensland diamonds.

Aggregation state estimates for 13 of the Chinese diamonds have been made directly from absolute absorption coefficients (Milledge, Unpublished data) and as a result have considerably lower associated uncertainties (*ca.* ± 15%) than most other aggregation state determinations presented in this thesis. These samples are all typified by very low degrees of nitrogen aggregation, and the maximum observed proportion of B-aggregates is 27% in diamond C7. The mean proportion of B-aggregates is 6% and more than 75% of samples contain less than 10% B-aggregates (Figure 4.12). Three samples with type II spectra (C10, C17, C18) contained sufficient nitrogen for analysis (33, 104 and 201 ppm respectively), and the remaining spectral type II diamond (C6) was nitrogen free.

There is no obvious relationship between nitrogen aggregation state and either nitrogen content or carbon isotopic composition for the Chinese diamonds, and nor is there any visible relationship between nitrogen aggregation state and diamond colour or morphology. In this respect, the Chinese diamonds are similar to the Northern Queensland and Morelli's Fox diamonds, which also show no general relationship

between nitrogen aggregation state and either nitrogen content or carbon isotopic composition.

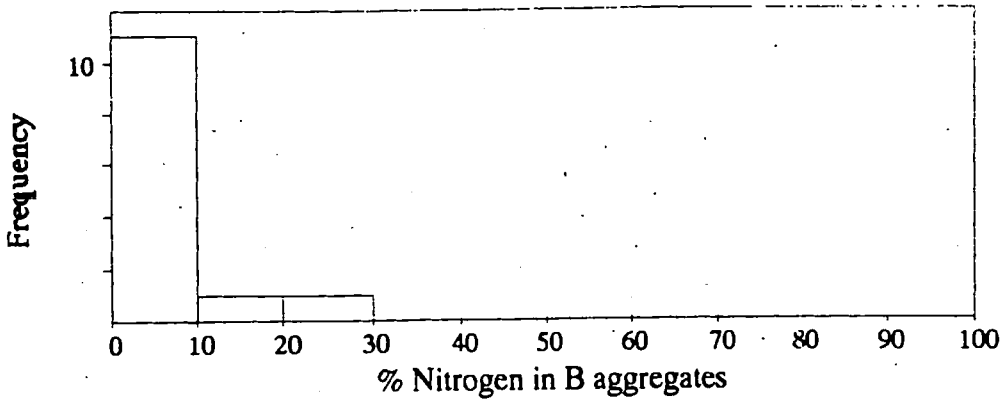

Figure 4.12: Histogram of the nitrogen aggregation state of Chinese diamonds.

The Morelli's Fox and Northern Queensland diamonds comprise both aggregated and less aggregated samples and in this respect they are distinct from the Chinese diamond population with only low degrees of nitrogen aggregation (See Figures 4.10 to 4.12). Low degrees of nitrogen aggregation are also evident at Ellendale 4 (See Figure 2.19) although, unlike the Chinese samples, a single outlier with 80% B-aggregates exists. Morelli's Fox diamonds have a similar range in nitrogen aggregation states to Argyle diamonds. The different sub-populations of the Morelli's Fox suite do not however correspond directly to Argyle peridotitic or eclogitic paragenesis diamonds, although the range of aggregation states displayed by Argyle type Morelli's Fox diamonds encompasses the range for Argyle eclogitic paragenesis diamonds.

Northern Queensland and Ellendale 9 diamonds have a similar range of nitrogen aggregation states, and the median values for these two populations are 16% and 17% B-aggregates respectively. The two populations are also similar in that both have a number of samples with 30% to 50% B-aggregates, and at Ellendale 9, these are all of eclogitic paragenesis (median = 31% B-aggregates). The lack of inclusion paragenesis data for the Northern Queensland diamonds prevents an evaluation of whether this is also the case for the Northern Queensland diamonds.

4.2.3.3 Nitrogen isotopic composition

The nitrogen isotope compositions of Morelli's Fox, Northern Queensland and Chinese diamonds are summarised in Table 4.7 and 4.8. The Morelli's Fox diamonds have nitrogen isotopic compositions within the range $-14.2‰ \leq \delta^{15}N \leq +16.1‰$ but the different morphological types have different $\delta^{15}N$ distributions and this is shown in Figure 4.13. Argyle type samples are ^{15}N enriched, and Plateau type diamonds, ^{15}N depleted relative to the Frosted octahedra and Discoid diamonds.

On a $\delta^{15}N$ *vs.* $\delta^{13}C$ plot (Figure 4.14) there is near total overlap of the Frosted Octahedral field with that of the Discoid type samples. Argyle type samples plot in a region with very negative $\delta^{13}C$ and positive $\delta^{15}N$ and do not overlap with any of the other groups. Plateau type samples in contrast, plot at less negative $\delta^{13}C$ values and at very negative $\delta^{15}N$ values. They overlap the Discoid diamonds, but do not intercept the Frosted Octahedra field.

Sample	Range (‰)	Mean and std. error on mean (‰)		Median (‰), population std. deviation (‰) and n		
All Morelli's Fox	-14.2 to +16.1	+2.9	1.7	+3.5	7.6	19
Frosted octahedra	-0.6 to +10.6	+4.3	1.7	+1.6	4.5	7
Discoid type	-10.6 to +10.1	+2.0	2.4	+3.6	6.8	8
Plateau type	-12.2 & -3.6	-8.9	5.3	Not applicable		2
Argyle type	+10.6 & +16.1	+13.4	2.8	Not applicable		2

Table 4.7: Descriptive statistics for $\delta^{15}N$ values from Morelli's Fox diamonds.

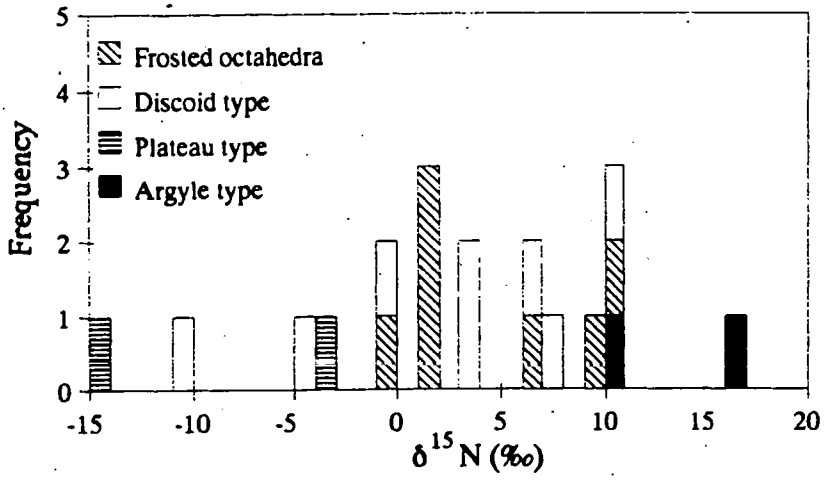

Figure 4.13: Histogram showing $\delta^{15}N$ distribution of the different groups of Morelli's Fox diamonds.

The North Queensland diamonds include the two most ^{15}N depleted terrestrial diamonds yet analysed (N.Q. 33, $\delta^{15}N$ = -28.4‰ and N.Q 25, $\delta^{15}N$ = -22.8‰) and this locality is also unusual in the presence of a large number of low-$\delta^{15}N$ samples (Figure 4.15). Seven of the 22 diamonds for which $\delta^{15}N$ values have been determined (32%) have $\delta^{15}N < -12$‰. Of these seven, 1 is blue and 6 white, 5 have irregular morphology and 2 are octahedra. These seven diamonds include five of the six most ^{15}N depleted natural, terrestrial diamonds yet analysed. There are similar ranges in $\delta^{15}N$ value for octahedra, dodecahedra and irregular Northern Queensland diamonds, however dodecahedra contain a larger proportion of samples with $\delta^{15}N > 0$‰ (2/4) than either of the other two groups (Octahedra - 1/7; Irregular diamonds - 1/11).

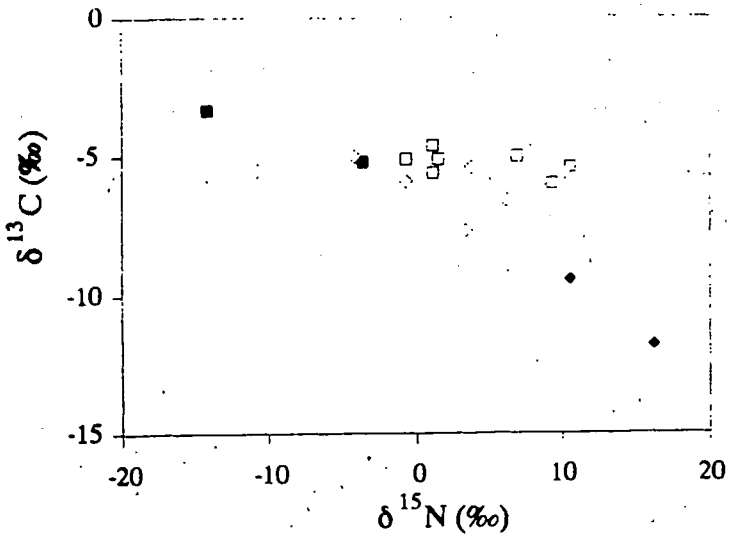

Figure 4.14: $\delta^{15}N$ - $\delta^{13}C$ plot for Morelli's Fox diamonds. Frosted Octahedra shown by open squares, Discoid type diamonds by open diamonds, Plateau type samples by filled squares and Argyle type diamonds by filled diamonds.

Sample	Range (‰)	Mean and std. error on mean (‰)		Median (‰), population std. deviation (‰) and n		
All N.Q. diamonds	-28.4 to +9.7	-6.2	2.1	-4.7	9.9	22
White	-28.4 to +8.0	-7.2	2.4	-4.7	10.0	18
Brown	Both type II					
Blue	-17.0 & -8.2	-12.6	4.4		Not applicable	2
Yellow	+3.6 & +9.7	-6.7	3.1		Not applicable	2
Octahedra	-22.8 to +1.9	-7.4	3.1	-5.3	2.7	7
Dodecahedra	-22.8 to +8.0	-4.5	6.7	-6.2	4.2	4
Irregular	-28.4 to +9.7	-7.7	3.4	-8.2	11.4	11
All Chinese diamonds	-20.7 to +6.1	-3.8	1.7	-3.5	7.4	19

Table 4.8: Descriptive statistics for $\delta^{15}N$ values from North Queensland and Chinese diamonds.

There are no relationships between $\delta^{15}N$ value and nitrogen content, nitrogen aggregation state or carbon isotopic composition on the basis of shape or colour for any of these North Queensland diamonds, and this is evident from a $\delta^{15}N$ - $\delta^{13}C$ plot for the North Queensland diamonds on which diamond colour is shown (Figure 4.16). When diamond morphology is considered, the octahedral diamond group is totally overlapped by the irregular shaped diamonds, and this group also overlays most of the dodecahedral samples, the exception being white diamond N.Q. 36 which has $\delta^{15}N$ = +2.0‰ and $\delta^{13}C$ = -14.8‰.

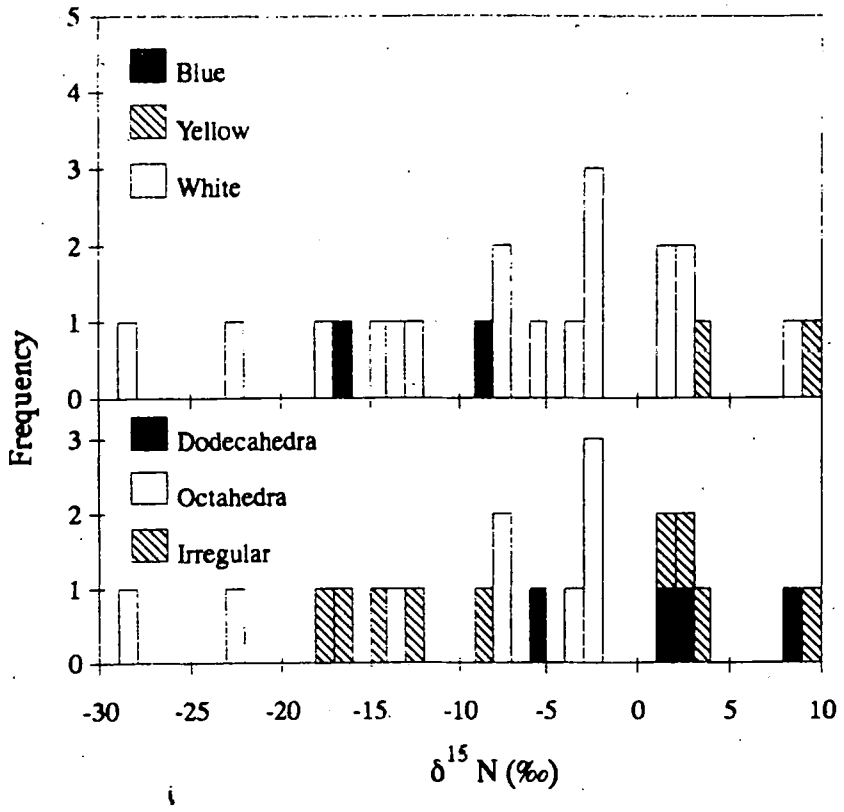

Figure 4.15: The $\delta^{15}N$ distribution of North Queensland diamonds. Different morphologies and colours are shown.

The wide range in the nitrogen isotopic composition of these Chinese diamonds (Table 4.8) is illustrated in Figure 4.17. Seven of the Chinese diamonds have $\delta^{15}N$ >0‰ (Table 4.9), seven have $\delta^{15}N$ values between -7‰ and 0‰ and four have $\delta^{15}N$ < -11‰. One of the four samples with $\delta^{15}N$ values < -11‰, diamond C.3 ($\delta^{15}N$ = -20.7‰ and -13.7‰) is the third most ^{15}N depleted diamond yet analysed. The seven samples with $\delta^{15}N$ values > 0‰ have $\delta^{13}C$ values falling between -12.2‰ and -0.7‰ and the samples with $\delta^{15}N$ values between 0‰ and -7‰ have $\delta^{13}C$ values between -2.4‰ and -16.2‰ (Figure 4.18). The most negative $\delta^{15}N$ samples have a narrower range in $\delta^{13}C$ values, from 2.0‰ to -4.9‰ (Figure 4.18). The mean nitrogen contents of these three groups are 359 ppm, 300 ppm and 699 ppm respectively. Nitrogen aggregation state in the 7 samples with $\delta^{15}N$ < -11‰ ranges from 0% to 3% B-aggregates, and estimates of the proportion of nitrogen in B-aggregates ranges from 0% to 5% for samples that have $\delta^{15}N$ between 0‰ and -7‰. Only in samples that have $\delta^{15}N$ values > 0‰, is nitrogen in a more advanced state of aggregation (up to 27% B-aggregates). There are no obvious morphological or colour characteristics that correlate with these groups, and further data are clearly required in order to investigate their significance.

The Morelli's Fox diamonds differ from the Northern Queensland and Chinese diamonds in that they have a positive mean $\delta^{15}N$ value (Table 4.7 and 4.8) and these differences in nitrogen isotopic composition are also reflected in the relative proportions of diamonds with positive and negative $\delta^{15}N$. Only 32% of the Morelli's Fox diamonds have $\delta^{15}N$ <

0‰, whereas 68% of the Northern Queensland and 63% of the Chinese samples have negative $\delta^{15}N$ values.

Group 1 $\delta^{15}N > 0‰$	Group 3 $\delta^{15}N < -11‰$	Group 2 $-7‰ < \delta^{15}N < 0‰$
C2	C3	C1
C7	(2 analyses)	C4
C10	C9	C8
C11	C19	C13
C12	C20	C14
C16		C15
C18		C17

Table 4.9: Samples comprising the different groups apparent in Chinese diamonds on the basis of nitrogen stable isotope ratios. The type II diamond, C6 has not been classified.

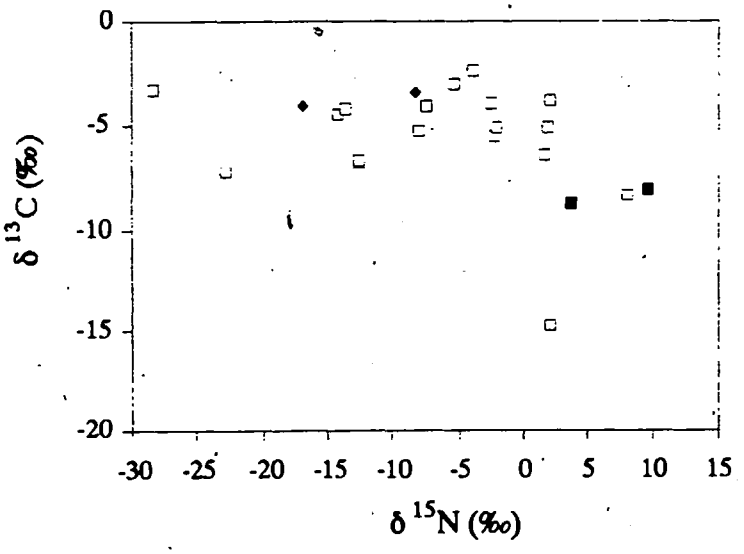

Figure 4.16: $\delta^{15}N$ - $\delta^{13}C$ plot for North Queensland diamonds. Blue diamonds shown by filled diamonds, yellow diamonds by filled squares and white diamonds by open squares.

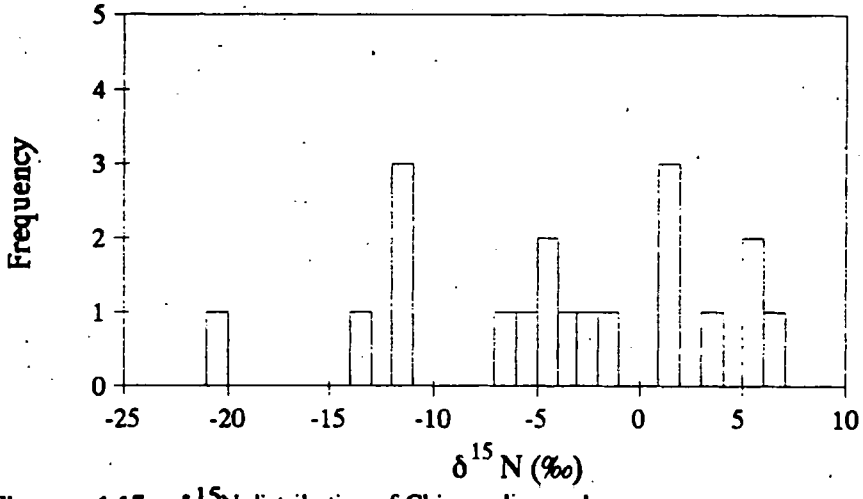

Figure 4.17: $\delta^{15}N$ distribution of Chinese diamonds.

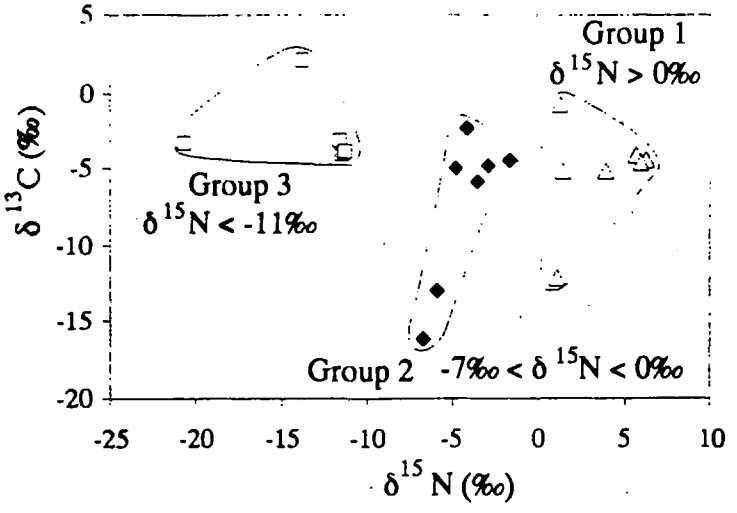

Figure 4.18: $\delta^{15}N$ - $\delta^{13}C$ plot for Chinese diamonds. The three groups are shown.

Diamonds from Morelli's Fox, Northern Queensland and China all show wider ranges in nitrogen isotopic composition than the Argyle or Ellendale diamonds, and there is no correspondence between Argyle and Ellendale diamonds of known paragenesis and any of the groups or subgroups from Morelli's Fox, Northern Queensland or China. When nitrogen and carbon isotopic covariation is considered (Figure 4.19), the considerable overlap between the Morelli's Fox, Northern Queensland and Chinese diamonds is evident. Morelli's Fox, and Northern Queensland diamonds are both elongated along the $\delta^{15}N$ axis and this is similar to the Ellendale diamonds described in Chapter 2. The Chinese diamonds in contrast, have a lesser elongation along the the $\delta^{15}N$ axis, but have a wider $\delta^{13}C$ range and this is similar to the Argyle diamond population. None of the diamond populations from Morelli's Fox, Northern Queensland or China correspond directly to diamonds of known paragenesis from Argyle or Ellendale 9, although the Chinese diamonds wholly enclose the peridotitic paragenesis diamonds (Figure 4.20).

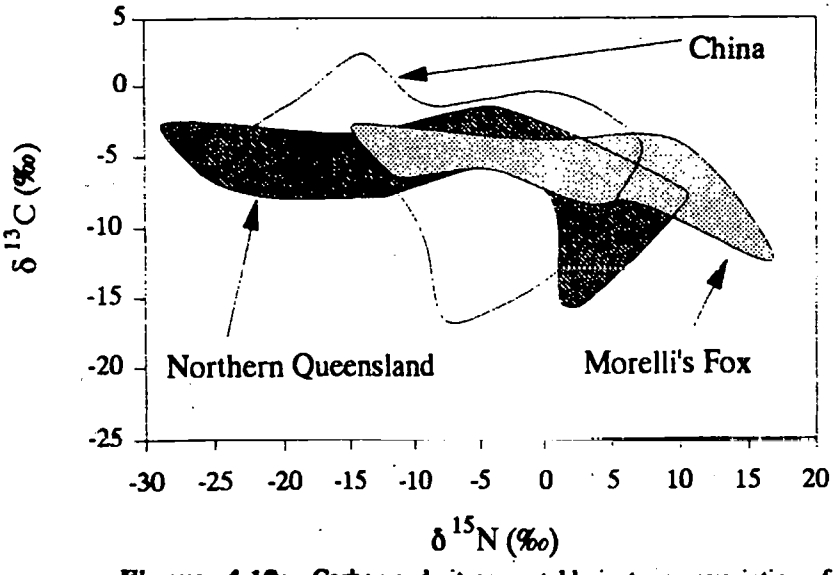

Figure 4.19: Carbon and nitrogen stable isotope covariation of Morelli's Fox, Northern Queensland and Chinese diamonds.

The relative abundance of ^{15}N depleted diamonds amongst the Northern Queensland samples is worthy of particular note. Not only do the two diamonds with the most negative $\delta^{15}N$ values determined come from this source, but seven of the 22 analysed samples have $\delta^{15}N$ values < -10. For comparison, of all the samples analysed by Boyd (1988) only two samples from Finsch (E12 & ladder 7/1),and one from Premier (P#1) had $\delta^{15}N$ values lower than -10‰. The 109 analyses of nitrogen isotopic composition made by Boyd (1988) include analyses of 13 Finsch and 5 Premier diamonds.

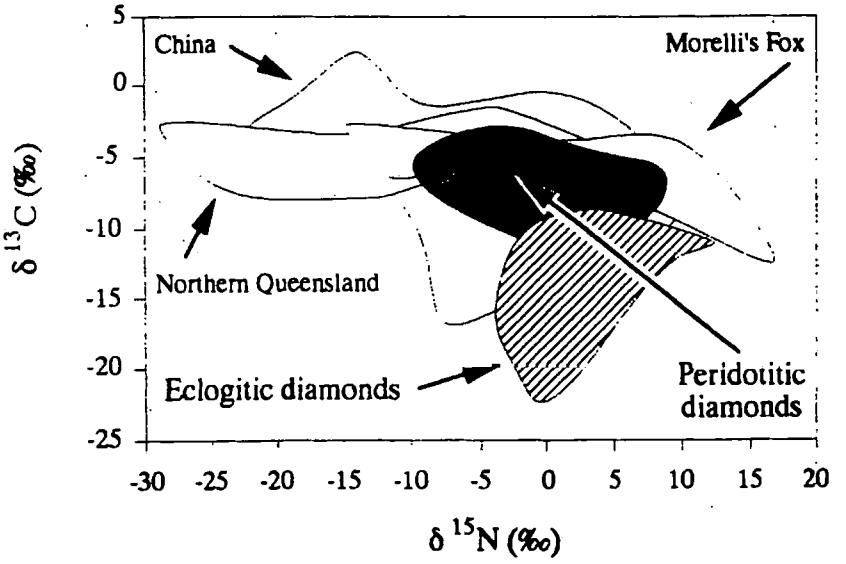

Figure 4.20: As for Figure 4.19, but showing eclogitic paragenesis (striped field) and peridotitic paragenesis (black fields) diamonds from Argyle and Ellendale 9.

4.2.4 Summary

There is considerable overlap in the characteristics of the individual diamond populations examined in this study, and no single parameter is able to effectively differentiate between them. Furthermore, no combination of these variables is effective in allocating diamonds from an unknown source to the characterised diamond deposits without there being some ambiguity.

Morelli's Fox: A variety of crystal forms occur amongst the Morelli's Fox diamonds and no particular morphology is distinctive of this group of samples. They have a wide range in $\delta^{13}C$ and $\delta^{15}N$ values. The $\delta^{13}C$ values cluster around "normal" mantle and the $\delta^{15}N$ values are positive more often than negative. The Morelli's Fox diamonds show some evidence for nitrogen aggregation and nitrogen contents are usually low. A variety of sub-groups may occur in the Morelli's Fox diamonds.

Northern Queensland: The relative rarity of resorbed dodecahedral forms amongst the Northern Queensland samples is notable, as is the extreme ^{15}N depletion evident in several samples from this group. The $\delta^{15}N$ values are mostly negative and $\delta^{13}C$ values

have a wide distribution centered about $\delta^{13}C = -5‰$. A single diamond with a positive $\delta^{13}C$ value occurs in this group, and a further two samples have $\delta^{13}C$ values more positive than -3‰. Northern Queensland diamonds have low nitrogen content and some nitrogen aggregation has occurred.

China: The most characteristic features of these Chinese diamonds are the polished, rounded morphology and the scarcity of aggregated nitrogen. In addition, the group is characterised by a wide spread of carbon isotopic compositions, centered around $\delta^{13}C \approx -4‰$, and includes a single sample with a positive $\delta^{13}C$ value. Nitrogen isotopic composition has a similar spread, also centered around $\delta^{15}N = -4‰$, and 12 of the 18 Chinese diamonds for which $\delta^{15}N$ have been determined, have $\delta^{15}N < 0‰$, and with 4 diamonds having $\delta^{15}N$ values more negative than -11‰. The third most ^{15}N depleted terrestrial diamond is one of these Chinese diamonds.

4.3 DISCUSSION

4.3.1 On the diamond source region

There appear to be sub-groups evident in the diamonds from two of these localities. At Morelli's Fox these are defined largely on the basis of morphology, while in the Chinese diamonds, they are defined on the basis of nitrogen isotopic composition. There are no distinct sub-populations in the diamonds from Northern Queensland. Sub-groups in diamond $\delta^{13}C$ value and nitrogen content have been reported previously (*e.g.* Deines *et al.*, 1984, 1987, 1989, 1991a, 1991b; Otter, 1989; Hill, 1989; Galimov, 1991) and there is strong evidence that diamond paragenesis plays a significant role in determining the stable isotope ratios of, at least, carbon and sulphur in diamond (Kirkley *et al.*, 1991; Eldridge *et al.*, 1991). It would be interesting therefore to consider whether diamond paragenesis is a significant controlling factor in the characteristics of the diamonds described in this chapter. There is, however, a problem with such a study. Firstly, few data are available for the Morelli's Fox, Northern Queensland and Chinese data and the existence of genuine sub-groups needs to be confirmed. This is particularly necessary in order to establish whether diamonds that have very negative $\delta^{15}N$ values ($\delta^{15}N < -10‰$) are indeed a genuine sub-group, or whether they simply represent a few extreme cases. Secondly, no data are available as to the paragenesis of the diamonds described in this chapter. Further studies need to be made on samples that contain inclusions, so that the type of diamond source region (eclogitic, harzburgitic or lherzolitic) may be identified.

4.3.2 Isotopic fractionation models

In Chapter 2, theoretical fractionation curves were fitted to diamonds from Argyle and Ellendale and it was shown that closed system fractional crystallization may be an appropriate model for explaining the isotopic variation within some diamonds. In this section the modelled fractionation factors for carbon and nitrogen determined in Chapter 3 are applied in an investigation as to whether the range of stable isotopic compositions of the Morelli's Fox, Northern Queensland and Chinese diamonds may also be explained by closed system fractional crystallization, or whether some other, more complex model is necessary.

4.3.2.1 Morelli's Fox.

The range in $\delta^{13}C$ values for the Morelli's Fox diamonds is from -11.8‰ to -3.3‰ and the corresponding $\delta^{15}N$ range is from -12.2‰ to +16.1‰ (Figures 4.14 and 4.19). It is possible to generate this range in isotopic compositions by simple closed system fractional crystallization (equation 3.1), using fractionation factors of $\alpha = 1.001$ for carbon and $\alpha = 1.004$ for nitrogen provided that the initial $\delta^{13}C$ value is -6‰ and the initial $\delta^{15}N$ value is +12‰. For both carbon and nitrogen, almost total crystallization are required with $F \leq 0.001$ (99.9% crystallized). The $\delta^{13}C_{initial}$ value of -6‰ is consistent with the major mode in diamond $\delta^{13}C$ values, and the fractionation factors are from Chapter 3.

Thus simple closed system fractional crystallization may adequately explain the stable isotopic compositions of the Morelli's Fox diamonds, provided that large degrees of crystallization have occurred.

4.3.2.2 Northern Queensland

The Northern Queensland diamonds have a wider range in $\delta^{13}C$ values than the Morelli's Fox diamonds, with $-14.8‰ \leq \delta^{13}C \leq +1.9‰$. The range in nitrogen stable isotope compositions is from $\delta^{15}N$ = -28.4‰ to +9.7‰ (See Figures 4.16 and 4.19). It is not possible to produce the range in carbon isotopic compositions found in the Northern Queensland diamonds by simple closed system fractional crystallization with a carbon fractionation factor of 1.001 or less (as is indicated in Chapter 3) regardless of the initial $\delta^{13}C$ value. If, however the larger fractionation factor of 1.0026 is applicable (Mattey *et al.*, 1990), then 99.9% crystallization will account for the observed range in $\delta^{13}C$ values from a source with $\delta^{13}C_{initial}$ = -1‰.

A carbon source with $\delta^{13}C$ = -1‰ is not within the range usually accepted as being representative of primary mantle. It may however be possible to produce a diamond precursor phase by melting a mantle source with $\delta^{13}C \approx$ -5‰, in the presence of CO_2.

The isotopic fractionation associated with CO_2 (α = 1.004, *e.g.* Javoy *et al.*, 1978) should alter the melt $\delta^{13}C$ to more positive values and these may be reflected in diamonds precipitated from such a melt.

The range in nitrogen isotopic compositions seen in the Northern Queensland diamonds cannot be produced by a simple fractional crystallization process, regardless of the source composition, for 99.9% crystallization when α = 1.004. It is therefore suggested that, as with Argyle and Ellendale 9, the stable isotope characteristics of the Northern Queensland diamonds do not result from simple closed system fractional crystallization and that the range of carbon and nitrogen stable isotopic compositions are more likely to arise from some other process.

4.3.2.3 China

The range in $\delta^{13}C$ values amongst the Chinese diamonds is from -16.2‰ to +2.0‰, which is similar to the range seen in the Northern Queensland samples. The $\delta^{15}N$ compositional range is from $\delta^{15}N$ = -20.7‰ to +6.1‰ (See Figures 4.18 and 4.19).

As with the Northern Queensland diamonds the range in Chinese diamond $\delta^{13}C$ values cannot be produced by simple closed system fractional crystallization for 99.9% crystallization and a fractionation factor α = 1.001. The minimum fractionation factor needed is α = 1.0026, and in order to generate all the $\delta^{13}C$ values observed in the Chinese diamonds a $\delta^{13}C_{initial}$ of -1‰ is required. This may, as described above, be produced by melting of a source mantle in the presence of CO_2.

The range in nitrogen isotopic compositions seen in the Chinese diamonds can be explained by closed system fractional crystallization, using the α = 1.004 fractionation factor obtained in Chapter 2, from a source material with $\delta^{15}N_{initial}$ = +2‰ when crystallization is 99.9% complete (*i.e.* F = 0.001).

4.3.2.4 Summary

The range in carbon and nitrogen stable isotopic compositions seen in the Morelli's Fox, and Chinese diamonds may be explained by a simple fractional crystallization model, using believable fractionation factors. However, large degrees of crystallization are necessary (99.9%), and the initial $\delta^{13}C$ value for China ($\delta^{13}C_{initial}$ = -1‰) is not within the range usually accepted as being characteristic of "normal mantle". This ^{13}C enrichment in the diamond source material may be produced by a melting event in which mantle ($\delta^{13}C \approx$ -5 or -6‰) melts in the presence of CO_2 with an associated 4‰ isotopic fractionation, but such a model becomes complex in that it requires a two-stage isotopic fractionation. The range of nitrogen stable isotope ratios that occur in Northern Queensland diamonds preclude simple, closed system fractional crystallization as a

genetic model for the formation of these diamonds, if the nitrogen fractionation factor determined in Chapter 2 is correct.

Thus, although isotopic fractionation may be a cause of the isotopic heterogeneity evident in the Morelli's Fox and Chinese diamonds, the viability of such a model must be considered in conjunction with other possible causes of isotopic variation within the mantle. These include primary mantle heterogeneity and the possibility that the mantle stable isotopic compositions may be modified by the addition of a crustal component with a distinct composition by subduction. The data presented in this Chapter and in Chapter 2 are used in Chapter 6 in order to generate a possible model of diamond formation in the mantle.

A feature of the models of nitrogen isotopic fractionation presented in Chapter 3 and in this Chapter is the positive $\delta^{15}N_{initial}$ values that are necessary for successful modelling. The initial $\delta^{15}N$ values of Morelli's Fox ($\delta^{15}N = +12‰$) and Chinese diamonds ($\delta^{15}N = +2‰$) are both greater than 0‰, in agreement with the results obtained from Argyle and Ellendale diamonds plates (Chapter 2) and this implies a source region that is ^{15}N enriched relative to the present atmosphere. Such a diamond source region with a positive $\delta^{15}N$ value is not in agreement with other (rare) estimates of mantle $\delta^{15}N$ value which are usually < 0‰ and may be as low as $\delta^{15}N = -40‰$ (*e.g.* Javoy *et al.*, 1984, 1986; Boyd *et al.*, 1987, 1992). Mantle $\delta^{15}N$ values are also discussed in Chapter 6.

4.3.3 Differences between lamproitic and alluvial diamonds

There are no discernable differences in the colour or primary shape characteristics of these alluvial diamonds and the lamproitic diamonds from Argyle or Ellendale, although only good quality Chinese diamonds have survived fluvial transport. There are also no significant differences in the range of nitrogen contents and the nitrogen aggregation state of the diamonds described in this chapter and the Argyle and Ellendale lamproitic diamonds. Furthermore, the mean $\delta^{13}C$ (Table 4.3 and 4.4) and $\delta^{15}N$ (Tables 4.7 and 4.8) values of these alluvial diamonds are close to the corresponding values determined for lamproitic diamonds. Hall and Smith (1984) have shown that kimberlitic and lamproitic diamonds are essentially indistinguishable, and it is therefore highly likely that the diamonds in the Morelli's Fox, Northern Queensland and Chinese alluvial deposits are of magmatic origin.

Despite the similarities in many of the characteristics of lamproitic and the limited alluvial diamonds described in this chapter, there are also differences between the two types of diamond source. The Morelli's Fox, Northern Queensland and Chinese diamonds all have a wider range in nitrogen stable isotope ratios than the ranges that have been

determined for individual magmatic diamond sources. Morelli's Fox, Northern Queensland and Chinese diamonds have a range in $\delta^{15}N$ value of 30.3‰, 38.1‰ and 26.8‰ respectively (Tables 4.7 and 4.8), whereas the the widest $\delta^{15}N$ range from a single magmatic diamond source is 22.5‰ (from $\delta^{15}N$ = -9.3‰ to +13.2‰) found at Ellendale 9 (See also Table 5.1). The Northern Queensland and Chinese diamonds also have a wider range in $\delta^{13}C$ values than is usual for most magmatic diamonds (See Table 1.3).

There are too few data available to state categorically that diamonds from a single alluvial source have more variable $\delta^{15}N$ values than magmatic diamonds from a single source. It is possible, perhaps even likely, that the range in $\delta^{15}N$ values that exists in the Morelli's Fox, Northern Queensland and Chinese diamonds is the result of multiple primary sources contributing diamonds to the placer deposit. The range of $\delta^{15}N$ values in an alluvial diamond deposit with a single primary source, for example the crater facies diamonds from Orapa, Botswana, must be investigated. If this shows, as is expected, that the $\delta^{15}N$ values of diamonds in alluvial deposits simply mimics that of the primary source, then the wide range of diamond $\delta^{15}N$ values measured in the Morelli's Fox, Northern Queensland and Chinese diamonds is indicative of either unusually heterogeneous primary primary diamond sources, or is a valuable prospecting tool in that it is indicative of more than one primary magmatic diamond source of these diamonds.

If single primary sources can be identified for each of the Morelli's Fox, Northern Queensland and Chinese deposits, then this may indicate that the mantle is more variable than is currently expected from the nitrogen stable isotope ratios determined from other diamond sources (Chapter 2 and Boyd, 1988), and this possibility needs further investigation.

---

5 Microdiamonds from Australia

5.1 OVERVIEW

Microdiamonds are diamonds or fragments of diamond that are too small to extract and market economically. They have not been formally defined by the diamond industry, however the size limit is usually taken as being smaller than about 1mm across. Complete diamond crystals, smaller than 40μm across have also been described (*e.g.* Sobolev and Shatsky, 1990) and these would be considered by mineralogists to be "true microdiamonds".

Unlike macro-diamonds, which are now accepted as being xenocrysts in the primary magmatic host (*e.g.* Gurney, 1989), the origin of microdiamonds is still unconstrained, largely due to their occurrence in a number of different environments. Magmatic microdiamonds are those that occur in both kimberlite and lamproite pipes (McCandless, 1989; McCandless *et al.*, 1991), and in xenoliths therein, but microdiamonds also occur in placer deposits (*e.g.* Atkinson, 1989) and they have also been recovered from impact craters, picrites, ophiolites and alkali basalts (Orlov, 1977; Kaminsky, 1980; Kaminsky *et al.*, 1986; Pearson *et al.*, 1989). Furthermore, microdiamonds have also been found in very high grade metamorphic rocks from Siberia (Sobolev and Shatsky, 1990) and from China (Shutong *et al.*, 1992), and these are usually termed ultra-metamorphic microdiamonds. Both microdiamonds and smaller nanometer sized diamonds are known to occur in iron meteorites (Lewis *et al.*, 1987, 1989), in ureilites (Grady *et al.*, 1988) and in the enstatite chondrite meteorite Abee (Russell *et al.*, 1991). Microdiamonds have also been found in detonation residues (Greiner *et al.*, 1988).

It has been suggested that some magmatic microdiamonds may be related to a kimberlitic or lamproitic magma and that they precipitated during diatreme emplacement, *i.e.* be of phenocrystal origin (*e.g.* Gurney, 1989). They have also been related to the thermal cracking of CO_2 dominated fluids within the diamond stability field in the mantle (Wyllie, 1989), and as such would represent xenocrysts in whatever magma transported them to the surface. Regardless of whether they are xenocrystal or phenocrystal, such microdiamonds are derived from, and form potentially valuable probes of, the mantle. In contrast, it has been suggested that microdiamonds in metamorphic rocks are the product of the very high pressure recrystallization of (possibly organic) crust derived carbon (Sobolev and Shatsky, 1990). These microdiamonds will be representative of the Earth's crust rather than the mantle. Other microdiamonds have been related to disaggregating meteorites, and the microdiamond belt across north western Australia may represent one such dispersal plume (Atkinson, 1989). The presence of microdiamonds

in impact related structures and nanodiamonds in the Cretaceous - Tertiary boundary clay at Alberta (Carlisle and Braman, 1991) may also indicate the existence of naturally occurring shock synthesized diamonds.

This study is not concerned with microdiamonds of possible cosmological origin, but rather with the microdiamonds that occur in the Argyle and Ellendale lamproite pipes and in a number of placer deposits (exploration sites) from northern and western Australia. The lamproite-derived microdiamonds are unequivocally magmatic in origin whereas the placer microdiamonds may have either a magmatic source, or they may be a product of ultra-high pressure metamorphic events, similar to those described for Siberia and China (Sobolev and Shatsky, 1990; Shutong *et al.*, 1992. See also Becker and Altherr, 1992 for evidence of metamorphism at pressures within the diamond stability field). One of the aims of this study is to investigate the source material and region of formation of the microdiamonds found in placer deposits. If these can be shown to have been the result of the high pressure metamorphic events associated with collisional tectonics, they may be used to constrain the tectonic evolution of Western Australia. They may also, in an indirect way, help to resolve the long standing debate about the role of subduction in diamond genesis, by showing that the presence of a crustal component in, at least some diamonds is physically possible. If these microdiamonds are instead shown to be of magmatic origin, they may be the indicator minerals of potentially economic macrodiamond deposits. Diamond itself is, after all, the most effective tracer of diamond deposits (Levinson *et al.*, 1987).

Another aim of this study is to investigate the relationships between the microdiamond and macrodiamond populations from the same lamproite pipe. If microdiamond and macrodiamond populations are related to one another, then the microdiamonds can provide a valuable indicator of diamond grade that is both easy and cheap to collect. Such a relationship has been reported previously for diamonds from Argyle (Deakin and Boxer, 1989), although microdiamond abundances do not, as a general rule, correlate with the overall kimberlite or lamproite grade (Gurney, Unpublished data). If there is no relationship between microdiamonds and macrodiamonds this implies a non-cogenetic origin, as has been suggested by Rombouts (1991) for the Argyle diamonds. On the basis of a statistical analysis of diamond size distributions, Rombouts (1991) suggests that the Argyle microdiamonds are related to pipe emplacement, rather than to the xenocrystal macrodiamond population.

A third aim of this study is to investigate the stable isotope characteristics of microdiamonds having different morphologies. Microdiamonds can occur in cubic as well as octahedral and dodecahedral crystal forms (*e.g.* Shutong *et al.*, 1992), as well as having a "mixed morphology" with variable development of cube and octahedral faces

(Sobolev and Shatsky, 1990). Sunagawa (1990; See also Chapter 1) has shown that the morphology of a diamond is dependent on the formation conditions and a comparison of cubic and irregular microdiamonds from an exploration site near Coanjula in the Northern Territory, Australia is presented in this Chapter. This examines isotopic differences between these two microdiamond morphologies, and attempts to relate these to the microdiamond formation process.

The major aim of this chapter however, is to provide a formal definition of microdiamonds. It is suggested that **diamonds showing little evidence for resorption, and having a primary growth form that is smaller than about 1 mm in diameter**, are microdiamonds *sensu strictu*. This definition is tested in this chapter by comparing microdiamonds as defined above, with samples that fulfill the size criteria but have broken and resorbed morphology. An attempt is made to show that the broken and resorbed microdiamonds are related to the macrodiamond population in their source lamproite, and thus differ from the true microdiamonds.

The results presented here are the first stable isotope data from Australian microdiamonds, although some of the Northern Territory microdiamonds used in this study have also been described by Lee *et al.*, (1991). The Argyle and Ellendale samples used were initially selected by Chris Smith of ADM and a variety of samples were supplied. Microdiamonds of unequivocally magmatic origin, between 0.83 mm and 0.12 mm in diameter were obtained from Ellendale 4, Ellendale 9 and the Argyle lamproites, and in addition, samples from a magmatic dyke at Argyle and three peridotite nodules from Argyle were examined. Samples from a Northern Queensland exploration site and a Northern Territory exploration site, provided by Dearn Lee of Ashton Mining, were also examined and in both of these cases, the primary source of the microdiamonds is not known. The different microdiamond groups, and the number of analyses of these are listed in Table 5.1.

The study presented in this Chapter is primarily one of carbon stable isotope ratios. However, an analysis of the aggregation state, concentration and isotopic composition of nitrogen in a diamond is desirable as it can assist in further constraining the origin of the sample. Mass spectrometric methods for measuring nitrogen concentration and isotopic composition were attempted on samples from all the microdiamond groups, and in most cases, these were not successful due to a combination of low nitrogen content and very small sample size. Five measurements were however obtained; three on Argyle R.O.M microdiamonds, one on an Ellendale 4 microdiamond and one on a Northern Territory cube. These are the first determinations of nitrogen content and isotopic composition made from any microdiamonds. FTIR spectra were collected on all microdiamonds used in this study, however the combination of small sample size and non-parallel and often

etched sample surfaces resulted in very poor quality spectra and for this reason, no attempt has been made to determine nitrogen content spectroscopically. For the same reason, no attempt has been made to estimate the proportion of nitrogen occurring in B-aggregates, although in some cases, diamond type could be qualitatively identified.

			$\delta^{13}C$	FTIR	$\delta^{15}N$	[N]
Argyle	Magmatic dyke		2			
	Run of Mine	+600 fraction	7	7		
		+425 fraction	3	7	3	3
	Peridotite nodule	958075	5			
		958324	8			
		958330	2			
Ellendale 4			11	9	1	1
Ellendale 9			5			
Northern Queensland			6	1		
Northern Territory	Cubes		27	23	1	1
	Irregular		18	3		
			94	50	5	5

Table 5.1: Microdiamonds used in this study and the number of analyses from each group. The two different size fractions for the Argyle run of mine microdiamonds are those with nominal diameters of between 600μm and 850 μm (+600 fraction) and of between 425 μm and 500 μm (+425 fraction).

5.2 RESULTS

5.2.1 Diamond morphology

With the exception of the Run of Mine (R.O.M.) microdiamonds from Argyle, the magmatic microdiamonds from Argyle, Ellendale 4 and Ellendale 9 are all sharp-edged octahedra and they range in size from 0.4 mm down to 0.12 mm. In contrast, the Argyle R.O.M. microdiamonds are all broken fragments which often show evidence of resorption and occasionally, curvilinear crystal faces. Samples of up to 0.825 mm were analysed, although both larger and smaller R.O.M. samples do occur. No octahedral R.O.M. microdiamonds were supplied, despite their occurrence at concentrations of $\approx$1% in the Argyle diamond population (Davy, Pers. Comm.).

The shape of the Argyle dyke and peridotite nodule microdiamonds and the Ellendale microdiamonds differs from that common amongst the macrodiamond populations. The dyke and nodule microdiamonds are characterised by a sharp-edged octahedral morphology whereas the macrodiamond populations are dominated by rounded dodecahedra (*e.g.* Hall and Smith, 1984). Octahedral diamonds, usually of peridotitic paragenesis (C.B. Smith, Pers. Comm.) do occur in the Argyle lamproite, and these are akin to the dyke and nodule microdiamonds. The Argyle R.O.M. microdiamonds

however, have a similar morphology to the bulk of the macrodiamond population when remnant crystal faces occur on these microdiamonds.

The North Queensland and Northern Territory microdiamonds occur in a variety of shapes, including cubes, octahedra and dodecahedra and irregular samples. Lee *et al.*, (1991) have described the Northern Territory microdiamond population and report that more than 70% of these microdiamonds are opaque cubes with a fibrous structure, with a further 4% being colourless, yellow or green non-fibrous cubes. The remaining samples are octahedral, dodecahedral or irregular This dominance of cubic morphology crystals is unusual and is unlike any recorded for kimberlitic or lamproitic diamonds (Lee *et al.*, 1991). The fibrous structure is also unusual, but has been reported for rapidly grown diamond forming the coat on coated stones (Boyd *et al.*, 1987, 1992). The majority of the Northern Queensland and Northern Territory microdiamonds are 0.2 mm in size and samples more than 0.5 mm in diameter are rare. Amongst the Northern Queensland samples, only N.Q. 3 is cubic, the remainder being irregular fragments.

5.2.2 Carbon isotopic composition

Whole microdiamond samples were usually combusted off-line (See Appendix 2) prior to analysis of the carbon isotopic composition in a SIRA 24 dynamic mass spectrometer. FTIR spectra suggested that nitrogen analysis might be possible for 5 microdiamonds, and these samples were prepared in the same manner as the macrodiamond samples described in Chapters Two and Three, however their small size meant that the complete, unbroken sample was analysed. The $\delta^{13}C$ values of these samples were obtained from CO_2 collected during combustion in the nitrogen experiment. Full details of the analytical procedure are presented in Appendix 2.

5.2.2.1 Argyle

Two microdiamonds from the magmatic dyke at Argyle were available for analysis and their $\delta^{13}C$ values are -5.6‰ and -6.9‰ respectively. Run of mine microdiamonds in two size fractions, +425 (which are between 425μm and 500μm across) and +600 (600μm to 850μm across) were analysed (See Table 5.1). The $\delta^{13}C$ values of the smaller size fraction ranged from -9.6‰ to a minimum of -14.9‰, and the range of $\delta^{13}C$ values for the larger size fraction was from a maximum of -10.0‰ to a minimum of -14.0‰. The mean $\delta^{13}C$ value for all 10 R.O.M microdiamonds is -11.7‰, and there is no discernable difference between the +425 size fraction (mean $\delta^{13}C$ value = -11.6‰) and the +600 size fraction (mean $\delta^{13}C$ value = -11.8‰).

The $\delta^{13}C$ distribution of the Argyle run of mine microdiamonds is shown relative to the magmatic dyke microdiamonds in Figure 5.1. From this it is evident that all R.O.M.

microdiamonds have $\delta^{13}C$ values that are more negative than the $\delta^{13}C$ values of microdiamonds derived from the Argyle magmatic dyke.

Microdiamonds from three peridotite nodules from Argyle were analysed, and all had carbon isotopic composition within the range $-4.6‰ \leq \delta^{13}C \leq +0.1‰$ (Figure 5.1). The widest range occurs in nodule 958324 which has microdiamond $\delta^{13}C$ values between -4.2‰ and +0.1‰, and the mean $\delta^{13}C$ value of diamonds from this nodule is $\delta^{13}C = -2.7‰$. The two $\delta^{13}C$ measurements from nodule 958330 are -2.9‰ and -1.9‰ respectively, only 1‰ different. The microdiamonds from nodule 958075 have a minimum $\delta^{13}C$ value of -4.6‰ and a maximum of -2.7‰, which makes them almost distinct from 958330 microdiamonds, but they do overlap with microdiamonds from nodule 958324. This maximum was measured on a composite sample, comprising 5 very small microdiamonds (≈0.12 mm diameter). The mean $\delta^{13}C$ value for all the microdiamonds from this nodule is -4.0‰. When all the analysed microdiamonds from all three peridotite nodules are considered together, they have a mean $\delta^{13}C$ value of -3.1‰. This is more negative than the mean $\delta^{13}C$ value for either magmatic dyke microdiamonds or R.O.M. microdiamonds, and the separation of nodule microdiamonds from those derived directly from the host lamproite is evident on Figure 5.1.

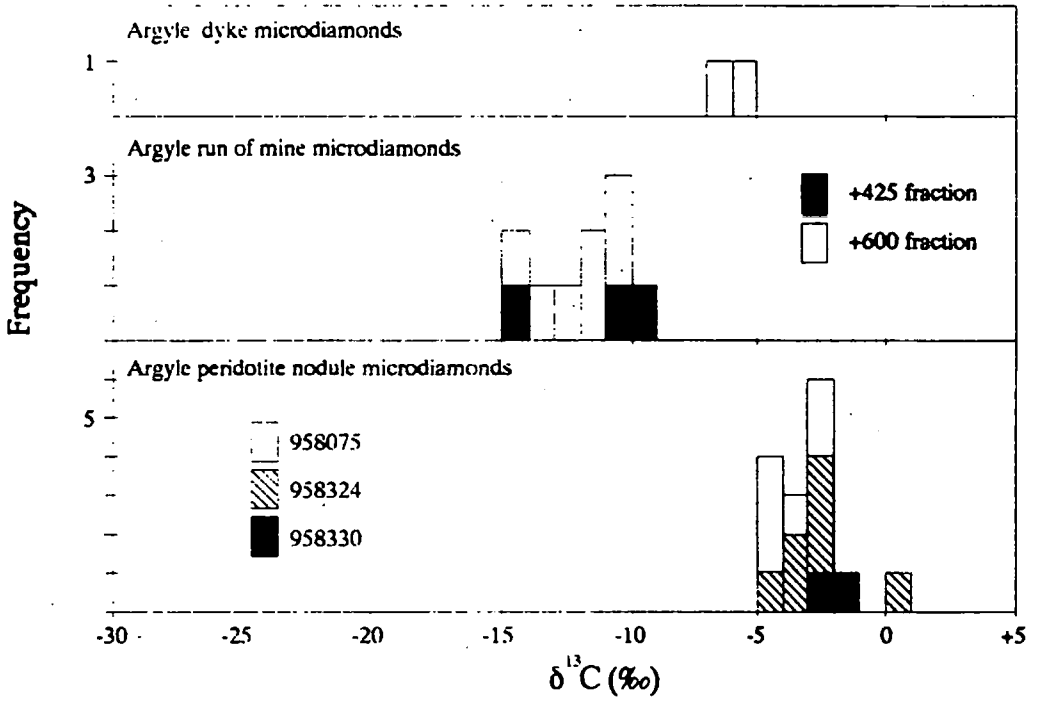

Figure 5.1: The $\delta^{13}C$ distribution of microdiamonds from Argyle. The median $\delta^{13}C$ value for magmatic dyke microdiamonds is -6.3‰, for R.O.M. microdiamonds is -11.1‰ and for microdiamonds derived from peridotite nodules is -3.0‰.

A comparison of the $\delta^{13}C$ values of the Argyle microdiamonds with the macrodiamond population is shown in Figure 5.2. The carbon isotopic composition of the dyke, two of the +425 μm R.O.M. microdiamonds and all of the +600 μm fall within the range

defined by the Argyle macrodiamond population (Figure 5.2). The remaining +425 μm R.O.M microdiamond, with a $\delta^{13}C$ value of -14.9‰ is just more negative than the the minimum $\delta^{13}C$ value for Argyle macrodiamonds which is $\delta^{13}C$ = -14.1‰. None of the R.O.M microdiamonds have $\delta^{13}C$ values above -9.6‰ whereas 38% (23/60) of the 2mm diamonds have this composition. The two dyke microdiamonds have $\delta^{13}C$ values within the limits of the 2 mm stones, at the high side of the distribution.

The $\delta^{13}C$ values of microdiamonds derived from the peridotite nodules do not overlap with measured $\delta^{13}C$ values from peridotitic paragenesis macrodiamonds, despite their occurrence in a peridotitic host rock. Indeed, the only 2mm diamond that has a $\delta^{13}C$ value within the range measured for these microdiamonds is the eclogitic paragenesis sample A3, which has $\delta^{13}C$ = -4.5‰. The minimum $\delta^{13}C$ value from the nodule microdiamonds is -4.6‰, whereas the maximum $\delta^{13}C$ value of peridotite paragenesis 2mm diamonds is -6.0‰.

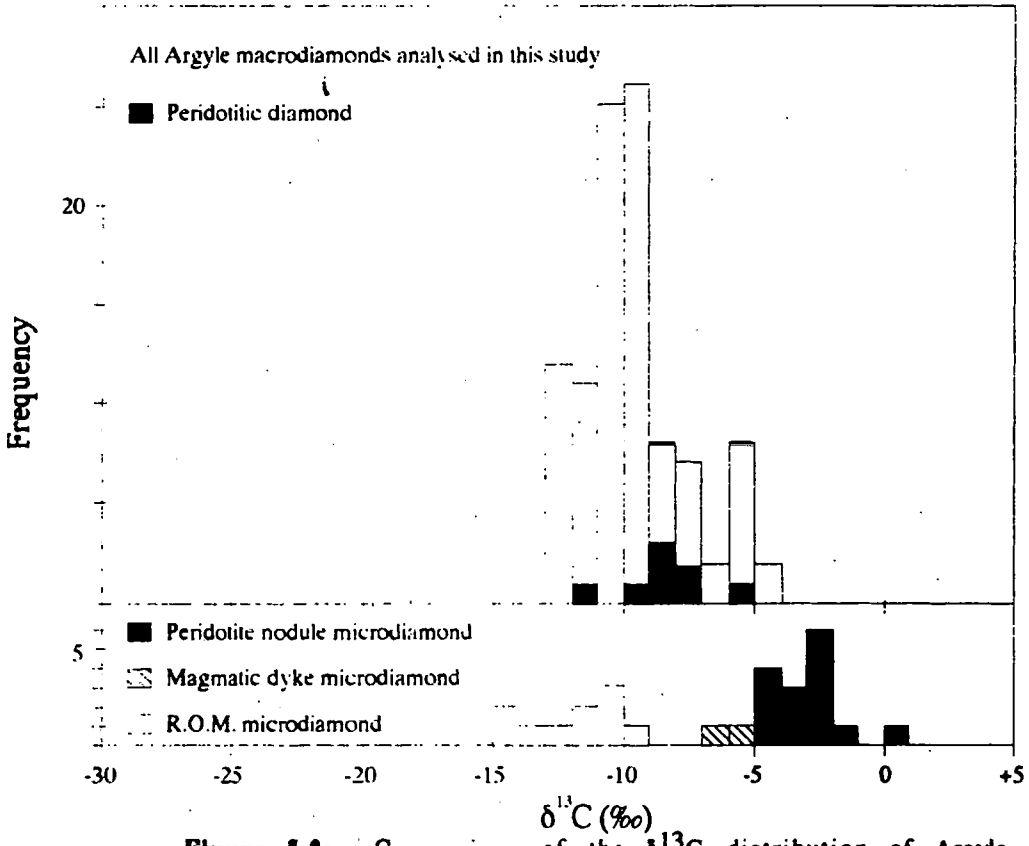

Figure 5.2: Comparison of the $\delta^{13}C$ distribution of Argyle microdiamonds and macrodiamonds.

5.2.2.2 Ellendale 4 and Ellendale 9

Microdiamonds from both the Ellendale 4 and Ellendale 9 lamproite have a range of just over 3.1‰ in their measured $\delta^{13}C$ values, and minimum and maximum values are also similar for diamonds from each lamproite. Ellendale 4 microdiamonds have $\delta^{13}C$ values within the range -6.7‰ to -2.9‰, whereas Ellendale 9 microdiamonds range from $\delta^{13}C$

= -6.8‰ to -3.3‰. The mean $\delta^{13}C$ value for Ellendale 4 microdiamonds is -4.5‰ and the mean for Ellendale 9 microdiamonds is -5.0‰.

A histogram showing the $\delta^{13}C$ distribution of the Ellendale microdiamonds is shown in Figure 5.3. Although data are scarce, it is apparent that these microdiamonds have a mode around $\delta^{13}C \approx -5‰$, similar to the distribution of diamonds in general (See Chapter 1, Figure 1.3 and Galimov, 1991).

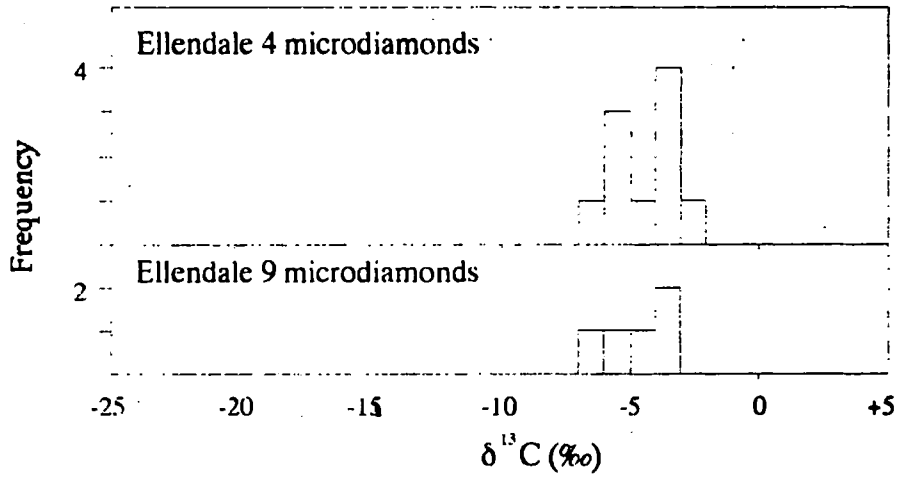

Figure 5.3: The $\delta^{13}C$ distribution of microdiamonds from the Ellendale 4 and Ellendale 9 lamproites.

Whereas the morphological characteristics of the Ellendale macrodiamond and microdiamond suites are distinct, the same is not the case for the carbon isotopic compositions (Figure 5.4).

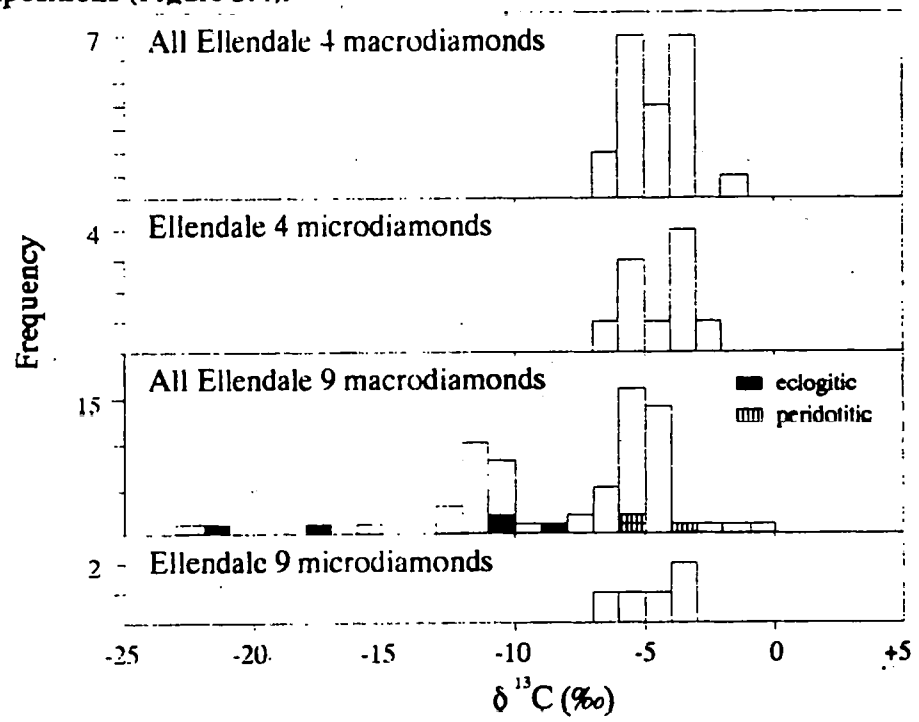

Figure 5.4: Comparison of the $\delta^{13}C$ distributions of Ellendale macrodiamond and microdiamond populations.

Ellendale 4 macrodiamonds have $\delta^{13}C$ values between -6.2‰ and -2.0‰, and microdiamonds from the same pipe have a $\delta^{13}C$ range from -6.7‰ to -2.9‰. The $\delta^{13}C$ values of the microdiamonds from Ellendale 9 are also similar to the major mode in the Ellendale 9 macrodiamond population (Figure 5.4), which is centered around $\delta^{13}C$ = -5‰. Amongst the macrodiamonds however, nearly a third of the stones analysed (10 of the 27) have $\delta^{13}C$ values outside the range $-7‰ < \delta^{13}C \geq -3‰$, yet none of the 5 microdiamonds have $\delta^{13}C$ values falling outside this range. The Ellendale 9 microdiamonds, with $\delta^{13}C$ values between -6.8‰ and -3.4‰ do not overlap with macrodiamonds of confirmed eclogitic paragenesis, but their $\delta^{13}C$ values are similar to those from peridotitic paragenesis Ellendale 9 macrodiamonds. Both Ellendale 4 and Ellendale 9 diamonds have carbon isotopic composition within the range expected for "normal" mantle.

5.2.2.3 Northern Queensland microdiamonds

The Northern Queensland samples are unusual in that they are highly ^{13}C depleted. The $\delta^{13}C$ values range from a maximum of -9.7‰, down to a minimum of -20.7‰ and the mean $\delta^{13}C$ value is -15.6‰. The minimum $\delta^{13}C$ value occurs in the only cubic sample, N.Q. 3. A $\delta^{13}C$ histogram for these Northern Queensland microdiamonds is presented in Figure 5.5. This shows the range of $\delta^{13}C$ values recorded for these samples, and on comparison with Figures 5.1 and 5.3, it is evident that these microdiamonds do not overlap with diamonds from the Argyle dyke or peridotite nodule, or with the Ellendale octahedral microdiamonds. The Argyle R.O.M. samples however all fall within the range of these Northern Queensland samples.

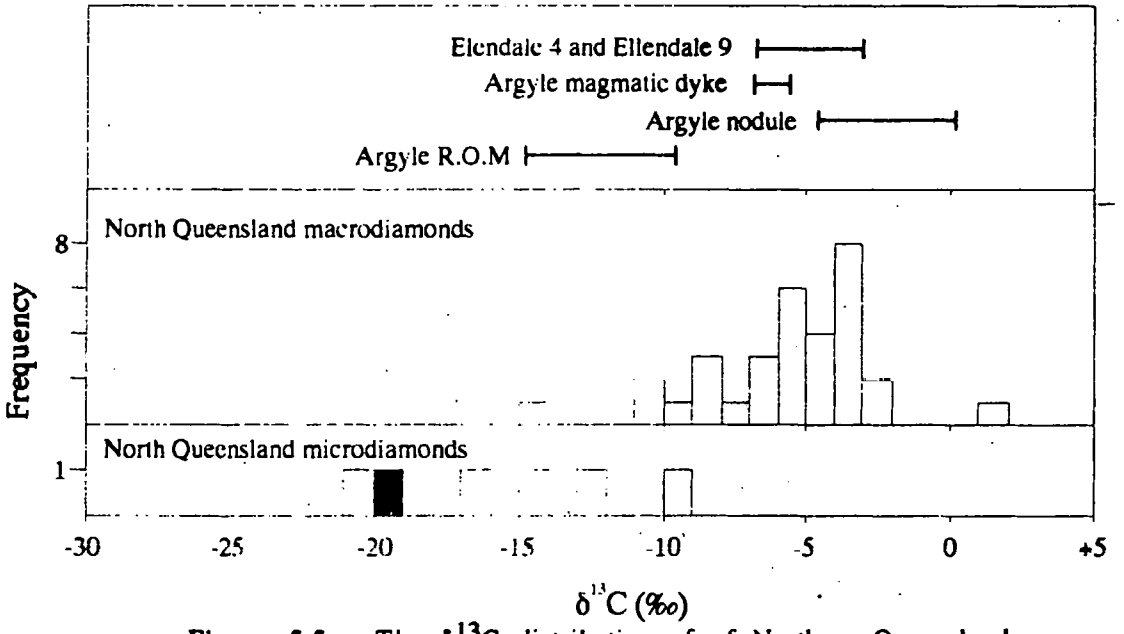

Figure 5.5: The $\delta^{13}C$ distribution of of Northern Queensland microdiamonds. The shaded sample is N.Q. #4, a rare type Ib diamond and the implications of this are discussed in section 5.4.1.3. The $\delta^{13}C$ ranges for Argyle and Ellendale microdiamonds and the histogram of the Northern Queensland macrodiamonds are shown.

The carbon isotopic composition of the three least ^{13}C depleted Northern Queensland microdiamonds fall within the $\delta^{13}C$ range of the Northern Queensland macrodiamonds (Figure 5.5), but the mean $\delta^{13}C$ values of the macrodiamond and microdiamond populations is distinct. Microdiamonds (mean $\delta^{13}C$ = -15.6‰) are ^{13}C depleted relative to the macrodiamond population which has a mean $\delta^{13}C$ value of -5.9‰ (t - statistic = -6.41, Degrees of freedom = 38, significant at 99% confidence).

5.2.2.4 Northern Territory microdiamonds

Microdiamonds from the Northern Territory are particularly useful in this study, for not only are many more samples available than at other localities (45 in total), but their morphology and trace element composition have been described (Lee *et al.*, 1991). Furthermore, the Northern Territory microdiamonds are readily divided on the basis of morphology.

The $\delta^{13}C$ values of cubic microdiamonds from this Northern Territory site have a broad, Gaussian distribution between the limits of $\delta^{13}C$ = -27.5‰ and $\delta^{13}C$ = -10.1‰ (Figure 5.6). The mean $\delta^{13}C$ value is -17.8‰ and the standard deviation is 3.8‰. From Figure 5.6, it is evident that there is a mode in the data at $\delta^{13}C$ = -16‰ to -18‰. This suite of microdiamonds includes the most ^{13}C depleted microdiamonds analysed in this study (N.T. 6, $\delta^{13}C$ = -27.5‰), and 4 of the 26 analysed microdiamonds had $\delta^{13}C$ values more negative than even the most ^{13}C depleted Northern Queensland microdiamonds. No cubic microdiamonds with $\delta^{13}C$ values near the mantle $\delta^{13}C$ value of ≈ -5‰ were measured.

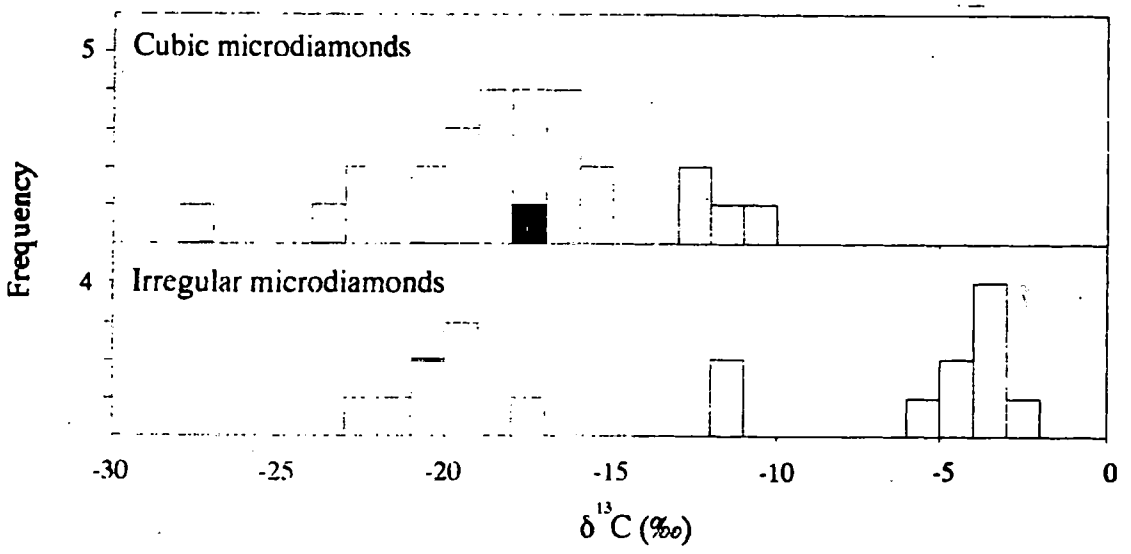

Figure 5.6: Histogram showing the carbon isotopic composition of Northern Territory microdiamonds. The shaded sample is the cubic microdiamond N.T. 1-16 , and is a sample for which nitrogen content and isotopic composition have been determined.

All the irregular microdiamonds from this Northern Territory site have a trimodal $\delta^{13}C$ distribution in the range $-22.2‰ \leq \delta^{13}C \leq -2.5‰$ (See Figure 5.6 and Table 5.2). The intermediate group comprises two microdiamonds (N.T. 16 and N.T. 7) which are more than 3 standard deviations away from the mean $\delta^{13}C$ value of either of the other two groups, and for this reason it is likely that they define a third population.

	range (‰)	mean (‰)	σ (‰)	n
Most ^{13}C depleted samples	-22.2 to -17.7	-20.2	1.4	8
Least ^{13}C depleted samples	-2.5 to -5.6	-4.0	1.0	8
Intermediate samples	-11.5			2

Table 5.2: The three modes in the Northern Territory irregular microdiamonds. See also Figure 5.6.

Microdiamonds with $\delta^{13}C$ values of between -2‰ and -6‰ fall within the range of primary mantle $\delta^{13}C$ measurements (See Chapter 1). The remaining microdiamonds from this group fall within the $\delta^{13}C$ range of the cubic Northern Territory microdiamonds. The mean $\delta^{13}C$ value of the most ^{13}C depleted group of irregular microdiamonds is not significantly different from that of the cubic microdiamonds and nor is there a significant difference (99% confidence level) between cubes and the two microdiamonds with $\delta^{13}C$ values of -11.5‰.

5.2.3 Nitrogen

FTIR spectra were collected for all microdiamonds used in this study, but only in the case of 50 of the 101 samples examined could diamond type be identified. The distribution of the different spectral types by locality are listed in Table 5.3. Nitrogen abundance determinations were attempted on samples for which FTIR spectra indicated significant amounts of nitrogen, and on the largest microdiamonds from each site, however only 5 measurements were successful. Three of these are from type IaB Argyle R.O.M. microdiamonds, one is from a type IaA Ellendale 4 sample and one is a cubic microdiamond from the Northern Territory samples for which the spectral type could not be identified.

In the case of nitrogen measurements from the Argyle R.O.M. and Ellendale 4 microdiamonds, high nitrogen yields on combustion† render blank correction of the data unnecessary. This is not the case for the cubic microdiamond from the Northern

† Argyle R.O.M +425 fraction, sample #3: Nitrogen yield = 160 ng
#5: Nitrogen yield = 435 ng
#6: Nitrogen yield = 500 ng
Ellendale 4, microdiamond #9: Nitrogen yield = 12 ng

Territory which has been corrected for a 0.7 ng blank (25%) measured at the start of the days run. This blank correction, for various assumed isotopic compositions of the blank is shown in Table 5.4.

	IIa	IIb	Ib	IaA	IaAB	IaB	Unknown
Argyle							
+425 R.O.M	2	1	-	-	-	4	-
+600 R.O.M	3	-	-	1	1	2	-
Dyke	-	-	-	-	-	-	Both
Nodule	-	-	-	-	-	-	All 18*
Ellendale 4	6	-	-	3	-	-	2
Ellendale 9	-	-	-	-	-	-	All 5
Northern Queensland	-	-	1	-	-	-	5
Northern Territory							
cubes	13	-	-	1	1	8	4
irregular	-	-	-	3	-	-	15
	24	1	1	8	2	14	51

Table 5.3: The occurrence of different spectral types in the microdiamonds described in this Chapter. * Includes a composite of 5 individual diamonds from nodule 958075.

5.2.3.1 Argyle R.O.M. microdiamonds

Both type II and type IaB diamonds occur in the +425 size fraction of the Argyle R.O.M microdiamonds, and the type II diamonds include a rare type IIb sample (#4). The $\delta^{13}C$ value of this diamond has not been determined. Three of the four type IaB diamonds contain platelets and nitrogen concentration and isotopic composition have been determined for these samples. No type IaA or type IaAB diamonds were found in the +425 size fraction, although a single example of each of these occurs in the +600 size fraction. Three of the +600 size fraction are type II diamonds and the remaining +600 microdiamonds are both type IaB diamonds and contain platelets. In the +600 size fraction, the sample with the highest $\delta^{13}C$ value (#5, $\delta^{13}C$ = -10.1‰) is the type IaA sample. The next highest $\delta^{13}C$ value (-12.7‰, sample #6) corresponds to the type IaAB sample and the most negative $\delta^{13}C$ measurements both come from the type IaB microdiamonds (#4 and #7). The three type II microdiamonds have $\delta^{13}C$ values higher than those of the type IaAB and type IaB samples.

The +425 size fraction microdiamonds have spectral characteristics that differ from the Argyle macrodiamond population. Both type IaA and IaAB diamonds occur amongst the macrodiamonds, but were not found in the +425 microdiamond population. In addition, the rare type IIb microdiamond does not have a counterpart amongst the Argyle macrodiamonds analysed in this study. Microdiamonds from the +600 size fraction however are similar to the macrodiamond population in that type II and type IaB spectra are most common.

Nitrogen isotopic compositions determined for three of the +425 size fraction Argyle R.O.M microdiamonds are $\delta^{15}N$ = +5.5‰, $\delta^{15}N$ = +5.8‰ and $\delta^{15}N$ = +0.8‰, and these correspond to nitrogen contents of 405 ppm, 1198 ppm and 1961 ppm respectively. All three of these are type IaB diamonds. The sample with the highest $\delta^{15}N$ value (#5, $\delta^{15}N$ = +5.8‰) has the most negative $\delta^{13}C$ value (-14.9‰) and the diamond with the lowest $\delta^{15}N$ value (+0.8‰) is that with the highest $\delta^{13}C$ value (-9.6‰). This is illustrated in Figure 5.7.

The $\delta^{15}N$ values determined for the three +425 microdiamonds are similar to those from the macrodiamond population in that all three are above than 0‰. Nitrogen abundances measured from the microdiamond and macrodiamond populations are however different. Nitrogen contents in the Argyle 2 mm diamonds are generally low. Of the 60 samples described in Chapter 2, only 6 (10%) contain more than 1000 ppm nitrogen, and these 6 comprise two peridotitic paragenesis diamonds, the grey diamond, a white macle and two yellow diamonds. In contrast, two (out of 7) or 29% of the +425 microdiamonds have nitrogen contents of more than 1000 ppm.

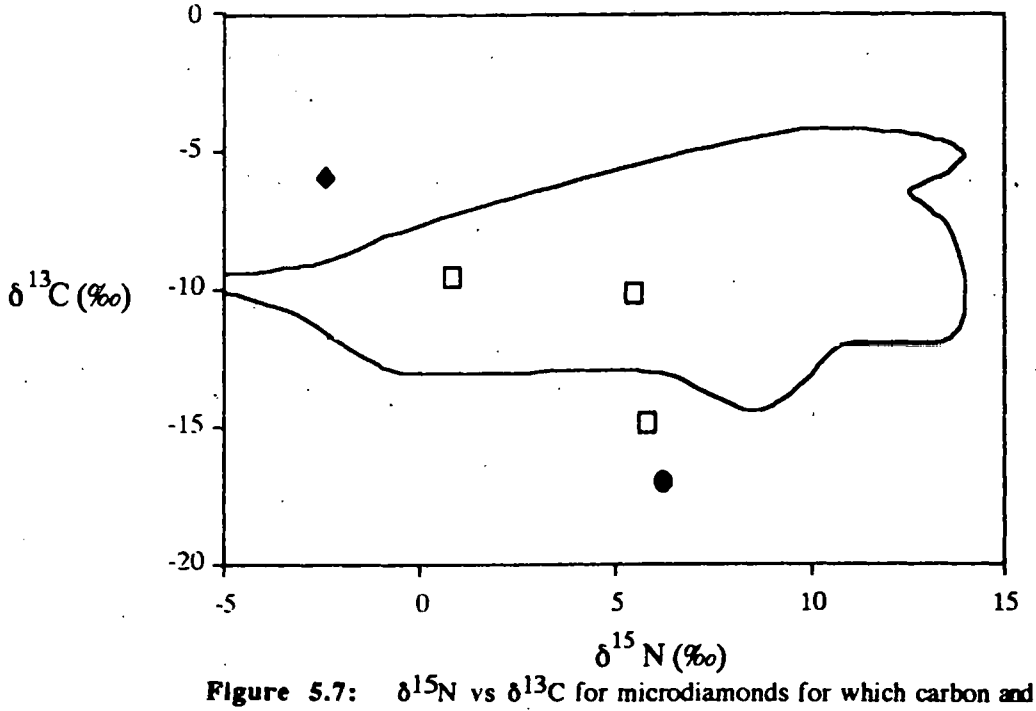

Figure 5.7: $\delta^{15}N$ vs $\delta^{13}C$ for microdiamonds for which carbon and nitrogen isotopic composition are known. Argyle R.O.M samples shown by open squares. Ellendale 4 sample #9 is shown by a filled diamond and the cubic microdiamond from the Northern Territory is shown by a filled circle. The outline field is that for all the Argyle diamonds described in Chapter 2.

5.2.3.2 Ellendale 4 microdiamonds

Type II diamonds dominate the Ellendale 4 microdiamond population, with 6 of the 11 samples containing no spectroscopically detectable nitrogen. The remaining 3 samples, for which diamond type is identifiable are type IaA, and two of these contain platelets,

suggesting at least some formation of B-aggregates, although this is not readily detectable on the spectra. This differs from the macrodiamond population, in which no type II samples were found, and for which only 4 of the 30 samples were type IaA (with some platelet formation). The remaining macrodiamonds are all spectral type IaAB, and all contain platelets.

The largest Ellendale 4 microdiamond, sample #9 (mass 537.4μg), a platelet-bearing type IaA contains 22 ppm nitrogen and this has an isotopic composition of $\delta^{15}N$ = -2.4‰ ($\delta^{13}C$ = -5.7‰). This is within the range of $\delta^{15}N$ (and $\delta^{13}C$) values measured for the 2 mm diamonds from Ellendale 4, and also within the range, but towards the lower limit, of macrodiamond nitrogen abundance measurements. This sample is plotted on the $\delta^{13}C$ *vs.* $\delta^{15}N$ plot shown on Figure 5.7.

5.2.3.3 Northern Queensland microdiamond

A provisional identification of green, cubic North Queensland microdiamond #3 as a type Ib sample has been made (Milledge, Pers. Comm. 1990) on the basis of the FTIR spectra shown in Figure 5.8. Mass spectrometric analysis of nitrogen was not successful for this sample, which has a $\delta^{13}C$ value of -20.7‰. Type Ib diamonds are very rare amongst naturally occurring microdiamonds and are indicative of low temperatures and/or very short periods of mantle storage. This has important implications for the genesis of this microdiamond, which will be discussed in section 5.4.1.3.

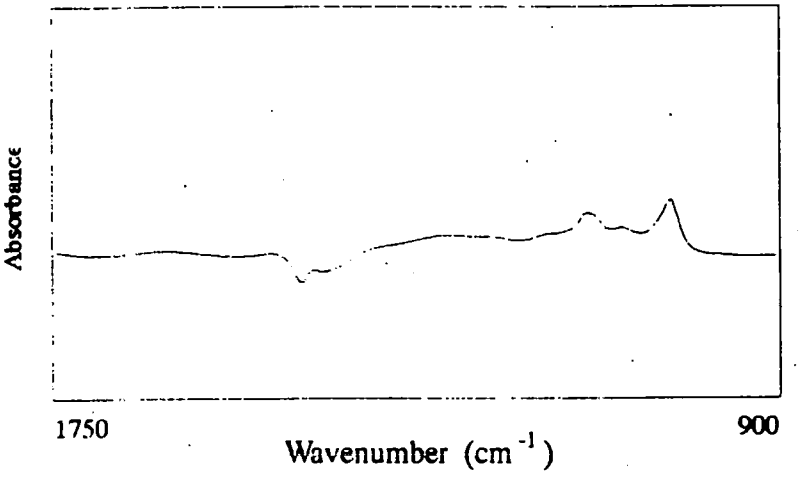

Figure 5.8: Fourier transform infrared spectrum of North Queensland microdiamond #4. This has been interpreted (Milledge, Pers. Comm. 1990) as an example of a type Ib absorbance spectrum. Such samples are usually considered to be thermally immature.

5.2.3.4 Northern Territory cubic microdiamond

A single nitrogen measurement was obtained from one of the larger cubic Northern Territory cubic samples (N.T. 1-16). Diamond type was not ascertainable for this

sample, which has a mass of 24.1 μg, and on combustion yielded 2.8 ng of nitrogen. The isotopic composition and concentrations determined for this nitrogen have been "blank corrected" for a 0.7 ng blank measured at the start of the days run (Table 5.4), however as this blank contributes 25% of the measured nitrogen, these results should be treated as tentative.

If the system blank is assumed to have a $\delta^{15}N$ value between +5‰ and -5‰, in accordance with the isotopic composition measured at times of high system blank, then this sample is characterised by a $\delta^{15}N$ value of between +6.6‰ and +9.9‰. Sample N.T. 1-16 is also shown on Figure 5.7, where it is plotted at the minimum $\delta^{15}N$ value (6.6‰), which assumes a blank $\delta^{15}N$ value of +5‰. The $\delta^{13}C$ value of this microdiamond is -17.1‰.

		Yield (ng)	[N] ppm	$\delta^{15}N$ ‰	± ‰
N.T. 1-16, as measured	(75%)	2.8	116	6.2	1.2
Blank as measured	(25%)	0.7			
Blank corrected:	Assumed blank $\delta^{15}N$ = -5‰		87	9.9	1.2
	Assumed blank $\delta^{15}N$ = 0‰		87	8.2	1.2
	Assumed blank $\delta^{15}N$ = +5		87	6.6	1.2

Table 5.4: Nitrogen content and isotopic composition of N.T. cube # 1-16, corrected for a 0.7 ng blank of various assumed isotopic compositions. The isotopic composition of this blank could not be determined due to insufficient gas, however isotopic compositions measured at times of higher system blank are usually of the order of $\delta^{15}N$ = +5‰.

The only macrodiamond available from the Northern Territory for comparison with this cubic Northern Territory microdiamond is the type IaA specimen CAL 039 which was reported by Boyd (1988). CAL 039 contains abundant silicate micro-inclusions and it has a $\delta^{15}N$ value of -8.7‰, a nitrogen content of 330 ppm and a $\delta^{13}C$ value of -4.1‰. This sample is therefore quite unlike the Northern Territory cubic microdiamond NT 1-16.

5.4 DISCUSSION

5.4.1 On the origin of these microdiamonds

5.4.1.1 Argyle

A number of distinct populations are evident amongst the Argyle diamond suite. Some of these, like the peridotite nodule microdiamonds and the dyke-derived microdiamonds are morphologically similar to peridotitic macrodiamonds, while others like the R.O.M. microdiamonds are more akin to the bulk of the macrodiamond population. Similar comparisons may also be made for carbon isotopic composition, nitrogen aggregation

state when diamond type could be ascertained, nitrogen content and isotopic composition, and when used together, these data can provide clues as to the origin of the microdiamonds.

The magmatic dyke microdiamonds are unquestionably of magmatic origin, but whether they are phenocrystal or xenocrystal remains to be determined. Evidence for a xenocrystal origin can however be found in the morphology of these crystals. Sharp edged octahedra are associated with slow diamond growth (Sunagawa, 1990) and octahedra and octahedra-related forms (*e.g.* dodecahedra) are commonly interpreted as being of xenocrystal origin, unlike fibrous cubes which are often interpreted as being phenocrystal (*e.g.* Gurney, 1989). Furthermore, the carbon isotope composition of these dyke microdiamonds is also consistent with growth in an environment in which isotopic fractionation was restricted. The $\delta^{13}C$ values of the dyke microdiamonds are similar to those expected from "normal" mantle, and they are also similar to those for the peridotitic paragenesis macrodiamonds from Argyle.

If these microdiamonds are indeed xenocrysts in the magmatic dyke, the lack of resorption is unusual, but it is not unheard of at Argyle. Peridotite paragenesis macrodiamonds also have sharp-edged octahedral morphology and this has been interpreted as being a consequence of the armouring of diamond within a peridotite nodule (Jaques *et al.*, 1990), and a similar hypothesis has been advanced to explain the octahedral morphology of microdiamonds from Sloan (McCandless, 1989). Thus it is considered likely that these dyke microdiamonds are of a similar origin to the peridotitic paragenesis macrodiamonds from the Argyle lamproite. It is expected that they were liberated from a late disaggregating peridotite nodule during lamproite emplacement, which resulted in their well preserved crystal morphology.

When considered together, the +425 and +600 R.O.M. microdiamonds have carbon and nitrogen isotopic composition, nitrogen aggregation state and nitrogen contents similar to the Argyle macrodiamond population. They are also all broken and irregular fragments, many of which show evidence for resorption and occasionally, curvilinear crystal faces. In addition, Deakin and Boxer (1989) report a constant 3 parameter lognormal size distribution for Argyle diamonds extending down to below the size limits of these R.O.M. microdiamonds. On the basis therefore of the similar morphologies, carbon and nitrogen stable isotopic compositions, nitrogen aggregation state and nitrogen content as well as the apparently constant size distribution, it is considered likely that these R.O.M. microdiamonds are intimately related to the bulk of the macrodiamond population. They are thought to simply represent the smaller-sized lamproitic diamonds. If this is indeed correct, then these microdiamonds extend the range of $\delta^{13}C$ values of diamonds from the Argyle main population to a minimum $\delta^{13}C$ value of -14.9‰; a ^{13}C depletion of 0.8‰

relative to the diamond with the next lowest $\delta^{13}C$ value (Plate 150701 #12-8, piece H which has $\delta^{13}C$ = -14.1‰).

Microdiamonds from the three peridotite nodules define a group that is morphologically and isotopically distinct from the bulk of the Argyle macrodiamond population. Furthermore, these peridotitic paragenesis (by definition, assuming that these diamonds are primary features of the host peridotite, as described by Jaques *et al.*, 1990) microdiamonds and the peridotite paragenesis macrodiamonds do not have any overlap in $\delta^{13}C$ value. Rather, the microdiamonds are ^{13}C enriched relative to all peridotitic paragenesis macrodiamonds from Argyle (See Figure 5.2), and a statistical t - test (t statistic = -9.7; degrees of freedom = 26) shows that the mean $\delta^{13}C$ values of nodule microdiamonds and peridotitic paragenesis microdiamonds are significantly different at a 99.9% confidence level. It is therefore suggested that the nodule microdiamonds represent a discrete diamond population, different to the 2 mm peridotitic paragenesis diamonds.

The nodule microdiamonds are also unusual in that they have a mode in $\delta^{13}C$ values that is more positive than that of most other mantle-derived material (See Figure 1.4). The implications of such ^{13}C enrichment, which is most similar to that for CO_2 occurring in wehrlite xenoliths from alkali basalts (Pineau and Mathez, 1990), are discussed in Chapter 6.

As the nodule microdiamonds form an apparently distinct population, it becomes evident that there are at least two different populations in the $\delta^{13}C$ values of the Argyle diamonds. The first group contains the nodule microdiamonds and the second group comprising the macrodiamonds, regardless of paragenesis and the run of mine microdiamonds. The microdiamonds from the Argyle magmatic dyke are enigmatic. Their $\delta^{13}C$ values are intermediate between the two populations and they may belong to either group, or may even form a third group. Additional $\delta^{13}C$ data from dyke microdiamonds are required in order to resolve this problem. Nitrogen data may also be useful in confirming the existence of two diamond populations at Argyle.

5.4.1.2 Ellendale

At both Ellendale 4 and Ellendale 9, the microdiamonds have carbon isotopic composition corresponding to the major mode in $\delta^{13}C$ value of the macrodiamond population. In addition, at Ellendale 9, the microdiamonds have a $\delta^{13}C$ range encompassing that of peridotitic paragenesis macrodiamonds. This similarity in carbon isotopic composition may be evidence for a similar origin of the macro and microdiamond populations at these two lamproites, however the morphological differences between the two size fractions needs to be addressed. One possibility is that these microdiamonds have been derived

from peridotite xenoliths that disaggregated relatively late, relative to the bulk of the macrodiamond population. They have thus been armoured against the caustic effects of metasomatising fluids or lamproite, and the primary diamond morphology has therefore been preserved. A second possibility is that these microdiamonds represent a second diamond growth event, from a source with a carbon and nitrogen isotopic composition that has not changed significantly throughout time. This second growth phase would have to have taken place after the events that modified the morphology of the bulk of the macrodiamond population and may, perhaps, be related to lamproite emplacement.

Evidence in support of the second hypothesis comes from nitrogen aggregation state. Type IaAB diamonds dominate the Ellendale 4 macrodiamonds (see Chapter 2). Ellendale 4 microdiamonds, for which diamond type could be determined however appear to be either type II or type IaA. The existence of these less aggregated type IaA microdiamonds implies either a cooler storage environment which is unlikely given that macrodiamonds and microdiamonds have been sampled by the same lamproite. The alternative is that the less aggregated microdiamonds have experienced a shorter period of mantle storage. This second possibility is more likely, but this conclusion must however be regarded as preliminary. Nitrogen aggregation state determinations for the macrodiamonds have large associated uncertainties (See Chapter 2 and Appendix 2) and the identification of diamond type for these microdiamonds is tentative. Further detailed spectroscopic investigation of the relationships between Ellendale macro- and microdiamonds are required before either hypothesis can be expressly favoured.

The morphology of these crystals argues against a phenocrystal relationship between the microdiamonds and the host lamproite. Their octahedral morphology is consistent with slow diamond growth during periods of low supersaturation of carbon (Sunagawa *et al.*, 1984). These conditions are expected to prevail in the mantle, rather than in a magma where rapid precipitation of diamond usually results in fibrous crystal growth (*e.g.* Boyd *et al.*, 1992; Moore and Lang, 1972; Walmsley and Lang, 1992b).

It is therefore suggested that the Ellendale microdiamonds and macrodiamonds are related to one another in that they are derived from similar source regions, albeit at different times, and that this source region has undergone little change in carbon and nitrogen stable isotopic composition.

5.4.1.3 Northern Queensland

Only morphological evidence suggests that the Northern Queensland microdiamonds are of magmatic rather than of possible crustal origin. Samples from this source are commonly resorbed, and most appear to have been derived from octahedral primary growth forms (D.C. Lee, Pers. Comm. 1993) consistent with a magmatic rather than

metamorphic origin. Furthermore, sample N.Q. 4, a rounded reddish coloured fragment with a $\delta^{13}C$ value of -19.5‰ contained a red, possibly garnet, inclusion. Whether the microdiamonds are of phenocrystal or xenocrystal origin cannot however be debated without further data. It is evident however, from their significantly different mean $\delta^{13}C$ values, that the macrodiamond and microdiamond populations need not be related.

The Northern Queensland samples are also unusual in that a single sample, the green cube N.Q. 3 is a type Ib diamond. Type Ib diamonds are considered to be thermally immature and are very rare in natural diamonds. The type Ib to type IaA transition has a low activation energy (See Chapter 1 and Table 1.4) and this results in most diamonds that are of magmatic origin usually showing evidence of at least sufficient nitrogen aggregation to form IaA centres. The coat on coated stones, often interpreted as being related to kimberlite emplacement (*e.g.* Boyd *et al.*, 1987, 1992) for example, is always type IaA diamond. The presence of a type Ib microdiamond therefore implies either cool conditions (sub magmatic) or very rapid diatreme emplacement, with insufficient time for the formation of A-aggregates. The first of these is considered to be more likely. Very rapid, or explosive diatreme emplacement should be evident either in the presence of lonsdaleite rather than diamond (Erskine and Nellis, 1991) or the diamonds being poorly formed polycrystalline aggregates of submicron size crystallites (Sunagawa, 1990) rather than cubic or irregular crystals.

Microdiamonds of "metamorphic" origin have been reported from the Kokchetav massif, Kazakhstan (Sobolev and Shatsky, 1990) and from Dabi Shan, China (Shutong *et al.*, 1992). Most of these samples are octahedra or cubo octahedral forms and many of the Kokchetav samples show evidence for fibrous growth. The Kokchetav microdiamonds are also characterised by ^{13}C depletion, with $\delta^{13}C \leq$ -8.7‰. The cubic morphology, type Ib FTIR spectrum and marked ^{13}C depletion of N.Q. 3 suggest that this green, cubic microdiamond from Northern Queensland may possibly be similar to the crustal microdiamonds described by Sobolev and Shatsky, (1990) and by Shutong *et al.*, (1992). This possibility should be investigated further.

5.4.1.4 Northern Territory

The Northern Territory diamonds are unusual in that, like the Northern Queensland diamonds, they are ^{13}C depleted, and in this case, have $\delta^{13}C$ values down to -27.5‰. Furthermore, cubic diamonds, and particularly cubic diamonds with fibrous growth dominate, indicative of rapid diamond growth. This dominance of fibrous cubes is quite unlike any other known microdiamond occurrence (Lee *et al.*, 1991).

Two distinct types of cubic diamond have been described previously. The first of these, termed C_a by Boyd (1988) is characterised by $\delta^{13}C$ values of near -5‰, has high

nitrogen contents (*ca.* 1000 ppm) and is ubiquitously type IaA diamond. It is also marked by fibrous growth habit and by the presence of abundant fluid and mineral micro-inclusions. Type Ca cubic diamond forms the coat on coated diamonds, and is thought to be associated with the presence of probably asthenospheric, volatile-rich fluids within the diamond source region (Boyd *et al.*, 1992). The second type of cubic diamond, termed C_b by Boyd (Pers. Comm., 1990) is characterised by a type Ib spectral signature (hence C_b), also has a fibrous growth habit and is characterised by low nitrogen abundances and $\delta^{13}C$ values of -10‰ or less. Type C_b diamonds have been reported by Galimov (1984b), and the diamonds of crustal origin occurring in the Kokchetav massif (Sobolev and Shatsky, 1990) and Dabi Shan, China (Shutong *et al.*, 1992) are thought to be type C_b. It has been suggested that this type of diamond may be the result of the subduction and subsequent exhuming of crustal carbon (Sobolev and Shatsky, 1990; Shutong *et al.*, 1992). The lack of significant nitrogen aggregation in the C_b diamonds (their "thermal immaturity") reflects this mode of origin. Note however that recent spectral analysis of some of the diamonds recovered directly from the Kokchetav massif garnets have shown these to be type IaA diamonds whereas diamonds recovered from an associated placer are both type IaA and type Ib (Verchovsky *et al.*, 1992).

There are similarities between the Northern Territory cubes and type C_b cubic diamonds. Both types are marked by $\delta^{13}C$ values considerably more negative than those characteristic of "normal mantle", and a large proportion of the Northern Territory cubic microdiamonds are type II (13/26) and hence contain (if any) very small amounts of nitrogen. However, a significant number of the Northern Territory cubic microdiamonds (8/26) contain aggregated nitrogen. Seven of these are type IaB and one is a type IaAB diamond, and these samples are indistinguishable on the basis of $\delta^{13}C$ values from the type II microdiamonds. Thus, if a similar crustal origin for the Northern Territory cubic microdiamonds and the Kokchetav microdiamonds is postulated, then more intense metamorphism occurred in western Australia than occurred in the Kokchetav massif, and elevated temperatures facilitated nitrogen aggregation. Metamorphic temperatures in excess of 1100°C have been reported from the western Alps (Becker and Altherr, 1992), suggesting that this is possible. The peak metamorphic temperatures in the Kokchetav massif and in the Dabi Shan are between 900° and 1000°C (Sobolev and Shatsky, 1990; Shutong *et al.*, 1992).

There is however, some evidence which argues against a "metamorphic" origin for these Northern Territory cubic microdiamonds. Lee *et al.*, (1991) report that one of the samples contains abundant micro-inclusions of a highly potassic, alumino-silicate melt phase (Table 5.5), and these have Mg# (atomic Mg/(Mg+Fe)x100) ranging from 30.9 to 43.1 which is similar to the primary, mantle-derived melt inclusions reported by Navon *et al.*, (1988) from diamond coat (C_a diamond). Furthermore, the trace element patterns

measured on the Northern Territory cubic microdiamonds are similar to those from Argyle microdiamonds (Lee *et al.*, 1991), and inclusions within these microdiamonds have compositions similar to eclogitic paragenesis diamonds.

On balance of evidence it seems likely that the Northern Territory microdiamonds are of magmatic origin, and it is suggested that the distinctly negative $\delta^{13}C$ values found in these diamonds are similar to those found in eclogitic paragenesis diamonds from other sources (*e.g.* Kirkley *et al.*, 1991). Further data are however needed to confirm the origin of these cubic microdiamonds, and good quality FTIR spectra are an absolute pre-requisite.

	Inc 1	Inc 2	Inc 3	Inc 4	Inc 5	Inc 6	Inc 7	Diamond coat
SiO_2	54.66	52.41	53.99	54.13	53.28	55.23	51.54	30.3 to 67.7
TiO_2	0	0	0	0	0	0	0	2.0 to 4.2
Al_2O_3	23.46	23.77	23.49	22.74	23.96	22.73	23.49	2.9 to 6.1
FeO	4.32	5.61	5.27	4.92	4.32	6.08	5.46	3.3 to 15.7
MgO	4.22	3.24	3.03	3.93	3.90	3.96	3.71	1.3 to 8.0
CaO	0	0	0	0	0	0	0	1.6 to 18.7
Na_2O	3.89	5.64	1.32	3.01	4.72	0.98	4.96	1.0 to 4.8
K_2O	9.44	9.33	12.60	10.65	9.82	11.02	10.46	11.6 to 29.7
Mg#	43.1	31.0	30.9	38.3	41.2	33.6	34.5	22.0 to 40.0

Table 5.5: Frozen melt inclusions in Northern Territory microdiamonds, reproduced from Lee *et al.*, (1991). The range in compositions for diamond coat is from Navon *et al.*, (1988). These two phases are not identical. That from the Northern Territory micro-inclusions is more aluminous, and contains less TiO_2 (less than detection limits) than the micro-inclusions from diamond coat. This may reflect the addition of some crustal component in the source of the Northern Territory micro-inclusions. Mg# = atomic Mg/(Mg + Fe) x 100.

Notwithstanding their origin , these Northern Territory microdiamonds show at least two distinct sub-populations on the basis of carbon isotopic composition. When cubic and irregular samples are considered together, the first group has a range of $\delta^{13}C$ values from -27.5‰ to -10.1‰ and this encompasses all the cubic and 10 of the irregular microdiamonds. The second group comprises 8 irregular microdiamonds and has a $\delta^{13}C$ range from -5.6‰ to -2.5‰. This second group has $\delta^{13}C$ values close to, and marginally ^{13}C enriched relative to, the range accepted as being characteristic for normal mantle-derived samples. But, without further data, and particularly inclusion and spectral data nothing more can be said about the origin of these diamonds.

5.4.2 Testing the definition for microdiamonds

In the past, the absence of a formal definition has led some confusion as to what exactly constitutes a microdiamond, so at the beginning of this Chapter, microdiamonds were strictly defined on size and shape criteria. By these criteria, the Argyle R.O.M samples would not be classified as microdiamonds whereas the remaining samples described here would be microdiamonds. This definition of microdiamonds can now be seen to be valid. The Argyle R.O.M samples for example, despite being less than a millimeter across are, from isotope evidence, clearly part of the main Argyle diamond population. On the other hand, the sharp-edged crystal forms of the microdiamonds from Argyle peridotite nodules, the Northern Territories and perhaps Ellendale, are distinct from the larger, often resorbed, commercial diamonds. The well preserved crystal morphology is also a characteristic of the microdiamonds from Sloan described by McCandless (1989) and the "metamorphic" microdiamonds described by Sobolev and Shatsky (1990) and by Shutong *et al.*, (1992). It is suggested that this preservation of the primary growth form of the microdiamond be acknowledged in a strict definition.

5.4.3 On the validity of microdiamonds as grade indicators

Microdiamonds may be valuable indicators of the macrodiamond grade in kimberlites or lamproites provided that the macrodiamond and microdiamond populations are related. This relationship has been shown for the Argyle run of mine "microdiamonds" and, as expected, a good correlation is found between diamond grade predicted from microdiamonds and the recovered diamond grade (Deakin and Boxer 1989). The coincidence of predicted and actual diamond grades are shown in Table 5.6

This is not always the case for true microdiamonds however. Although the microdiamond population of a specific lamproite pipe may hold valuable information as to the macrodiamond grade, unless microdiamonds can be shown to be intimately related to, and representative of, the macrodiamond population, the use of microdiamonds for grade estimation should be approached with extreme caution. In the case of the Ellendale 4 and Ellendale 9, the macrodiamond population has a similar $\delta^{13}C$ distribution to the microdiamond population, and there are gross similarities in the micro– and macrodiamond crystal morphologies. It is therefore possible that there will be a correlation between microdiamond abundance and the overall grade of the lamproite. The situation in the case of the Northern Queensland and Northern Territory microdiamonds is more difficult to assess. Without additional analyses of the carbon stable isotopic composition of the Northern Queensland microdiamonds, a relationship between these and the Northern Queensland macrodiamonds cannot be confirmed, and care should be exercised in projecting the diamond grades of potential primary sources.

Care should also be exercised in estimating possible diamond grades for the primary source of the Northern Territory microdiamonds. This primary source is clearly unusual in that fibrous cubes dominate and the $\delta^{13}C$ values are very negative. This primary source may not even be a lamproite or kimberlite!

	Estimated grade ($ct.t^{-1}$)	Recovered grade ($ct.t^{-1}$)
A:	11.59	10.50
B:	5.89	6.27
C:	4.01	4.67

Table 5.6: Comparison of estimated diamond grade and recovered diamond grade from large diameter cores of the Argyle lamproite. Data from Deakin and Boxer (1989).

Clearly, considerable effort has to be applied to a full characterisation of the entire diamond population at any given locality before microdiamonds can be used as reliable grade indicators. In this study, magmatic microdiamonds from the host lamproite at Ellendale 4, Ellendale 9 and Argyle may provide reasonable estimates of the macrodiamond grade, but this is not necessarily a general conclusion for all magmatic microdiamonds.

6 Nitrogen in the mantle

6.1 AN ESTIMATE OF MANTLE $\delta^{15}N$ VALUE

6.1.1 Compilation of diamond $\delta^{15}N$ data

There is, as yet, no consensus what $\delta^{15}N$ value is characteristic of primary mantle material, unlike the $\delta^{13}C$ value of -5‰ to -7‰ assumed for the carbon isotopic composition of primary mantle material. Various estimates of the mantle $\delta^{15}N$ value, made from the analysis of diamond, have however been published, and these range from marginally positive values (*e.g.* Wand *et al.*, 1980; $\delta^{15}N$ = 0.15‰ and Becker, 1982; $\delta^{15}N$ = 0‰ to +5‰) to considerably more negative values of $\delta^{15}N$ = -16‰ to -40‰ (Javoy *et al.*, 1984, 1986) or $\delta^{15}N$ = -5‰ (Boyd *et al.*, 1987, 1992). The most negative $\delta^{15}N$ value that has been suggested as possibly representative of primary mantle nitrogen is $\delta^{15}N \approx$ -40‰ (Javoy *et al.*, 1986), and this estimate is based largely on the analysis of diamonds from Mbuji Mayi, Zaire. In this section, a compilation of all available diamond $\delta^{15}N$ data is presented in an attempt to reconcile this wide range of $\delta^{15}N$ estimates and to examine whether there are additional parameters that may further constrain mantle nitrogen. In particular, from the evidence of diamond $\delta^{13}C$ values which show a relationship to diamond paragenesis (*e.g.* Kirkley *et al.*, 1991), paragenesis may be equally important in understanding the behaviour of nitrogen in diamonds.

There are now 514 analyses of the $\delta^{15}N$ value of diamonds of known provenance and these come from 16 different localities worldwide. They are summarised in Tables 6.1 and 6.2, and histograms of these data are shown in Figure 6.1 and 6.2. Where available, diamond paragenesis as determined from inclusion studies, is given. Only a mean $\delta^{15}N$ value of the thirteen diamonds analysed by Wand *et al.*, (1980) was presented and for this reason, this is not included in the calculations reported in Table 6.2 and nor is it included in Figures 6.1 and 6.2. The 21 small Zaire stones and the 26 western Australian analyses reported by Boyd (1988) are of uncertain provenance and for this reason, they are not included in Figure 6.2 or in Table 6.1. They are included in the composite $\delta^{15}N$ histogram (Figure 6.1) and in the calculation of diamond $\delta^{15}N$ statistics (Table 6.2). In both of these cases the number of analyses, n, = 561 and this represents 280 different diamonds. With the exception of the 14 diamonds analysed by Javoy *et al.*, (1984) and the 13 small stones of Wand *et al.*, (1980), all the diamonds listed in Table 6.1 were analysed in the same mass spectrometer described by Boyd *et al.*, (1988), Wright *et al.*, (1988) and in Appendix 2.

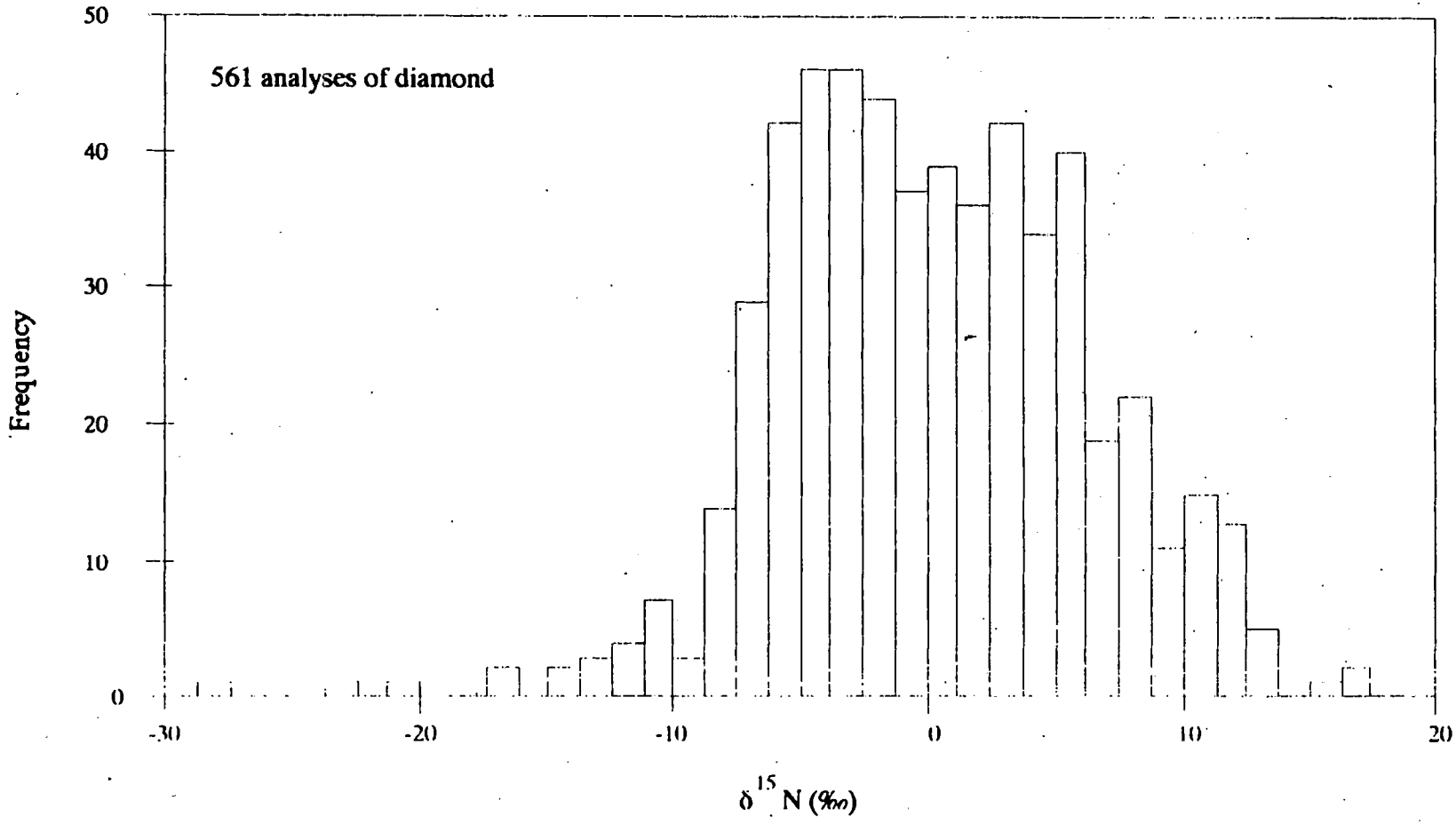

Figure 6.1: Histograms of δ^{15} N values in diamonds Data sources as per Table 5.1, including samples of uncertain origin. Data of Wand *et al* (1980) omitted.

Locality	Mean	Median	Max.	Min.	Range	n	Modes at	Ref.
Angola	-1.8	-1.6	2.7	-6.2	7.9	14	-1	4
Argyle	5.8	5.5	13.6	-4.6	18.2	101	4, 12	6
eclogitic	5.2	4.5	13.6	-4.6	18.2	42	4, 12	6
peridotitic	6.0	5.5	10.6	0.1	10.5	15	4, 8	6
Arkansas	6.0	5.4	16.6	-2.1	18.7	10	5, 17	4
China	-3.8	-3.5	6.1	-20.7	26.8	19	-12, -5, 5	6
Ellendale 4	2.3	-1.02	3.7	-10.4	14.1	20	-8, 1	6
Ellendale 9	0.1	-0.9	13.2	-9.3	22.5	66	-2	6
eclogitic	1.4	0.0	8.6	-3.3	11.9	5	0	6
peridotitic	-3.1	-3.6	3.7	-9.3	13.0	4	-3?	6
Finsch	-2.7	-2.8	5.9	-10.8	16.7	31	-4, -1, 5	4,5,7
Jagersfontein	1.1	2.9	5.6	-6.0	11.6	9	-2, 4	4
Jwaneng	0.4	-4.2	12.0	-6.5	18.5	14	-6, +12	4
Mbuji Mayi	-1.7	-3.3	13.4	-11.2	24.6	130	-6, 0, 4	2,3,4
Morelli's Fox	2.9	3.5	16.1	-14.2	30.3	19	1?, 10?	6
Namibia	1.5	----------notgiven----------				13	?	1
North Queensland	-6.2	-4.7	9.7	-28.4	38.1	22	?	6
Premier	-6.4	-5.9	-1.0	-12.3	11.3	8	-11, -6, -1	4
Sierra Leone	0.3	-1.1	7.7	-5.2	12.9	29	-5, 0, 5	4
Udachnaya	-0.8	-0.4	1.7	-4.1	5.8	17	0	4
Williamson	-0.8	0.5	3.3	-7.7	11.0	5	1?	4

Table 6.1: Compilation of diamond $\delta^{15}N$ values from a variety of sources. All values are in ‰, except "n", the number of analyses. Data from 1 = Wand *et al.*, (1980), 2 = Javoy *et al.*, (1984), 3 = Boyd *et al.*, (1987), 4 = Boyd, (1988), 5 = Milledge *et al.*, (1989), 6 = this thesis and 7 = van Heerden (Unpublished data - see Appendix 1). Of the 527 analyses listed, 247 are described in Chapters 2 and 3. Samples from unknown sources, for example those of Becker *et al.*, (1982) and the commercially sourced stones of Boyd (1988) from western Australia and Zaire are not included in this list. Note that the Namibian data of Wand *et al.*, (1980) is not included in the calculations reported in Table 6.2 or in Figures 6.1 and 6.2

Mean	+0.2	Std. error on mean	0.3
Median	-0.1	Number of analyses	561
Maximum	16.6	Minimum	-28.4
Range	45.0		
Variance	37.4	Standard deviation	6.1
Skewness	-0.2	Kurtosis	0.8
Coefficient of variation	3065		

Table 6.2: Statistics of the $\delta^{15}N$ values of diamonds. All values in ‰ except the number of analyses. Data of Wand *et al.*, (1980) omitted, otherwise data sources as per Table 6.1.

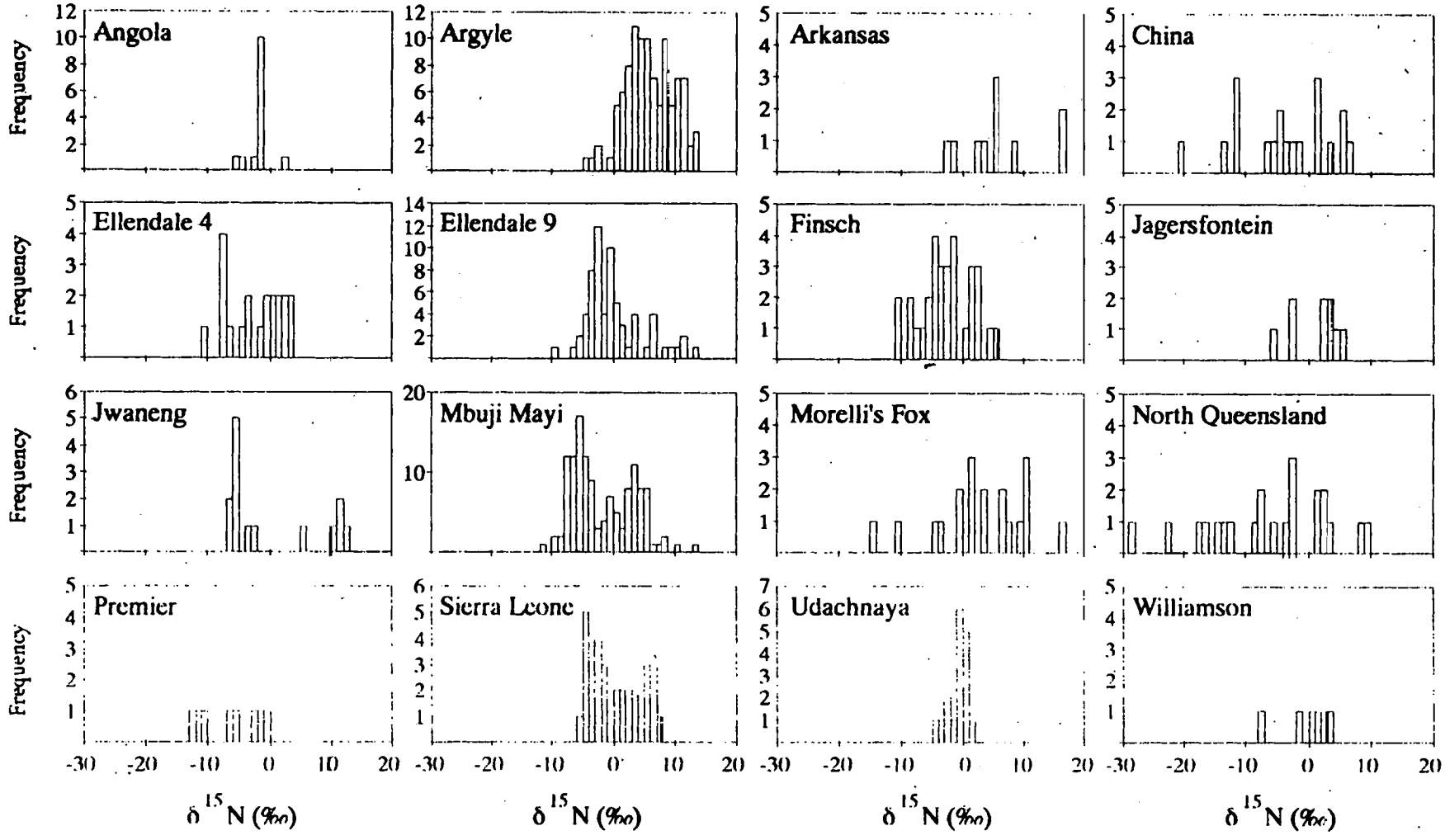

Figure 6.2: Histograms of δ^{15}N values in diamonds from individual pipes. Data sources as per Table 5.1.

The combined $\delta^{15}N$ histogram (Figure 6.1) has a near Gaussian distribution with a mean $\delta^{15}N$ value (0.2‰) that corresponds very closely to that of nitrogen in the Earth's atmosphere (0.0‰). The three most negative $\delta^{15}N$ analyses (out of 561) are more than 3 standard deviations from the mean, and two of these come from Northern Queensland and the third is a Chinese diamond. The three most positive $\delta^{15}N$ values fall between $\delta^{15}N$ = +16‰ and +17‰ and two of these are from Arkansas (Boyd, 1988) and the third is a Morelli's Fox diamond. The "bulge" on the positive $\delta^{15}N$ side of the histogram is a result of both the abundance of diamonds with positive $\delta^{15}N$ values in the Argyle suite (95 analyses with $\delta^{15}N > 0$‰) and the occurrence of a mode in the Mbuji Mayi $\delta^{15}N$ distribution at positive $\delta^{15}N$ values (49 analyses of $\delta^{15}N > 0$‰; Figure 6.2).

Given that the major mode in the diamond $\delta^{13}C$ distribution (Figure 6.3) is near -5‰; the value characteristic of most peridotitic paragenesis diamonds and thought to be characteristic of primary mantle material, it is suggested that the corresponding $\delta^{15}N$ value of sub-continental, lithospheric, upper mantle material is ≈0‰. There is however, considerable variation in measured diamond $\delta^{15}N$ values and it is more illustrative to state that the $\delta^{15}N$ value characteristic of this mantle material lies in the range $-6‰ \leq \delta^{15}N \leq +6‰$. This is not in agreement with the estimates of Javoy *et al.*, (1984, 1986) who suggest that a more negative $\delta^{15}N$ value is characteristic of the mantle, and reasons for this discrepancy are discussed in the following section. This estimate of mantle $\delta^{15}N$ value is close to the estimates of Boyd *et al.*, (1987, 1992) and Boyd (1988).

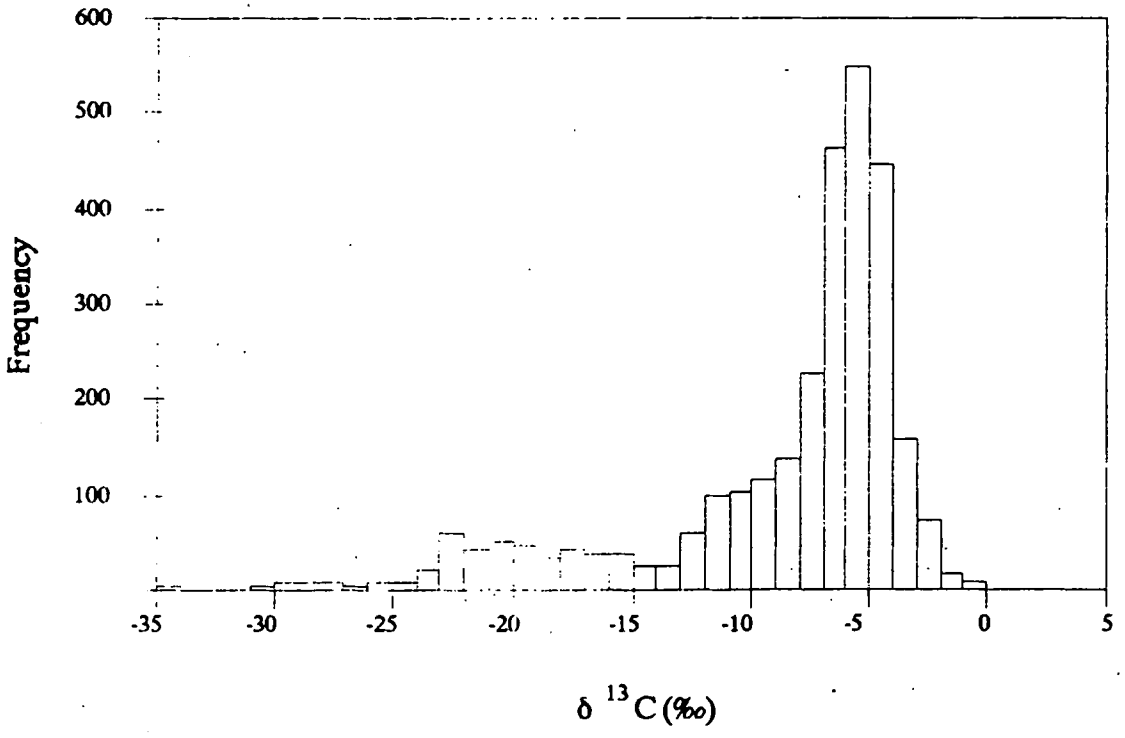

Figure 6.3: A histogram showing the distribution of $\delta^{13}C$ values from diamond. A total of 2946 analyses are shown. Data sources are listed in the caption to Table 1.3 and additional data are from Galimov (1991) and this thesis.

From Figure 6.2, it is evident that although there are gross similarities in the distribution of $\delta^{15}N$ values from diamonds from different localities, for example Ellendale 9 and Finsch or Mbuji Mayi and Sierra Leone, there is no general $\delta^{15}N$ distribution that is characteristic of all diamond sources. Diamonds from each kimberlite, lamproite or alluvial deposit appear, from the available data, to have a characteristic set of $\delta^{15}N$ values that is representative of that diamond source region. There is however considerable overlap in the $\delta^{15}N$ values for different pipes. Without speculating on the cause of the differences between pipes, this "preferred $\delta^{15}N$ value" may place some constraints on the lateral scale of mantle nitrogen heterogeneity. For example, the significant difference, at a 99% confidence level, in the mean $\delta^{15}N$ value of the Ellendale 4 ($\delta^{15}N$ = -2.3‰, σ = 4.4) and the Ellendale 9 diamonds (mean $\delta^{15}N$ = 0.1‰, σ = 4.7) indicates that heterogeneities in the mantle exist on a scale at least as small as the horizontal separation of these two lamproites, which is 15 km. Possible causes of this heterogeneity are discussed in section 6.2.

It is also apparent from Figure 6.2 that the alluvial diamonds from China, Northern Queensland and Morelli's Fox exhibit a wider range of $\delta^{15}N$ values than those occurring at the 13 unequivocally magmatic diamond sources. The widest range in $\delta^{15}N$ values measured from any individual magmatic source is 19.2‰ at Ellendale 9† (from $\delta^{15}N$ = -9.3‰ to +9.9‰) whereas the $\delta^{15}N$ ranges measured on diamonds from China, Northern Queensland and Morelli's Fox are 26.8‰, 30.3‰ and 38.1‰ respectively. One possible cause of this extended $\delta^{15}N$ range is that these alluvial diamond occurrences represent the contribution of several magmatic sources to form composite deposits. This possibility may be resolved once the primary magmatic sources of these alluvial diamonds are traced.

6.1.2 Diamond paragenesis and stable isotope ratios

A relationship between diamond paragenesis and $\delta^{13}C$ value was first reported by Sobolev *et al.*, (1979) and this has been subsequently reported from a majority of primary diamond sources (See Kirkley *et al.*, 1991 for a review). A compilation of available data (1592 analyses of the $\delta^{13}C$ value of diamonds of known paragenesis) is shown in Figure 6.4 and it can be seen that both eclogitic and peridotitic paragenesis diamonds have the major peak in their $\delta^{13}C$ distribution at the "normal mantle" $\delta^{13}C$ value near -5‰, but eclogitic paragenesis diamonds are further characterised by two

† The $\delta^{15}N$ range at Mbuji Mayi is wider, but a number of pipes contribute to the deposit.

additional modes; one centered on $\delta^{13}C \approx -12‰$ and one near $\delta^{13}C = -20‰$. Few peridotitic paragenesis diamonds have $\delta^{13}C$ values that are this negative.

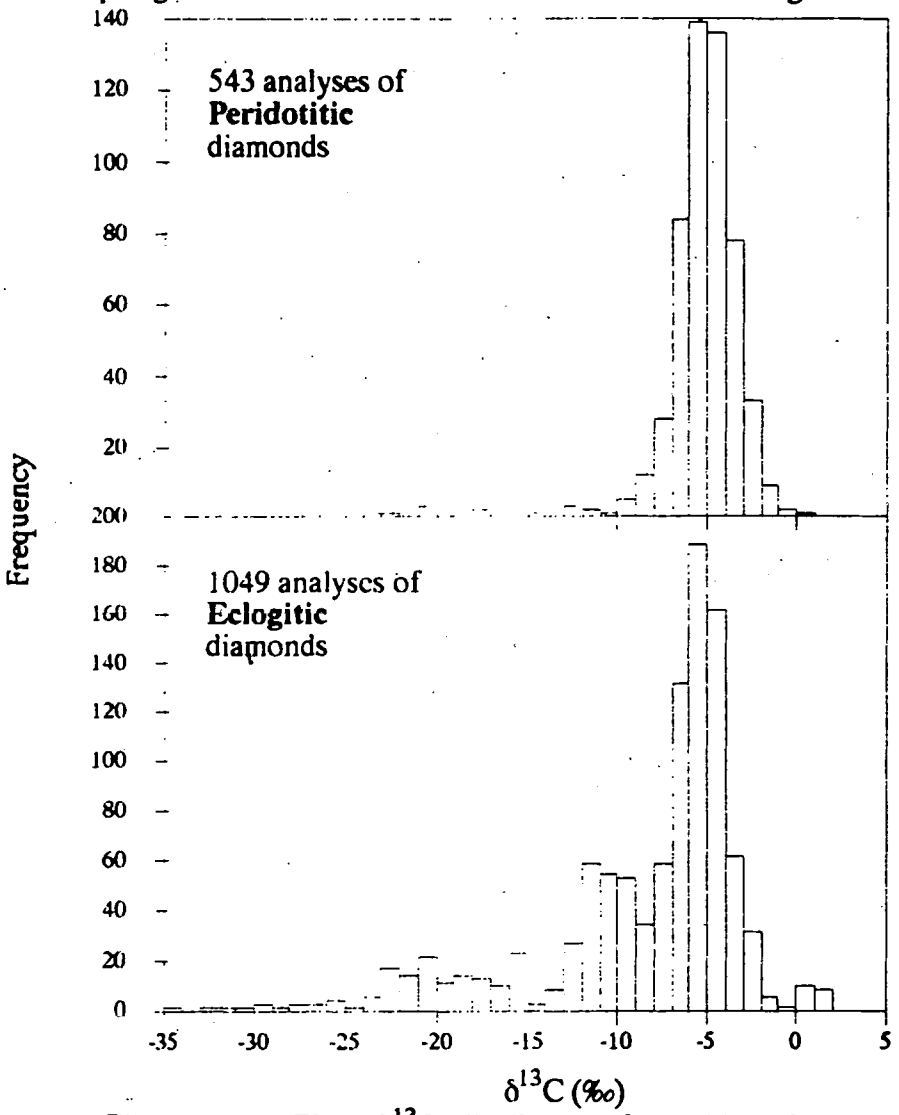

Figure 6.4: The $\delta^{13}C$ distribution of eclogitic and peridotitic paragenesis diamonds. Data sources as for Table 6.4. A total of 1592 analyses are shown.

In addition to having $\delta^{13}C$ distributions that are significantly different from those of peridotitic diamonds, eclogitic diamonds also differ in terms of equilibration temperatures and age. They formed at temperatures up to 200°C hotter than peridotitic paragenesis diamonds (Gurney 1989), and they are Proterozoic rather than Archaean in age (Richardson *et al.*, 1990). Eclogitic inclusions also have more variable sulphur and lead stable isotope ratios (Eldridge *et al.*, 1991) and $\delta^{18}O$ values (Deines *et al.*, 1991b) than inclusions from peridotitic paragenesis diamonds. Unsupported, radiogenic Sr may also be a characteristic of some eclogitic paragenesis diamonds (Smith *et al.*, 1991).

The first-order separation of diamonds into only the eclogitic and peridotitic parageneses is however not sufficiently detailed. Peridotitic diamond should be sub-divided into the lherzolitic and harzburgitic parageneses on the basis of inclusion mineral composition

(Table 6.3). The $\delta^{13}C$ distributions for lherzolitic and harzburgitic diamonds from the Finsch, Jagersfontein, Koffiefontein, Orapa, Premier and Roberts Victor kimberlites, Southern Africa; the only sources from which both $\delta^{13}C$ and mineral data of sufficient quality are readily available from peridotitic samples, are shown in Figure 6.5, and their $\delta^{13}C$ distributions are described in Table 6.4, along with the $\delta^{13}C$ distribution of eclogitic paragenesis diamonds. A statistical test (t-test, t = 3.289 for 182 degrees of freedom) shows that in Southern African examples there are significant differences in the mean $\delta^{13}C$ values of lherzolitic and harzburgitic paragenesis diamonds at a 99.8% confidence level.

Eclogitic	Lherzolitic	Harzburgitic	Websteritic
Garnets			
Orange colour <0.2% Cr_2O_3	Deep red >0.2% Cr_2O_3 Lie to the right of the "85%" line of Gurney (1984) on a CaO *vs.* Cr_2O_3 plot.	Purple >0.2% Cr_2O_3 Lie to the left of the 85% line	Orange Elevated TiO_2 (up to 1%)
Olivines			
Not present	90 to 92.5% Forsterite	Fo > 92.5%	Fo < 90%
Clinopyroxene			
Omphacite elevated K_2O	Cr-diopside	Not present	Coexists with olivine and garnet
Chromite			
Absent	Absent	Present	Absent

Table 6.3: Criteria used to classify diamond paragenesis. Note that these criteria only apply to diamond inclusions and are subject to exceptions. These are the criteria currently in use at the University of Cape Town.

	Range (‰)	Mean and std. error on mean (‰)		Median (‰), population std deviation (‰) and n		
Eclogitic diamonds	-34.5 to +1.5	-8.6	0.2	-6.5	5.8	1049
Peridotitic diamonds	-23.5 to +0.1	-5.4	0.1	-5.2	2.6	543
lherzolitic diamonds	-12.7 to -1.9	-4.8	0.4	-4.5	2.2	27
harzburgitic diamonds	-9.6 to -2.0	-5.8	0.1	-5.8	1.2	157

Table 6.4: Statistics of the $\delta^{13}C$ distribution of eclogitic and peridotitic diamonds illustrated in Figures 6.4 and 6.5. The difference between the mean $\delta^{13}C$ values of the two paragenetic groups is significant, at better than a 99.9% confidence level. The differences between lherzolitic and harzburgitic diamonds are also statistically significant at a 99.8% confidence level.

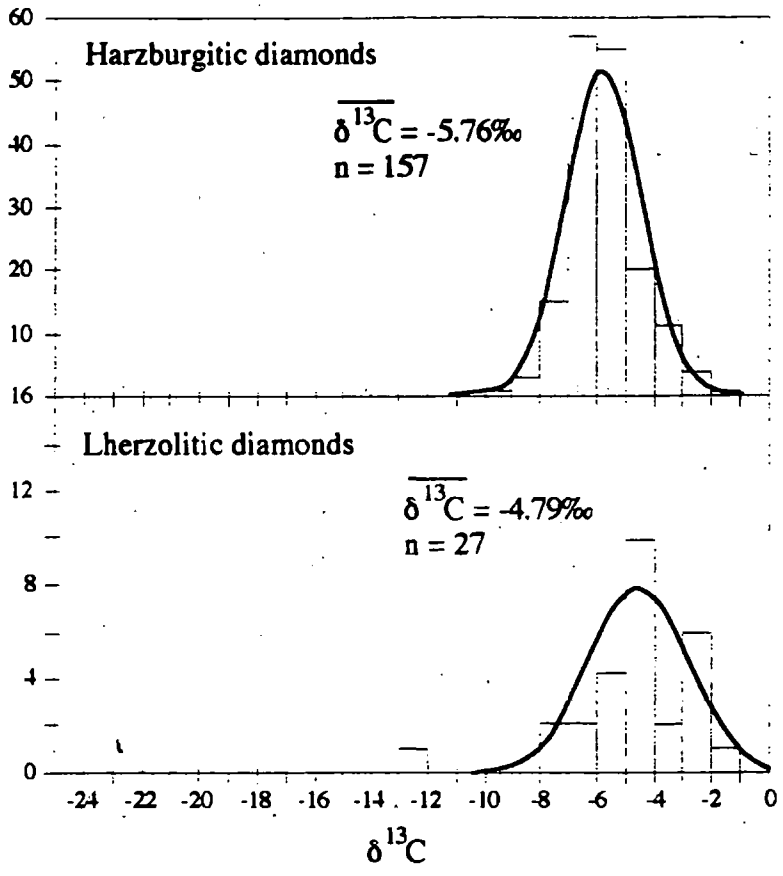

Figure 6.5: The $\delta^{13}C$ distributions of lherzolitic and harzburgitic diamonds from Southern Africa. Data from Deines *et al.*, (1984, 1987, 1989, 1991).

Given the above differences in the $\delta^{13}C$ values of eclogitic and peridotitic paragenesis diamonds, it is worth examining $\delta^{15}N$ values for differences between the two parageneses. There are 66 $\delta^{15}N$ analyses available for 38 diamonds of known paragenesis, from two localities. There are 21 eclogitic and 9 peridotitic diamonds from Argyle, and 5 eclogitic and 3 peridotitic diamonds from Ellendale 9. From the diamond inclusion analyses presented by Jaques *et al.*, (1986b) and Griffin *et al.*, (1988); the presence of diamonds within a lherzolite nodule (Chapter 4), and the complete absence of harzburgite nodules in the Argyle xenolith suite (Jaques *et al.*, 1986b), the Argyle peridotitic paragenesis diamonds may be further classified as belonging to the lherzolitic paragenesis. For similar mineral-chemical reasons, it is probable that the Ellendale 9 peridotitic paragenesis inclusions are also lherzolitic, although mantle-derived xenoliths from the West Kimberley province comprise dunites, harzburgites and spinel– and clinopyroxene-poor lherzolites (Jaques *et al.*, 1986b). These 47 $\delta^{15}N$ analyses from eclogitic diamonds and 19 $\delta^{15}N$ analyses from peridotitic diamonds are illustrated in Figure 6.6.

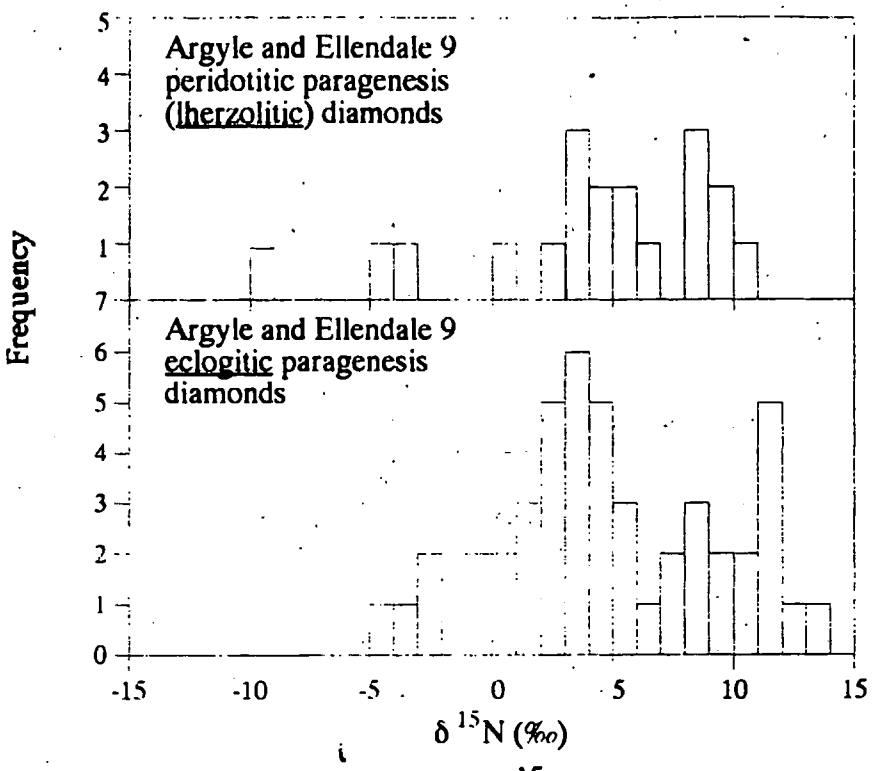

Figure 6.6: Histogram showing the $\delta^{15}N$ distribution of eclogitic and lherzolitic paragenesis diamonds.

The descriptive statistics of these two $\delta^{15}N$ distributions are listed in Table 6.5. The eclogitic and lherzolitic paragenesis diamonds have similar mean $\delta^{15}N$ values that are not significantly different at a better than a 99% confidence level (t statistic = 0.65, Degrees of freedom (d.o.f) = 64).

	Range (‰)	Mean and std. error on mean (‰)		Median (‰), population std deviation (‰) and n		
Eclogitic diamonds	-4.6 to +13.6	4.9	0.7	4.2	4.6	47
Lherzolitic diamonds	-9.3 to 10.6	4.1	1.2	4.9	5.2	19

Table 6.5: Statistics of the $\delta^{15}N$ distribution of eclogitic and lherzolitic diamonds illustrated in Figure 6.6. The mean $\delta^{15}N$ values of the two paragenetic groups are not significantly different, at better than a 99.9% confidence level.

From the available data, it can be seen that there are no significant differences in the $\delta^{15}N$ values of eclogitic paragenesis and these lherzolitic paragenesis diamonds from Western Australia. Whether this is a general conclusion for all peridotitic diamonds must now be tested. In order to do this, published eclogitic:peridotitic ratios need to be considered, as no further $\delta^{15}N$ data are available from diamonds from which inclusions have been extracted and examined.

Gurney *et al.*, (1991) report that 98% of the diamonds extracted from the Finsch mine are of peridotitic paragenesis and that these are particularly enriched in harzburgitic diamonds. Boyd (1988) report 21 $\delta^{15}N$ measurements from 12 Finsch diamonds and a

further 10 analyses from a central cross diamond from Finsch are listed in Appendix 1 (van Heerden, Unpublished data). The $\delta^{15}N$ values of these 13 diamonds from Finsch range from -10.8‰ to +5.9‰, and the mean $\delta^{15}N$ value is -2.7‰ with a standard deviation σ = 4.2‰ (See also Figure 6.2). This population differs significantly, at a 99.9% confidence level, from both the eclogitic paragenesis (t-statistic = 7.4, d.o.f = 76) and lherzolitic paragenesis (t-statistic = 5.0, d.o.f = 48) Western Australian diamonds.

This difference suggests that there may be a paragenetic control on the $\delta^{15}N$ value of these diamonds. If this is the case, and these Finsch diamonds with their mostly negative $\delta^{15}N$ values are characteristic of harzburgitic diamonds in general, then the nitrogen stable isotope characteristics of harzburgitic, lherzolitic and eclogitic paragenesis diamonds may be summarised as follows (Figure 6.7.):

Eclogitic paragenesis	Variable $\delta^{15}N$ values between -5‰ and +14‰ in Western Australian samples, with the mode at positive $\delta^{15}N$ values, and with a positive mean $\delta^{15}N$ value.
Lherzolitic paragenesis	Variable $\delta^{15}N$ values, between -10‰ and +11‰, in Western Australian samples. The mode and mean of the Western Australian samples occur at positive $\delta^{15}N$ values.
Harzburgitic paragenesis	Variable $\delta^{15}N$ values between -11‰ and +6‰, with a negative mean $\delta^{15}N$ value.

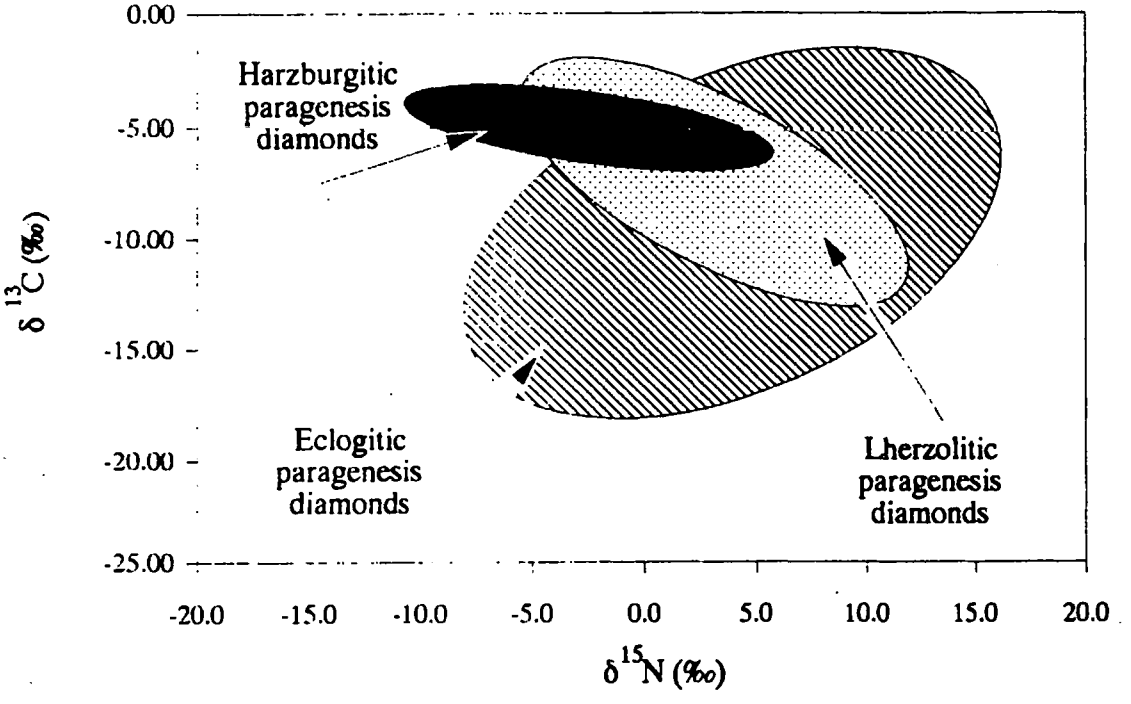

Figure 6.7: Graphical summary of the suggested differences in carbon and nitrogen stable isotope ratios of diamond, as a function of paragenesis. The calculated bivariate ellipses each contains 95% of the available analytical data and were calculated using the Systat Inc. program Systat© 5.

It must be emphasised that the $\delta^{13}C$ - $\delta^{15}N$ relationship is provisional and further stable isotope data are required from diamonds of confirmed paragenesis, from localities other than Western Australia and Finsch, in order to quantify any paragenetic control on diamond $\delta^{15}N$ values.

A paragenetic control on the $\delta^{15}N$ value of diamonds is one possible reason for the very negative estimates of mantle $\delta^{15}N$ value made by Javoy *et al.*, (1984, 1986). These estimates were based predominantly on the analysis of Mbuji Mayi diamonds, augmented in the later publication by the inclusion of a few analyses of komatiites and volcanic gases and an analysis of the $\delta^{15}N$ value of Kasai kimberlite. Of the material analysed, only diamond had $\delta^{15}N$ values less than -6.4‰. From these data, Javoy *et al.*, (1986) postulated a degassing model for mantle nitrogen and suggested that the minimum $\delta^{15}N$ value for primary mantle material may be as low as $\delta^{15}N$ = -40‰. However, the eclogitic:lherzolitic:harzburgitic ratio is not known for diamonds from Mbuji Mayi, and there are no data available to suggest that the Mbuji Mayi diamonds are characteristic of all diamond sources. Indeed, this is highly unlikely given the common occurrence of coated diamonds, which are rare elsewhere (Gurney Pers. Comm.), at Mbuji Mayi! Furthermore, the histograms of $\delta^{15}N$ values from different locations shown in Figure 6.2 illustrate the inadvisability of generalising bulk mantle parameters from a single diamond source. For these reasons, the estimate of mantle $\delta^{15}N$ value based on a compilation of diamond analyses from a number of sources worldwide presented earlier, rather than an estimate from a single locality is preferred.

The diamond coat analysed by Boyd *et al.*, (1987, 1992) and Boyd (1988) from a wide variety of sources has been shown to be have uniform isotopic and nitrogen aggregation state characteristics. It is thus another useful indicator of mantle stable isotope ratios. Diamond coat has a negative mean $\delta^{15}N$ value of -3.8‰ (52 analyses from Boyd *et al.*, 1987) and the mean $\delta^{13}C$ value is -6.8‰ (70 analyses from Boyd *et al.*, 1987) and both of these values are close to values accepted here as being representative of primary mantle material. The paragenetic associations of diamond coat have not been definitively shown, although it occludes numerous solid and fluid inclusions (See Section 1.3.3.1 and 1.3.3.2), some of which (biotite, coesite, sanidine) are thought to be associated with the eclogitic rather than peridotitic paragenesis (*e.g.* Navon, 1991). There is also an overlap of the diamond coat field on a $\delta^{15}N$ - $\delta^{13}C$ plot with that of eclogitic paragenesis diamonds (Figure 6.8). There is also however, a close correspondence between the carbon and nitrogen stable isotope ratios of Finsch harzburgitic diamonds and diamond coat (Figure 6.8). Clearly, the paragenetic associations of diamond coat need further investigation.

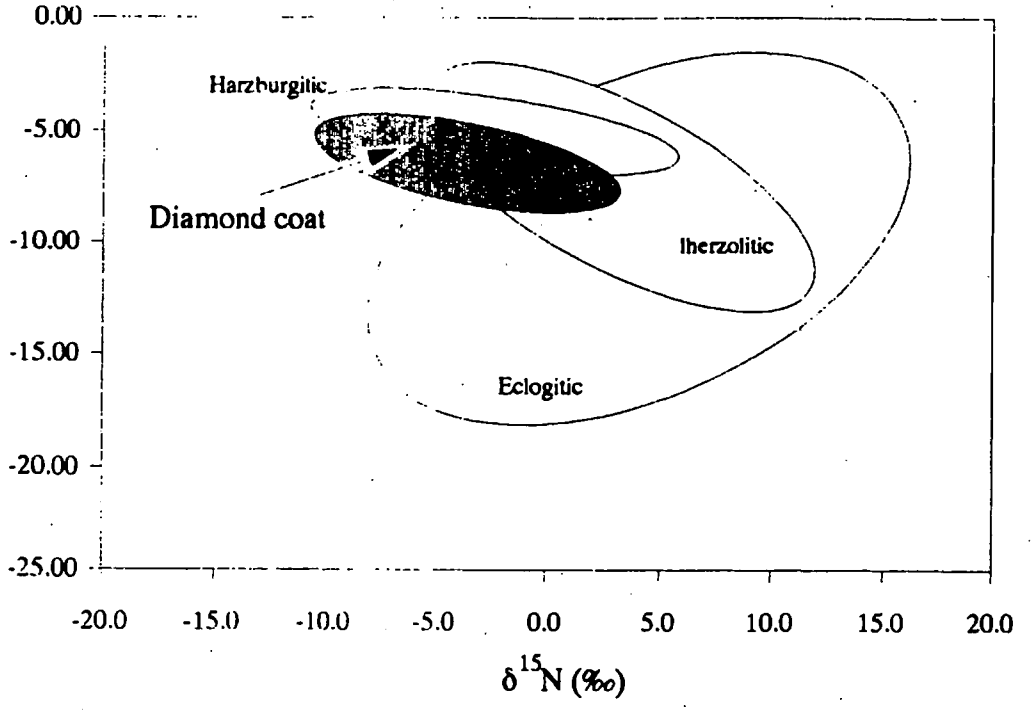

Figure 6.8: A $\delta^{15}N$ - $\delta^{13}C$ plot showing the bivariate ellipse containing 95% of the diamond coat data presented in Boyd *et al.*, (1987). Also shown are the corresponding ellipses for Western Australian eclogitic and lherzolitic paragenesis, and Finsch (harzburgitic) diamonds from Figure 6.7. Diamond coat overlaps both peridotitic paragenesis and eclogitic paragenesis diamonds.

The origin of diamond coat is associated with the presence of volatile-rich mantle fluids (See section 1.3.3.2) and may be related to kimberlite magmatism (Boyd *et al.*, 1992). It is thus highly likely that the stable isotope ratios in diamond coat are fractionated to some extent. Nevertheless, diamond coat has a mean $\delta^{15}N$ value within the $-6‰ \leq \delta^{15}N \leq +6‰$ range, and near to the 0.2‰ mean $\delta^{15}N$ suggested in this chapter as being representative of the mantle in general.

6.1.3 Implications of this estimate of mantle $\delta^{15}N$ value

Earlier estimate of the $\delta^{15}N$ value characteristic of the mantle (*e.g.* Javoy *et al.*, 1986, Boyd 1988) suggested that it was negative - between -5‰ and -40‰ but if this is indeed the case, an isotopic and geometric imbalance is generated by the formation of the atmosphere (Javoy and Pineau, 1986). It is usually accepted that the Earth's atmosphere arose, largely, by accumulation of the volatiles degassed from the Upper mantle, and the crust would thus be expected to have a $\delta^{15}N$ value intermediate to those of the crust and upper mantle. This is not the case for a negative $\delta^{15}N$ mantle however. The atmosphere, by definition has a $\delta^{15}N$ value of 0‰ and the crust is characterised by ^{15}N enriched nitrogen and has a positive $\delta^{15}N$ value (See Section 6.2.3.2 and Table 1.9). The ^{15}N enriched crust is therefore sandwiched between two relatively ^{15}N depleted reservoirs. In addition, degassing is expected to be accompanied by a kinetic isotope

fractionation (*e.g.* Hoefs, 1987) with the preferential migration of the lighter ^{14}N isotope into the atmosphere, resulting in an atmosphere that is ^{15}N depleted relative to the source mantle.

There are a number of possible models for rationalising this apparent anomaly. For example, Javoy *et al.*, (1986) suggest that the Earth's atmosphere formed from volatile fluxes significantly different from those pertaining now, whereas Boyd (1988) prefers a case in which an extra-terrestrial component is added to the early atmosphere. Alternatively, early atmosphere loss, either a the result of meteorite impacts or the hydrodynamic escape of nitrogen as a result of comic ray bombardment (McElroy *et al.*, 1976) may have significantly fractionated the nitrogen stable isotope ratios. All of these models are complex and require multiple stages and none of them are necessary if the mantle is accepted as being heterogeneous and having a mean $\delta^{15}N$ value of $0 \pm 6‰$, for in this case the anomaly does not arise. During Rayleigh processes (See Appendix 3, Figure A3.1), the average δ value of separated and accumulated distillate approaches that of the source material as degassing continues, and the atmosphere therefore simply represents the well mixed accumulation of all the degassed products of the upper mantle. The range of $\delta^{15}N$ values measured on diamonds worldwide (Figure 3.1) records the various $\delta^{15}N$ values in the upper mantle during it's geological evolution from at least the Archaean (harzburgitic diamonds) to at least the Proterozoic (eclogitic diamonds). The formation of the atmosphere is however not likely to be the only process that affects the $\delta^{15}N$ value of the upper mantle, and further causes of variations in the nitrogen stable isotope ratio of the upper mantle are discussed in Section 6.2.

6.1.4 Summary

The $\delta^{13}C$ value of primary mantle material is commonly accepted as being $\approx$ -5‰ to -7‰ and it is suggested from the composite diamond $\delta^{15}N$ histogram that the corresponding mean $\delta^{15}N$ value is $\approx 0‰ \pm 6‰$. There is however considerable variation in mantle $\delta^{15}N$ value, and the scale on which the heterogeneity exists is 15 km or less. Some of this variability is thought be a function of diamond paragenesis. More than 95% of diamonds that have very negative $\delta^{13}C$ values ($\leq$ -10‰) are of eclogitic paragenesis. In addition, the majority of Western Australian diamonds in this study are of eclogitic paragenesis and most have positive $\delta^{15}N$ values. The limited data available indicate that lherzolitic paragenesis diamonds may also be characterised by positive $\delta^{15}N$ values and they do have $\delta^{13}C$ values that are significantly different to harzburgitic paragenesis diamonds.

Diamond coat has carbon and nitrogen stable isotope ratios that fall within the preferred mantle range. The fact that the coat $\delta^{15}N$ value is negative may be a result of an isotope

fraction mechanism during coat precipitation or may be the result of some other process. One possibility is that coat, if phenocrystal (*e.g.* Kamiya and Lang, 1965) and by implication considerably younger than the core diamond, records changes in mantle carbon and nitrogen stable isotope ratios through time.

6.2 CAUSES OF STABLE ISOTOPE VARIATION

Several models have been proposed in order to explain the range of carbon stable isotope ratios occurring in mantle-derived material, and these models can now be evaluated using nitrogen stable isotope data as an additional constraint. The three models are:

(1) The primordial heterogeneity model, in which the full range of carbon isotopes measured on mantle-derived material have existed in the mantle since the accretion of the Earth and its initial segregation.
(2) The isotope fractionation model in which a homogeneous mantle gives rise to the range of measured $\delta^{13}C$ values as the result of open and closed system isotope fractionation processes.
(3) The subduction model, in which carbon is recycled from the crust back into the mantle *via* subduction zones. Some of this recycled material may be significantly ^{13}C depleted as a result of the involvement of organic processes.

Each of these models is now considered individually, and the behaviour of nitrogen examined.

6.2.1 Primordial heterogeneity

The basis of this model is that diamonds record stable isotope heterogeneities that have existed since the accretion of the Earth 4.6 Ga ago. The model arose from firstly, the conclusion of Deines (1980a) that, in all probability, diamond $\delta^{13}C$ values were inherited from their source mantle, and secondly, from the close agreement between the $\delta^{13}C$ values obtained from diamonds and from the more common meteorite groups (Javoy *et al.*, 1986), as well as from the similarities between Mbuji Mayi diamond and chondritic $\delta^{15}N$ values (Javoy *et al.*, 1986). Diamond $\delta^{15}N$ and $\delta^{13}C$ ranges are compared to those from the common meteorite classes in Figure 6.9.

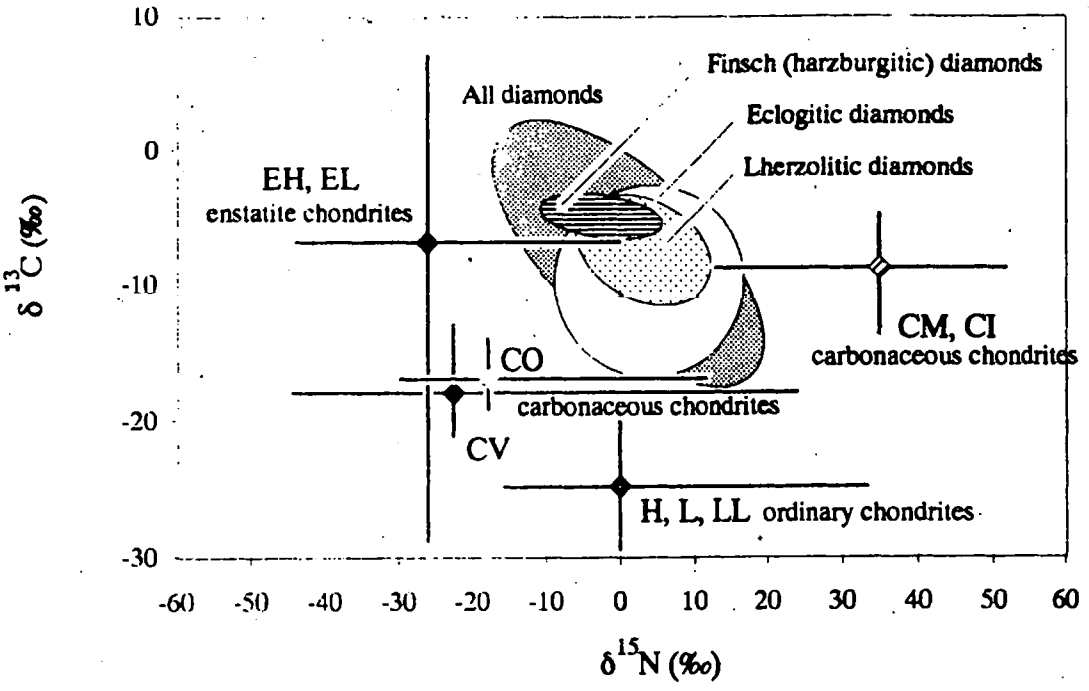

Figure 6.9: Isotopic composition of diamonds plotted in relation to the common stony meteorite classes. Bivariate ellipses for known paragenesis samples contain 95% of data. The bivariate ellipse for all diamonds is a 99% ellipse. Meteorite ranges from Kung and Clayton (1978), Kerridge (1985) and Grady *et al.*, (1986).

Although there is much overlap of diamond and meteorite $\delta^{13}C$ values, it is evident that this is not the case for diamond $\delta^{15}N$ values and those of the common stony meteorites. However, the $\delta^{15}N$ values of eclogitic paragenesis diamonds do overlap (just) with those of CM and CI carbonaceous chondrites whereas peridotitic paragenesis diamonds (both lherzolitic and harzburgitic) overlap with the enstatite chondrites. Clearly, the most simple model of the Earth's mantle - that in which it is approximated in composition by carbonaceous CI chondrites cannot be appropriate in the case of diamond bearing-mantle. However, a mixture of enstatite and carbonaceous chondrites can explain the $\delta^{13}C$ and $\delta^{15}N$ values that have been obtained from diamonds. Such a mix, in the proportions 58% enstatite chondrite to 42% carbonaceous chondrite will have a mean $\delta^{15}N$ value of ≈ 0‰, consistent with that found in diamonds. The mean $\delta^{13}C$ value of such a mix is ≈ -8‰ which is marginally lower than that expected for primordial mantle, but still very close to the mantle range. Javoy *et al.*, (1986) also suggested a mantle comprising a mixture of enstatite and carbonaceous chondrite. In their model, enstatite chondrite comprises ≈98% of the mantle, however this proportion was calculated from the assumption of a very negative mantle $\delta^{15}N$ value (maximum -16‰, possibly as low as -40‰).

Kung and Clayton (1978), Kerridge (1985) and Grady *et al.*, (1986) have all reported on the heterogeneity of the carbon and nitrogen stable isotopes and nitrogen contents in enstatite and/or carbonaceous chondrites. In all cases, these are heterogeneous (see for

example Figure 6.9) and a mixture of two heterogeneous components is one reasonable explanation for the range of carbon and nitrogen isotope values found in diamonds.

Boyd (1988) argues against mantle heterogeneity being relict from the primary accretion of meteoritic material on the following grounds: The uniformity of the carbon and nitrogen stable isotope ratios in the coat of coated diamonds (Boyd *et al.*, 1987) and the similarity between coat and variety 1 diamonds† from around the world indicates the existence of a fairly uniform asthenospheric reservoir that has changed little since the mid-Archaean. This in turn suggests that the homogenization process following Earth accretion went almost to completion. In order to survive this homogenization process, any primordial heterogeneity would have had to be frozen into the lithosphere at an early stage, and diamonds associated with the heterogeneous material (^{13}C depleted diamonds) would be associated with old (>3.3 Ga) sub-continental lithosphere. However, primary sources rich in ^{13}C depleted diamonds tend to be concentrated along craton margins (*e.g.* Arkansas, Jagersfontein, Orapa, Mbuji Mayi, Sierra Leone) or even off craton (Argyle). They are thus associated with younger rather than older lithosphere, which is confirmed by the radiogenic ages of Argyle diamonds of 1.5 Ga (Richardson, 1986). Boyd (1988) thus suggests that the survival of primordial carbon heterogeneity in the mantle is not supported, and primordial nitrogen heterogeneity is equally unlikely to have survived.

It has subsequently been shown that harzburgitic paragenesis diamonds, which are Archaean in age (Richardson *et al.*, 1984) are associated with the root zones of the stable Archaean cratonic areas (these are occasionally referred to as Archons; Boyd *et al.*, 1993), whereas eclogitic paragenesis and lherzolitic paragenesis diamonds are associated with both younger Archaean and Proterozoic lithosphere (Richardson *et al.*, 1993). Using the Boyd (1988) argument presented above, any primordial mantle heterogeneity should be associated with the older diamonds yet harzburgitic paragenesis samples are less variable in terms of carbon and nitrogen stable isotope ratios, than either eclogitic or lherzolitic paragenesis samples. This is not consistent with the survival of mantle heterogeneity from the time of Earth accretion and alternative explanations for the range of stable isotope compositions found in diamonds therefore need to be considered.

6.2.2 Fractionation of stable isotope ratios

The fractionation of stable isotope ratios is a probable cause of at least some of the variability evident in the $\delta^{13}C$ and $\delta^{15}N$ values of Western Australian and other

---

† Diamonds with "normal mantle" $\delta^{13}C$ values and negative $\delta^{15}N$ values, as are common for example, at Finsch. The are thought by Boyd (1988) to represent primary mantle.

diamonds. Such fractionations may occur either during diamond growth (fractional crystallization) or they may occur subsequent to diamond growth, possibly as a function of nitrogen aggregation.

The effects of fractional crystallization and mixing processes were quantitatively modelled in Chapter 3. They were examined as possible mechanisms for explaining the inter-sample and intra-sample variation of the $\delta^{13}C$ and $\delta^{15}N$ values of diamonds from Argyle and Ellendale, and it was shown that simple, closed system fractional crystallization could account for the variation of $\delta^{15}N$ and $\delta^{13}C$ values within some samples. The results of the modelling also showed that a heterogeneous source material is required, in order for the observed $\delta^{13}C$ and $\delta^{15}N$ variation to be consistent with an origin by fractional crystallization. Modelled initial $\delta^{13}C$ values range from -5‰ to -10‰ and modelled initial $\delta^{15}N$ values range from +5‰ to +10‰. Such heterogeneity must occur on a local scale as different diamonds from the same pipe, in this case Argyle, exhibit this 5‰ variation in modelled initial δ values.

Although fractional crystallization can explain a large proportion of the carbon and nitrogen stable isotope variability within diamonds from the same source region, it cannot alone explain the approximately 40‰ range in the observed $\delta^{15}N$ and $\delta^{13}C$ values when all diamonds are considered, assuming believable fractionation factors and degrees of crystallization. It is however likely that some isotopic fractionation will occur, both during diamond precipitation and on the production of the diamond precursor phase, but the magnitude of these fractionations are expected to be limited. The efficiency of Rayleigh isotope fractionation mechanisms is illustrated by restricted range in intra-diamond $\delta^{13}C$ and $\delta^{15}N$ values. In diamonds that do not show evidence for multi-stage growth, *i.e.* not coated stones, the maximum reported range in $\delta^{13}C$ values is 7.1‰† (Harte and Otter, 1992) for a single diamond from Bultfontein (See Table 1.3), and the maximum reported range in $\delta^{15}N$ values is 12.9‰ for the Ellendale 9 diamond plate E9037, described in Chapter 2. Using the fractionation factors determined in Chapter 3, the range in carbon and nitrogen δ values must represent more than 96%, and possibly as much as 99.9% crystallization. It is therefore suggested that these maximum reported $\delta^{13}C$ and $\delta^{15}N$ ranges probably approach the limit of stable isotope ratio variations that can be caused by simple Rayleigh processes alone.

---

† A piece of type II diamond heatsink, of unknown provenance has been analysed by this author and this has a $\delta^{13}C$ range of 11.3‰, from $\delta^{13}C$ = -5.1‰ at one edge to $\delta^{13}C$ = -16.4‰ at the other edge. This sample is not visibly zoned, but the change in carbon isotope ratios is as abrupt as it is in coated stones, and this may be a result of multiple growth events. The $\delta^{13}C$ values of this diamond are presented in Appendix 1 Table A1.32.

Thus, although isotope fractionation processes may alter the stable isotope ratios of carbon and nitrogen in diamonds, possibly by as much as 10‰ or 12‰ in extreme cases, fractional crystallization alone does not explain either the full range of $\delta^{15}N$ (≈45‰) or $\delta^{13}C$ (≈37‰) values measured from diamonds. However, the range in modelled initial $\delta^{13}C$ and $\delta^{15}N$ values (Chapter 3) is strong evidence for a heterogeneous diamond source region.

The second possible stable isotope fractionation process that is likely to be important is the within diamond diffusion of nitrogen leading to nitrogen aggregation. The nitrogen aggregation state within simply zoned Western Australian diamonds correlates with the $\delta^{15}N$ value (See Table 2.13) and this suggests that there may be a causal relationship between nitrogen aggregation and the nitrogen stable isotope ratio, although the poor quality of the aggregation state determination prevents quantitative assessment of the relationship between these two variables. There is however evidence from synthetic diamonds (Boyd *et al.*, 1988a) that a relationship is to be expected and the consistent ^{15}N enrichment of nitrogen in more aggregated forms seen in simply zoned Western Australian diamonds, is the association that would be expected for a mass-dependent, diffusion driven fractionation. The heavier ^{15}N isotope has a higher vibrational frequency than the lighter ^{14}N isotope and as a result of this is expected to be more strongly bound into the diamond lattice (Collins and Woods, 1987) resulting in the preferential retention of this isotope during diffusion.

The approximately 10% lattice dilation around substitutional nitrogen atoms within the diamond crystal (See Table 1.1) provides a "driving force" promoting nitrogen diffusion, and subsequent aggregation. There is no energetic advantage driving carbon diffusion, and this provides a possible explanation for the restricted carbon isotope variability within simply zoned Western Australian diamonds (maximum range in $\delta^{13}C$ of 4.8‰ in 150701 #12-8) when compared to the range of $\delta^{15}N$ value that occur within the same diamond (up to 12.9‰ range within a single stone). Simply stated, nitrogen is fractionated to a greater extent than carbon, because it is more likely to diffuse within the diamond lattice.

Nitrogen aggregation state variations in simply zoned Western Australian diamonds are discussed in more detail in section 3.3, with reference to the age of diamonds.

6.2.3 Subduction

6.2.3.1 Summary of previous work

The possibility that subduction may play a role in the genesis of eclogitic paragenesis diamonds has been widely debated. The transport of organic carbon and nitrogen deep into the mantle along what have come to be known as subduction zones was first mooted

by Frank (1967) prior to the development of plate tectonics theory, and subsequently a number of authors have related crustal carbon components to diamonds and to xenoliths in kimberlite. For example, Milledge *et al.*, (1983) suggested that type II diamonds may derive their variable carbon isotope ratios from recycled crustal material, and from the observation of Sobolev *et al.*, (1979) that eclogite paragenesis diamonds had variable $\delta^{13}C$ values, suggested that type II diamonds may be related to this paragenesis. Certainly eclogite-paragenesis garnets and eclogite xenoliths in kimberlite had long been suggested to be related to subducted, former oceanic crust (*e.g* Nichols and Ringwood, 1973; Ringwood, 1975; Helmstaedt and Doig, 1975), and this interpretation is also valid for most South African eclogite xenoliths (Helmstaedt and Gurney, 1984). There is now considerable geochemical evidence in favour of a subduction origin for the eclogite xenoliths in many kimberlites (*e.g.* Ater *et al.*, 1984; Jagoutz *et al.*, 1984; MacGregor and Manton, 1986; Kirkley *et al.*, 1993), and this provides a convenient framework for explaining the anomalous isotopic characteristics of eclogitic paragenesis diamonds, and particularly their marked ^{13}C depletion (see Figure 6.4).

A compilation of isotopic data for carbon in sedimentary rocks (Schidlowski *et al.*, 1983) indicates that the $\delta^{13}C$ value of carbonate material has remained constant at 0‰ ± 2‰ since the Archaean, whereas organic carbon and inorganic reduced carbon are characterised by a large ^{13}C depletion, with $\delta^{13}C$ values as low as -50‰ being possible. During burial, organic material is expected to be subjected to dehydration, decarboxylation, and the loss of methoxyl (CH_3O), carbonyl (C=O) and amine (NH_2) functional groups accompanied by an increase in the proportion of aromatic structures until these coalesce to form graphite (Degens, 1969). These structural changes are expected to be accompanied by some isotopic fractionation, towards less negative $\delta^{13}C$ values, however the maximum isotope shift likely has been estimated to be ≈20‰ (McKirdy and Powell, 1974) and the maximum $\delta^{13}C$ value achieved on the metamorphism of organic carbon to graphite is -10‰ (McKirdy and Powell, 1974; Hoefs and Frey, 1976). A compilation of the $\delta^{13}C$ values of graphite in ancient sediments (Kirkley *et al.*, 1991) has a mode at $\delta^{13}C$ = -22‰ (Figure 6.10) and this is probably characteristic of the organic material carried into the diamond source region by subduction; a process that has been shown by Javoy *et al.*, (1982) and Des Marais (1985) to be necessary to balance global carbon budgets. As the fractionation factor between graphite and diamond is small, < 0.5‰ at temperatures above 700°C (Bottinga 1969), conversion of this graphite to diamond will not be accompanied by a significant isotopic shift and hence ^{13}C depleted diamonds may result from the deep burial of organic carbon. This graphite - diamond fractionation factor is incidentally very similar to that modelled for diamond plates from Argyle and Ellendale 4 in Chapter 2.

During metamorphism, graphite in calc-silicate assemblages has been shown to attain $\delta^{13}C$ values of -2±4‰ as a result of C isotope exchange with carbonate (Valley and O'Neil, 1981) and this carbon is interpreted by Kirkley *et al.*, (1991) to be responsible for the more positive $\delta^{13}C$ values exhibited by some eclogite paragenesis diamonds (See Figure 6.4). This interpretation is supported by an association between Ca-rich garnet inclusions in these ^{13}C enriched (relative to "normal" mantle) eclogitic diamonds (Sobolev, 1984; Hill, 1989) and by the occurrence of a dolomite inclusion in such a diamond (Hill, 1989) which consistent with diamond crystallization in a carbonate rich host rock. Thus diamonds with both ^{13}C depletion and ^{13}C enrichment may be derived from subducted carbon and varying degrees of mixing may produce any $\delta^{13}C$ value seen in eclogitic paragenesis diamonds.

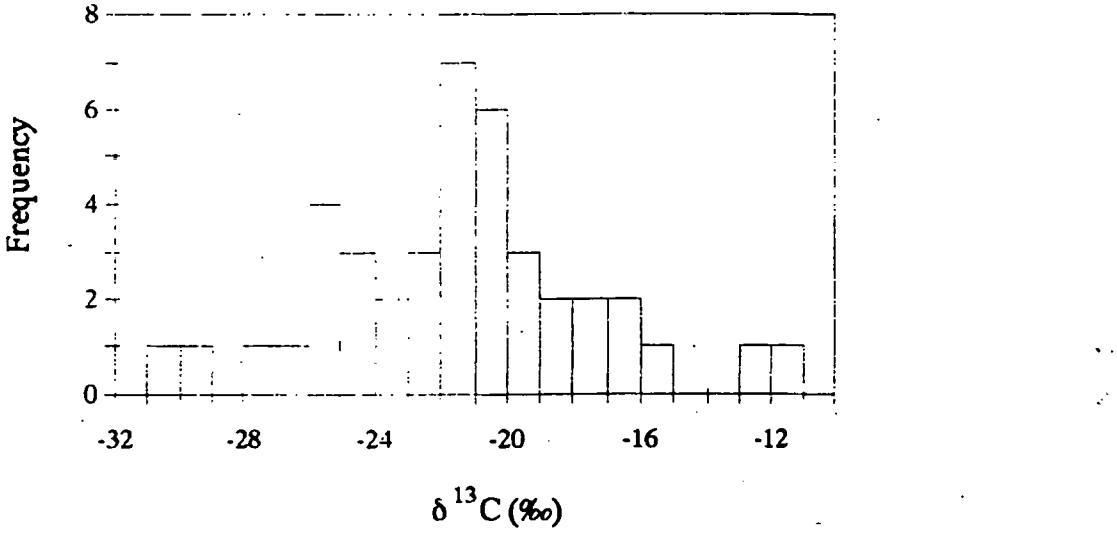

Figure 6.10: The $\delta^{13}C$ distribution of graphite in metasedimentary rocks over 1000 Ma old, and above amphibolite grade. Compiled by Kirkley *et al.*, (1991).

Further independent evidence of the presence of a subduction-related component in eclogite paragenesis minerals and diamonds is available. Eldridge *et al.*, (1991) report sulphur isotope ratios of sulphide inclusions in diamonds and their $\delta^{34}S$ data correlate with the Ni content of the sulphide inclusions. Ni content is thought to be indicative of diamond paragenesis (Sobolev, 1984), and low Ni (<8%) sulphide inclusions are thought to be of eclogitic paragenesis. The low Ni, eclogite paragenesis diamond inclusions examined by Eldridge *et al.*, (1991) have $\delta^{34}S$ values more variable than is usual for primary mantle material and deviate from $\delta^{34}S$ = 0‰ by over 4‰, and by up to 14‰. In contrast, sulphide inclusions with more than 8% Ni, which are thought to be of peridotitic paragenesis have $\delta^{34}S$ values that show little (<4‰) deviation from $\delta^{34}S$ = 0‰. The variation in the $\delta^{34}S$ values of diamond-inclusion sulphides from -11‰ to +14‰ is interpreted by Eldridge *et al.*, (1991) as being entirely consistent with a subducted origin for these diamonds, as oceanic crust and sediment have very variable $\delta^{34}S$ values.

Additional stable isotope evidence for the presence of a crustal component in the diamond source region is provided by the $\delta^{18}O$ values measured on eclogite xenoliths. Mantle peridotite xenoliths have a restricted range of whole rock $\delta^{18}O$ values, typically between +5‰ and +6.5‰ (*e.g.* Kyser *et al.*, 1981) whereas the $\delta^{18}O$ values of eclogite xenoliths are more variable and range from $\delta^{18}O$ = +2‰ to +8‰ (See Kirkley *et al.*, 1991 and references therein). This has been interpreted as a result of the low temperature sea water alteration of subducted material (Jagoutz *et al.*, 1984) as seen in modern oceanic crust (*e.g.* Muehlenbachs and Clayton, 1976).

There is also circumstantial evidence supporting the presence of a subduction related component in the mantle. Back arc basin basalts (BABB) are interpreted to contain a subduction-related component from the correlations between trace element contents of trench sediments and the associated arc volcanics (Plank and Langmuir, 1993) and also from the presence of spallogenic ^{10}Be in arc volcanic rocks (Morris *et al.*, 1990; Sigmarsson *et al.*, 1990). ^{10}Be has a short half life (1.5 Ma), does not occur naturally in the mantle and yet is concentrated in many arc-derived lavas (Morris *et al.*, 1990). The $\delta^{13}C$ values of BABB have been determined by Mattey *et al.*, (1984) and Exley *et al.*, (1986b) and these have been found to show moderate ^{13}C depletion relative to MORB, with $\delta^{13}C$ = -13.2‰ to -9.8‰ (See Figure 1.4). These negative $\delta^{13}C$ values are interpreted by both Mattey *et al.*, (1984) and by Exley *et al.*, (1986b) as being most probably related to the presence of a subduction-related organic component. This component could also be reflected in diamond $\delta^{13}C$ values, provided that subduction can carry crustal material to the depths of diamond formation (Kirkley *et al.*, 1991).

Thus there is an accumulating body of evidence for the role of a crustal component transported into the diamond source region by subduction, in the genesis of, at least some eclogitic paragenesis diamonds. Up to now, peridotitic paragenesis diamonds have not been associated with a subduction origin, largely due to their more restricted $\delta^{13}C$ values (Figure 6.4). Much of the $\delta^{13}C$ variability of peridotitic paragenesis diamonds can be attributed to small scale isotope shifts around the $\delta^{13}C$ value characteristic of "normal" mantle *vis.* $\delta^{13}C$ = -5‰ or -6‰, as may be caused by Rayleigh fractionations or by homogenization of primordial carbon (Kirkley *et al.*, 1991). It is now pertinent to consider whether the nitrogen stable isotope ratios of ^{13}C depleted diamonds are also consistent with a subduction origin.

6.2.3.2 Nitrogen in the subduction model

The nitrogen content of sedimentary and crustal igneous rocks can be high (200 to 4000 ppm; Wedepohl, 1969) particularly in mica rich rocks, for nitrogen as NH_4^+, substitutes readily for K^+ (Honma and Ithara, 1981). The nitrogen content of the mantle on the other hand is estimated to be of the order of 1 to 20 ppm (*e.g.* Gregor *et al.*, 1988). The

nitrogen stable isotope ratio of the mantle is estimated to be $\delta^{15}N = 0‰ \pm 6‰$ (See Section 6.1) whereas nitrogen stable isotope ratios at the surface of the Earth are usually characterised by positive $\delta^{15}N$ values (See Table 1.9). If the mantle is indeed characterised by a low or zero $\delta^{15}N$ value, then the addition of a positive $\delta^{15}N$ – component by subduction could have a significant effect.

Bebout and Fogel (1992) have examined the effect of prograde metamorphism on nitrogen content, and more particularly on nitrogen stable isotope ratios in the metasedimentary rocks of the Catalina Schist subduction zone metamorphic complex, California. They report a decrease in the nitrogen content of the metasedimentary rocks with increasing metamorphic grade, accompanied by an increase in the $\delta^{15}N$ values of these rocks, and they interpret this as a Rayleigh distillation effect, arising from the devolatilization of the subducting material. The highest metamorphic grade rocks examined by Bebout and Fogel (1992) are high-grade amphibolites that have reached temperatures of about 750°C and pressures that correspond to depths of up to 45 km. These samples are reported to contain 30 ppm to 250 ppm nitrogen with $\delta^{15}N$ values in excess of +4‰, and are estimated to have lost 74% to 78% of the original nitrogen, based on lower-grade rocks with similar K_2O contents (Bebout and Fogel, 1992). Bebout (1991) estimates that the maximum devolatilization of the Catalina Schist occurred at relatively low temperature (350°C to 600°C) by reactions involving the breakdown of chlorite, and the existence of non-negligible nitrogen contents in high grade metamorphic rocks indicates that at least some nitrogen can survive subduction, with an enhanced (more positive) $\delta^{15}N$ value. It is pertinent to consider whether such nitrogen may be implicated in diamond genesis. Certainly sediment related potassium can be transported to, and beyond depths at which melting occurs (Wyllie and Sekine, 1982; Rogers *et al.*, 1987) where it becomes stabilised in phlogopite-bearing assemblages at depths in excess of about 150 km. If NH_4^+ substitution for K^+ continues to operate, then ^{15}N enriched nitrogen may also be stable within the lithosphere, and it may become involved in diamond genesis. The fate of nitrogen as N_2 is less well constrained. N_2 is unreactive in most geochemical cycles (Gregor *et al.*, 1988) and any produced from the breakdown of ammonia should behave in a similar manner to the noble gases. Staudacher and Allègre (1988) conclude that these are effectively returned to the Earth's external reservoirs during subduction, however Poreda and Craig (1989) and Porcelli *et al.*, (1992) suggest that at least some subduction-related He can be detected in rocks associated with volcanic arcs. If this He is indeed derived from the subducted slab, it implies that slab-derived nitrogen (as N_2) can also reach deep levels in the lithosphere.

It therefore seems likely that at least some crustal nitrogen can survive subduction and be transported into the diamond-stable regions of the lithosphere, either as NH_4^+ or as N_2. Transport by subduction will however, undoubtedly, be accompanied by decreases in

nitrogen content and by increases in $\delta^{15}N$ value, as the subducting slab looses volatile phases and any component introduced into the mantle should thus be characterised by positive $\delta^{15}N$ values. A crude mass balance calculation showing the effect of adding nitrogen-bearing sediment into the mantle is shown in Table 6.6. Two extreme and an intermediate cases for the nitrogen content and $\delta^{15}N$ values of sediment are used (Wedepohl, 1969; Letolle, 1980; Bebout and Fogel, 1992). The Gregor *et al.*, (1988) estimates of mantle nitrogen content are used, and the $\delta^{15}N$ value of the mantle is assumed to be 0‰ throughout.

A

Mantle: [N] assumed to be 2 ppm, $\delta^{15}N$ assumed to be 0‰

Sediment: [N] assumed to be 4000 ppm, $\delta^{15}N$ assumed to be +20‰

Proportion of added sediment (%)	Mixture $\delta^{15}N$ (‰)	Mixture [N] (ppm)
.001	0.4	2
.01	3.4	2
.05	10	4
.10	13	6
.15	15	8
.20	16	10

B

Mantle: [N] assumed to be 20 ppm, $\delta^{15}N$ assumed to be 0‰

Sediment: [N] assumed to be 250 ppm, $\delta^{15}N$ assumed to be +5‰

Proportion of added sediment (%)	Mixture $\delta^{15}N$ (‰)	Mixture [N] (ppm)
1	1	22
5	2	32
10	3	43
15	3	55
20	4	66
30	4	89

C

Mantle: [N] assumed to be 10 ppm, $\delta^{15}N$ assumed to be 0‰

Sediment: [N] assumed to be 250 ppm, $\delta^{15}N$ assumed to be +4‰

Proportion of added sediment (%)	Mixture $\delta^{15}N$ (‰)	Mixture [N] (ppm)
1	1	12
5	2	22
10	3	34
15	3	46
20	3	58

Table 6.6: (A); The effect of adding a sedimentary component with very high nitrogen content and $\delta^{15}N$ value into low-nitrogen mantle. (B); The effect of adding a sedimentary component with a low nitrogen content and $\delta^{15}N$ value into low-nitrogen mantle. (C); As for (B) except that the added phase has a $\delta^{15}N$ value and nitrogen content the same as that measured from the Catalina Schist metamorphic rocks (Bebout and Fogel, 1992). Nitrogen content estimates from Wedepohl (1969) and Gregor *et al.*, (1988) throughout, and in A and B, sediment $\delta^{15}N$ estimates are from Letolle (1980).

From Table 6.6 it can be seen that subduction-related nitrogen may significantly perturb the $\delta^{15}N$ value and nitrogen content of the mantle, when large amounts of ^{15}N enriched nitrogen are present in the sediment (Case A). In more realistic cases, for example if the component has a nitrogen composition and $\delta^{15}N$ value similar to that of the Catalina Schist metamorphic rocks, the effect on the diamond source region is more restricted and may in fact be obscured by the $\delta^{15}N$ heterogeneity intrinsic to the mantle. The effect on nitrogen content can however be marked.

Nitrogen stable isotope ratios in diamond do not therefore provide direct, unequivocal evidence for the presence of a subduction-related component within the sub-continental lithosphere. It is however equally true to state that the nitrogen stable isotope ratios in ^{15}N enriched ($\delta^{15}N > 0‰$) diamonds do not preclude the addition of a crust-derived component into the source region of these samples.

6.2.4 Synthesis

An explanation for the apparent $\delta^{15}N$ heterogeneity of the diamond source region is necessary, and this can be based on the relationships between diamond $\delta^{15}N$ value and paragenesis. The model presented here is based on the framework of the sub-continental lithospheric upper mantle model developed by the Kimberlite Research Group, University of Cape Town, and this mantle model is based on numerous studies of kimberlite-derived material from southern Africa. It is summarised in Gurney *et al.*, (1991), and is illustrated in Figure 6.11.

In southern Africa, the lithospheric mantle increases in thickness from the margins towards the centre reaching a maximum approaching 200 km. This deep cratonic root is cool, consists mainly of coarse grained garnet and chromite harzburgite with minor garnet lherzolite and may have persisted since the Archaean. The harzburgites show evidence of an ancient metasomatism (K, U, Rb and LREE enriched) and may also be carbonated. At shallower levels in the lithospheric mantle, the dominant rock is also coarse grained peridotite (garnet lherzolite and harzburgite) and this has been subjected to several metasomatic processes over a period of the order of Ga's. Phlogopite has been introduced at depths in excess of 120 km, accompanied by potassic richterite or other amphiboles at shallower levels where the modal metasomatism may be very intensely developed. The highly metasomatized regions of the lithosphere are veined with

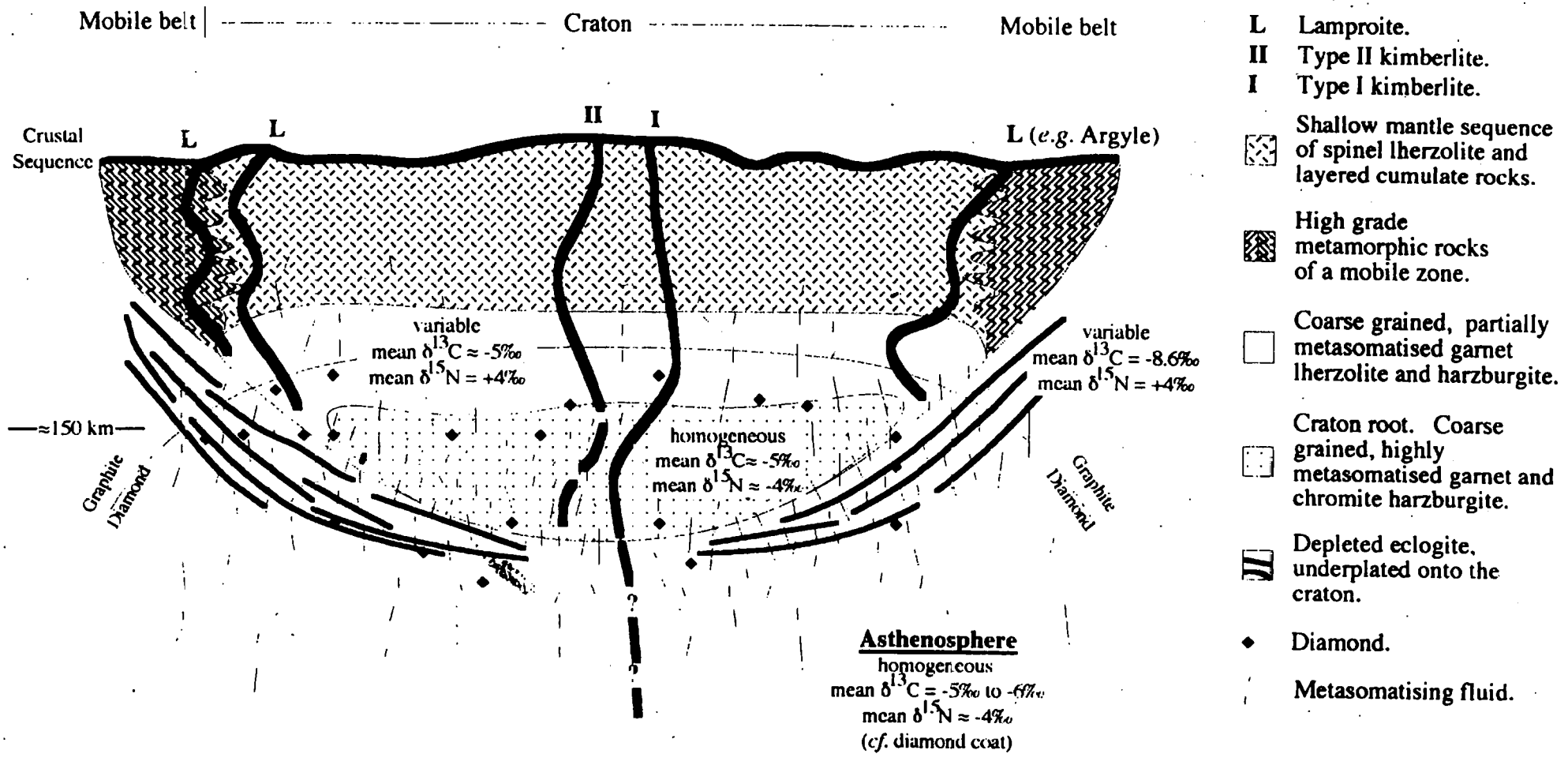

Figure 6.11: A generalised model of craton structure, based on that of Gurney *et al.*, (1991). The asthenosphere and eclogite are chemically depleted (large volumes of mafic melt extracted) whereas the harzburgite and lherzolite are very enriched and mildly enriched respectively, by the action of metasomatic fluids. The carbon and nitrogen stable isotope characteristics of each part of the sub-continental lithospheric mantle are from Table 6.4 and the text. The approximate position of the graphite-diamond stability curve is shown.. This diagram is not to scale.

MARID† (Erlank *et al.*, 1987) mineral assemblages. Unmetasomatised peridotite is a chemically depleted rock, capable of producing only small amounts of basaltic melt, and appears to be a major, old (>1 Ga) component of the lithosphere. Underplated onto the harzburgitic lithospheric keel are eclogites (Group 1) that are thought to have formed near the lithosphere/asthenosphere boundary in an igneous process in which recycled oceanic crust is involved.

This model is also considered to be broadly applicable to the Kimberley Craton, Western Australia. The lamproites and kimberlites of the East, West and North Kimberley provinces are all close to the craton edge, and the lamproite source region has been shown to be largely metasomatized peridotite (Fraser *et al.*, 1985; Hawkesworth *et al.*, 1985; Fraser, 1987), characterised by elevated incompatible element contents, particularly K, Rb, Ba, Sr, REE, P and Zr, consistent with the presence of phlogopite in the source (Wilson, 1989 p.381). Furthermore, lherzolite xenoliths, particularly high temperature, sheared lherzolites, are more common than harzburgite xenoliths in the Western Australian lamproites (Jaques *et al.*, 1986b, p. 251) and eclogite paragenesis diamonds are most abundant in the Argyle lamproite. The source region of these lamproites is thus considered to be close to the region in which metasomatized lherzolite abuts underplated eclogite and this is illustrated in Figure 6.11. The scarcity of harzburgite xenoliths and absence of harzburgite paragenesis diamonds from Argyle and Ellendale suggests that the cool harzburgite root of the Kimberley craton may be less well developed, or less well preserved, than the harzburgite keel of the Kaapvaal craton.

Assuming that diamonds directly reflect the stable isotope ratios of their source region, why should the eclogitic, lherzolitic and harzburgitic sub-continental lithospheric mantle have differing $\delta^{15}N$ values? One significant clue lies in the recent results of Richardson *et al.*, (1993). Harzburgitic diamonds are ancient (>3 Ga; Richardson *et al.*, 1984) whereas eclogitic diamonds are much younger (Proterozoic; Richardson, 1986; Richardson *et al.*, 1990) and lherzolitic paragenesis diamonds are of intermediate age (≈1930 Ma; Richardson *et al.*, 1993). Furthermore, Richardson *et al.*, (1993) report that the source region for first generation harzburgitic diamonds from Premier mine, South Africa is characterised by a strongly enriched precursor isotopic and trace element signature (elevated Nd, Sr in garnet, Sm/Nd and $^{143}Nd/^{144}Nd$ lower, and $^{87}Sr/^{86}Sr$

---

† MARID: Mica, amphibole, rutile, ilmenite, diopside. A class of mantle xenolith produced by the metasomatism of the upper mantle. They crystallized from fluids that were enriched in O, F, Na, Al, P, Cl, K, Ca, Ti, Mn, Fe, Rb, Sr, Y, Zr, Ba, LREE, Ta, Th and U (Basaltic Volcanism Study Project, 1981, page 304)

higher than bulk earth at time of emplacement). The corresponding signature for second generation lherzolitic paragenesis diamonds is one of only mild enrichment (εNd = -3), and in contrast, the third generation eclogitic diamonds have a precursor isotopic signature that is strongly depleted.

The correspondence of diamond age, the degree of metasomatism of the source region and the nitrogen stable isotope characteristics of diamonds of differing parageneses, summarised in Table 6.7 has at least two possible explanations, which are not mutually exclusive. The first of these entails a relationship between the $\delta^{15}N$ characteristics of diamonds and the metasomatism of the diamond source region. With increasing degrees of metasomatism, the nitrogen stable isotope ratios are progressively homogenized, resulting in the $\delta^{15}N$ characteristics of harzburgitic diamonds eventually approaching those of the metasomatic agent. The second possibility is that the increase in the variability of diamond $\delta^{15}N$ values, and the increase in the mean $\delta^{15}N$ values of the different parageneses is a function of time, *i.e.* an initially relatively homogeneous, ^{15}N depleted source (harzburgite) becomes progressively more variable and more enriched in ^{15}N with time. These possibilities are now considered individually.

Harzburgite	**Lherzolite**	**Eclogite**
3.2 Ga	1.9 Ga	1.2 Ga
Highly Enriched	Mildly enriched	Depleted
(most metasomatized)	(less metasomatized)	(least metasomatized)
Least variable $\delta^{15}N$	variable $\delta^{15}N$	most variable $\delta^{15}N$
mean $\delta^{15}N < 0‰$	positive mean $\delta^{15}N$	positive mean $\delta^{15}N$

Table 6.7: Characteristics of harzburgitic, lherzolitic and eclogitic diamond source regions. Isotope geochemistry and ages from Richardson *et al.*, (1993).

(1) Metasomatic homogenization of diamond source $\delta^{15}N$ values

Metasomatism of the diamond stable region of the sub-continental lithospheric upper mantle is accepted as occurring, and has been identified as being responsible for the enriched geochemical signatures of lamproites and group II kimberlites from a variety of localities in southern Africa and Western Australia (Wilson, 1989). The metasomatic process involves the transfer of incompatible, high field strength and rare earth elements including K, and a "metasomatic fluid" phase, either a small volume silicic melt or a H_2O-dominated fluid, is usually invoked as being the responsible agent (Morris and Pasteris, 1987 and references therein). It is highly likely that NH_4, if present, will also be enriched in the metasomatic fluid. The origin of these fluids is poorly constrained, but if they are derived from the convecting asthenosphere they are likely to be homogeneous over a wide geographical extent. Such fluids may correspond to the coat formed on coated stones that has been described by Boyd *et al.*, (1992) and by Navon and others (Navon *et al.*, 1988; Navon 1991). Certainly the fluid inclusions in diamond coat are highly potassic (Navon *et al.*, 1988) and the nitrogen isotope ratios measured

from diamond coat (Boyd *et al.*, 1992) are very close to those measured from assumed harzburgitic diamonds from Finsch (See Figure 6.8). The $\delta^{15}N$ value of metasomatic fluids should however be directly measured by examining the nitrogen stable isotope ratios in MARID and other metasomatized xenoliths.

A drawback of this paradigm is that it requires the source of the metasomatic fluid to be the convecting and hence well mixed, asthenosphere. If however, the volatile precursors to diamond genesis are derived from a subducting slab, as is favoured for example by Kesson and Ringwood (1989), it is difficult to envisage how the low $\delta^{15}N$ values of the most metasomatized diamonds are generated. Although volatile-rich, water dominated fluid phases are likely to be trapped in subducting slab to below the depths of amphibole breakdown (Watson and Lupulescu, 1993), this should be accompanied by a kinetic fractionation of the associated nitrogen to more positive $\delta^{15}N$ values as has been shown for example in the Catalina schists (Bebout and Fogel, 1992).

(2) Source $\delta^{15}N$ values and time

This model suggests a global relationship between the $\delta^{15}N$ values of different parts of the sub-continental lithospheric upper mantle. As the Earth evolves, there is an increase in the mean $\delta^{15}N$ value of the sub-continental lithospheric mantle, and such an increase in the $\delta^{15}N$ value of the lithospheric mantle is consistent with a kinetic nitrogen fractionation during mantle degassing to form the atmosphere. The more mobile ^{14}N isotope should be preferentially degassed, leaving a residue relatively enriched in ^{15}N. Evidence in support of this hypothesis is to be found in the similarity of the $\delta^{15}N$ value of the atmosphere (the well mixed product of mantle degassing) and the mean $\delta^{15}N$ value suggested for all diamonds (representative of the original, undegassed source material), both of which are close to $\delta^{15}N = 0‰$. Further circumstantial evidence is to be found in the $\delta^{15}N$ values reported for MORB, the youngest known upper mantle samples. These mostly have $\delta^{15}N$ values > 0‰ (Becker and Clayton, 1977; Sakai *et al.*, 1984; Exley *et al.*, 1987. See also Chapter 1, section 1.3.2.2.2) and they may thus represent the residue of the most degassed mantle.

It is difficult to quantitatively investigate either of these two hypotheses. Although mantle degassing to form the terrestrial atmosphere is generally accepted (Allègre *et al.*, 1993), the time at which the atmosphere become nitrogen-dominated is not known and the global nitrogen cycle is poorly constrained. Furthermore, the precise chemistry of, and source of metasomatic fluids is still the subject of contentious debate and the behaviour of nitrogen in such fluids is totally unknown. It is likely to be a function of oxygen fugacity, and this is equally poorly constrained. Nevertheless, the two possibilities presented are not mutually exclusive and both may combine to generate the range of nitrogen stable isotope ratios measured in diamond samples from the sub-

continental lithospheric upper mantle. Useful tests that should be undertaken include (1) analyses of the $\delta^{15}N$ values of ultra-deep asthenospheric diamonds (Moore and Gurney, 1985, 1989) to investigate whether these are similar to diamond coat and thus possibly constrain the stable isotope systematics of the postulated metasomatic fluids and (2) a detailed investigation of the nitrogen contents of harzburgite, lherzolite and eclogite. Is there evidence of decreasing mean nitrogen content in this series, consistent with increasing amounts of nitrogen loss to form the present atmosphere?

Richardson *et al.*, (1993) link the three generations of diamond growth at the Premier Mine, South Africa to three regional tectonic events. Archaean harzburgitic diamonds are related to widespread komatiitic magmatism (which would doubtless have been accompanied by significant amounts of mantle outgassing) and the 1.92 Ga lherzolitic diamonds are linked to the emplacement of the Bushveld Igneous Complex; a very significant mafic melting event. Eclogitic diamonds in contrast are only marginally younger than the host kimberlites and Richardson *et al.*, (1993) suggest that diamond formation and diatreme emplacement may be causally related, with kimberlitic precursor fluids being the source material for eclogitic paragenesis diamonds. In Western Australia, there are similar tectonic events that may perhaps be linked to diamond forming episodes. The date of formation of the crust that now underlies the Kimberley craton is not known, but Fraser (1987) reports that an event at ≈3.5 Ga is required to model the lead evolution of the source material of the West Kimberley lamproites. A further Pb event is modelled at 2.1 Ga (Fraser 1987) and this is very similar to the age of the extensional tectonism that thinned Archaean crust allowing deposition of the Halls Creek Group (Hancock and Rutland, 1984). It is also similar to the maximum ages calculated from the Argyle diamond plates 150701 #8 (peridotitic paragenesis) and 150701 #12-1 (unknown paragenesis) on the basis of nitrogen aggregation state estimates (See Section 2.3.5). Compression and uplift occurred between 1920 Ma and 1830 Ga (Hancock and Rutland, 1984) resulting in the eventual stabilization of the Halls Creek and King Leipold mobile zones. It is suggested that these three episodes may be related to the formation of harzburgitic, lherzolitic and eclogitic diamonds from Western Australia. The only diamonds for which formation ages have however been determined are eclogitic paragenesis Argyle samples (1580 ± 60 Ma; Richardson 1986) and Richardson (1986) suggested that these may be related to the stabilization of the Halls Creek Mobile Zone. Clearly, age determinations must be made for peridotitic paragenesis diamonds from Western Australia in order to test this suggestion.

6.2.5 Conclusion

Diamonds are derived from the sub-continental lithospheric mantle and it is suggested that the mean $\delta^{13}C$ and $\delta^{15}N$ values of this are -5‰ to -6‰ and 0‰ respectively. From

numerous diamond inclusion and xenolith studies and from the petrology of lamproites and kimberlites, it is known that the evolution of the sub-continental mantle is complex, involving repeated cycles of melting, enrichment and depletion in incompatible-, large ion lithophile-, and high field strength elements, metasomatism and intrusion by volatile rich, possibly asthenospheric fluids (*e.g.* Boyd, 1973; Fraser, 1987; Griffin *et al.*, 1988, 1992, 1993; Jaques *et al.*, 1990; Gurney *et al.*, 1991; Boyd *et al.*, 1992 and Boyd *et al.*, 1993). It is also likely that a number of processes affect the stable isotope ratios of the diamond source region and the diamonds themselves. Rayleigh type isotope fractionation is likely to occur during melting and metasomatic episodes and similarly, mantle outgassing to form the atmosphere is likely to be accompanied by a relative increase in the proportion the heavy isotope (^{13}C or ^{15}N) in the residue. Subduction will also affect the carbon, nitrogen and other stable isotope ratios in the diamond source region. The presence of subducted crustal components has been suggested in eclogite xenoliths and eclogite paragenesis diamonds (*e.g.* Kirkley *et al.*, 1991, 1993) and water and other volatiles may be trapped and transported to sufficient depths (Watson and Lupulescu, 1993) to provide the triggering mechanism for further magmatism.

It is thus naive to expect a single simple process to explain the entire range in $\delta^{13}C$ and $\delta^{15}N$ values measured in diamonds. It is more likely that a combination of degassing history, isotopic fractionation processes during metasomatism and the transport of volatile-rich phases during the recycling of crustal components to the mantle by a subducting slab will act in concert to generate the stable isotope characteristics of any particular diamond source region.

Some primordial mantle heterogeneity may even be preserved. The Northern Queensland diamonds (N.Q 33 and N.Q 25) have very negative $\delta^{15}N$ values ($\delta^{15}N$ = -28.4‰ and -22.8‰ respectively) that are not readily explained by the paragenesis controlled model suggested above. They are however close to the mean $\delta^{15}N$ values for enstatite chondrites (Grady *et al.*, 1986; Kung and Clayton 1978) and CV chondrites (Kerridge 1985) and may represent the primordial constituents of the Earth. Equally however, these very ^{15}N depleted diamonds may have simply had a long and complex history, involving repeated cycles of precipitation and dissolution in a variety of environments. Without age and paragenetic data (and the samples are inclusion free so this will not be forthcoming), these possibilities cannot be resolved. In general however, the restricted range in δ values shown by Archaean harzburgitic diamonds suggests that the initial homogenization of the Earth went nearly to completion.

7 Conclusions and recommended research

From the results presented in this thesis it has been possible to derive a number of conclusions as to the nature of Western Australian diamonds; their source regions and the processes involved in their formation. For the most part, these have been discussed in the relevant chapters and thus only a brief summery is presented here.

Single diamond crystals are heterogeneous with respect to their $\delta^{13}C$ and $\delta^{15}N$ values, nitrogen content and nitrogen aggregation state. The maximum variation seen in the $\delta^{13}C$ values of a single Western Australian diamond is 4.8‰ in the Argyle plate 150701 #12-8 (from $\delta^{13}C$ = -14.1‰ to -9.3‰) and this is close to the maximum reported $\delta^{13}C$ variation in non-coated diamonds of 7.1‰ from a Bultfontein diamond reported by Harte and Otter (1992). The maximum $\delta^{15}N$ variation in any diamond occurs in the Ellendale 9 sample E9037 and is 12.9‰ from $\delta^{15}N$ = +0.3‰ to +13.2‰. Nitrogen contents measured by mass spectrometry can also vary within individual diamonds. This variation may be by as much much as 1382 ppm (Argyle plate 150701 #8) and the maximum nitrogen content in this sample (1435 ppm) is 26 times higher than the minimum measured nitrogen content (53 ppm)! Nitrogen aggregation state variations across diamonds can also be extreme and both samples 150701#1 and 150701 #8 from Argyle show a range from pure type II diamond to nearly 100% B-aggregates. Nitrogen aggregation state has been used to calculate nominal mantle resident times for the Argyle and Ellendale plates and the intra-sample variation in these samples indicates that diamond growth is a very slow process. The age difference between the oldest and youngest portion of an Argyle plate is nearly 1200 Ma (150701 #12-1) and this implies that diamond growth started at ≈2.4 Ga; a date for the commencement of diamond growth that is also appropriate for the oldest Ellendale diamond (E9037). This heterogeneity indicates that in future, whole diamonds rather than fragments broken from diamonds should be examined.

With certain exceptions, there are no consistent relationships between the carbon and nitrogen stable isotope ratios and the colour, shape, nitrogen content or nitrogen aggregation state of individual diamond crystals. In some simple crystals from Argyle and Ellendale 9 however, higher concentrations of more aggregated nitrogen occur in the central regions of the diamonds than are found towards the rims. These concentrations of aggregated nitrogen are also associated with a ^{15}N enrichment relative to the rims of the stones. The zonation patterns in these simple crystals are consistent with their formation by simple closed system fractional crystallization, within a reservoir that is approximately the same size as the diamond itself. Mixing of two or more reservoirs

with different $\delta^{13}C$ and $\delta^{15}N$ values may also be responsible for the zoning patterns seen in sample 150701 #12-1.

The fractional crystallization of 4 single diamonds has been quantitatively modelled and fractionation factors determined. These fractionation factors are low; mostly less than $\alpha = 1.001$ for carbon and approximately $\alpha = 1.004$ for nitrogen at the temperatures appropriate for diamond growth. It is likely that variations in the fractionation factors for individual samples are affected by crystallization temperature, mantle fO_2 and the composition of the diamond source material. The starting material does not have a uniform composition and initial δ values may vary by up to 5‰ for individual diamonds within a single lamproite.

When many diamonds from individual lamproites are considered, it is evident that the diamond source region is also heterogeneous. The diamonds from single source can have a range of $\delta^{13}C$ and $\delta^{15}N$ values and in Western Australia this range of 22‰ for carbon (Ellendale 9) and 23‰ for nitrogen (Argyle and Ellendale 9) is larger than the variation seen within individual crystals. Some of this variation may be ascribed to the existence of several generations of diamond growth in the Western Australian deposits studied, which means that the use of microdiamonds as grade indicators in prospecting must be approached with caution. The major control on diamond stable isotope ratios is however paragenetic. Eclogitic and lherzolitic Western Australian diamonds have significantly different carbon stable isotope ratios although the nitrogen stable isotope ratios of these two parageneses do not differ significantly. The nitrogen stable isotope ratios in Finsch diamonds which are presumed to be dominantly harzburgitic are however distinct from the Western Australian eclogitic and lherzolitic parageneses. It is therefore provisionally suggested that the carbon and nitrogen stable isotope ratios of diamonds may be used to discriminate the eclogitic, lherzolitic and harzburgitic parageneses. The suggested characteristics are:

Eclogitic variable $\delta^{13}C$ values and a mean $\delta^{13}C$ value more negative than $\approx$ -5‰ to -7‰. $\delta^{15}N$ values are mostly positive and the mean $\delta^{15}N$ value is +4.3‰ for Western Australian examples.

Lherzolitic $\delta^{13}C$ values within the mantle range and a mean $\delta^{13}C$ value of -5‰. $\delta^{15}N$ values are mostly positive and the mean for Western Australian diamonds is +4.1‰.

Harzburgitic $\delta^{13}C$ values are characteristic of normal mantle at $\delta^{13}C$ = -5‰ to -6‰. $\delta^{15}N$ values are negative. If Finsch diamonds are indeed characteristic of harzburgitic diamonds, the mean $\delta^{15}N$ value is $\approx$ -3‰, which is very similar to that of diamond coat.

When all available nitrogen stable isotope data for diamonds are combined, the mean $\delta^{15}N$ value is +0.2‰ with a standard deviation of 6‰. It is therefore suggested that the sub-continental lithospheric upper mantle has a $\delta^{15}N$ value of 0±6‰. This estimate of the upper mantle $\delta^{15}N$ value is remarkably similar to that of the atmosphere, and is wholly consistent with atmosphere being the accumulated product of the outgassed upper mantle. Mantle outgassing is also broadly in line with the differences in the mean $\delta^{15}N$ values of harzburgitic, lherzolitic and eclogitic paragenesis diamonds. Richardson *et al.*, (1993) shows that these three paragenesis represent a trend of decreasing age and they also have increasing $\delta^{15}N$ values. This is explained by the expected kinetic fractionation associated with nitrogen outgassing, which will result in the mantle residue becoming progressively ^{15}N enriched with time.

Several lines of evidence point to the involvement of fluid phases in diamond genesis. These include the presence of frozen melt inclusions in the Coanjula (Northern Territory) microdiamonds; the ubiquitous presence of resorbed diamonds and the existence of non-negligible carbon and nitrogen fractionation factors. This fluid phase is thought to be a small volume, highly enriched silicic, or perhaps carbonatitic, melt but its origin is not known. It may be derived from the asthenosphere and be similar to the material implicated in the metasomatism of the lithospheric mantle, in which case it might be expected to have stable isotope characteristics similar to those of diamond coat. Alternatively, this fluid may be related to subduction zones, and be derived from, or related to, volatile fluxing off a subducting slab. Organic carbon has been implicated in the genesis of ^{13}C depleted eclogitic paragenesis diamonds (Kirkley *et al.*, 1991) and graphite of organic origin transported into the mantle along a subduction zone may give rise to the ^{13}C depleted diamonds of Western Australia. Similarly, ^{13}C enriched lherzolitic paragenesis diamonds, for example those that occur in lherzolite nodules from Argyle, may be related to either marine carbonates or abyssal peridotite transported on subducting slabs into the mantle. The nitrogen stable isotope ratios in diamond do not provide definitive proof (or disproof) of the involvement of an organic N component within diamonds. Crust-derived nitrogen is however ^{15}N enriched relative to the atmosphere (positive $\delta^{15}N$ values) and this is also the case for most lherzolitic and eclogitic diamonds from Western Australia. If subduction was indeed involved in their genesis, the Halls Creek mobile zone may represent the fossil subduction zone.

Diamond genesis is a complex process. The stable isotope characteristics of any diamond will be a function of the source region characteristics and the processes that have been involved in that diamonds crystallization. Temperature, pressure and fO_2 are all likely to be important variables in determining the composition of that diamond. Care is thus needed when drawing general conclusions based on any particular group of diamonds. Furthermore, in light of the heterogeneity shown in the composition and the

ages of the diamonds described in these chapters it is suggested that future diamond studies be undertaken on complete samples, rather than on fragments broken from whole stones. This will be particularly important if diamond crystallization processes are to be further characterised, and is relatively easily implemented by using modern ion probe analytical techniques.

Some specific questions have been raised by this thesis and they need to be addressed. These included a detailed study of the relationship between diamond paragenesis, $\delta^{15}N$ value and age and it is suggested that eclogitic, lherzolitic and harzburgitic paragenesis diamonds from the same source be studied. All three parageneses occur in the Premier kimberlite, South Africa and as the radiogenic isotopes in inclusions from these diamonds have already been examined by Richardson *et al.*, (1993), this would be a sensible source of diamonds for such an examination. A second problem that must be addressed concerns that age zonation seen in some of the Western Australian diamonds. Semi-quantitative estimates of nitrogen aggregation state have indicated that diamond growth is very slow and this should be quantified by using good quality FTIR spectra, preferably from traverses across diamonds from which temperature can be accurately determined. Whether such age zonations exist in diamonds from other sources should also be examined.

Additional problems that need to be addressed include: (1) the effect of temperature on the C and N fractionation factors that pertain to diamond growth, and an experimental study is indicated here. (2) The variation of nitrogen content with age must be examined for diamonds and other mantle-derived samples. Is there a net decrease of the amount of nitrogen in the mantle over geological time, as would be expected for a degassing mantle? (3) What are the $\delta^{15}N$ and $\delta^{13}C$ characteristics of metasomatic fluids? Are they similar to diamond coat or not, and this may be assessed by measuring these ratios in MARID xenoliths and in other metasomatized samples.

The final question concerns the origin of the very ^{15}N depleted diamonds that occur in the Northern Queensland and Chinese placer deposits. These may represent the extremes of isotopic fractionation, the presence of primordial (meteorite-derived) carbon and nitrogen in diamonds or may have a more mundane explanation. More of these samples, and particularly inclusion-bearing samples need to be examined.

List of References

Allen B.P and Evans T (1981). Aggregation of nitrogen in diamond including platelet formation. *Proc. Roy. Soc. Lond.*, **A375**: 93 - 104.

Allègre C.J, Sarda P and Staudacher T (1993). Speculations about the cosmic origin of He and Ne in the interior of the Earth. *Earth Planet. Sci. Lett.*, **117**: 229 - 233.

Ammerlaan C.A.J (1981). *Inst. Phys. Conf. Ser.*, **59**: 81 - 94.

Amundsen H.E.F and Neumann E.-R (1992). Redox control during mantle/melt interaction. *Geochim. Cosmochim. Acta*, **56**: 2405 - 2416.

Angus J.C and Hayman C.C (1988). Low pressure, metastable growth of diamond and "diamondlike" phases. *Science*, **241**: 913 - 921.

Argyle Project Briefing (1984). Argyle diamond mines joint venture project briefing. *Argyle diamond mines Pty. Ltd. Perth, Western Australia, August 1984*, 96p.

Ash R.D (1990). Intersteller dust from primative meteorites: A carbon and nitrogen isotope study. *Ph.D Thesis (Unpubl.). Open University, Milton Keynes.*

Ater P.C, Eggler D.H and McCallum M.E (1984). Petrology and geochemistry of mantle eclogite xenoliths from Colorado-Wyoming kimberlites; recycled ocean crust? *In: Kornprobst J (Ed.). Kimberlites II. The mantle andcrust-mantle relationships. Developments in petrology IIA. Elsvier, Amsterdam*, : 309 - 318.

Atkinson W.J (1989). Diamond exploration philosophy, practise, and promises; a review. *In: Ross J, Jaques A.L, Ferguson J, Green D.H, O'Reilly S.Y.O, Danchin R.V and Janse A.J.A (Eds.). Kimberlites and related rocks. Volume 2. Their mantle/crust setting, diamonds and diamond exploration.*, **Geological Society of Australia Spec. Publ. 14**: 1075 - 1107.

Atkinson W.J, Hughes F.E and Smith C.B (1982). A review of the kimberlitic rocks of Western Australia. *Terra Cognita*, **2**: 204.

Atkinson W.J, Hughes F.E and Smith C.B (1984). A review of the kimberlitic rocks of Western Australia. *In: Kornprobst J (Ed.). Kimberlites I: Kimberlites and related rocks. Developments in petrology IIA. Elsvier, Amsterdam*, 195 - 244.

Balhaus C (1993). Oxidation state of lithospheric and asthenospheric upper mantle. *Contrib. Mineral. Petrol.*, **114**: 331 - 348.

Balhaus C, Berry R.F and Green D.H (1990). Oxygen fugacity controls in the Earth's upper mantle. *Nature*, **348**: 437 - 440.

Basaltic Volcanism Study Project. (1981). Basaltic volcanism on the terrestrial planets *Pergammon Press, Inc. New York, U.S.A.*

Bebout G.E (1991). Field based evidence for devolatilization in subduction zones: Implications for arc magmatism. *Science*, **251**: 413 - 416.

Bebout G.E and Fogel M.L (1992). Nitrogen-isotope compositions of metasedimentary rocks in the Catalina Schist, California: Implications for metamorphic devolatilazation history. *Geochim. Cosmochim. Acta*, **56**: 2839 - 2849.

Becker H and Altherr R (1992). Evidence from ultra-high pressure marbles for recycling of sediments into the mantle. *Nature*, **358**: 745 - 748.

Becker R.H (1982). Nitrogen isotopic ratios of individual diamond samples. *Proc. 5th Int. Conf. Geochronology, Cosmochronology & isotope geology*, 21 - 22.

Becker R.H and Clayton R.N (1977). Nitrogen isotopes in igneous rocks. (Abs.). *EOS, Trans. Am. Geophys. Union*, **58**: 536.

Berger S.D and Pennycook S.J (1982). Detection of nitrogen at {100} platelets in diamond. *Nature*, **298**: 635 - 637.

Berman R and Simon F (1955). The graphite diamond equilibrium. *Z. Electrochem.*, **59**: 333 - 345.

Bibby D.M (1982). Impurities in natural diamonds. *In: Thrower P.A. (Ed.). Chemistry and Physics of carbon. Vol 18. Marcell Drekker*, **1**: 1 - 91.

Blacic J.D, Mathez E., Maggiore C, Mitchell T.E and Fogel R (1991). Oxygen in diamond by the nuclear microprobe: Analytical technique and initial results. *Proc. 5th Int. Kimberlite Conference, Araxá (Abstract volume)*, 20 - 22.

Blundy J.D, Broadholt J.P and Woods B.J (1991). Carbon-fluid equilibria and the oxidation state of the upper mantle. *Nature*, **349**: 321 - 324.

Bottinga Y (1969). Carbon isotope fractionation between graphite, diamond and carbon dioxide. *Earth Planet. Sci. Lett.*, **5**: 301 - 307.

Bottinga Y and Javoy M (1989). MORB degassing: evolution of CO_2. *Earth Planet. Sci. Lett.*, **95**: 215 - 225.

Bottinga Y and Javoy M (1990). MORB degassing: Bubble growth and ascent. *Chem. Geol.*, **81**: 255 - 270.

Boyd F.R (1973). A pyroxene geotherm. *Geochim. Cosmochim. Acta*, **37**: 2533 - 2546.

Boyd F.R, Pearson D.G, Nixon P.H and Mertzman S.A (1993). Low-calcium garnet harzburgites from southern Africa: their relation to craton structure and diamond crystallization. *Contrib. Mineral. Petrol.*, **113**: 352 - 366.

Boyd S.R (1988). A study of carbon and nitrogen isotopes from the Earth's mantle. *Ph.D Thesis (Unpubl.). Open University, Milton Keynes.*

Boyd S.R and Pillinger C.T (1991). Rubidium sulphate - ammonium sulphate solid solution: A standard for use during the determination of nitrogen abundance and isotopic composition at the ppm level by static vacuum mass spectrometry. *Anal. Chem.*, **63**: 1332 - 1335.

Boyd S.R, Mattey D.P, Pillinger C.T, Milledge H.J, Mendelsson M and Seal M (1987). Multiple growth events during diamond genesis: an integrated study of C and N isotopes and N aggregation state in coated stones. *Earth Planet. Sci. Lett.*, **86**: 341 - 353.

Boyd S.R, Pillinger C.T, Milledge H.J, Mendelsson M.J and Seal M (1988a). Fractionation of N isotopes in a synthetic diamond of mixed crystal habit. *Nature*, **331**: 604 - 607.

Boyd S.R, Pillinger C.T.P, Milledge H.J, Mendelssohn M.J and Seal M (1992). C and N isotopic composition and the infrared absorption spectra of coated diamonds: evidence for the regional uniformity of CO_2 - H_2O fluids in lithospheric mantle. *Earth Planet. Sci. Lett.*, **108**: 139 - 150.

Boyd S.R, Wright I.P, Franchi I.A and Pillinger C.T (1988b). Preparation of sub-nanamole quantities of nitrogen gas for stable isotope analysis. *J. Phys. E: Sci. Instrum.*, **21**: 876-885.

Bryndzia L.T, Wood B.J and Dick H.J.B (1989). The oxidation state of the earths sub-oceanic mantle from oxygen thermobarometry of abyssal spinel peridotites. *Nature*, **341**: 526 - 527.

Burgess R, Turner G and Harris J.W (1992). ^{40}Ar - ^{39}Ar laser probe studies of clinopyroxene inclusions in eclogitic diamonds. *Geochim. Cosmochim. Acta*, **56**: 389 - 402.

Burgess R, Turner G, Laurenzi M and Harris J.W (1989). $^{40}Ar/^{39}Ar$ laser probe dating of individual clnopyroxene inclusions in Premier diamonds. *Earth Planet. Sci. Lett.*, **94**: 22 - 28.

Calvert S.E, Nielsen B and Fontugne M.R (1992). Evidence from nitrogen isotope ratios for enhanced productivity during formation of eastern Mediterranian sapropels. *Nature*, **359**: 223 - 225.

Carlisle D.B and Braman D.R (1991). Nanometer sized diamonds in the Cretaceous Tertiary boundary clay of Alberta. *Nature*, **352**: 708 - 709.

Chen Y.D, Pearson N.J, O'Reilly S.Y and Griffin W.L (1991). Applications of olivine-orthopyroxene-spinel oxygen barometers to the redox state of the upper mantle. *J. Petrol.*, **Orogenic lherzolites and mantle processes, special volume**: 291 - 306.

Chrenko R.M, Tuft R.E and Strong H.M (1977). Transformation of the state of nitrogen in diamond. *Nature*, **271**: 141 - 144.

Clackson S.G, Moore M, Walmsley J.C and Woods G.S (1990). The relationship between platelet size and the frequency of the B' infrared absorption peak in type Ia diamond. *Philos. Mag. B*, **62**: 115 128.

Clark C.D and Davey S.T (1984). One phonon infrared absorption in diamond. *J. Phys. C. Solid State Phys.*, **17**: 1127 - 1140.

Cline J.D and Kaplan I.R (1975). Isotope fractionation of dissolved nitrate during denitrification in the eastern tropical Pacific Ocean. *Marine Chem.*, **3**: 271 - 299.

Collins A.T (1978). Migration of nitrogen in electron irradiated type Ib diamond. *J. Phys. C. Solid State Phys.*, **11**: L417 - 412.

Collins A.T (1980). Vacancy enhanced aggregation of nitrogen in diamond. *J. Phys. C. Solid State Phys.*, **13**: 2641 - 2650.

Collins A.T (1989). The polarised absorption and cathodoluminescence associated with the 1.40 eV center in synthetic diamond. *J. Phys. Condensed Matter*, **1**: 439 - 450.

Collins A.T and Woods G.S (1987). Isotope shifts of nitrogen related localised mode vibrations in diamond. *J. Phys. C. Condensed state physics*, **20**: L797 - L801.

Cooper G.I, Mendelssohn M.J and Milledge H.J (1989). High temperature/high pressure experiments with natural diamonds. *Diamond Conference Abstracts, Bristol*, 13 - 14.

Cox K.G, Bell J.D and Pankhurst R.J (1979). The interpretation of igneous rocks. *George Allen and Unwin, London. 450 pp.*

Craig H (1953). The geochemistry of the stable carbon isotopes. *Geochim. Cosmochim. Acta*, **3**: 53 - 92.

Daniels L.R.M (1991). Diamonds and related minerals from the Dokolwayo kimberlite, Kingdom of Swaziland. *Ph.D thesis (Unpubl.). University of Cape Town, South Africa.*

Daniels L.R.M and Gurney J.J (1991). Oxygen fugacity constraints on the southern African lithosphere. *Contrib. Mineral. Petrol.*, **108**: 154 - 164.

Davies G (1976). The A nitrogen aggregate in diamond. Its symmetry and possible structure. *J. Phys. C. Solid State Phys.*, **9**: L537 - 532.

Davies G (1979). Dynamic Jahn-Teller distortions at trigonal optical centers in diamond. *J. Phys. C. Solid State Phys.*, **12**: 2551 - 2566.

Davies G (1981). Decomposing the IR absorption spectra of diamonds. *Nature*, **290**: 40 - 41.

Davies G (1984). Diamond. *Adam Hilgar, Bristol*, 255pp.

Davies G, Welbourn C.M and Loubser J.H.N (1978). Optical and electron paramagnetic effects in yellow type Ia diamonds. *Diamond Res.*, 22 - 30.

Dawson J.B (1980). Kimberlites and their xenoliths. *Springer Verlag, New York*, 252pp.

Dawson J.B (1989). Geographic and time distribution of kimberlites and lamproites: relationship to tectonic processes. *In: Ross J, Jaques A.L, Ferguson J, Green D.H, O'Reilly S.Y.O, Danchin R.V and Janse A.J.A (Eds.). Kimberlites and related rocks. Volume 2. Their mantle/crust setting, diamonds and diamond exploration.*, **Geological Society of Australia Spec. Publ. 14**: 323 - 342.

Dawson J.B and Smith J.V (1975). Occurrence of diamond in a mica-garnet lherzolite from kimberlite. *Nature*, **254**: 580 - 581.

De Sa E.S and Davies G (1977). Uniaxial stress studies of the 2.498 eV (H4), 2.417 and 2.536 eV vibronic bands in diamond. *Proc. Roy. Soc. Lond.*, **A357**: 231 - 251.

Deakin A.S and Boxer G.L (1989). Argyle AK1 diamond size distribution; the use of fine diamonds to predict the occurrence of commercial sized diamonds. *In: Ross J, Jaques A.L, Ferguson J, Green D.H, O'Reilly S.Y.O, Danchin R.V and Janse A.J.A (Eds.). Kimberlites and related rocks. Volume 2. Their mantle/crust setting, diamonds and diamond exploration.*, **Geological Society of Australia Spec. Publ. 14**: 1117 - 1122.

Degens E.T (1969). Biogeochemistry of stable carbon isotopes. *In: Eglington G and Murphy M.T.J (Eds.). Organic geochemistry; methods and results*, : 304 - 329.

Deines P (1970). The carbon and oxygen isotopic composition of carbonates from the Oka carbonatite complex, Quebec, Canada. *Geochim. Cosmochim. Acta*, **34**: 1199 - 1225.

Deines P (1980a). The carbon isotopic composition of diamonds: relationship to diamond shape, color, occurrence and vapour composition. *Geochim. Cosmochim. Acta*, **44**: 943 - 961.

Deines P (1980b). The isotopic composition of reduced organic carbon. *In; Fritz P and Fontes J.Ch (Eds.). Handbook of environmental geochemistry. Elsvier*, **Vol. 1**: 239 - 406.

Deines P and Gold D.P (1973). The isotopic composition of carbonatite and kimberlite carbonates and their bearing on the isotopic composition of deep-seated carbon. *Geochim. Cosmochim. Acta*, **37**: 1703 - 1733.

Deines P, Gurney J.J and Harris J.W (1984). Associated chemical and carbon isotopic composition variations in diamonds from Finsch and Premier kimberlite, South Africa. *Geochim. Cosmochim. Acta*, **48**: 325 - 342.

Deines P, Harris J.W and Gurney J.J (1987). Carbon isotopic composition, nitrogen content and inclusion composition of diamonds from the Roberts Victor kimberlite, South Africa: Evidence for ^{13}C depletion in the mantle. *Geochim. Cosmochim. Acta*, **51**: 1227 - 1243.

Deines P, Harris J.W and Gurney J.J (1991a). The carbon isotopic composition and nitrogen content of lithospheric and asthenospheric diamonds from the Jagersfontein and Koffiefontein kimberlites, South Africa. *Geochim. Cosmochim. Acta*, **55**: 2615 - 2626.

Deines P, Harris J.W and Gurney J.J (1993). Depth-related carbon isotope and nitrogen concentration variability in the mantle below the Orapa kimberlite, Botswana, Africa. *Geochim. Cosmochim. Acta*, **57**: 2781 - 2796.

Deines P, Harris J.W, Robinson D.N, Gurney J.J and Shee S.R (1991b). Carbon and oxygen isotope variations in diamond and graphite eclogite eclogites from Orapa, Botswana and the nitrogen contents of their diamonds. *Geochim. Cosmochim. Acta*, **55**: 515 - 524.

Deines P, Harris J.W, Spear P.M and Gurney J.J (1989). Nitrogen and ^{13}C contents of Finsch and Premier diamonds and their implications. *Geochim. Cosmochim. Acta*, **53**: 1367 - 1378.

Derjaguin B.V and Fedoseev D.V (1977). Growth of diamond and graphite from the gas phase. *Nauka, Moscow.*

Des Marais D.J (1985). Carbon exchange between the mantle and the crust and its effect on the atmosphere: today compared to Archean time. *Geophys. Mono.*, **32**: 602 - 611.

Des Marais D.J and Moore J.G (1984). Carbon and its isotopes in mid-oceanic basaltic glasses. *Earth Planet. Sci. Lett.*, **69**: 43 - 57.

Eckermann H. von, Ubisch H. von and Wickman F.E (1952). A preliminary investigation into the isotopic composition of carbon from some alkaline intrusions. *Geochim. Cosmochim. Acta*, **2**: 207 - 210.

Eldridge C.S, Compston W, Williams I.S, Harris J.W and Bristow J.W (1991). Isotope evidence for the involvement of recycled sediments in diamond formation. *Nature*, **535**: 649 - 653.

Erlank A.J, Waters F.G, Hawkesworth C.J, Haggerty S.E, Allsopp H.L, Rickard R.S and Menzies M (1987). Evidence for mantle metasomatism in mantle peridotite nodules from the Kimberley Pipes, South Africa. *In: Menzies M.A and Hawkesworth C.J (Eds.). Mantle metasomatism. Academic Press Geology Series*: 221 - 311.

Erskine J.D and Nellis W.J (1991). Shock induced martensitic phase transformation of oriented graphite to diamond. *Nature*, **349**: 317 - 319.

Evans T (1976). Diamond. *Contemp. Phys.*, **17**: 45 - 70.

Evans T and Harris J.W (1989). Nitrogen aggregation, inclusion equilibration temperatures and the age of diamonds. *In: Ross J, Jaques A.L, Ferguson J, Green D.H, O'Reilly S.Y.O, Danchin R.V and Janse A.J.A (Eds.). Kimberlites and related rocks. Volume 2. Their mantle/crust setting, diamonds and diamond exploration.*, **Geological Society of Australia Spec. Publ. 14**: 1001 - 1006.

Evans T and Phaal C (1962). Imperfections in type I and type II diamonds. *Proc. Roy. Soc. Lond.*, **A270**: 538 - 552.

Evans T and Qi Z (1982). The kinetics of the aggregation of nitrogen atoms in diamond. *Proc. Roy. Soc. Lond.*, **A381**: 159 - 178.

Evans T, Qi Z and Maguire J (1981). The stages of nitrogen aggregation in diamond. *J. Phys. C. Solid State Phys.*, **14**: L379 - 384.

Eversole W.G (1962). U.S. Patent *3030*, **188**.

Exley R.A, Boyd S.R, Mattey D.P and Pillinger C.T (1987). Nitrogen isotope geochemistry of basaltic glasses: implications for mantle degassing and structure. *Earth Planet. Sci. Lett.*, **81**: 163 - 174.

Exley R.A, Mattey D.P, Boyd S.R, and Pillinger S.R (1986a). Nitrogen isotope geochemistry of basaltic glasses. *Terra Cognita*, **6**: 191.

Exley R.A, Mattey D.P, Claque D.A and Pillinger C.T **(1986b).** Carbon isotope systematics of a mantle "hotspot": a comparison of LOIHI Seamount and MORB glasses. *Earth Planet. Sci. Lett.*, **78**: 189 - 199.

Fallick A.E **(1980).** On the measurement of the valve-mixing correction of the changeover valve of a duel inlet gas source mass spectrometer. *Int. J. Mass Spec. Ion Physics*, **36**: 47 - 55.

Foley S.F **(1988).** The genesis of continental basic alkaline magmas. An interpretation in terms of redox melting. *J. Petrol*, **Spec. Lithos Issue**: 139 - 161.

Frank F.C **(1967).** Defects in diamond. *In: Burls J (Ed.). Science and technology of industrial diamonds, Vol. 1. Science Ind. Diamond Info. Bur., London*, : pp119 - 136.

Fraser K **(1987).** Petrogenesis of kimberlites from South Africa and lamproites from Western Australia and North America. *Ph.D Thesis (Unpubl.). Open University, Milton Keynes.*

Fraser K.J, Hawkesworth C.J, Erlank A.J, Mitchell R.H and Scott-Smith B.H **(1985).** Sr, Nd and Pb isotope and minor element geochemistry of lamproites and kimberlites. *Earth Planet. Sci. Lett.*, **76**: 57 - 70.

Friedman I and O'Neil J.R **(1977).** Compilation of the stable isotope fractionation factors of geochemical interest. *Fleischer M (Ed.). Data of Geochemistry, Sixth edition. Geological Survey Professional paper 440,* **Chapter KK**.

Galimov E.M **(1984a).** $^{13}C/^{12}C$ of diamonds. Vertical zonality of diamond formation in the lithosphere. *Doklady. Proc. 27th Int. Geol. Congress, Moscow*, **11**: 279 - 307.

Galimov E.M **(1984b).** The relation between formation conditions and variations in stable isotope compositions of diamonds *Geokhimiya*, **8**: 1091 - 1118.

Galimov E.M **(1991).** Isotope fractionation related to kimberlite magmatism and diamond formation. *Geochim. Cosmochim. Acta*, **55**: 1697 - 1708.

Ganpathy R and Anders E **(1974).** Bulk compositions of the moon and Earth, estimated from meteorites. *Proc. 5th Lunar Sci. Conf.*, 1181 - 1206.

Gee R.D **(1979).** Structure and tectonic style of the Western Australian Shield. *Tectonophysics*, **58**: 327 - 369.

Grady M.M Wright I.P, Swart P.K and Pillinger C.T **(1988).** The carbon and oxygen isotopic composition of meteoritic carbonates. *Geochim.Cosmochim. Acta*, **52**: 2855 - 2866.

Grady M.M, Wright I.P, Carr L.P and Pillinger C.T **(1986).** Compositional differences in enstatite chondrites based on carbon and nitrogen stable isotope measurements. *Geochim. Cosmochim. Acta*, **50**: 2799 - 2813.

Gregor C.B, Garrels R.M, Mackenzie R.T and Maynard J.B **(1988).** Chemical cycles in the evolution of the Earth. *John Wiley and sons. New York*, **276pp**.

Greiner N.R, Phillips D.S, Jahnson J.D and Volk F **(1988).** Diamonds in detonation soot. *Nature*, **333**: 440 - 442.

Griffin W.L, Gurney J.J and Ryan C.G **(1992).** Variations in trapping temperatures and trace elements in peridotite suite inclusions from African diamonds: evidence for two inclusion suites and implications for lithosphere stratigraphy. *Contrib. Mineral. Petrol.*, **110**: 1 - 15.

Griffin W.L, Jaques A.L, Sie S.H, Ryan C.G, Cousens D.R and Suter G.F **(1988).** Conditions of diamond growth: a proton microprobe study of inclusions in West Australian diamonds. *Contrib. Mineral. Petrol.*, **99**: 143 - 158.

Griffin W.L, Sobolev N.V, Ryan C.G, Pokhilenko N.P, Win T.T and Yefimova E.S **(1993).** Trace elements in garnets and chromites: Diamond formation in the Siberian lithosphere. *Lithos*, **29**: 235 - 256.

Gurney J.J **(1986).** Diamonds. *Proc. 4th Int. Kimberlite Conference, Perth (Abstract volume)*, 363 - 367.

Gurney J.J **(1989).** Diamonds. *In: Ross J, Jaques A.L, Ferguson J, Green D.H, O'Reilly S.Y.O, Danchin R.V and Janse A.J.A (Eds.). Kimberlites and related rocks. Volume 2. Their mantle/crust setting, diamonds and diamond exploration.*, **Geological Society of Australia Spec. Publ. 14**: 935 - 965.

Gurney J.J **(1991).** Diamonds deliver the dirt. *Nature*, **535**: 601 - 602.

Gurney J.J, Harris J.W and Rickard R.S **(1984).** Silicate and oxide inclusions in diamonds from the Orapa Mine, Botswana. *In: Kornprobst J (Ed.). Kimberlites II: The mantle and crust-mantle relationships; Developments in petrology IIB*: 3 - 9.

Gurney J.J, Moore R.O, Otter M.L, Kirkley M.B, Hops J.J and McCandless T.E **(1991).** Southern African kimberlites and their xenoliths. *In: Kampunzu A.B and Lubala R.T. (Eds.). Magmatism in extensional structural settings. The Phanerozoic African Plate. Springer-Verlag, Berlin*, **14**: 495 - 536.

Guthrie G.D Jr, Veblen D.R, Navon O and Rossman G.R **(1991).** Submicrometer fluid inclusions in turbid diamond coats. *Earth Planet. Sci. Lett.*, **105**: 1 - 12.

Haggerty S.E **(1986).** Diamond genesis in a multiply-constrained model. *Nature*, **320**: 34 - 38.

Hall A.E and Smith C.B **(1984).** Lamproite diamonds - Are they different? *In: Glover J.E and Harris P.G (Eds.). Kimberlite occurrence and origin: A basis for conceptual models in exploration. Geol. dept. & Univ. extension, Univ. Western Australia Publication*, **8**: 167 - 212.

Hancock S.L and Rutland R.W.R **(1984).** Tectonics of an early proterozoic geosuture: The Halls Creek orogenic sub-province, Northwestern Australia. *J. Geodynamics*, **1**: 387 - 432.

Hargraves R.B and Onstott T.C **(1980).** Palaeomagnetic results from some southern African kimberlites and their tectonic significance. *J. Geophys. Res.*, **85**: 3587 - 3596.

Harris J.W (1987). Recent physical chemical and isotopic research of diamond. *In: Nixon P.H (Ed.) Mantle xenoliths. Wiley, Chichester, England*, 427 - 500.

Harris J.W and Collins A.T (1985). Studies of Argyle diamond. *Ind. Diamond Rev.*, **Mar-85**: 128 - 130.

Harris J.W, and Spear P.M (1986). Systematic studies of nitrogen in diamonds. *Proc. 4th Int. Kimberlite Conference, Perth (Abstract volume)*, 398 - 400.

Hart R.J, Damarupurshad A, Sellschop J.P.F, Meyer H.O.A, McCallum M.E and Koeberl C (1991). The trace element anlysis of single diamond crystal by neutron activation analysis. *Proc. 5th Int. Kimberlite Conference, Araxá (Abstract volume)*, 163 - 166.

Harte B and Otter M (1992). Carbon isotope measurements on diamonds. *Chem. Geol. (Isotope Geoscience Section)*, **101**: 177 - 183.

Hawkesworth C.J, Fraser K.J and Rogers N.W (1985). Kimberlites and lamproites: extreme products of mantle enrichment processes. *Trans. Geol. Soc. S. Af.*, **88**: 439 - 448.

Hawthorne J.B (1975). Model of a kimberlite pipe. *Phys. Chem. Earth*, **9**: 1 - 15.

Helmstaedt H and Doig R (1975). Eclogite nodules from kimberite pipes of the Colorado Plateau - samples of subducted Fransiscan-type lithosphere. *In: Ahrens L.H, Dawson J.B, Duncan A.R and Erlank A.J (Eds.). Physics and chemistry of the Earth, 9. Pergammon Press, Oxford*, : 95 - 112.

Helmstaedt H and Gurney J.J (1984). Kimberlites of South Africa - are they related to subduction? *In: Kornprobst J (Ed.). Kimberlites 1: Kimberlites and related rocks. Developments in petrology IIA. Elsvier, Amsterdam*, : 425 - 434.

Hill S.J (1989). A study of the diamonds and xenoliths of the Star kimberlite, Orange Free State, South Africa. *Ms.C Thesis (Unpubl.). University of Cape Town, South Africa.*

Hirsch P.B, Hutchison J.L and Titmarsch J.M (1986a). Voidites in diamond: Evidence for a crystalline phase containing nitrogen. *Diamond Conference abstracts, London.*

Hirsch P.B, Pirous P and Barry J.C (1986b). The transformation of platelets into dislocation loops and voidites. *Diamond Conference abstracts, London.*

Hoefs J (1987). Stable isotope geochemistry. *3rd edition, Springer - Verlag, Berlin. 241pp.*

Hoefs J and Frey M (1976). The isotopic composition of organic matter in a metamorphic profile from the Swiss Alps. *Geochim. Cosmochim. Acta*, **40**: 945 - 951.

Hoering T (1956). Variations in the nitrogen isotope abundance. *Proc. 2nd Conf. Nucl. Process. Geol. Settings.*

Honda M, Reynolds J.H, Roedder E and Epstein S (1987). Noble gases in diamonds: Occurences of solarlike helium and neon. *J. Geophys. Res.*, **92**: 12507 - 12521.

Honma H and Ithara Y (1981). Distribution of ammonium in minerals of metamorphic and granitic rocks. *Geochim. Cosmochim. Acta*, **45**: 983 - 988.

Ionov D.A and Wood B.J (1992). The oxidation state of subcontinental mantle: oxygen thermobarometry of mantle xenoliths from central Asia. *Contrib. Mineral. Petrol.*, **111**: 179 - 193.

Jagoutz E, Dawson J.B, Hoernes S, Spettel B and Wänke H (1984). Anorthositic ocean crust in Archean earth. *14th. LunarPlaet. Sci. Conf. Lunar Planet. Sci. Inst., Houston, Texas.*, : pp 395 - 396.

Jambon A (1980). Isotopic fractionation; a kinetic model for crystals growing from magmatic melts. *Geochim. Cosmochim. Acta*, **44**: 1373 - 1380.

Jaques A.L, Boxer G, Lucas H and Haggerty S.E (1986a). Mineralogy and petrology of the Argyle lamproite pipe, Western Australia. *Proc. 4th Int. Kimberlite Conference, Perth (Abstract volume)*, 48 - 50.

Jaques A.L, Gregory G.P, Lewis J.D and Ferguson J (1982). The ultrapotassic rocks of the West Kimberley region, Western Australia, and a new class of diamondiferous kimberlite. *Terra Cognita*, **2**: 251 - 252.

Jaques A.L, Hall A.E, Sheraton J.W, Smith C.B, Sun S.S, Drew R.M, Foudoulis C and Ellingsen K (1989). Composition of crystalline inclusions and C-isotopic composition of Argyle and Ellendale diamonds. *Geol. Soc. Australia, Special Publ. 14*, **#2**: 966 - 989.

Jaques A.L, Lewis J.D and Smith C.B (1986b). The kimberlitic and lamproitic rocks of Western Australia. *Geol. Survey. Western Australia Bulletin*, **132**.

Jaques A.L, Lewis J.D, Smith C.B, Gregory G.P, Ferguson J, Chappell B.W and McCulloch M.T (1984a). The diamond - bearing ultra potassic (lamproitic) rocks of the West Kimberley region, Western Australia *In: Kornprobst J (Ed.). Kimberlites 1: Kimberlites and related rocks. Developments in petrology IIA. Elsvier, Amsterdam*, 225 - 254.

Jaques A.L, O'Neill H.St.C, Smith C.B, Moon J and Chappell B.W (1990). Diamondiferous peridotite xenoliths from the Argyle (AK1) lamproite pipe, Western Australia. *Contrib. Mineral. Petrol.*, **104**: 255 - 276.

Jaques A.L, Webb A.W, Fanning C.M, Black L.P, Pidgeon R.T, Ferguson J, Smith C.B and Gregory G.P (1984b). The age of the diamond-bearing pipes and associated leucite lamproites of the West Kimberley region, Western Australia. *J. Australian Geol. and Geophys.*, **9**: 1 - 7.

Javoy M, and Pineau F (1986). Nitrogen isotopes in mantle materials. *Terra Cognita*, **6**: 103.

Javoy M, Pineau F and Allègre C.J (1982). Carbon geodynamic cycle. *Nature*, **300**: 171 - 173.

Javoy M, Pineau F and Delorme H (1986). Carbon and Nitrogen isotopes in the mantle. *Chem. Geol.*, **57**: 41 - 62.

Javoy M, Pineau F and Demaiffe D (1984). Nitrogen and Carbon isotopic composition in the diamonds of Mbuji Mayi (Zaire). *Earth Planet. Sci. Lett.*, **68**: 399 - 412.

Javoy M, Pineau F and Iiyama I (1978). Experimental determination of the isotopic fractionation between gaseous CO_2 and carbon dissolved in tholeiitic magma. *Contrib. Mineral. Petrol.*, **67**: 35 - 39.

Kaiser W and Bond L (1959). Nitrogen, a major impurity in common type I diamond. *Phys. Rev.*, **115**: 857 - 863.

Kaminsky F (1980). Notes of the All-American mineralogical company. *Translated from the Russian by Ashton Mining Ltd., Western Australia*, **Chapter 6**: 488 - 493.

Kaminsky F, Chernaya I.P and Cherny A.V (1986). Occurrence of diamond in alkaline picrites and alkaline ultrabasic rocks. (In Russian) *Mineral. Zh.*, **8**: 39 - 45.

Kamiya Y and Lang A.R (1965). On the structure of natural diamonds. *Philos. Mag. B*, **11**: 347 - 356.

Kendall C and Grim E (1990). *Anal. Chem.*, **62**: 526 - 529.

Kennedy G.C and Nordlie B.E (1976). The genesis of diamond deposits. *Econ. Geol.*, **63**: 495 - 503.

Kerridge J.F (1985). Carbon, Hydrogen and Nitrogen in carbonaceous chondrites: Abundances and isotopic composition in bulk samples. *Geochim. Cosmochim. Acta*, **49**: 1707 - 1714.

Kesson S.E and Ringwood A.E (1989). Slab-mantle interactions 2. The formation of diamonds. *Chem. Geol.*, **78**: 97 - 118.

Kim K-R and Craig H (1990). Two - isotope characterisation of N_2O in the Pacific Ocean and constraints on its origin in deep water. *Nature*, **347**: 58 - 61.

Kirkley M.B, Gurney J.J, Otter M.L, Hill S.J and Daniels L.R (1991). The application of C isotope measurements to the identification of the source of C in diamonds: a review. *App. Geochemistry*, **6**: 477 - 494.

Kirkley M.B, Harte B and Gurney J.J (1993). Crustal plagioclase-rich protoliths for Roberts Victor kyanite eclogites. *Contrib. Mineral. Petrol.*, **Submitted**.

Kirkley M.B, Smith H.S and Gurney J.J (1986). Kimberlite carbonates: A carbon - oxygen stable isotope study. *Proc. 4th Int. Kimberlite Conference, Perth (Abstract volume)*, 57 - 59.

Kovalsky V.V, Galimov E.M and Prohorev V.S (1972). The carbon isotopic composition of the Yakut coloured diamond varieties. *Dokl. Acad. Nauk. SSSR*, **203**: 440 - 443.

Kramers J.D (1979). Pb, U, Sr, K and Rb in inclusion bearing diamonds and mantle derived xenoliths from southern Africa. *Earth Planet. Sci. Lett.*, **42**: 58 - 70.

Kramers J.D, Smith C.B, Lock N.P, Harmon R.S and Boyd F.R (1981). Can kimberlites be generated from an ordinary mantle? *Nature*, **291**: 53 - 56.

Kratsov A.I, Kropotova O.I, Voytov G.I and Ivanov V.A (1977). Isotopic composition of carbon of diamonds and carbon compounds in pipes of the East Siberian diamond province. *Dokl. Acad. Nauk. SSSR*, **279**: 206 - 208.

Kung C-C and Clayton R (1978). Nitrogen abundances and isotopic compositions in stony meteorites *Earth Planet. Sci. Lett.*, **38**: 421 - 435.

Kyser T K (1986). Stable isotope variations in the mantle. *In: Valley J.W, Taylor H.P and O'Neil J.R (Eds.). Stable isotopes in high temperature geological processes.*, **Reviews in mineralogy, V16. Mineralogical Society of America**: 141 - 164.

Kyser T.K (1990). Stable isotopes in the continental lithospheric mantle. *In: Menzies M (Ed.) Continental mantle.*, **Clarendon Press, Oxford**: 127 - 156.

Kyser T.K, O'Neil J.R and Carmichael I.S.E (1981). Oxygen isotope thermometry of basic lavas and mantle nodules. *Contrib. Mineral. Petrol.*, **77**: 11 - 23.

Lal D (1989). An important source of ^4He (and ^3He) in diamonds. *Earth Planet. Sci. Lett.*, **96**: 1 - 7.

Lang A.R (1964). A proposed structure for nitrogen impurity platelets found in diamond. *Proc. Phys. Soc.*, **84**: 871 - 876.

Lang A.R (1979). Internal structure. *In: Field J.E (Ed.). The properties of diamond*, 425 - 469.

Lang A.R and Walmsley J.C (1983). Apatite inclusions in natural diamond coat. *Phys. Chem. Minerals*, **9**: 6 - 8.

Langmuir C.H, Vocke R.D. Jr., Hanson G.N and Hart S.R (1978). A general mixing equation with applications to Icelandic basalts. *Earth. Planet. Sci. Lett.*, **37**: 380 - 392.

Lee D.C, Boyd S.R, Griffin B.J, Griffin B.W and Reddicliffe T (1991). Coanjula diamonds, Northern Territory, Australia. *Proc. 5th Int. Kimberlite Conference, Araxá (Abstract volume)*, 231 - 233.

Lerman A, Mackenzie F.T and Ver L.M (1993). Global nitrogen cycle within the coupled C - N - P system. *Chem. Geol.*, **107**: 389 - 392.

Levinson A.A, Bradshaw P.M.D and Thomson I (1987). Practical problems in exploration geochemistry. *Applied Publishing Ltd. Wilmette, Illinois*, 269pp.

Lewis R.S, Anders and Draine B.T (1989). Properties, detectability and origin of intersteller diamonds in meteorites. *Nature*, **339**: 117 - 121.

Lewis R.S, Tang M, Wacker J.F, Anders E and Steel E (1987). Intersteller diamonds in meteorites. *Nature*, **326**: 160 - 162.

Létolle R (1980). Nitrogen - 15 in the natural environment. *In: Fritz P and Fontes JCh (Eds). Handbook of environmental geochemistry. Elsvier Amsterdam*, 407 - 433.

Loubser J.H.N and Wright A.C.J (1973). Discussion of the ENDOR and ESR spectra of diamonds with the N3 optical system. *Diamond Res.*, 16 - 20.

Lubala R.T (1991). African kimberlites: Introduction. *In: Kampunzu A.B and Lubala R.T. (Eds.). Magmatism in extensional structural settings. The Phanerozoic African Plate. Springer-Verlag, Berlin*, 490 - 494.

MacGregor I.D and Manton W.I (1986). Roberts Victor eclogites: Ancient oceanic crust. *J. Geophys. Res.*, 91: 14063 - 14079.

Mainwood A (1979). Substitutional impurities in diamond. *J. Phys. C*, 12: 2543 - 2549.

Marty B and Jambon A (1987). $C/^3He$ in volatile fluxes from the solid earth: implications for carbon geodynamics. *Earth Planet. Sci. Lett.*, 83: 16 - 26.

Masuda A and Akagi T (1988). The cause of misleading K-Ar ages of diamonds, actually young but apparently older than the solar system. *Geochem. J.*, 22: 139 - 142.

Mathez E.A (1987). Carbonaceous matter in mantle xenoliths: composition and relevance to the isotopes. *Geochim. Cosmochim. Acta*, 51: 2339 - 2347.

Mattey D.P (1991). Carbon dioxide solubility and carbon isotopic fractionation in basaltic melt. *Geochim. Cosmochim. Acta*, 55: 3467 - 3475.

Mattey D.P, Exley R.A and Pillinger C.T (1989). Isotopic composition of CO_2 and dissolved carbon species in basaltic glass. *Geochim. Cosmochim. Acta*, 53: 2377 - 2386.

Mattey D.P, Taylor W.R, Green D.H and Pillinger C.T (1990). Carbon isotope fractionation between CO_2 vapour, silicate and carbonate melts: an experimental study to 30kbar. *Contrib. Mineral. Petrol.*, 104: 492 - 505.

Mattioli G.S, Baker M.B, Rutter M.J and Stolper E.M (1989). Upper mantle oxygen fugacity and its relationship to metasomatism. *J. Geol.*, 97: 521 - 536.

McCallum D.E and Eggler D.H (1976). Diamonds in an upper mantle nodule in Southern Wyoming. *Science*, 192: 253 - 256.

McCandless T.E (1989). Microdiamonds from Sloan 1 and 2 kimberlites, Colorado, U.S.A. *Workshop on diamonds. 28th International Geological Congress, Washington (Abstract)*, 44 - 46.

McCandless T.E and Gurney J.J (1989). Sodium in garnet and potassium in clinopyroxene: criteria for classifying mantle eclogites. *In: Ross J, Jaques A.L, Ferguson J, Green D.H, O'Reilly S.Y.O, Danchin R.V and Janse A.J.A (Eds.). Kimberlites and related rocks. Volume 2. Their mantle/crust setting, diamonds and diamond exploration.*, **Geological Society of Australia Spec. Publ. 14**: 827 - 832.

McCandless T.E, Kirkley M.B, Robinson D.N, Gurney J.J, Griffin W.L, Cousens D.R and Boyd F.R (1989). Some initial observations on polycrystalline diamonds mainly from Orapa: abstract. *Workshop on diamonds. 28th International Geological Congress, Washington (Abstract)*, 47 - 51.

McCandless T.E, Waldman M.A and Gurney J.J (1991). Macro- and micro-diamonds from Arkansas lamproites; morphology, inclusions and isotope geochemistry. *Proc. 5th Int. Kimberlite Conference, Araxá (Abstract volume)*, 264 - 266.

McCulloch M.T, Jaques A.L, Nelson D.R and Lewis J.D (1983). Nd and Sr isotopes in kimberlites and lamproites from Western Australia: an enriched mantle origin. *Nature*, 302: 400 - 403.

McElroy M.B, Yung Y.L and Nier A.O (1976). Isotopic composition of nitrogen: Implications for the past history of Mars' atmosphere. *Science*, 194: 70 - 72.

McKenzie D (1989). Some remarks on the movements of small melt fractions in the mantle. *Earth Planet. Sci. Lett.*, 95: 53 - 72.

McKenzie D and Bickle M.J (1988). The volume and composition of melt generated by extension of the lithosphere. *J. Petrol*, 29: 625 - 679.

McKinney C.R. McCrea J.M, Epstein S, Allen H.A and Urey H.C (1950). Improvements in mass spectrometers for the measurement of small abundance ratios. *Rev. Sci. Instr.*, 21: 724 - 730.

McKirdy D.M and Powell T.G (1974). Metamorphic alteration of carbon isotopic composition in ancient sedimentary organic matter: new evidence from Australia and South Africa. *Geology*, 2: 591 - 595.

Menzies M.A (1988). Mantle melts in diamonds. *Nature*, 335: 769 - 770.

Meyer H.O.A (1985). Genesis of diamond: a mantle saga. *Am. Mineral.*, 70: 344 - 355.

Meyer H.O.A (1987). Inclusions in diamond. *In: P.H. Nixon (Ed.). Mantle xenoliths. John Wiley and Sons*, 501 - 524.

Milledge H.J and Meyer H.O.A (1962). Nitrogen 14 in natural diamonds. *Nature*, 195: 171 - 172.

Milledge H.J, Mendelssohn M.J, Boyd S.R, Pillinger C.T, van Heerden L and Seal M (1989). Investigations of a suite of diamonds from the Finsch mine. *Diamond Conference Abstracts, Bristol.*

Milledge H.J, Mendelssohn M.J, Seal M, Rouse J.E, Swart P.K and Pillinger C.T (1983). Carbon isotope variation in spectral type II diamonds. *Nature*, 303: 791 - 792.d

Mitchell R.H (1986). Kimberlites, mineralogy, geochemistry, petrology. *Plenum Press. London*, 442pp.

Moore M (1985). Diamond morphology. *Ind. Diamond Rev.*, 45 #507: 67 - 71.

Moore M (1988). X-ray studies of the growth of natural diamond. *Ind. Diamond Rev.*, Feb-88: 59 - 64.

Moore M and Lang A.R (1972). On the internal structure of natural diamonds of cubic habit. *Philos. Mag. B*, 26: 1313 - 1325.

Moore R.O (1986). A study of kimberlites, diamonds and associated rocks and minerals from the Monestry Mine, South Africa. *Ph.D Thesis (Unpubl.). University of Cape Town, South Africa.*

Moore R.O and Gurney J.J (1985). Pyroxene solid solution in garnets included in diamond. *Nature*, **318**: 553 - 555.

Moore R.O and Gurney J.J (1989). Mineral inclusions in diamond from the Monestry kimberlite, South Africa. *In: Ross J, Jaques A.L, Ferguson J, Green D.H, O'Reilly S.Y.O, Danchin R.V and Janse A.J.A (Eds.). Kimberlites and related rocks. Volume 2. Their mantle/crust setting, diamonds and diamond exploration.*, **Geological Society of Australia Spec. Publ. 14**: 1029 - 1041.

Morris E.M and Pasteris J.D (Eds.) (1987). Mantle metasomatism and alkaline magmatism. **Geol. Soc. America Spec. Publ. 215**: 383pp.

Morris J.D, Leeman W.P and Tera F (1990). The subducted component in island arc lavas: constraints from Be isotopes and B-Be systematics. *Nature*, **344**: 31 - 36.

Muehlenbachs K and Clayton R.N (1976). Oxygen isotope composition of the oceanic crust and and its bearing on seawater. *J. Geophys. Res.*, **81**: 4365 - 4369.

Nadeau S, Pineau F, Javoy M and Francis D (1990). Carbon concentrations and isotopic ratios in fluid-inclusion-bearing upper-mantle xenoliths along the northwestern margin of North America. *Chem. Geol.*, **81**: 271 - 297.

Navon O (1991). High internal pressure in diamond fluid inclusions determined by infrared absorption. *Nature*, **353**: 746 - 748.

Navon O, Hutcheon I.D, Rossman G.R and Wasserburg G.J (1988). Mantle-derived fluids in diamond micro-inclusions. *Nature*, **335**: 784 - 789.

Nichols I.A and Ringwood A.E (1973). Effect of water on olivine stability in tholeiites and the production of SiO_2-saturated magmas in the island arc environment. *J. Geol.*, **81**: 285 - 300.

Nier A.O and Gulbransen E.A (1939). Variations in the relative abundance of carbon isotopes. *J. Am. Chem. Soc.*, **61**: 697 - 698.

Norris T.L and Shaeffer O.A (1982). Total nitrogen content of deep sea basalts. *Geochim. Cosmochim. Acta*, **46**: 371 - 379.

O'Neil J.R (1977). Stable isotopes in mineralogy. *Phys. Chem. Minerals*, **2**: 105 - 123.

O'Neil J.R (1986). Theoretical and experimental aspects of isotopic fractionation. *In: Valley J.W, Taylor H.P and O'Neil J.R (Eds.). Stable isotopes in high temperature geological processes.*, **Reviews in mineralogy, V16. Mineralogical Society of America**: 1 - 40.

O'Neill H.St.C, Jaques A.L, Smith C.B and Moon J (1986). Diamond bearing peridotite xenoliths from the Argyle (AK1) pipe. *Proc. 4th Int. Kimberlite Conference, Perth (Abstract volume)*, 300 - 302.

Orlov Yu, L (1977). The mineralogy of diamond. *Wiley, New York*, 235pp.

Otter M.L (1989). Diamonds and their mineral inclusions from the Sloan diatremes of the Colorado - Wyoming state line kimberlite district, North America. *Ph.D thesis (Unpubl.), University of Cape Town, South Africa.*

Ozima M (1989). Gases in diamonds. *Ann. Rev. Earth Planet. Sci.*, **17**: 361 - 384.

Ozima M, Zashu S and Nitoh O (1983). $^{3}He/^{4}He$ ratio, noble gas abundance and K-Ar dating of diamonds. *Geochim. Cosmochim. Acta*, **47**: 2217 - 2224.

Ozima M, Zashu S, Takigami Y and Turner G (1989). Origin of the anomalous ^{40}Ar-^{39}Ar age of Zaire cubic diamonds: excess ^{40}Ar in pristine mantle fluids. *Nature*, **337**: 226 - 229.

Ozima M, Zashu S, Tomura K and Matsuhisa Y (1991). Constraints from noble gas contents on the origin of carbonado diamonds. *Nature*, **351**: 472 - 474.

Pearson D.G, Davies G.R, Nixon P.H and Milledge H.J (1989). Graphitised diamond from a peridotite massif in Morocco and implications for anomalous diamond occurrences. *Nature*, **338**: 60 - 62.

Pidgeon R.T, Smith C.B and Fanning C.M (1989). Kimberlite and lamproite emplacement ages in Western Australia. *In: Ross J, Jaques A.L, Ferguson J, Green D.H, O'Reilly S.Y.O, Danchin R.V and Janse A.J.A (Eds.). Kimberlites and related rocks. Volume 2. Their mantle/crust setting, diamonds and diamond exploration.*, **Geological Society of Australia Spec. Publ. 14**: 369 - 381.

Pineau F and Javoy M (1983). Carbon isotopes and concentrations in mid-ocean ridge basalts. *Earth Planet. Sci. Lett.*, **62**: 239 - 257.

Pineau F and Mathez E.A (1990). Carbon isotopes in xenoliths from the Hualalai Volcano, Hawaii and the generation of isotopic variability. *Geochim. Cosmochim. Acta*, **54**: 217 - 227.

Pineau F, Javoy M and Bottinga Y (1976). $^{13}C/^{12}C$ ratios of rocks and inclusions in the popping rocks of the mid-Atlantic ridge and their bearing on the problem of isotopic composition of deep-seated carbon. *Earth Planet. Sci. Lett.*, **29**: 413 - 421.

Plank T and Langmuir C.H (1993). Tracing trace elements from sediment input to volcanic output at subduction zones. *Nature*, **362**: 739 - 743.

Plumb K.A (1979). The tectonic evolution of Australia. *Earth Sci. Rev.*, **19**: 205 - 249.

Plumb K.A and Gemuts I (1976). Precambrian geology of the Kimberley Region, Western Australia. *25 Int. Geol. Congress Sydney Excursion guide*, **44C**: 69pp.

Plumb K.A, Derrick G.M, Needham R.S and Shaw R.D **(1981).** The proterozoic of Northern Australia. *In: D.R. Hunter (Ed.). The Precambrian geology of the Southern Hemisphere. Elsvier, Amsterdam,* 205 - 307.

Podosek F.A, Pier J, Nitoh O, Zashu S and Ozima M **(1988).** Normal potassium, inherited argon in Zaire cubic diamonds. *Nature,* **334**: 607 - 609.

Polyikov V.B and Kharlashina N.N **(1989).** The effect of pressure on isotope fractionation. *Dokl. Akad. Nauk. SSSR,* **306** (N2): 390 - 395.

Porcelli D.R, O'Nions R.K, Galer S.J.G, Cohen A.S and Mattey D.P **(1992).** Isotopic relationships of volatile and lithophile trace elements in continental ultramafic xenoliths. *Contrib. Mineral. Petrol.,* **110**: 528 - 538.

Poreda R and Craig H **(1989).** Helium isotope ratios in circum-Pacific volcanic arcs. *Nature,* **338**: 473 - 478.

Raal F.A **(1957).** A spectrographic study of the minor element content of diamond. *Am. Mineral.,* **42**: 354 - 361.

Rayleigh J.W.S **(1896).** Theoretical considerations respecting the separation of gases by diffusion and similar processes. *Philos. Mag.,* **42**: 493 - 498.

Richardson S.H **(1986).** Latter-day origin of diamonds of eclogitic paragenesis. *Nature,* **322**: 623 - 626.

Richardson S.H **(1986).** Origin of diamonds of peridotitic and eclogitic paragenesis. *Proc. 4th Int. Kimberlite Conference, Perth (Abstract volume),* 418 - 419.

Richardson S.H, Erlank A.J, Harris J.W and Hart S.R **(1990).** Eclogitic diamonds of proterozoic age from Cretaceous Kimberlites. *Nature,* **346**: 54 - 56.

Richardson S.H, Gurney J.J, Erlank A.J and Harris J.W **(1984).** Origin of diamonds in old enriched mantle. *Nature,* **310**: 198 - 202.

Richardson S.H, Harris J.W and Gurney J.J **(1993).** Three generations of diamonds from old continental mantle. *Nature,* **366**: 256 - 258.

Richet P, Bottinga Y and Javoy M **(1977).** A review of H, C, N, O, S and Cl stable isotope fractionation among gaseous molecules. *Ann. Rev. Earth Planet. Sci.,* **5**: 65 - 110.

Rickard R.S, Harris J.W, Gurney J.J and Cardoso P **(1989).** Mineral inclusions in diamonds from Koffiefontein mine. *In: Ross J, Jaques A.L, Ferguson J, Green D.H, O'Reilly S.Y.O, Danchin R.V and Janse A.J.A (Eds.). Kimberlites and related rocks. Volume 2. Their mantle/crust setting, diamonds and diamond exploration.,* 1054 - 1062.

Ringwood A.E **(1975).** Composition and petrology of the Earth's mantle. *McGraw-Hill. New York,* : 618pp.

Robertson R, Fox J.J and Martin A.E **(1934).** Two types of diamond. *Philos. Trans. Royal Soc.,* **A232**: 463 - 535.

Robey J.V.A **(1981).** Kimberlites of the central Cape Province, R.S.A *Ph.D Thesis (Unpubl.). University of Cape Town, South Africa.*

Robinson D.N **(1979).** Surface textures and other surface features of diamonds. *Ph.D Thesis (Unpubl.). University of Cape Town, South Africa.*

Rogers N.W, Hawkesworth C.J, Mattey D.P, and Harmon R.S **(1987).** Sediment subduction and the source for potassium in orogenic leucitites. *Geology,* **15**: 451 - 453.

Rombouts L **(1991).** Statistical distributions for diamonds. *Proc. 5th Int. Kimberlite Conference, Araxá (Abstract volume),* 342 - 343.

Russell S.S, Arden J.W and Pillinger C.T **(1991).** Evidence for multiple sources of diamond from primative chondrite. *Science,* **254**: 1188 - 1191.

Saino T and Hatori A **(1980).** ^{15}N natural abundance in oceanic suspended particulate organic matter. *Nature,* **283**: 752 - 754.

Sakai H, Des Marais D.J, Ueda A and Moore J.G **(1984).** Concentrations and isotope ratios of carbon, nitrogen and sulphur in ocean floor basalts. *Geochim. Cosmochim. Acta,* **48**: 2433 - 2441.

Schidlowski M, Hayes J.M and Kaplan IR **(1983).** Isotopic inferences of ancient biochemistries: Carbon, supfur, hydrogen and nitrogen. *In: Schopf J.W (Ed.) Earth's earliest biosphere. Princeton University Press, Princeton, N.J.,* 149 - 186.

Scott-Smith B.H and Skinner E.M.W **(1984).** Diamondiferous lamproites. *J. Geol.,* **92**: 433 - 438.

Shee S.R, Gurney J.J and Robinson D.N **(1982).** Two diamond-bearing peridotite xenoliths from the Finsch kimbelite, South Africa. *Contrib. Mineral. Petrol.,* **81**: 79 - 87.

Shutong Xu, Okay A.I, Shouyuan Ji, Sengör A.M.C, Wen Su, Yican Liu and Liali Jiang **(1992).** Diamonds from the Dabbi Shan metamorphic rocks and its implications for tectonic setting. *Science,* **256**: 80 - 82.

Sigmarsson O, Condomines M, Morris J.D and Harmon R.S **(1990).** Uranium and ^{10}Be enrichments in fluids in Andean arc magmas. *Nature,* **346**: 163 - 165.

Skinner E.M.W, Smith C.B, Bristow J.W, Scott-Smith B.H and Dawson J.B **(1985).** Proterozoic kimberlites and lamproites and a preliminary age for the Argyle lamproite pipe, Western Australia. *Trans. Geol. Soc. S. Af.,* **88**: 335 - 340.

Smirnov G.I, Mofolo M.M, Lerothai P.M, Kaminsky F.V, Galimov E.M and Ivanovskaya I.N **(1979).** Isotopically light carbon in diamonds from some kimberlite pipes from Lesotho. *Nature,* **278**: 630.

Smith C.B **(1984).** The genesis of diamond deposits of the west Kimberley, W.A. *In: Purcell P.G. (Ed.). The Canning Basin W.A. Proc. Geol. Soc. Aust. Symp. Perth,* 463 - 473.

Smith C.B, Gurney J.J, Harris J.W, Otter M.L, Kirkley M.B and Jagoutz E **(1991).** Neodimium and Strontium isotope systematics of eclogite and websterite paragenesis inclusions from single diamonds, Finsch and Kimberley pool, R.S.A. *Geochim. Cosmochim. Acta,* **55**: 2579 - 2590.

Smith J.V and Dawson J.B (1985). Carbonado: Diamond aggregates from early impacts of crustal rocks. *Geology*, 13: 342 - 343.

Smith V.W, Sorokin D.P , Gelles I.L and Lasher G.J (1959). Electron spin resonance of nitrogen donors in diamond. *Phys. Rev.*, 115: 1546 - 1552.

Sobolev N.V (1984). Kimberlites of the Siberian platform: their geological and mineralogical features. *In Glover J.E and Harris P.G (Eds.). Kimberlite occurrence and origin: a basis for conceptual models in mineral exploration. Geology Dept. and Univesity Extn., University of Western Australia, Publication*, 8: 275 - 287.

Sobolev N.V and Shatsky V.S (1990). Diamond inclusions from metamorphic rocks: a new environment for diamond formation. *Nature*, 343: 742 - 746.

Sobolev N.V, Galimov E.M, Ivanoskaya I.N and Efimova E.S (1979). Isotopic composition of carbon in diamonds containing crystalline inclusions. *Dokl. Akad. Nauk. SSSR*, 249: 1217 - 1220.

Sobolev N.V, Galimov E.M, Smith C.B, Yefimova E.S, Maltsev K.A, Hall A.E and Usova L.V (1989). A comparative study of the morphology, inclusions and carbon isotopic composition of diamonds from alluvials of the King George River and Argyle lamproite (Western Australia), and of cubic diamonds from Northern Australia. *Geologiya i Geofizika*, 30: 3 - 19.

Staudacher T and Allègre C.J (1988). Recycling of oceanic crust and sediments: the noble gas barrier. *Earth Planet. Sci. Lett.*, 89: 173 - 183.

Stevenson F.J (1959). On the presence of fixed ammonium in rocks. *Science*, 130: 221 - 222.

Sunagawa I (1990). Growth and morphology of diamond crystals under stable and metastable conditions. *J. Crystal Growth*, 99: 1156 - 1161.

Sunagawa I, Tsukomota K and Yasuda T (1984). Surface microtopographic and X-ray topographic study of octahedral crystals of natural diamond from Siberia. *In: Sunagawa I (Ed.). Materials science of the Earth's interior.* , **Terra Scientific, Tokyo**: 331 - 349.

Sutherland G.B.B.M, Blackwell D.E and Simeral W.G (1954). The problem of the two types of diamond. *Nature*, 174: 901 - 904.

Swart P.K, Pillinger C.T, Milledge H.J and Seal M (1983). Carbon isotope variations within individual diamonds. *Nature*, 303: 793 - 795.

Taylor H.P and Epstein S (1963). O^{18}/O^{16} ratios in rocks nd coexisting minerals from the Skaergaard intrusion, East Greenland. *J. Petrol.*, 4: 51 - 74.

Taylor W.R, Jaques A.L and Ridd M (1990). Nitrogen-defect aggregation characteristics of some Australasian diamonds: Time-temperature constraints on the source regions of pipe and alluvial diamonds. *Am. Mineral.*, 75: 1290 - 1310.

Tingle T.N (1989). More on the mantle carbon flux. *EOS, Trans. Am. Geophys. Union*, 70: 1513 - 1514.

Turner G, Burgess R and Bannon M (1990). Volatile rich mantle fluids inferred from inclusions in diamond and mantle xenoliths. *Nature*, 344: 653 - 655.

Valley J.W and O'Neil J.R (1981). $^{13}C/^{12}C$ exchange between calcite and graphite: a possible thermometer in Grenville marbles. *Geochim. Cosmochim. Acta*, 45: 411 - 419.

van Tendeloo G, Luyten W and Woods G.S (1990). Voidites in pure type IaB diamonds. *Philos Mag. Letters*, 61: 343 - 348.

van Wyk J.A (1982). Carbon^{13} hyperfine interaction of the unique of the P2 (ESR) or N3 (optical) centre in diamond. *J. Solid State Phys.*, 15: 981 - 983.

Verchovsky A.B, Bergmann F, Ott, U, Jagoutz E, Shatsky V, Sobolev N, Pillinger C.T, Milledge H.J and Mendelssohn M.M (1992). Noble gases, carbon and nitrogen in microdiamonds from the Kokchetav massif, Northern Kazakhtan. *Diamond Conference, Cambridge (Abstract)*, 3.1 - 3.4.

Vinadagorev A.P, Kropotova O.I, Orlov Yu,L and Grinenko V.A (1966). Isotopic composition of diamond and carbonado crystals. *Geochem. Int.*, 2: 1123 - 1125.

Walmsley J.C and Lang A.R (1992a). On sub-micrometer inclusions in diamond coat: crystallography and composition of ankerites and related rhombohedral carbonates. *Min. Mag.*, 56: 533 - 543.

Walmsley J.C and Lang A.R (1992b). Oriented biotite inclusions in diamond coat. *Min. Mag.*, 56: 106 - 111.

Wan G (1989). The distribution pattern of kimberlites and associated rocks in Shandong, China. *In: Ross J, Jaques A.L, Ferguson J, Green D.H, O'Reilly S.Y.O, Danchin R.V and Janse A.J.A (Eds.). Kimberlites and related rocks. Volume 2. Their mantle/crust setting, diamonds and diamond exploration.*, **Geological Society of Australia Spec. Publ.** 14: 401 - 406.

Wand U, Nitzsche H-M, Mühle K and Wetzel K (1980). Nitrogen isotope composition in natural diamonds - first results. *Chemie der Erde*, 39: 85 - 87.

Waples D.W and Sloan J.R (1980). Carbon and nitrogen diagenesis in deep sea sediments. *Geochim. Cosmochim. Acta*, 44: 1463 - 1470.

Wasson J.T (1985). Meteorites: their record of early solar-system history. *Freeman, New York*, 267 pp.

Watson B.E and Lupulescu A (1993). Aqueous fluid connectivity and chemical transport in clinopyroxene-rich rocks. *Earth Planet. Sci. Lett.*, 117: 279 - 294.

Watson B.E, Brenan J.M and Baker D.R (1990). Distribution of fluids in the continental mantle. *In: Menzies M (Ed.).. Continental mantle. Clarendon Press, London.* **Chapter 6**: 111 - 125.

Wedepohl K.H (1969). Handbook of Geochemistry. *Springer Verlag. Berlin*, **Vol. 1**.

Wedlake R.J (**1979**). Technology of diamond growth. *In: Field J.E (Ed.). The properties of diamond. Academic Press, London.*, 501 - 535.

Wickman F.E (**1956**). The cycle of carbon and the stable carbon isotopes. *Geochim. Cosmochim. Acta*, **9**: 136 - 153.

Wilding M.C and Harte B (**1991**). Carbon isotope variation in a single diamond from the Bultfontein mine determined by ion microprobe. *Frontiers in isotope geosciences, Keyworth (Abstarct)*, 13 - 14.

Wilson M (**1989**). Igneous petrogenesis *Unwin Hyman, London*, 466 pp.

Wood B.J and Virgo D (**1989**). Upper mantle oxidation state: ferric iron contents of lherzolite spinels by ^{57}Fe Mössbauer spectroscopy and resultant oxygen fugacities. *Geochim. Cosmochim. Acta*, **53**: 1277 - 1291.

Woods G.S (**1985**). Platelets and infrared absorption in type Ia diamonds. *Diamond Conference abstracts*, **1985**: 95 - 102.

Woods G.S, Purser G.C, Mtimukuku, A.S.S and Collins A.T (**1990**). The nitrogen content of type Ia natural diamonds. *J. Phys. Chem. Solids*, **51**: 1191 - 1197.

Wright I.P, Boyd S.R, Franchi I.A and Pillinger C.T (**1988**). High-precision determinations of nitrogen stable isotope ratios at the sub-nanomole level. *J. Phys. E: Sci. Instrum.*, **21**: 865 - 875.

Wyllie P.J (**1989**). The genesis of kimberlites and some low-SiO_2, high-alkali magmas. *In: Ross J, Jaques A.L, Ferguson J, Green D.H, O'Reilly S.Y.O, Danchin R.V and Janse A.J.A (Eds.). Kimberlites and related rocks. Volume 1. Their composition, occurrence, origen and emplacement.*, **Geological Society of Australia Spec. Publ. 14**: 603 - 615.

Wyllie P.J and Sekine T (**1982**). The formation of mantle phlogopite in subduction zone hybridisation. *Contrib. Mineral. Petrol.*, **79**: 375 - 380.

Yacoot A and Moore M (**1993**). X-ray topography of natural tetrahedral diamonds. *Min. Mag.*, **57**: 223 - 230.

Yamamoto N, Spence J.C and Fathy D (**1984**). Cathodoluminescence and polarization studies from individual dislocations in diamond. *Philos. Mag. B*, **49**: 609 - 629.

Zashu S, Ozima M and Nitoh O (**1986**). K-Ar isochron dating of Zaire cubic diamonds. *Nature*, **323**: 710 - 712.

Zhang P, Hu S and Wan G (**1989**). A review of the geology of some kimberlites in China. *In: Ross J, Jaques A.L, Ferguson J, Green D.H, O'Reilly S.Y.O, Danchin R.V and Janse A.J.A (Eds.). Kimberlites and related rocks. Volume 2. Their mantle/crust setting, diamonds and diamond exploration.*, **Geological Society of Australia Spec. Publ. 14**: 392 - 400.

Appendix 1: Data tables

In this appendix, the following convention is applied to the sample descriptions that follow the sample number;

Paragenesis (if known), colour, shape, inclusion mineralogy

The following abbreviations are used:

Paregenesis		**colour**		**shape**		**inclusion mineralogy**	
Eclogitic	E	Clear	C	Octahedral	O	Garnet	Gt
Peridotitic	P	White	W	Dodecagedral	D	Olivine	Ol
Lherzolitic	Lhz	Brown	Br	Macled	M	Clinopyroxene	Cpx
Harzburgitic	Hz	Yellow	Y	Cubic	C	Orthopyroxene	Opx
		Green	Gr	Irregular	I	Kyanite	Ky
		Grey	G	Resorbed	R	Rutile	Rut
		Blue	B	Aggregate	A	Not recovered	nr
						Unknown	U

Thus a moderately resorbed, green eclogitic diamond with dodecahedral morphology and containing garnet and clinopyroxene inclusions would be described as E, Gr, RD, Gt Cpx.

Sample	Type	$\delta^{13}C$	$\delta^{15}N$	[N]	% B
A1 E, W, MO, Gt	IaB+p	-10.99	11.3	475	83
A2 Y, M, nr	IaB	-4.6			
A3 Y, O, nr	IaAB	-4.54			
A4 E, Y, MO, Gt	II	-11.05	9.7	372	
A5 E, Y, MD, Gt	IaB	-9.33	4.7	363	
repeat	"	-9.57	2.4	35	
A7 Y, I, nr	IaAB	-11.10	3.5	15	
A8 Y, MI, nr	IaAB	-10.47	-2.5	25	
A11 Y, MO, nr	II	-10.68	3.0	215	
A13 G, MA, nr	IaB	-9.47	3.3	30	
A15 E, Br, MD, Gt Rut	II	-10.22		0	
A18 E, Br, MD, Gt	IaAB	-10.02	5.3	277	
A20 Br, MO, nr	IaB	-12.09	5.1	41	
A21 Br, MO, nr	IaAB+p	-8.90	5.0	185	83
A22 E, Br, MD, Gt Cpx	IaB	-10.47	11.6	79	
A23 E, Br, MD, Gt	IaAB+p	-10.59	11.3	118	74
A25 E, Br, MD, Gt Ky	IaB	-10.83	11.8	55	78
A26 E, Br, MD, Cpx	IaAB+p	-9.91	3.8	45	20
A28 E, Br, O, Gt	IaB	-10.48	6.6	257	
A32 E, Br, MD, Gt Rut	IaB	-10.35			90
A39 E, Br, MD, Gt Cpx coesite	II	-11.47	2.0	17	
A41 E, Br, O, Gt coesite	IaA+p	-12.96	0.0	14	
A50 E, Br, MD, Gt	IaAB	-12.01	4.0	35	
A55 E, W, MD, Gt	IaAB	-11.75	8.4	571	81

Table A1.1: Argyle diamonds with eclogitic paragenesis inclusions.

Sample	Type	$\delta^{13}C$	$\delta^{15}N$	[N]	% B
Possibly peridotitic diamond: A1	IaB+p	-5.79	8.4	580	77
A2	IaA	-8.99	6.7	1317	3
A3	IaB	-7.98	0.1	973	
A4	IaAB	-9.39	2.3	1181	3
Probably peridotitic diamond: A1	IaAB	-7.23	4.9	174	6
A2	IaAB	-8.14	3.6	79	0
A3	II	-11.99	4.3	97	
A4	II	-8.19	8.5	555	

Table A1.2: Peridotitic paragenesis diamonds from Argyle, identified as such on the basis of sharp-edged octahedral morphology.

Sample	Type	$\delta^{13}C$	$\delta^{15}N$	[N]	% B
pink diamond : A1	IaB	-7.98	13.5	93	44
pink diamond : A2	II	-9.80	1.7	33	
grey diamond: A1		-9.10	4.5	1364	
Repeat A1			4.7		
yellow diamond: A1	IaAB+p	-10.25	4.0	1881	22
yellow diamond: A2	IaAB+p	-9.73	2.3	2198	12
yellow diamond: A3	II	-11.41		0	
yellow/white macle: A1	II	-11.04	3.1	625	

Table A1.3: Inclusion free, coloured diamonds from Argyle.

Sample	Type	$\delta^{13}C$	$\delta^{15}N$	[N]	% B
octahedra: A1	IaAB+p	-10.46		0	40
dodecahedra: A1	IaAB+p	-10.58	11.3	98	17
2	IaAB	-11.61	13.4	85	66
3	II	-11.08	1.2	12	
4	II	-10.78	7.7	10	
5	IaB	-10.64	4.6	110	
6	IaB	-10.83	7.4	26	100
macle: A1	IaA+p	-10.09	4.1	1074	4
A2	IaAB+p	-9.17	8.6	549	80
A3	IaAB+p	-8.19	11.9	236	40

Table A1.4: Inclusion free, white diamonds from Argyle.

Sample	Type	$\delta^{13}C$	$\delta^{15}N$	[N]	% B
octahedra: A1	IaAB	-9.79	8.8	197	29
Repeat A1	IaB	-9.79	10.8	197	29
dodecahedra: A1	II	-6.21	10.3	30	4
2	IaAB+p	-9.19	8.4	100	70
3	IaAB	-9.18	8.5	71	16
4	IaAB+p	-10.97	8.7	31	85
5	II	-10.43	9.4	98	
6	II	-9.42	10.7	42	
7	IaB+p	-9.78	12.1	291	97
8	II	-10.90	6.4	23	
macle: A1	IaAB+p	-11.43	6.7	111	63
A2	II				
A3	IaAB	-7.81	5.7	54	73
A4	IaAB	-7.84	5.7	39	23

Table A1.5: Inclusion free, brown diamonds from Argyle.

Sample	Type	$\delta^{13}C$	$\delta^{15}N$	[N]	% B
150701/1/0	IaAB+p	-10.12	1.2	107	50
150701/1/1	IaAB+p	-8.66		107	58
150701/1/2	IaAB+p	-10.19	1.9	148	86
150701/1/3	?	-9.33	4.7	110	62
150701/1/4	IaAB+p	-9.39	-0.7	147	46
150701/1/5	IaB	-9.90	4.2	140	75
150701/1/6	IaB	-10.07	2.0	380	92
150701/1/7	IaAB	-10.22	3.3	247	79
150701/1/8	II	9.77	4.6	181	0
150701/1/9	II	-9.87	-3.7	203	0
150701/1/10	IaB+p	-9.86	-2.5	456	69

Table A1.6: Argyle plate 150701#1. This is a pale yellow dodecahedron and contained an eclogitic garnet inclusion.

Sample	Type	$\delta^{13}C$	$\delta^{15}N$	[N]	% B
150701/8/0	IaAB+p	-6.64	2.7	105	38
150701/8/1/1	IaAB+p	-5.75	9.8	402	74
150701/8/1/2	IaAB+p	-5.91	7.1	145	74
Weighted mean, block 1		-5.83	8.0	227	
150701/8/1A/1	IaB+p	-5.71	10.5	588	94
150701/8/1A/2	IaB+p	-5.63	7.9	1267	94
150701/8/1A/3	IaB+p	-5.47	13.6	1056	94
Weighted mean, block 1A		-5.69	10.1	840	
150701/8/2/1	IaAB+p	-5.96	12.2	447	84
150701/8/2/2	IaAB+p	-4.51	10.3	284	84
150701/8/2/3	IaAB+p	-5.44	11.1	1435	84
Weighted mean, block 2		-5.30	11.7	551	
150701/8/3/1	IaAB+p	lost	2.5	53	45
150701/8/3/2	IaAB+p	lost	4.3	124	45
150701/8/3/3	IaAB+p	lost	8.3	232	45
Weighted mean, block 3			4.5	120	
150701/8/4	II	lost			0

Table A1.7: Argyle plate 150701#8. This is a slightly resorbed brown octahedron. It contains an eclogitic garnet inclusion.

Sample	Type	$\delta^{13}C$	$\delta^{15}N$	[N]	% B
150701 #12-4/A	IaAB+p	-12.33	0.9	114	43
150701 #12-4/B	IaAB+p	-12.65	2.6	106	
150701 #12-4/C	IaB	-12.56			74
150701 #12-4/D	IaB	-12.58			78
150701 #12-4/E	IaB	-12.63	6.1	253	69
150701 #12-4/F	IaB	-12.86	7.4	108	75
150701 #12-4/G	IaAB	-12.69	6.6	157	86
150701 #12-4/H	IaAB	-12.48	3.3	192	60
150701 #12-4/I	IaAB	-12.62	5.7	89	63

Table A1.8: Argyle plate 150701 #12-4. This is a brown, very slightly resorbed octahedral diamond with no inclusions.

Sample	Type	$\delta^{13}C$	$\delta^{15}N$	[N]	% B
150701 #12-1/A	II	-8.52	1.1	41	18
150701 #12-1/B	IaAB+p+H	-7.96	6.9	74	83
150701 #12-1/C	IaB+H	-7.25	10.0	123	95
150701 #12-1/D	IaAB				47
150701 #12-1/E	IaAB	-8.85	0.9	19	17
(Second burn)	-9.07	3.0	23		

Table A1.9: Argyle plate 150701 #12-1. This is a white, very slightly resorbed octahedral diamond with no inclusions.

Sample	Type	$\delta^{13}C$	$\delta^{15}N$	[N]	% B
150701 #12-8/A	IaAB+p	-9.31	3.3	17	22
150701 #12-8/C	IaAB+p	-9.29	5.4	29	29
150701 #12-8/D	IaAB+p	-9.79	10.6	135	50
150701 #12-8/E	IaAB+p	-11.74	9.1	73	35
150701 #12-8/F	IaAB+p	-14.05	9.1	29	6
150701 #12-8/G	IaAB+p	-10.83	8.6	55	24
150701 #12-8/H	IaAB+p		5.5	34	40
150701 #12-8/IIaAB+p					

Table A1.10: Argyle plate 150701 #12-8. This is a brown, moderately resorbed octahedron, with a peridotitic paragenesis orthopyroxene inclusion.

Sample		Type	$\delta^{13}C$	$\delta^{15}N$	[N]	% B
E4001	Y, MD, U	IaAB+p	-3.05	-7.7	1408	20
E4002	W, D, Ky?	IaAB+p	-5.92	-3.5	60	29
E4003	Y, D, 3Gt	IaAB+p	-6.24	-3.9	1205	
E4005	Y, DA, 4U	IaAB+p	-6.12	1.6	218	30
E4006	Br, MD, U	IaAB+p	-5.41	3.7	797	46
E4008	Y, DA, 2U	IaA+p	-4.63	1.9	682	15
E4009	Y, D, 5Gt?	IaAB+p	-5.09	-0.9	665	24
E4010	Y, DA, 7U	IaAB+p	-4.27	2.1	230	21
E4011	Y, D, 2Gt? graphite	IaA+p	-4.89	-4.4	606	15
E4012	Y, MD, 2U	IaAB+p	-3.15	2.1	1425	26

Table A1.11: Ellendale 4 inclusion bearing diamonds. All unidentified inclusions are silicates.

Sample		Type	$\delta^{13}C$	$\delta^{15}N$	[N]	% B
E4013	Br, O/D	IaAB+p	-1.96	3.7	135	13
E4014	Br, O/D	IaAB+p	-3.85		0	18
E4015	Br, O/D	IaAB+p	-5.52	0.1	367	12
E4016	W, O/D	IaAB+p	-5.21	-0.8	1206	12
E4017	Br, O/D	IaAB+p	-3.40	-7.0	1344	13
E4018	CY, O/D	IaAB+p				27
E4019	CW, O	IaAB+p	-5.79	0.1	1570	17
E4020	CBr, O	IaAB+p	-4.73	-1.1	1502	21
E4021	CY, O	IaAB+p	-3.75	-10.4	4125	
	Repeat #1	IaAB+p	-3.75	-7.9	3650	
	Repeat #2	IaAB+p	-3.75	-7.9	2872	
E4022	W, O	IaAB+p	-5.20	-6.4	1963	19
E4023	Y, O	IaAB+p				
E4024	Br, O	IaAB+p				80
E4025	Br, O	IaAB+p				12
E4026	Br, O	IaAB+p				
E4027	Br, O	IaAB+p				9
E4028	Br, O	IaA+p				8
E4029	Br, O	IaA+p				5
E4030	Br, O	IaAB+p				36
E4031	Br, O	IaAB+p				14
E4032	Br, O	IaAB+p				15

Table A1.12: Ellendale 4 inclusion free diamonds.

Sample		Type	$\delta^{13}C$	$\delta^{15}N$	[N]	% B
E9001	E, Y, D, Gt	IaAB+p	-8.51	1.5	1294	46
E9002	E, W, D, Gt	IaAB+p	-11.20	8.6	63	31
E9004	E, Y, D, 3Gt	IaAB+p	-10.20	0.0	1413	38
E9005	W, D, U	IaAB+p	-5.34	-3.0	1082	46
E9006	P, W, D, Ol	IaA+p	-5.10	3.7	904	17
E9007	E, W, D, Gt Cpx	II	-17.49		0	5
E9008	P, Br, MD, Ol	IaAB+p	-2.97	-3.6	27	
E9009	Br, D, U	IaAB+p	-1.21	4.0	13	69
E9010	W, D, U	IaA+p	-5.40	2.5	79	17
E9011	Br, D, U	IaA+p	-0.01	5.7	19	14
E9012	E, W, D, Gt Cpx	IaA	-21.66	-0.1	27	0
	Repeat	IaA	-15.66	-3.3	16	0
E9013	P, W, D, Ol	IaA	-5.80	-9.3	45	6
	Repeat	IaA	-5.82	-4.0	48	6
E9014	W, D, U	IaAB+p	-12.09	0.8	44	28

Table A1.13: Ellendale 9 inclusion bearing diamonds.

Sample		Type	$\delta^{13}C$	$\delta^{15}N$	[N]	% B
E9015	Br, D,	IaAB+p	-22.14			55
E9016	Br, D,	IaA	-5.38	1.6	186	6
E9017	Br, D,	IaA	-5.33	-4.0	54	11
E9018	Br, D, graphite	IaAB+p	-6.35	-6.3	9	
E9019	Y, D,	IaAB+p	-6.80	-4.2	4438	
E9020	Y, D,	IaAB+p	-4.91	1.4	1510	73
E9021	Y, D,	IaAB+p	-6.62	-0.8	2230	
E9022	Y, D,	IaAB+p	-6.77	6.1	509	90
E9023	W, D,	IaAB+p	-7.72	9.9	380	8
E9024	W, D,	IaAB+p	-4.71	-5.9	411	9
E9025	W, DA,	IaAB+p	-6.88	3.1	1649	17
E9026	W, D, graphite	IaAB+p	-5.50	6.5	923	20
E9027	Y, D,	IaAB+p	-5.70	-2.8	1615	30
E9028	W, D,	IaA+p	-4.33	-2.4	1076	8

Table A1.14: Ellendale 9 inclusion free diamonds.

Sample	Type	$\delta^{13}C$	$\delta^{15}N$	[N]	% B
E9037/4	IaAB+p	-10.70	13.2	313	59
E9037/5	IaAB+p	-10.34	10.4	387	75
E9037/6	IaAB+p	-10.14	12.0	1052	77
E9037/7	IaAB+p	-10.20	11.2	453	63
E9037/8	IaAB+p	-10.79	6.9	340	33
E9037/9	IaAB+p	-10.85	7.0	398	51
E9037/10	IaAB+p	-9.37	3.8	299	48
E9037/u.n.	IaA	-7.90	0.3	213	0

Table A1.15: Ellendale 9 plate E9037. This is a brown, inclusion free dodecahedron.

Sample	Type	$\delta^{13}C$	$\delta^{15}N$	[N]	% B
E9038/u.n.	IaAB+p	-10.93	-2.0	1486	
E9038/1	IaAB+p	-11.97	-2.0	1691	24
E9038/2	IaAB+p	-11.51	-2.9	2052	27
E9038/3	IaAB+p	-11.62	-2.1	1986	26
E9038/4	IaAB+p	-11.62	-2.5	1858	27
E9038/5	IaAB+p	-11.91	-2.7	1659	24
E9038/6	IaAB+p	-12.05	-2.6	1042	23
E9038/7	IaAB+p	-12.00	-2.8	1279	23
E9038/8	IaAB+p	-11.94	-2.9	1418	26
E9038/9	IaAB+p	-11.75	-2.9	1757	27
E9038/10	IaAB+p	-11.62	-1.7	1928	27
E9038/u.n.	IaAB+p	-11.44	-0.7	2358	

Table A1.16: Ellendale 9 plate E9038. This is a yellow dodecahedron with a marginal, unidentified inclusion.

Sample	Type	$\delta^{13}C$	$\delta^{15}N$	[N]	% B
E9040/1	IaAB+p	-4.35	-3.6	1081	15
E9040/2	IaAB+p	-4.71	-4.0	1633	19
E9040/3	IaAB+p	-4.69	-3.8	1463	19
E9040/4	IaAB+p	-4.70	-2.5	1588	20
E9040/5	IaAB+p	-4.75	-5.0	1578	20
E9040/6	IaAB+p	-4.70	-3.2	1738	20
E9040/7	IaAB+p	-4.65	-4.0	1879	20
E9040/8	IaAB+p	-4.51	-4.0	1537	19
E9040/u.n.	IaA+p	-3.99	-1.2	953	11

Table A1.17: Ellendale 9 plate E9040. This is a yellow dodecahedron with tiny graphite inclusions.

Sample	Type	$\delta^{13}C$	$\delta^{15}N$	[N]	% B
E9041/u.n.	IaA+p	-5.10	0.1	805	8
E9041/1	IaA+p	-4.92	-0.9	887	4
E9041/2	IaA+p	-5.03	-0.7	545	11
E9041/3	IaAB+p	-5.17	-0.1	1084	19
E9041/4	IaAB+p	-5.14	-0.4	1716	25
E9041/5	IaAB+p	-5.18	-0.6	1712	28
E9041/6	IaAB+p	-4.99	-1.2	1257	27
E9041/7	IaAB+p	-4.94	-0.7	1072	22
E9041/8	IaAB+p	-5.01	-0.9	1040	17
E9041/9	IaA+p	-5.06	0.8	692	11

Table A1.18: Ellendale 9 plate E9041. This is a white dodecahedron with fine black graphite inclusions.

Sample		Type	$\delta^{13}C$	$\delta^{15}N$	[N]	% B
NQ1		II	-5.90			0
NQ2	W, O	IaAB+p	-4.10	-7.4	316	47
NQ3		IaAB+p	-2.60			14
NQ4	W, O	IaAB	-5.10	1.9	296	50
NQ5			-5.10			
NQ7	W, O	IaA	-5.09	-2.0	96	0
NQ8	Br,	II	-10.50			
NQ10	Y, I	IaAB+p	-8.10	9.7	154	30
NQ11	W, D	IaAB+p	-8.40	8.0	80	16
NQ12	Bl, I	IaA	-3.70	-17.0	63	7
NQ13	W, D	IaAB+p	-3.06	-5.4	182	32
NQ14		IaAB+p	-4.50			37
NQ15		IaA	1.90			12
NQ16	W, O	IaB	-5.45	-2.4	327	80
NQ17	Bl, I	II	-3.40	-8.2	25	0
NQ19	W, I	IaAB+p	-3.80	-17.2	104	26
NQ20			-10.40			
NQ21	Br,		-9.10			
NQ23	W, I	IaAB+p	-6.38	1.7	1196	13
NQ24		IaA	-6.75		20	40
NQ25	W, O	IaAB+p	-7.20	-22.8	410	66
NQ26			-3.10			
NQ28	W, O	IaAB+p	-3.90	-2.5	766	11
NQ29	W, I	IaA	-6.70	-12.6	120	7
NQ30		II	-11.10			
NQ31	W, I	IaA+p	-2.30	-4.0	211	0
NQ32	W, I	IaAB+p	-4.50	-14.2	216	49
NQ33	W, I	IaAB+p	-3.24	-28.4	446	57
NQ34	W, I	IaA	-3.80	2.0	187	0
NQ36	W, D	IaB+p	-14.79	2.0	2710	65
NQ37	W, O	IaA	-4.22	-13.6	47	4
NQ38	Y, I	IaAB+p	-8.70	3.6	64	2
NQ39		IaB	-5.29	-7.9	35	100
NQ40			-11.70			

Table A1.19: North Queensland diamonds. Initial sample descriptions by Yugi Sano.

Sample		Type	$\delta^{13}C$	$\delta^{15}N$	[N]	% B
Frosted octahedra						
MMF101	Br, O	IaA	-5.10	6.9	58	19
MMF102	Br, O	IaAB	-5.60	1.2	39	19
MMF103	Br, O	IaA	-5.12	-0.6	27	21
MMF104	Br, O	IaAB+p				39
MMF105	Br, O/D	IaAB+p	-5.07	1.6	32	38
MMF106	W, O/A	IaA	-5.96	9.2	180	8
MMF107	W, O	IaA+p	-4.56	1.1	976	15
MMF108	Gr, O	IaA	-4.09		18	7
MMF109	Br, MO	IaAB+p				44
MMF110	W, O	IaA	-5.41	10.6	49	15
Discoid type						
MMF111	Gr, D	IaAB+p				36
MMF112	Br, D	IaAB+p	-4.97	-4.2	216	80
MMF113	Y, D	IaAB+p	-6.62	6.2	281	54
MMF114	Y, D	IaAB+p				38
MMF115		IaAB+p	-5.56	10.1	171	14
MMF116	Br, D	IaAB+p	-5.53	-10.6	926	82
MMF117	Y, D	IaAB+p	-5.93	-0.7	1587	83
MMF118	Gr, D	IaAB+p	-4.39	7.8	819	16
MMF119	Br, D	IaA+p	-5.43	3.8	543	84
MMF120	Gr, D	IaAB+p	-7.64	3.5	1223	21
Plateau type						
MMF121	Br, O/D	IaAB+p				85
MMF122	Br, D	IaA+p				86
MMF123	W, D	IaA+p				87
MMF124	Br, O/D	IaAB+p	-3.30	-14.2	106	23
MMF125	Br, D	IaAB+p				21
MMF126	W, O/D	IaA+p				12
MMF127		IaA	-5.20	-3.6	79	14
MMF128	Gr, O	IaA				0
MMF129	Gr, O/D	IaB				90
MMF130	G, C/D	IaA				3
Argyle type						
MMF131	W, D/M	IaB	-9.44	10.6	105	67
MMF132	W, D/M	IaB+p				90
MMF133	W, D/M	IaB	-11.80	16.1	38	41
MMF134	Br, D/A	IaB				100
MMF135	Br, D	IaB				91

Table A1.20: Morelli's Fox diamonds.

Sample	Type	$\delta^{13}C$	$\delta^{15}N$	[N]	% B
C1	IaAB+p	-4.77	-2.9	367	4
C2	IaA+p	-5.07	3.8	1208	4
C3	IaA+p	-3.35	-20.7	193	
Repeat	IaA+p	+1.98	-13.7	107	
C4	IaA+p	-4.92	-4.9	1092	0
C6	II	-4.77			
C7	IaAB+p	-5.15	1.4	1047	27
C8	IaA	-2.40	-4.2	90	4
C9	IaA	-4.16	-11.4	127	2
C10	II	-0.73	1.3	33	
C11	IaB	-4.40	6.1	105	
C12	IaA	-4.14	5.6	62	4
C13	IaA	-5.86	-3.5	200	3
C14	IaA	-4.46	-1.7	120	5
C15	IaA	-13.08	-5.9	130	
C16	IaA	-4.65	6.0	2238	13
C17	II	-16.23	-6.7	104	
C18	II	-12.15	1.1	201	8
C19	IaA+p	-3.20	-11.5	477	3
C20	IaA	-3.84	-11.2	892	3

Table A1.21: Chinese diamonds. These samples are mostly dodecahedral.

Sample	Type	$\delta^{13}C$	$\delta^{15}N$	[N]	% B
+425 #1	II				
#2	IaB				
#3	IaB+p	-10.17	5.5	405	
#4	IIb				
#5	IaB+p	-14.90	5.8	1198	
#6	IaB+p	-9.57	0.8	1961	
#7	II				
+600 #1	II	-10.04			
#2	II	-11.07			
#3	II	-11.03			
#4	IaB+p	-13.38			
#5	IaA	-10.07			
#6	IaAB+p	-12.71			
#7	IaB+p	-14.02			

Table A1.22: Argyle run of mine microdiamonds.

Sample	Type	$\delta^{13}C$
958075 #1 (composite of 5)	?	-2.70
958075 #2	?	-4.60
#3	?	-3.80
#4	?	-4.20
#5	?	-4.50
958324 #1	?	0.10
#3	?	-2.40
#4	?	-2.80
#5	?	-3.00
#6	?	-3.70
#7	?	-4.20
#8	?	-2.30
958330 #1	?	-1.90
#2	?	-2.90

Table A1.23: Argyle peridotite nodule microdiamonds.

Sample	Type	$\delta^{13}C$
5	?	-5.58
11	?	-6.94

Table A1.24: Argyle dyke microdiamonds.

Sample	Type	$\delta^{13}C$
1	IaA	-5.23
2	IaA+p	-5.42
5	II	-4.38
7	II	-3.56
8	II	-3.76
10	II	-2.95
11	II	-4.00
2	?	-3.81
13	?	-6.65
15	II	-5.21

Table A1.25: Ellendale 4 microdiamonds.

Sample	Type	$\delta^{13}C$	$\delta^{15}N$	[N]	% B
E4 #9	IaA + p	-5.7	-2.4	22	-
N.T. cube 1 - 16	?	-17.1	6.2	109	-

Table A1.26: Western Australian microdiamonds for which [N] and $\delta^{15}N$ have been determined.

Sample	Type	$\delta^{13}C$
1	?	-4.83
2	?	-3.35
3	?	-5.90
5	?	-3.86
6	?	-6.84

Table A1.27: Ellendale 9 microdiamonds.

Sample		Type	$\delta^{13}C$
#1	Y, I	?	-16.66
#2	C, I	?	-12.57
#3	Gr, C	?	-20.72
#4	Gt? inclusion	Ib	-19.52
#5	Br/R, I, radiation damaged	?	-14.35
#6	Br/R, I, radiation damaged	?	-9.67

Table A1.28: North Queensland microdiamonds.

Sample	Type	$\delta^{13}C$
Batch 1 #2	IaA	-22.07
#3	?	-18.27
#4	IaB	-16.35
#5	IaAB	-17.88
#8	II	-16.94
#9	II	-10.13
#11	IaB	-20.55
#12	IaB	-19.05
#13	II	-18.08
#14	II	-11.17
#17	II	-18.37
#18	II	-12.69
Batch 2 #1	IaB	-15.24
#2	IaB	-16.52
#3	IaB	-19.38
#5	IaB	-23.26
#6	II	-27.52
#7	IaB	-20.74
#11	?	-17.27
#12	?	-22.53
#13	II	-17.64
#14	II	-16.00
#15	II	-19.12
#16	II	-12.87
#17	II	-16.62
#18	II	-18.44

Table A1.29: Northern Territory cubic microdiamonds.

Sample	Type	$\delta^{13}C$
batch 1 #1	?	-4.22
#3	?	-19.52
#5	?	-20.95
#6	?	-3.12
#7	IaA	-11.54
#9	?	-20.45
#10	?	-22.22
#15	?	-19.78
#16	?	-11.52
#17	?	-3.92
#?	?	-3.88
batch 2 #1	?	-17.74
#2	IaA	-2.52
#3	IaA	-5.60
#4	?	-4.90
#6	?	-3.73
#8	?	-21.53
#10	?	-19.60

Table A1.30: Northern Territory irregular microdiamonds.

Sample	Type	$\delta^{13}C$	$\delta^{15}N$	[N]	% B
FINJ00	IaA+p	-4.31	-4.6	308	4
FINJ01	IaA+p	-3.06	-3.6	456	2
FINJ02	IaA+p		-2.8	199	2
FINJ03	IaAB+p	-4.07	-1.3	390	1
FINJ04	IaAB+p +H	-4.43	1.3	657	14
FINJ05					10
FINJ06	IaAB+p +H	-5.07	2.3	392	7
FINJ07					11
FINJ08	IaAB+p +H	-5.00	1.5	1118	5
FINJ09					11
FINJ10	IaAB+p +H	-5.13	2.5	750	12
FINJ11					10
FINJ12	IaAB+p +H	-4.70	1.8	475	7
FINJ13					7
FINJ14	IaAB+p +H	-4.16	0.9	288	2

Table A1.31: Finsch central cross data for Chapter 5.

Sample	Type	$\delta^{13}C$
1	II	-5.8
2	II	-5.1
3	II	
4	II	-5.1
5	II	
6	II	-5.2
7	II	-10.6
8	II	-16.4

Table A1.32: Type II scrap; Honeycomb #7.

Appendix 2: Analytical Techniques

This appendix describes the technical specifications of mass spectrometers and associated hardware used in the determination of carbon and nitrogen stable isotope composition and nitrogen abundance. In addition the Fourier Transform Infrared (FTIR) spectrometer used and Davies (1981) method of spectral decomposition used are described.

The isotope ratio of sample nitrogen or carbon is expressed throughout this thesis in conventional "delta notation" where

$$\delta‰ = \left(\frac{R_{Sample}}{R_{Reference}} - 1\right) \times 1000‰$$

and $R = \frac{\text{heavy isotope}}{\text{light isotope}}$ (for light element stable isotopes)

and are expressed relative to the isotopic ratios of the commonly accepted standards - AIR for nitrogen and PDB (the Pee Dee formation belemnite) for carbon, both of which are defined as having δ values of zero. Enrichments in light isotopes relative to the standard are apparent from negative δ values while enrichments in the heavy isotope show up as positive values. A pure light end-member will have a δ value of -1000‰ and the pure heavy end-member has δ tending to + infinity. The scale is exponential but for the small enrichments evident in terrestrial samples is pseudo-linear. Working reference standards in the Planetary Sciences Unit (P.S.U.) are white spot grade cylinder nitrogen supplied by B.O.C ($\delta^{15}N = +1‰$) or nitrogen gas prepared from the international ammonium sulphate standards N-1 and N-2 (Boyd *et al.*, 1991) with $\delta^{15}N = +0.45‰$ or +20.35‰ respectively. A variety of CO_2 reference standards prepared from carbon dioxide ice are used and these have $\delta^{13}C$ between -41.701‰ and -2.823‰. To convert δ values measured against a reference standard (Ref) to δ values relative to the international standard (Std), the following relation is used:

$$\delta_{Std}^{Sample} = \delta_{Ref}^{Sample} + \delta_{Std}^{Ref} + \left(10^{-3}.\delta_{Ref}^{Sample} \times \delta_{Std}^{Ref}\right)$$

where δ_Y^X is δ value of X relative to Y (Hoefs, 1987).

NITROGEN

Mass spectrometer and associated hardware

The mass spectrometer used for nitrogen isotope ratio and abundance determinations is described in detail in Wright *et al.*, (1988) and only a summary is presented here.

The mass spectrometer is constructed from a V.G. 601 analyser head with a 6.2 cm flight tube and a 90° deflection and the static volume of $\approx 10^{-3}$ m^{-3} is pumped *via* CR38 bakeable valves by an ion pump during routine use and ancillary diffusion and rotary pumps are available for evacuation from high pressure or during bakeout. The ionisation source is of nude Nier design with a tungsten filament operated at 3A giving a trap current of 40μA. During idle periods the filament is operated at a 100μA trap current to aid degassing. Electrical supplies to the source are supplied by a modular system comprising a 0 - 5Kv high voltage supply, emission control regulator, a source monitor and a scan unit. Ion beams are scanned under control of a BBC micro-computer, by varying the accelerating voltage *via* a 16 bit digital to analogue convertor. Scanning can also be done manually using the scan unit.

Ion current signals are converted to voltages by a remote head high gain amplifier and transmitted to two variable gain second stage amplifiers. Amplifier outputs are returned to the BBC microcomputer *via* a 16 bit digital to analogue convertor and 1MHz interface bus and peak ratios calculated. Control software, written by S.R. Boyd and I.P. Wright, consists of a series of 6502 machine code routines nested within a basic program and is designed for maximum operating speed. Routine operation of the instrument is described in Boyd (1988), Chapter 2.

Gas inlet and nitrogen extraction system.

A description of the gas inlet and nitrogen extraction system (glass line) and appraisal of the glass line and mass spectrometer performance is described in detail by Boyd (Boyd *et al.*, 1988c; Boyd 1988) and thus only a precis is presented here. The glass line comprises four discrete sections; an inlet section, a purification section, a combustion section and a CO_2 recovery section and these are generally constructed from pyrex glass (o.d. 10mm, i.d. 8mm), the exceptions being sections where high temperatures are experienced and these are made of quartz glass (o.d. 6mm, i.d. 4mm) connected to the rest of the glass line *via* quartz-pyrex graded seals. Vacuum is maintained in a dual vacuum system by two water cooled oil diffusion pumps and the two circuits, referred to as the main and backing vacuum, have base pressures of $<7\times10^{-5}$ Pa and $\approx 7\times10^{-4}$ Pa respectively. The use of a backing system avoids atmospheric leaks into the high vacuum manifold past valve stems (Youngs greaseless, mostly of the special construction described by McNaughton *et al.*, (1983)) and ensures that the high vacuum circuit never intentionally sees atmosphere. The principle is described in McNaughton *et al.*, (1983).

The inlet section is used to control the amount of sample gas admitted to the mass spectrometer by means of a variety of fixed volume aliquotters and is also used to supply reference nitrogen from on-line storage reservoirs (one litre pyrex bulbs) at any pressure

using a variable volume aliquotter. All gas passing through the inlet system is allowed to equilibrate in a variable temperature cryotrap (V.T.C.) kept at -185°C for 90 seconds prior to admission to the mass spectrometer. This removes any remnant condensible impurities in sample gas after purification and the trace amount of condensible impurities present in the reference gas.

The purification section, comprising a 0.5nm molecular sieve, oxygen source (CuO furnace), V.T.C. and hot (1150°C) platinum catalyst is used in the following manner. Sample gas is frozen onto the molecular sieve at liquid nitrogen temperature (-196°C) for $3^1/_2$ minutes and the purification section isolated. The molecular sieve is then heated to 200°C by means of a Kanthal wire spiral desorbing sample nitrogen, and simultaneously the V.T.C. is cooled to -140°C trapping any condensible gasses (*e.g.* CO_2). The presence of the hot platinum catalyst expedites the decomposition of low molecular weight hydrocarbons and more importantly, aids the breakdown of oxides of nitrogen. Any oxygen transferred to the purification section is resorbed onto the CuO oxygen source at 600°C and then 450°C. Heating CuO to ≈850°C causes it to liberate oxygen while cooling it results in the resorption of oxygen. The CuO furnace serves a duel purpose by also converting any CO transferred to the purification section to CO_2 which is then frozen out in the V.T.C. The clean up procedure takes approximately ten minutes after which sample nitrogen is transferred to the inlet system for admission to the mass spectrometer. In a very comprehensive series of experiments, Boyd (Boyd, 1988; Boyd *et al.*, 1988b) showed the purification procedure to be capable of the total removal of CO, CO_2 and CH_4, all of which directly or indirectly lead to interferences at *m/z* 28 and 29; the major and minor peaks for nitrogen isotopic analyses.

The combustion section is supplied with a bulk loader capable of holding six samples, an on-line oxygen source and a V.T.C. The oxygen source, as with the one in the purification section consists of a quartz finger, lined with platinum foil and filled with wire form specpure® copper (II) oxide, which when heated to 850°C by means of a Kanthal wire spiral liberates oxygen. This oxygen can be resorbed by cooling of the CuO to first 600°C and then 450°C. Diamonds are individually loaded into the reaction vessel, a quartz tube surrounded by a furnace at 1050°C, by means of a magnetic slug and held at that temperature while pumping until vacuum base pressure is reached. This very effectively removes any contaminants that may be adsorbed onto the surface of the diamond or the platinum bucket in which it is wrapped. The combustion section is then closed, oxygen pressure raised by heating the CuO and the V.T.C. cooled to -180°C. Combustion takes ≈35 minutes and CO_2 produced is frozen onto the V.T.C., leaving nitrogen in the gaseous state for transferral to the purification section.

After transferral of sample nitrogen to the purification section, the CO_2 produced during diamond combustion is transferred to the CO_2 recovery section by freezing it onto a cold finger at liquid nitrogen temperature, while warming the combustion section V.T.C. to -100°C. This retains any condensible gases produced during combustion (*e.g.* H_2O) in the combustion section for later removal. Transfer takes ≈6 minutes after which the CO_2 recovery section is isolated and CO_2 allowed to expand by warming to room temperature. Gas pressure is measured in an oil manometer and as this is directly proportional to diamond mass that full combustion has occurred can be ascertained. Sample CO_2 is then frozen into a detachable "take off vessel" and transferred to the inlet manifold of a V.G. SIRA 24 dynamic mass spectrometer for determination of carbon isotopic ratios.

To test the efficacy of the extraction system at separating CO_2 and nitrogen, a series of experiments were run in which full procedural blank analyses were alternated with analysis of type II (nitrogen free) diamond. When the mass spectrometer is contaminated by CO_2 this very rapidly decays to CO interfering with the minor peak at *m/z* 29 and producing spuriously heavy results. This experiment was designed to show that even for large diamond fragments (500 or 600 μg) no CO_2 entered the mass spectrometer. Representative results are presented in Table A2.1. and show that with correct cryotrap settings, blank analyses are indistinguishable from analysis of nitrogen free diamonds.

	Yield ng	$\delta^{15}N$ ‰	error ‰
Full blank	0.98	-21.9	2.9
Type II diamond	0.87	-19.6	3.9
Full blank	0.60	-13.0	5.8

Table A2.1: Blank analyses compared to an analysis of a type II nitrogen free diamond. Isotopic composition of "diamond" nitrogen is within error of the isotopic composition of the blank.

Isotopic composition of blank amounts of nitrogen are extremely difficult to measure because of the small amounts of gas involved, although values of $\delta^{15}N$ between -21.9‰ and +15‰ have been obtained. Normal values are usually around +5‰ and the anomalously light blank composition determined above is largely the result of the inlet section having seen atmosphere some three weeks previously. As atmosphere is pumped away it shows evidence of kinetic fractionations with the lighter isotopes being removed first and with continued pumping, the blank composition gets heavier until it stabilises at ≈ +5‰. The amount of blank remains constant at <1ng after about three weeks of pumping. As all routine analyses are of amounts of gas larger than the blank, by at least an order of magnitude the affect on sample isotopic composition is negligible and thus discounted. A 1ng blank was considered to be the highest acceptable value for operation of the instrument, although values of < 0.5ng were more common. The smallest amount of nitrogen measured was 2.5ng and amounts >15ng were more usual.

Accuracy and precision

After a comprehensive series of experiments, Boyd and others (Boyd, 1988; Boyd *et al.*, 1988b; Wright *et al.*, 1988) reported the following evaluation of mass spectrometer performance:

- Internal precision = standard error on mean of $^{28}/_{29}$ ratios obtained from individual scans = 0.2‰ to ±0.5‰
- Reproducibility of m/z $^{28}/_{29}$ ratio = standard deviation (σ) on mean for replicate analyses of the same gas = ± 3‰ for 0.6 ng and < 0.6‰ for > 2 ng gas.

This quoted precision was tested by an examination of the variability of the m/z = 28 peak (*i.e.* the $^{28}/_{29}$ ratio) for aliquots of reference nitrogen, measured over two consecutive days, during which the machine was performing routine analyses (of the diamonds reported in Chapter 4). The days were chosen at random from the run book, and on the 13th and 14th of February, 1990, twenty five 20 - 40 ng aliquots of reference nitrogen were admitted to the mass spectrometer. These had a mean value of $^{28}/_{29}$ = 139.284 and the standard error on the mean was 0.031. The fractional error (*i.e.* {Standard error}/{$^{28}/_{29}$} x 1000) expressed in per mille is = 0.22‰ (Table A2.2) and this is similar to the precision quoted by Wright *et al.*, (1988). Over the course of a single days run, the instrumental precision is always better than this. Standard errors on the mean of the $^{28}/_{29}$ ratio measured during the course of a single day are typically better than 0.1‰ with a standard deviation of 0.3‰.

The accuracy of nitrogen analyses was monitored, by S.R. Boyd, as part of the routine maintenance program of the nitrogen mass spectrometer. This was done by the frequent analysis of the nitrogen reference material - ammonium sulphate N1 or N2, and later by the analysis of an ammonium sulphate – rubidium sulphate solid solution (See Boyd and Pillinger 1991 for a discussion of nitrogen standards), in order to check, and if necessary re-calibrate the "on-line" bulb of reference nitrogen gas. Thirty one analyses of ammonium sulphate N2 and eleven analyses of N1, done by S.R. Boyd during between January and October, 1990 are listed in Table A2.2. Ammonium sulphate N2 has a $\delta^{15}N$ value of 20.35‰ and the mean $\delta^{15}N$ value of the analyses listed in Table A2.2 are within one standard deviation (0.55‰) of the expected value. Ammonium sulphate N1 has a $\delta^{15}N$ value of 0.45‰ and analyses of this reference material are all well within one standard deviation of this value. The standard deviation of the 15 individual scans across the m/z = 28 peak that constitute each $\delta^{15}N$ determination of ammonium sulphate, are always less than 0.7‰, and are usually of the order of 0.3‰.

	$m/z = {}^{28}/_{29}$ on 13th and 14th of February, 1990	$\delta^{15}N$ value of $(NH_4)_2SO_4$ N2 (‰)	N1 (‰)
	139.38	20.6	0.38
	139.156	21.0	0.39
	139.447	20.4	0.25
	139.55	19.6	0.24
	139.44	19.57	0.29
	139.435	19.	0.35
	139.207	19.68	0.58
	139.294	19.2	0.78
	139.228	19.	0.62
	139.405	19.	0.31
	139.455	19.42	0.71
	139.311	20.95	
	139.242	20.97	
	138.843	21.01	
	139.365	20.98	
	139.213	19.79	
	139.306	19.25	
	139.355	20.51	
	139.451	19.58	
	139.166	19.73	
	139.174	19.93	
	139.155	20.63	
	139.169	19.89	
		20.16	
		19.8	
		19.8	
		20.07	
		20.49	
		20.29	
		20.16	
		20.1	
Mean	139.284	20.087	0.445
Standard error on the mean	0.031 (= 0.22‰)	0.99	0.058
Standard deviation	0.156 (= 1.1‰)	0.554	0.192
Expected $\delta^{15}N$ value (Kendall and Grim, 1990)		20.35 ± 0.02	0.45 ± 0.05

Table 2.2: Data for assessing the precision and accuracy of the nitrogen mass spectrometer. Precision is given by the std. error on the mean of analyses of reference nitrogen (Wright *et al.*, 1988) and is better than 0.25‰. Accuracy is shown by the standard deviation on replicate analysis of the ammonium sulphate standards N1 and N2 (See also Boyd and Pillinger, 1991). Analysis of $(NH_4)_2SO_4$ standards done by S.R. Boyd.

Nitrogen abundances are determined directly from the intensity of the *m/z* 28 ($^{14}N^{14}N^+$) ion beam. This was calibrated by S.R. Boyd, by admitting known amounts of nitrogen derived from ammonium sulphate standards into the mass spectrometer, and the initial calibration factor of 96.3 was determined. This was shown to be correct by the repeated analysis of three batches of Rb_2SO_4 with varying nitrogen contents, by Boyd and Pillinger (1991), which always gave measured N contents within 4% of the expected values. The mean uncertainty on nitrogen content measured for 18 rubidium sulphate solid solutions is 2.5% (Boyd and Pillinger, 1991). In this thesis it is assumed that nitrogen abundance determinations have an uncertainty of 5% or less.

Infrared analysis

The F.T.I.R spectrometer used in this study is a Brukker IFS45 equipped with a microscope and computer controlled stage and is in routine use in the Crystallography Department at University College, London. The following parameters are used for the collection of diamond spectra.

Resolution	8 cm^{-1}
Number of scans	200
Aperture	80μm

Spectral decomposition to obtain the relative proportions of A and B form nitrogen is done using the method of Davies (1981) using relative A and B feature absorbances. The following procedure is used with reference to Figure A2.1:

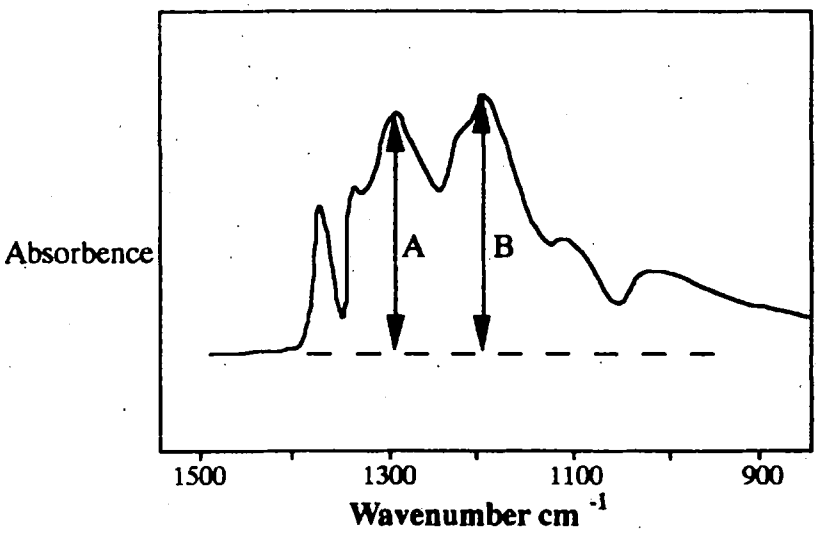

Figure A2.1: Type IaAB diamond spectrum. Lengths of lines A and B are proportional to $\mu(7.8)$ and $\mu(8.5)$ respectively.

1: Spectra (*e.g.* Figure A2.1) are baselined by inspection and the distances between the baseline and peak are measured for the peaks near 7.8μm (wavenumber 1280 cm^{-1}) and 8.5μm (wavenumber 1175 cm^{-1}) to $^1/_4$ mm and these values used for $\mu(7.8)$ and $\mu(8.5)$ respectively.

2: A and B spectra are separated by taking the ratio $m = \mu(7.8)/\mu(8.5)$ which is equal to A/B from Figure A2.1

3: The ratio of A and B feature absorbances at 7.8μm (r) is now calculated

$$r = (2.72m - 1) / (1 - 0.41m) \text{ when } m < 1.5$$

$$r = (1.88m - 1) / (1 - 0.5m) \text{ when } m > 1.5$$

4: The proportion of B nitrogen is now calculated from:

$$\mu^{B}_{7.8} = \mu(7.8)/(1+r) \qquad \text{(A2.1)}$$

which is equivalent to $A/(1+r)$.

Davies (1981) estimates equation A2.1 to give $\mu^{B}_{7.8}$ correct to ±5% of the total absorption at 7.8μm, however this is totally swamped by the large uncertainty on the measured values of A and B (Figure A2.1) which are estimated to be ±10%. Propagating through gives errors of 20% in m which leads to errors of 34% in r which is equivalent to a final uncertainty in excess of 40%, considerably larger than uncertainties obtained for Chinese diamonds where absolute absorbances are used in the determination of the proportion of B aggregate nitrogen. These are all <12% and usually <5% (Milledge Pers. Comm.).

CARBON

Dynamic carbon isotope mass spectrometry

A conventional commercial dynamic mass spectrometer was used for the analysis of diamond carbon isotopic composition. The instrument employed was a V.G. SIRA (**S**table **I**sotope **R**atio **A**nalyser) with an advertised precision of 0.005‰ on 1.46μmol of CO_2 (17.5μg carbon). Thirty four repeat analyses of the Planetary Sciences Unit internal standard gas, CO_2-6 over the 2 months from 14 February to 15 May 1990 (at least one analysis on each day that the mass spectrometer was in use) indicates an actual precision of 0.01‰ (standard error on the mean), and a reproducibility of the order of 0.08‰ (Table A2.3). Similar experiments conducted with diamond powder combusted "off line" have a precision of 0.02‰ and the reproducibility of 0.04‰ (Table A2.3).

The V.G. SIRA 24 is a 90° sector, 12cm actual radius (24 cm apparent radius due to the use of angled permanent magnet pole pieces and extended geometry) triple collecting mass spectrometer of the basic type pioneered by Nier (1940, 1947) incorporating the modifications described by McKinney *et al.*, (1950). The effective minimum sample size is 1.5μg carbon and this is accompanied by a decrease in precision to 0.1‰. For larger samples (>3μg) the precision is 0.01‰. The system incorporates a low volume McKinney type (McKinney *et al.*, 1950) change-over valve with tungsten shut off balls operated by solenoid switching under control of a Hewlett Packard HP9816 computer which also collects data, corrects for interfering ^{17}O, compensates for mixing in the change-over valve (Fallick, 1980), calculates δ values relative to laboratory reference gases and PDB, and monitors source parameters, the pumping system and a fully automated inlet.

Source gas ionisation efficiency is increased by internal source magnets increasing electron travel paths by spiralling and CO_2^+ ions are are accelerated, by a variable electric field supplying an accelerating voltage of 2.8 Kv, through a slit into the flight tube at the end of which, ion beams at masses 44, 45 and 46 are measured simultaneously by capturing ions in Faraday buckets. Amplified signals are passed to the HP9816 computer *via* three 1MHz voltage - frequency convertors. By measuring mass 46 ($^{12}C^{16}O^{18}O$) the isobaric interference of $^{12}C^{16}O^{17}O$ at mass 45 may be corrected for (See Ash, 1990 for details).

Sample and reference gas is admitted to the SIRA 24 from demountable bulbs or take off vessels (See Boyd *et al.*, 1988b) connected to an inlet manifold under control of the HP9816, by means of lightly greased cone and socket connectors. Internal Planetary Sciences Unit reference gases are used and these are produced from dry ice and are regularly calibrated against a variety of internal and NBS standards including NBS-22 (Table A2.3), as part of the routine maintenance of this mass spectrometer. The analysis of reference oil NBS-22 ($\delta^{13}C_{measured}$ = -29.79‰; $\delta^{13}C_{expected}$ = -29.73‰) indicate an accuracy of better than 0.1‰.

	CO_2 - 6		Diamond powder	NBS - 22
	-27.361	-27.333	-9.809	-29.711
	-27.300	-26.951	-9.808	-29.796
	-27.326	-27.252	-9.823	-29.862
	-27.355	-27.23	-9.726	
	-27.305	-27.299	-9.741	
	-27.275	-27.316		
	-27.365	-27.285		
	-27.423	-27.306		
	-27.335	-27.277		
	-27.414	-27.276		
	-27.292	-27.248		
	-27.325	-27.273		
	-27.335	-27.265		
	-27.414	-27.231		
	-27.292	-27.336		
	-27.38	-27.349		
	-27.217	-27.290		
number of analyses	34		5	3
Mean $\delta^{13}C$ value	-27.301		-9.78	-29.79
Standard error	0.014		0.02	0.04
Standard deviation	0.081		0.04	0.08
Expected value			-9.8	-29.73

Table A2.3: Replicate analyses of standard gas CO_2 - 6, diamond powder and the National Bureau of Standard oil, NBS - 22. All values except for the number of analyses are given in ‰.

Off line sample preparation

Carbon isotopic composition was measured for a number of samples without contemporaneous nitrogen analysis and these samples (*e.g.* Type II diamonds) were prepared off line for analysis on the SIRA 24 in the following way.

Cleaned diamond chips are placed in prebaked (1000°C, overnight) quartz buckets constructed by fusing one end of 2cm lengths of quartz tubes (o.d. 2 - 2.5mm, i.d. 1 - 1.5 mm). Quartz tubes are then filled with specpure ® powder form copper (II) oxide (B.D.H.Chemicals Ltd. Poole), precombusted in air at 500°C for 30 minutes and then dropped into quartz reaction vessels made by sealing one end of quartz tube (o.d. 6mm, i.d. 4mm). These are then evacuated using a turbo-molecular pump to a base pressure better than 10^{-3} Pa and sealed by collapsing the quartz tube ≈6cm above the sample with a hydrogen-oxygen flame. These quartz vials are then numbered with a diamond pencil and loaded into a muffle furnace where combustion occurs for at least 10 hours at a temperature of 1000°C, following which they are cooled to 600°C resorbing excess oxygen back onto the CuO.

CO_2 produced is recovered by cracking the quartz vial in a modified Youngs valve (See Boyd 1988) under vacuum and cracking is facilitated by first scoring the vial with a glass knife. Sample gas is frozen onto a cold finger at liquid nitrogen temperature (-196°C) *via* a trap containing copper gauze at 650°C which removes any unresorbed oxygen produced during combustion to CO_2. The cold finger is then isolated, warmed to ≈ -130°C by replacing the liquid nitrogen with an n-Pentane slush and the pressure of CO_2, now in the gaseous phase, measured in a capacitance manometer (baratron). Water and other condensible gases remain frozen in the cold finger. Baratron pressure is directly proportional to the mass of the diamond chip combusted, and this is used to ensure that full combustion has occurred. Samples with CO_2 yields that deviate by more than ≈5% from expected values are rejected. Clean sample CO_2 is then transferred from the baratron by freezing into a take off vessel and transferred to the SIRA 24 for carbon isotope ratio determination. CO_2 blanks in the system are too small for measurement on the SIRA 24.

crystallization alone however does negate other potential isotope fractionation mechanisms. In particular, melting processes, which are exactly analogous to Rayleigh distillation processes, are very effective at fractionating trace elements in magmatic systems (*e.g.* Cox *et al.*, 1979) and should also be effective at fractionating stable isotopes. Few authors however attempt to model changes in stable isotope ratios during melting rigorously. Furthermore, few attempts have been made to model the kinetic fractionations that may occur during diamond precipitation and this is due to the complexities of the mathematics involved, and the fact that at magmatic temperatures, kinetic effects are expected to be minimal (*e.g.* Hoefs, 1987). Jambon (1980) has, however produced a kinetic model for isotopic fractionations in crystals growing from magmatic melts. There are no published results available at present for the isotopic fractionations associated with the aggregation of nitrogen in diamonds, although it is likely that this diffusion-driven process will accompanied by some form of isotopic fractionation.

A3.1 EQUILIBRIUM CRYSTALLIZATION

On the crystallization of some source material (magma, melt or fluid), enrichments of the heavier isotope in the instantaneously forming product, say diamond, are given by the fractionation factor α. For example, diamond precipitating from CH_4 will concentrate ^{13}C by 4‰ for a fractionation factor $\alpha_{diamond\text{-}methane}$ of 1.004† at $\approx$ 1000°C. The enrichment of the heavier isotope in the product phase results in a corresponding depletion of that isotope in the source material, and thus both source material and product become progressively depleted in the heavy isotope as crystallization proceeds in a closed system. In equilibrium crystallization, the product phase remains in equilibrium with the source material and although the isotope ratios in product and source change with the amount of crystallization, the bulk isotope ratio remains constant and is equal to the isotope ratio of the source material before any crystallization. On 100% crystallization therefore, the mean $\delta^{13}C$ values of the diamonds will be the same as that in the original source. In closed system equilibrium crystallization, the maximum fractionation of δ values that is possible is equal to the Δ fractionation. Using the diamond precipitating from CH_4 example, the very first diamond to precipitate will have a $\delta^{13}C$ value 4‰

† For reactions in which the light isotope is concentrated in the product, *e.g.* diamond precipitating from CO_2, the fractionation factor α will be less than 1. A -4‰ fractionation has α = 0.996. Note also that $\alpha_{A\text{-}B} = 1\text{-}\alpha_{B\text{-}A}$.For example: a 4‰ C fractionation between diamond and methane with methane concentrating the light ^{12}C isotope has $\alpha_{diamond\text{ - }methane} = 1.004$ and $\alpha_{methane\text{ - }diamond} = 0.996$

Appendix 3: Theory of modelling

Fractionation of the stable isotope ratios of geological samples may arise from kinetic or equilibrium isotope effects (Hoefs, 1987). Kinetic effects occur in fast, incomplete or unidirectional processes like evaporation, diffusion or dissociation and arise from a sensitivity of the rate of chemical reaction to the atomic mass and bond strengths of the reacting species. Equilibrium fractionation effects are a result of the disproportional exchange of different isotopes due to differences in the binding energies. The magnitude of the fractionation is given by the fractionation factor α, and this is defined as the isotope ratio in one chemical compound A, divided by the corresponding ratio in another chemical compound B such that

$$\alpha = \frac{R_A}{R_B} \qquad \text{(A3.1)}$$

A more convenient way of expressing α is through the function $1000\ln\alpha$ which is the per mille fractionation between two species A and B and is very closely approximated by the Δ value where

$$\Delta_{A\text{-}B}(‰) = \delta_A(‰) - \delta_B(‰) \approx 1000\ln\alpha_{A\,-\,B} \qquad \text{(A3.2)}$$

Fractionation factors are related to the equilibrium constant (K) of the reaction causing the isotopic fractionation and are very dependent on temperature (Hoefs, 1987) and may be subject to a very small pressure effect (Polyikov and Kharlashina, 1989). As temperature decreases, the fractionation factor increases by

$$\ln\alpha = \frac{K}{T^2} + K' \qquad \text{(A3.3)}$$

Fractionation factors are determined by calculation (*e.g.* Bottinga 1969 for graphite, diamond and CO_2); by experiment (*e.g.* Mattey 1991 for C - CO_2 in basaltic melts) or by the observation of naturally occurring samples. There are, at present no fractionation factors available for nitrogen in diamond, the closest approximations being published by Richet *et al.*, (1977), for fractionations between the gaseous molecules N_2 and NH_4. Fractionation factors for carbon are however more readily available (*e.g.* Friedman and O'Neil, 1977).

Many previous attempts to model equilibrium isotopic fractionation have concentrated on Rayleigh processes (*e.g.* Swart *et al.*, 1983; Javoy *et al.*, 1986; Otter, 1989; Galimov, 1991), which are, for the most part, analogous to fractional crystallization or melting events. Fractional crystallization is valid as a model for fractionating the stable isotope ratios of diamonds, as other mantle derived material sampled by kimberlite magmas, particularly the megacryst suite of minerals, show clear fractional crystallization trends in trace element composition (*e.g.* Robey, 1981; Moore, 1986). Considering fractional

heavier than that of the starting material and the last CH_4 to precipitate will have a $\delta^{13}C$ value 4‰ lighter than that of the starting material.

In an open system where the stable isotopic composition of the source material is held constant, for example in the case of a very large reservoir, the precipitate will have a constant stable isotope ratio. This stable isotope ratio will however be displaced from that of the source region by an amount equal to the Δ fractionation. In the case of diamonds precipitating from CH_4, the diamond $\delta^{13}C$ values will be 4‰ more positive than the $\delta^{13}C$ value of the source CH_4. The offset in stable isotope ratios between product and source material during such crystallization depends solely on the magnitude and sign of the ‰ fractionation (Δ value). Based on extrapolated fractionation factors (Otter, 1989), diamonds crystallizing from CH_4 and graphite sources would be slightly ^{13}C enriched relative to the source material if crystallization occurred at 1100° and 1300°C. In contrast, diamonds precipitating from CO_2 or carbonate sources would be slightly ^{13}C depleted relative to the source.

A3.2 FRACTIONAL CRYSTALLIZATION

Fractional crystallization is a process which can effectively fractionate stable isotope ratios. This model differs from equilibrium crystallization in that crystallized material is isolated from the source material which becomes progressively enriched or depleted in the heavy isotope depending on the magnitude and sign of the fractionation factor. This may arise when diamond is precipitated from a fluid phase (*e.g.* silicate melt or metasomatic fluid), or by nitrogen fixed within a crystalline diamond, being unavailable for further reaction. This simple Rayleigh fractionation process (Rayleigh, 1896) is governed by the equation given by Hoefs (1987) for condensation:

$$\frac{R_v}{R_{v_o}} = F^{(\alpha - 1)} \qquad \text{(A3.4)}$$

Here α = the fractionation factor, F = the fraction of carbon remaining in the residue†, R_{v_o} = the isotope ratio in the source material and R_v = the isotope ratio in the residue. This equation can be written to show the fractionation of δ values (Taylor and Epstein 1963), where for carbon:

---

† F may be thought of as an indicator of the amount of crystallization. For no crystallization *i.e* at time t = 0, all carbon, or nitrogen, remains in the source material and thus F = 1. At 100% crystallization, F = 0. It should be noted that this terminology differs from that in many igneous petrology texts which use F as an indication of the degree of completion of a fractionation process *i.e.* at time t = 0, F = 0.

$$\frac{\delta^{13}C_{residue} + 1000}{\delta^{13}C_{initial} + 1000} = F^{\frac{\Delta}{1000}} \qquad \text{(A3.5)}$$

In this case, $\Delta \approx 1000\ln\alpha$ (from equation A3.2). This equation is equally valid for modelling nitrogen isotope fractionations, where $\delta^{15}N$ values are submitted in place of $\delta^{13}C$ values.

The effect of fractional crystallization is best illustrated graphically. On Figure A3.1, the change in δ value of source material and the precipitated phase (diamond) with increasing crystallization (decreasing F) is shown. This illustrates that, very large fractionations of isotope ratio are possible for large degrees of fractional crystallization. Given sufficient crystallization, any δ value between -1000‰ (pure light isotope, occurs for fractionation factors $\alpha > 1$) and +infinity ‰ (for fractionation factors $\alpha < 1$) may be achieved. At low degrees of crystallization however, changes in isotope ratio are slow. More than about 63% crystallization (F = 0.37) is necessary in order to fractionate isotope ratios by an amount equal to Δ‰. Fractional crystallization differs from equilibrium crystallization in the maximum change in δ value that can occur. This occurs at F = 0, and for equilibrium crystallization, is limited by the fractionation factor. In the case of carbon or nitrogen stable isotope ratios, the maximum change in δ value will be limited to a few per mille. For fractional crystallization, as detailed above, any δ value between -1000‰ and +infinity ‰ may be achieved, regardless of the fractionation factor.

Very high degrees of crystallization are unlikely to be accompanied by efficient separation of the source fluid and the crystalline residue in the case of silicate magmas and common mantle minerals (Cox *et al.*, 1979) and if this is also the case for diamonds in the mantle, then the efficacy of fractional crystallization as as a means of stable isotope fractionation in diamonds may be limited.

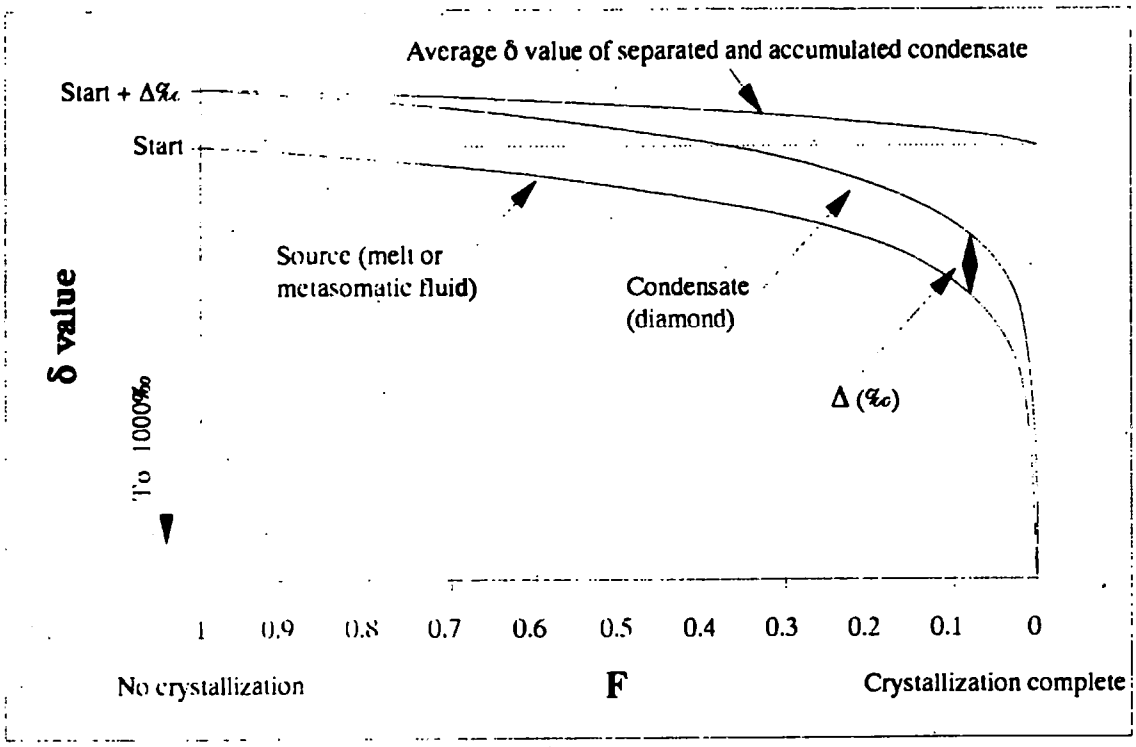

Figure A3.1: The effect of fractional crystallization on δ values. The effect for a positive fractionation factor is shown and condensed phases are enriched in the heavy isotope relative to the source material by Δ‰. The residue becomes progressively depleted in the heavy isotope with a consequent decrease in δ value. The maximum amount of fractionation possible would result when the source material has been totally depleted in the heavy isotope and this occurs at δ = -1000‰ when F = 0. For a negative fractionation factor (*i.e.* the condensed phases concentrating the lighter isotope), the curves have the same general form, but have positive slope and the maximum fractionation tends to + infinity.

A3.3 FRACTIONAL MELTING

Melt production is a mechanism by which stable isotope ratios could be effectively fractionated. It is equivalent to Rayleigh distillation and the equation governing the composition of the produced melt is (Hoefs, 1987):

$$\frac{R_v}{R_{v_o}} = \frac{1}{\alpha} F^{\left(\frac{1}{\alpha} - 1\right)} \qquad \text{(A3.6)}$$

As with equation A3.4, F = the fraction of residual material, α = the fractionation factor and R_{v_o} is the isotope ratio of the original material. This equation can be manipulated to give the isotopic fractionations for carbon:

$$\delta^{13}C_{residue} = \left((\delta^{13}C_{initial} + 1000) \times \left(\frac{-\Delta}{1000} + 1 \right) \times F^{\frac{-\Delta}{1000}} \right) - 1000 \quad \text{(A3.7)}$$

As with equation A3.5, Δ is the ‰ fractionation and is $\approx 1000\ln\alpha$ and F = the fraction of carbon remaining in the residue. Note the change of sign for Δ when compared to the fractional crystallization equation (A3.5). A melting curve is shown in Figure A3.2.

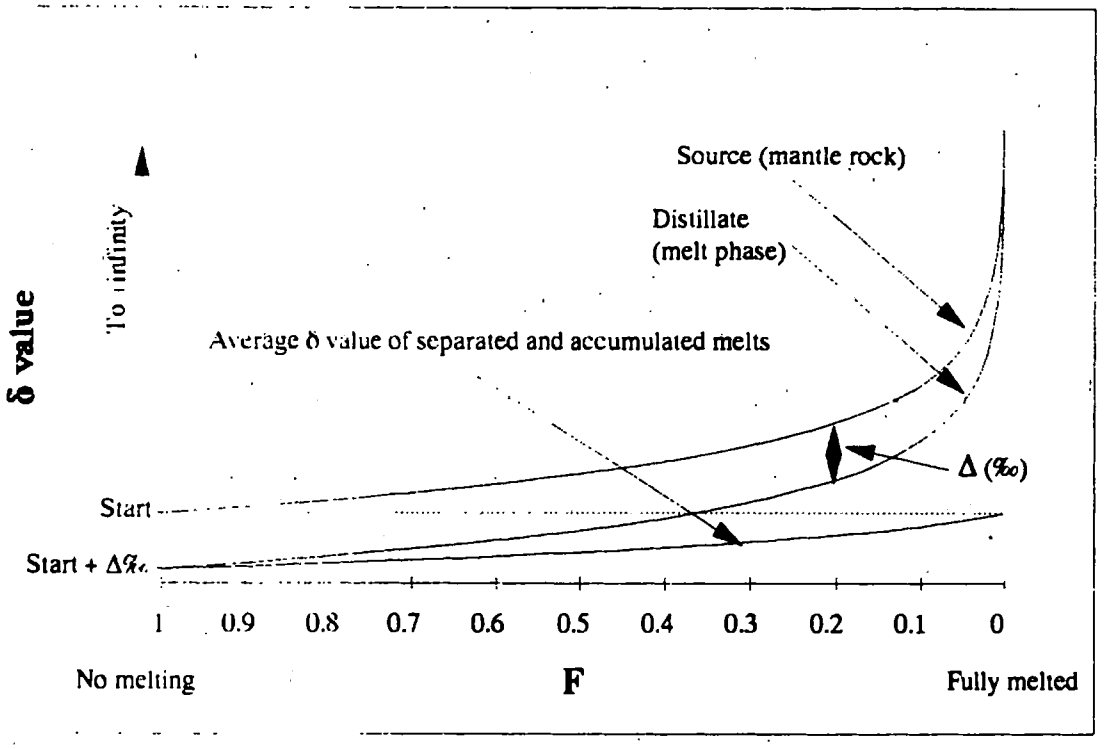

Figure A3.2: The effect of fractional (Rayleigh) melting on δ values. The same fractionation factor has been used as in Figure A3.1, and the melt product is enriched in the lighter isotope relative to the source material. This family of curves represents the limiting case for melting processes.

It is evident from Figure A3.2 that, as with fractional crystallization, large degrees of melting are required in order to significantly fractionate stable isotope ratios. In the case of diamonds, melting is analogous to the conversion of crystalline diamond to a supercritical "vapour" phase, and it is possible that all the diamond in any particular region may be so affected, fulfilling the conditions necessary for large degrees of isotope fractionation.

A3.4 BATCH MELTING

Batch melting is a more geologically reasonable model for the formation of fluid phases within the mantle, and very small volume melts (of the order of fractions of %; McKenzie and Bickle, 1988; McKenzie 1989) may be efficiently segregated from the source regions. While such small volume partial melts can cause extreme changes in the concentrations of incompatible trace elements, the changes that they can cause in stable

isotope ratios are less than those that can be caused in the limiting case of Rayleigh melting (described in the previous section). The maximum change in δ values occurs at infinitely small degrees of partial melt and is equal to the Δ value (in ‰). This limiting fractionation is due to the maintenance of equilibrium between produced melt and the solid residue until melt extraction. On 100% melting, the melt will have the same stable isotope ratio as the original source material. Batch melting is therefore not a particularly effective mechanism for generating large changes in stable isotope ratios.

A3.5 KINETIC EFFECTS

Kinetic effects are mathematically complex and are difficult to model. The may be relatively large (in excess of the per mille level) for major elements like C in diamond and for trace components may be even more significant (Jambon, 1980). Kinetic effects arise from the differing mass-dependent characteristics of different isotopes, particularly partition coefficients and diffusivities, which are, at present, poorly constrained. In the case of diamond, variation of the stable isotopic composition of carbon within individual samples of the order of several per mille have been reported (*e.g.* Javoy *et al.*, 1984; Otter, 1989; Wilding and Harte, 1991; Harte and Otter, 1992) and these are larger than the isotopic fractionation effects expected to be produced by kinetic fractionations alone (Jambon, 1980). The nitrogen stable isotopic composition may be affected by kinetic fractionations, particularly during nitrogen aggregation, however there are no data available for the differing diffusivities of different nitrogen isotopes in diamond, and thus kinetic isotopic fractionations are not discussed further here.

A3.6 MIXING PROCESSES

As with fractionation processes, mixing may be mathematically modelled, and a general mixing equation is presented by Langmuir *et al.*, (1978). The mixing equation is hyperbolic (Figure A3.3) and has the form:

$$Ax + Bxy + Cy + D = 0 \qquad \text{(A3.8)}$$

The coefficients of a mixing line between any two points may be calculated from the equations given by Langmuir *et al.*, (1978), and the symbols used are: x and y = general variables along the abscissa and ordinate respectively; x_i, y_i = coordinates of data point i; a_i = denominator of y_i (and $a_i = 1$ if y is not the ratio of two variables); b_i = denominator of x_i ($b_i = 1$ if x is not a ratio):

$$A = a_2b_1y_2 - a_1b_2y_1 \quad \text{(A3.9)}$$

$$B = a_1b_2 - a_2b_1 \quad \text{(A3.10)}$$

$$C = a_2b_1x_1 - a_1b_2x_2 \quad \text{(A3.11)}$$

$$D = a_1b_2x_2y_1 - a_2b_1x_1y_1 \quad \text{(A3.12)}$$

A measure of the hyperbolic curvature of the mixing curve is given by the parameter r. For straight lines, r = 1, and as r increases or decreases, the curvature of the hyperbola increases. The value of r is a function of coefficient B and is calculated from:

$$r = a_1b_2/a_2b_1 \quad \text{(A3.13)}$$

Mixing lines on single variable plots, for example $\delta^{13}C$ *vs.* nitrogen abundance, are straight lines. For straight lines, the value of coefficient B is always 0.

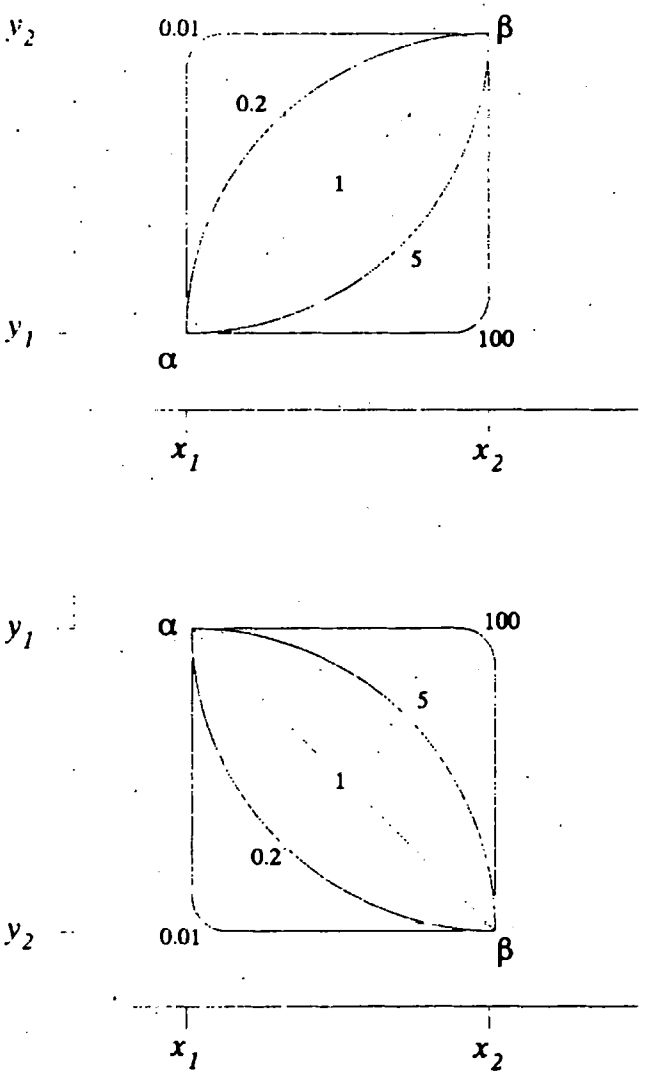

Figure A3.3: General mixing hyperbola for mixtures of α and β. The value of r is shown on each mixing hyperbola. The coordinates of α are $(\frac{x_1}{b_1} \cdot \frac{y_1}{a_1})$ and β is $(\frac{x_2}{b_2} \cdot \frac{y_2}{a_2})$. For single variable plots, a = b = 1.